Investigation of Response and Resistance to PARP Inhibition in Mouse Models of Human *BRCA2*-Mutant Breast Cancer

Thesis presented for Degree of Philosophiae Doctor
by

Liliana Ordonez

Cardiff School of Biosciences
Cardiff University

Declarations

This work has not previously been accepted in substance for any degree or award at this or any other university or place of learning, nor is being submitted concurrently in candidature for any degree or other award.

This thesis is being submitted in partial fulfilment of the requirements for the degree of PhD.

This thesis is the result of my own independent work/investigation, except where otherwise stated. Other sources are acknowledged by explicit references. The views expressed are my own.

I hereby give consent for my thesis, if accepted, to be available for photocopying and for inter-library loan, and for the title and summary to be made available to outside organisations.

I hereby give consent for my thesis, if accepted, to be available for photocopying and for inter-library loan after the expiry of a bar on access previously approves by the Graduate Development Committee.

Signed …….(candidate) Date……

Acknowledgements

I would like to dedicate this thesis to my boyfriend Matthew Allen and my best friend Kirsty Kemmett.

For many years Matthew and Kirsty has encouraged me to fulfil my goals and achievements, whether they be academic or climbing ten peaks for charity. They have always believed in me, even when I didn't believe in myself, and supported me through my career decisions. I would like to especially thank Matthew for putting up with my grumblings and emotional episodes, and being my rock throughout my PhD, always providing hugs and food when required.

I would also like to thank my parents; Andres and Iris Ordonez, and Katie and Lee Priday, for their continual support emotionally and financially throughout my education. I know that without their combined support I would not be where I am today. Along with my brother Sam, they have always encouraged me to pursue my goals.

I would like to thank everyone in the ARC group, past and present, for their helpful guidance. First and foremost I would like to thank my supervisor Alan, for providing me with such an interesting project, and allowing me to develop as a scientist by making my own decisions about the directions of the project, whilst providing guidance when needed. Secondly I would like to thank Trevor Hay for setting up the project, his continual guidance throughout the work, and also allowing me to take some leave from the lab by covering my daily injections from time-to-time. I would also like to thank Matthew Smalley, for his training and enthusiasm, and always being available for questions. I am also very grateful to everyone who I had contact with at AstraZeneca, especially Mark O'Connor, for their help with the project, but also for being friendly and accepting of someone who had no experience with industry. From ECSCRI I would also like to thank Maddy Young, for always making me laugh, Meera and Matt for their daily company in the basement, Steph and Elaine for making sure that I sometimes had a life outside of work, and the Friday night pub crew for their appreciation of after work drinks and crazy dancing! Finally I would like to thank everyone in ECSCRI for providing me with advice, humour and support.

Contents

List of figures

List of tables

Abbreviations and Definitions

Symbols

°C = Degrees Celsius

µg = Micrograms

µl = Microlitres

µm = Micrometre

µM = Micromolar

A

ABC = Avidin-Biotin Complex

AIF = Apoptosis-inducing factor

AME = Malignant Adenomyoepithelioma

AP site = Abasic site

ASQC = Metaplastic Adenosquamous carcinoma

ATM = Ataxia telangiectasia mutated protein

B

BARD1 = BRCA1-associated RING domain protein 1

BER = Base Excision Repair pathway

BLG = Beta-lactoglobulin

BlgCre = Beta-lactoglobulin Cre recombinase transgene

bp = Base pair

BRCA1= Breast cancer type 1 susceptibility protein

BRCA2 Breast cancer type 2 susceptibility protein

BRCT = BRCA1 C-terminal repeat

BSA = Bovine Serum Albumin

C

CK = Cytokeratin

cm = Centimetre

CSC = Cancer stem cells

C_T = Cycle time

D

DAB = 3,3'-diamionbenzidine

DCIS = Ductal carcinoma *in situ*

DNA = Deoxyribonucleic acid

DNase = Deoxyribonuclease

Dnmt1 = DNA (cytosine-5)-methyltransferase 1

DSBs = Double stranded breaks

DSBR = Double-strand break repair

E

E-cadherin = Epithelial cadherin

ECM = Extracellular matric

EGFR = Epidermal growth factor receptor

EMT = Epithelial-to-mesenchymal transition

ER = Oestrogen receptor

F

FEN-1 = 5'-flap endonuclease 1

H

H&E = Haematoxylin and eosin

HER2 = Human epidermal growth factor receptor

HR = Homologous repair pathway

I

IDC-NST = Invasive ductal carcinoma of no special type

IHC = Immunohistochemistry

IP = Interperitoneal

K

kDa = Kilodalton

K14 = Cytokeratin 14

L

loxP = locus of crossover of bacteriophage P1

M

MAPK = Mitogen-activated protein kinase

MDR = Multidrug resistance protein

MET = Mesenchymal-to-epithelial transition

mg = Milligram

MFU = Mammosphere forming unit

MMTV-LTR = Mouse mammary tumour virus –long terminal repeat

MRE11 = Mitotic recombinase 11

MSCC = Metaplastic spindle cell carcinoma

N

N-cadherin = Neural cadherin

NBS1 = Nijmegan breakage syndrome 1

NGS = Normal goat serum

NHEJ = Non-homologous end joining pathway

NLS = Nuclear localisation signal

NRS = Normal rabbit serum

P

PALB2 = Partner ad localiser of BRCA2

PAR = Poly(ADP-ribose)

PARG = Poly(ADP-ribose) glycohydrolase

PARP-1 = Poly(ADP-ribose) polymerase 1

PBS = Phosphate buffered saline

P-gps = P-glycoproteins

PI3K = Phosphatidylinositol 3-kinase

PLL = Poly-L-lysine

PR = Progesterone receptor

Q

qRT-PCR = Quantitative reverse transcription polymerase chain reaction

R

RNA = Ribonucleic acid

ROS = Reactive oxygen species

S

SDSA = Synthesis-dependent strand annealing

SMA = Smooth muscle actin

SSBs = Single stranded breaks

T

Taq = DNA polymerase from *Thermus aquaticus*

TDLU = Terminal duct lobular unit

TEBs = Terminal end buds

TGF-β1 = Transforming growth factor beta 1

TRF1 = Telomeric repeat-bindning factor-1

W

WAP = Whey acidic protein

123

53BP1 =p53 binding protein

Abstract

Breast cancer is the most common cancer in the UK, but despite recent encouraging increases in survival rates, is still the second most common cause of cancer death in women in the UK. To try to reduce systemic toxicity during treatment of cancer patients, a plethora of targeted therapies are in various stages of development. PARP inhibitors have been shown to be particularly effective in *BRCA*-deficient cells, making them a contender as a personalised therapy. One of the challenges for targeted therapies is that of resistance, which limits the extent of benefit to the patient. The work described in this study continues previous work within our laboratory, investigating the PARP inhibitor olaparib in a conditional mouse model of *BRCA2*-mutated human breast cancer.

The data presented here establish a correlation between histological tumour type and response to olaparib therapy, with poor responders classified exclusively as mesenchymal-like metaplastic spindle cell carcinomas (MSCC). This suggests that further patient stratification is required when deciding on whether this therapy may be suitable, and may explain why not all patients with *BRCA*-mutated breast cancer have benefitted from olaparib therapy in current clinical trials.

Investigation of olaparib resistance in this study indicated that several currently proposed mechanisms of resistance were not pertinent to the *Brca2/p53* model, hence novel mechanisms were sought. Histopathological analysis of resistant tumours showed that the majority were MSCCs, representing a significant change in the proportion compared to an untreated cohort. Other resistant tumour types had epithelial morphology, but showed an increase in expression in some mesenchymal-like genes compared to untreated cohorts, suggesting that mesenchymal features may be important in causing resistance to olaparib.

A similar tumour model, incorporating the additional deletion of E-cadherin, was used to investigate whether lack of this protein in tumours affected response and resistance to olaparib therapy. Loss of *Cdh1* led to an increase in invasive ductal carcinomas of no special type (IDC-NST) and the absence of MSCCs, suggesting that genetic loss of expression does not drive the formation of mesenchymal-like tumours. Correlating with this, loss of E-cadherin did not drive epithelial-to-mesenchymal transition in these tumours and had no effect on response to olaparib therapy or resistance to the inhibitor.

Taken together, the data presented in this thesis suggest that MSCCs have an intrinsic resistance to olaparib therapy, and tumours which initially respond to olaparib therapy harness or acquire certain mesenchymal characteristics in order to develop resistance during treatment.

1. Introduction

1.1 Mammary gland

1.1.1 Structure and Architecture

The female mammalian mammary gland functions to produce and secrete milk to nourish progeny. The milk is supplied by an exterior nipple which is connected to an interior network of epithelial ducts. The epithelial ducts branch throughout the fat pad, which comprises of adipocytes, fibroblasts, immune cells, neurons and blood vessels. In humans the nipple is connected to numerous epithelial ducts and pregnancy initiates the formation of alveoli, the sites of milk production. A collection of alveoli connected to one terminal duct is termed a terminal duct lobular unit (TDLU) (Figure 1.1A).

The epithelial ducts are comprised of two cellular layers surrounding a central lumen (Figure 1.1C) (Howard and Gusterson 2000). The inner layer of epithelial cells are termed luminal cells. These cells have an apical-basal polarity, are connected to adjacent luminal cells via tight junctions and are characterised by the expression of genes such as cytokeratin (CK) 8 and CK18. Approximately a third of the luminal cells express the oestrogen receptor (ER), enabling them to respond to oestrogen. The outer layer of cells surrounding the duct lumen are the basal cells. These cells are located between the luminal cells and the basement membrane and are characterised by the expression of CK5, CK14 or p63. Within this basal layer reside the myoepithelial cells, which contain features of both epithelial and smooth muscle cells and can be characterised by the expression of markers such as smooth muscle actin (SMA). These cells contract in response to the hormone oxytocin during lactation. The basement membrane functions to provide structural support for the epithelial cells and is composed of extracellular matrix proteins such as type IV collagen, fibronectin and laminin (Richert *et al.* 2000).

1.1.2 Key differences between the human and mouse mammary glands

Although the structure and development of the mammary glands in humans and mice are very similar, and studying the mouse mammary gland has achieved important advances in the knowledge of human mammary gland morphogenesis and disease, there are key differences between the two species. These include: (i) sexual dimorphism occurs during puberty in humans while in mice it occurs *in utero*; (ii) humans have one pair of mammary glands whereas mice have five; (iii) in humans the nipple is connected to multiple ducts and the alveoli are clustered in discrete TDLUs, whereas in mice the nipple is connected to one primary duct and the alveoli are located throughout the ductal network (Figure 1.1B) (Hovey *et al.* 2002). In addition the TDLUs in humans are encapsulated by intralobular stroma, which is predominantly composed of fibroblasts, and is bordered by a second, denser intralobular layer. In comparison the stroma in the mouse mammary gland is mainly composed of adipocytes (Howard and Gusterson 2000).

1.1.3 Changes during development

The mammary gland is a unique tissue in that the majority of its development occurs post-embryonically. The female mouse mammary gland undergoes dramatic morphological changes during puberty, pregnancy, lactation and involution (Figure 1.2A). At birth the interior mammary gland is composed of a rudimentary ductal structure (Richert et al. 2000). Oestrogen and progesterone initiate epithelial proliferation during puberty, creating secondary ducts, whose branching and elongation initiate from terminal end buds (TEBs), which are located at the growing tip of the duct. TEBs contain two cell types: cap cells and body cells. Cap cells compose the outer layer of the terminal end bud and form the basal cells, whereas the body cells form multilayers in the duct lumen and give rise to luminal cells (Figure 1.2B) (Williams and Daniel 1983; Hennighausen and Robinson 2005). The TEBs continue to cause ductal branching and elongation until they reach the capsule at the end of the mammary fat pad or become surrounded by other ducts, where they then regress to form terminal ducts (Howard and Gusterson 2000). Each oestrous cycle results in the formation of alveolar buds, but in the absence of pregnancy-related hormones these buds regress (Howard and Gusterson 2000). Rising levels of hormones such as prolactin, oestrogen and progesterone during pregnancy initiates further ductal branching and

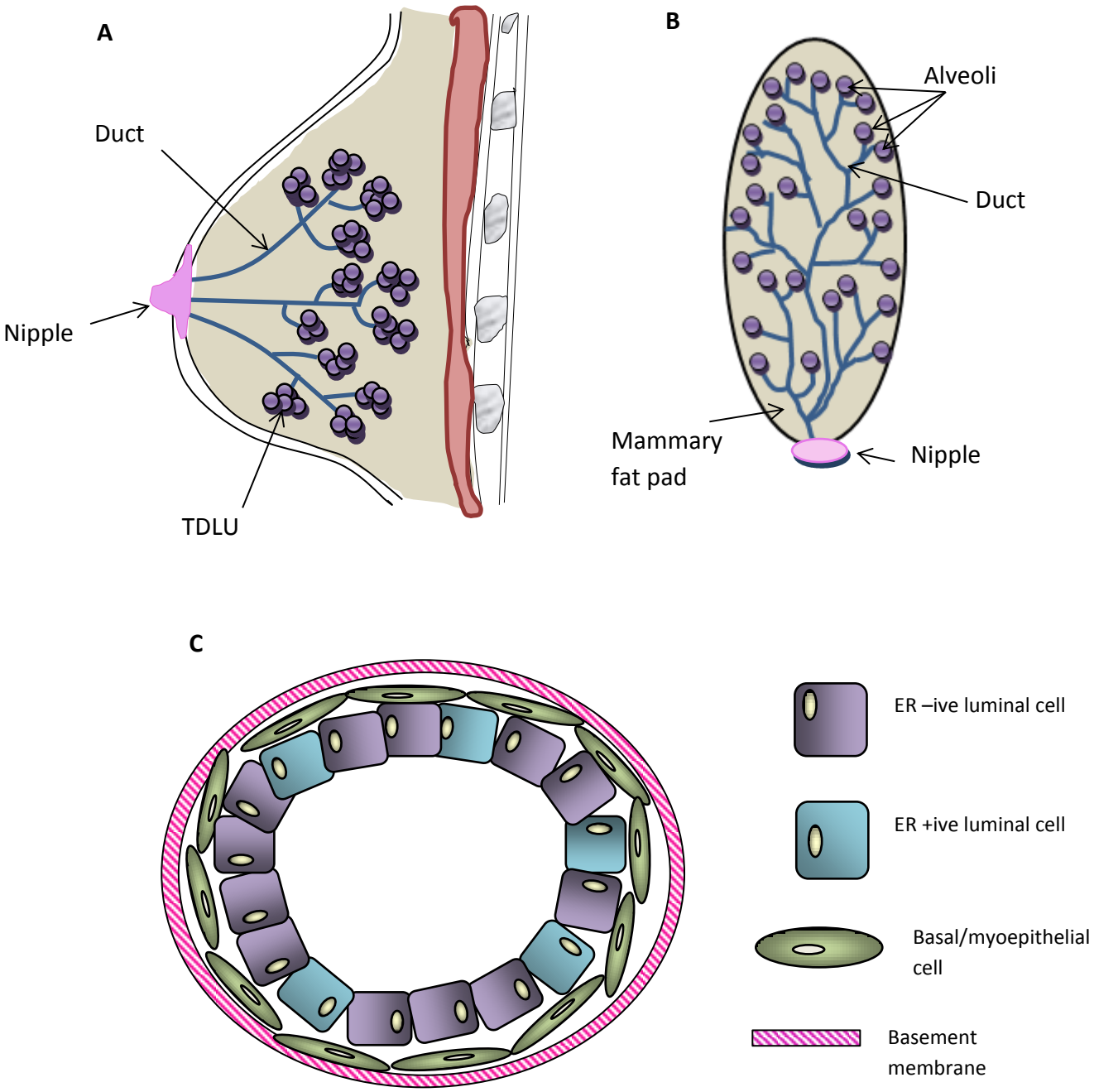

Figure 1.1 Structure of epithelial ducts within the mammary gland. *(**A**) The human mammary gland. (**B**) The mouse mammary gland. (**C**) Epithelial duct structure. TDLU: terminal ductal lobular unit.*

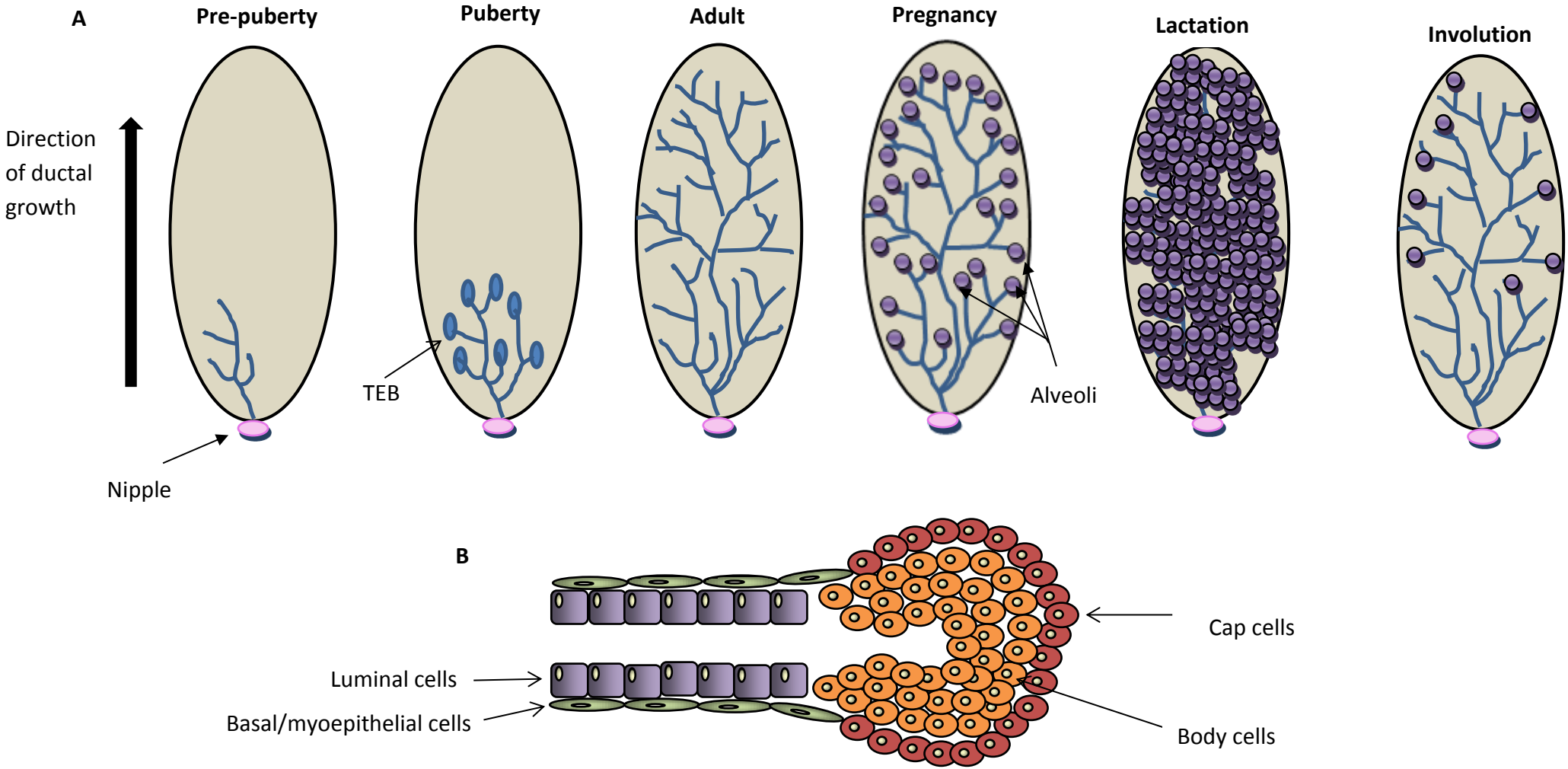

Figure 1.2 Post natal development of the mouse mammary gland. *(**A**) Changes in structure in pre-pubertal, pubertal, adult, pregnant, lactating and involuting mammary gland in mice. TEB: terminal end buds. (**B**) TEB structure. Figure adapted from Hennighausen and Robinson, 2005*

differentiation of the alveolar buds into alveoli. During lactation milk is produced in the alveoli and the contractile myoepithelial cells function to move the milk towards the nipple. Once lactation ceases the mammary gland undergoes a high rate of apoptosis and remodelling, a process known as involution, resulting in the morphology of the ductal network returning closely to the pre-pregnancy state (Howard and Gusterson 2000).

1.1.4 Mammary gland cell hierarchy

Cell hierarchy in the mammary gland remains controversial, with conflicting ideas as to whether the epithelial cell lineages arise from bipotent or unipotent stem cells (Figure 1.3A-B). Transplantation studies of small numbers of, or even single basal cells have been shown to regenerate entire mammary epithelial trees (Shackleton *et al.* 2006; Stingl *et al.* 2006), demonstrating the presence of bipotent stem cells in the basal layer. In contrast a study by Van Keymeulen and colleagues suggested that the luminal and basal lineages are uncoupled and are produced from distinct unipotent stem cell populations (Van Keymeulen *et al.* 2011). The in 2012, a study used lineage tracing to suggest that the epithelial cell lineages are maintained by unipotent stem cells during puberty and homoeostasis (van Amerongen *et al.* 2012). Cellular differentiation during pregnancy was also investigated in this study, with results suggesting that bipotent stem cells are able to produce both the luminal and basal lineages, and that alveolar cells differentiate from the luminal progenitor (Figure 1.3C). Following this, in early 2014 a study by Rios *et al* supported the bipotent theory by showing evidence of bipotent stem cells in the adult mouse mammary gland located in the basal layer (Rios *et al.* 2014).

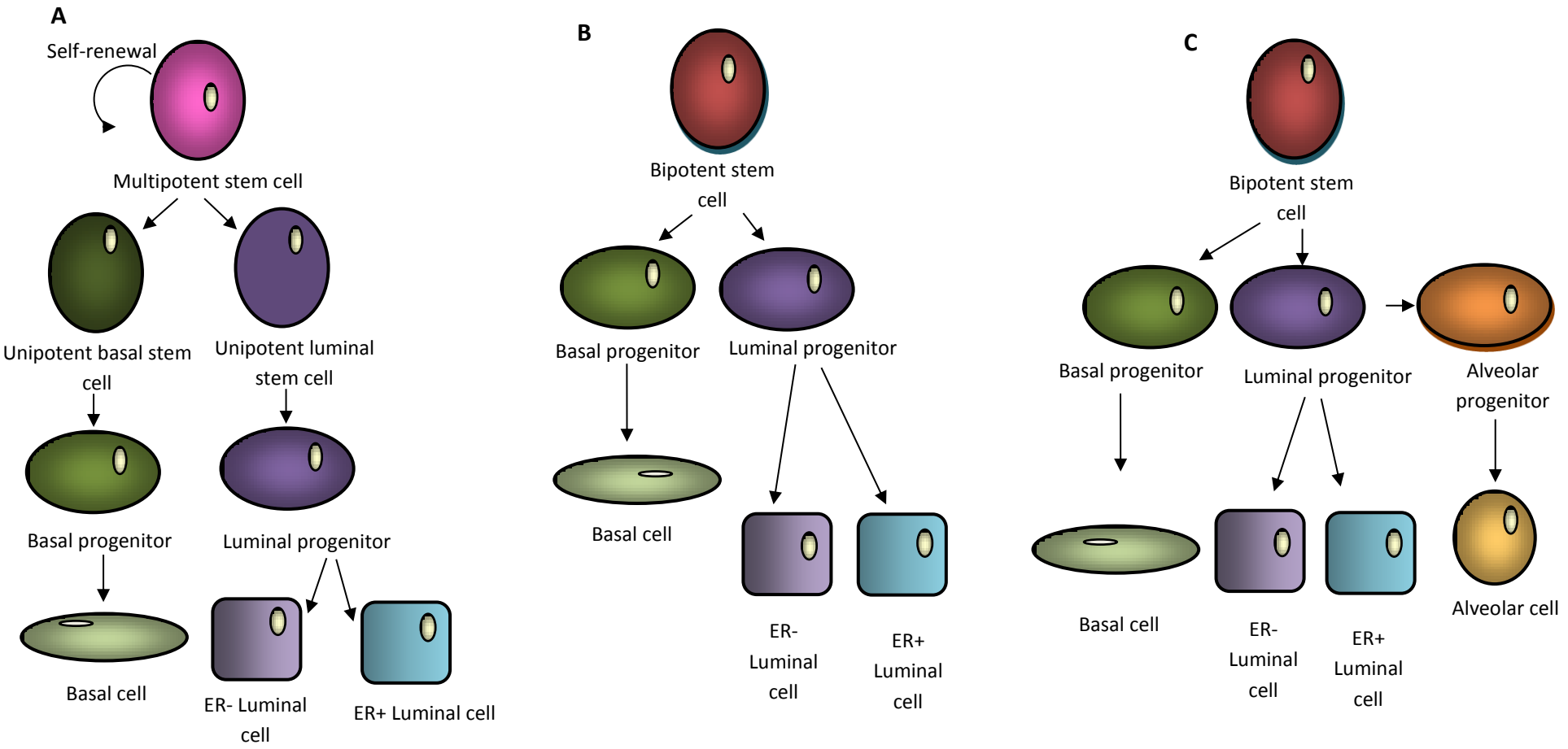

Figure 1.3 Theories of Mammary gland cell hierarchy. *(**A**) The mammary gland initially develops from a multipotent stem cell, then during puberty and adulthood the basal and luminal cells are maintained by unipotent stem cells. (**B**) In adults the epithelial lineages are maintained by bipotent stem cells. (**C**) During pregnancy bipotent stem cells are able to give rise to both epithelial lineages and alveolar cells are differentiated from luminal progenitors.*

1.2 Breast cancer

1.2.1 Incidence and survival

Breast cancer is the most common cancer in women in the UK, with almost 50,000 being diagnosed in 2010 (http://www.cancerresearchuk.org). Breast cancer is also the second most common cause of cancer death in women in the UK; however, despite the high incidence five year survival rates are increasing, currently at 85.1% (http://www.cancerresearchuk.org). The incidence of breast cancer in males is much lower, with around 400 being diagnosed in 2010. Factors that have been shown to increase the risk of breast cancer include: increased age, family history of the disease, obesity, high alcohol consumption, and exposure to hormone replacement therapy. There is also evidence to suggest that breast cancer risk can be reduced by both breastfeeding and an increased number of live births (Beral *et al.* 2002).

1.2.2 Progression of Breast cancer

The predominant location of breast tumour initiation in humans is in the TDLUs (Wellings *et al.* 1975). Breast cancer is thought to progress from hyperplasia to metastatic cancer via a series of stages (Mallon *et al.* 2000); Figure 1.4). The initial stage of epithelial hyperplasia is followed by atypical hyperplasia, which is the proliferation of epithelial cells with nuclear and morphological abnormalities. Atypical hyperplasia can result in ductal carcinoma *in situ* (DCIS), where the lumen is filled with abnormal epithelial cells. Once cells invade through the basement membrane and into the surrounding stroma it is classed as invasive breast cancer. Invasive cells can then enter the lymphatic or vasculature system and metastasise to secondary sites in the body. In humans, breast cancer metastasis via the lymphatic and the vascular system, with the most common sites of metastasis being lymph nodes, lung and bone, however in the mouse metastasis is predominantly through the vascular system (Mallon *et al*. 2000).

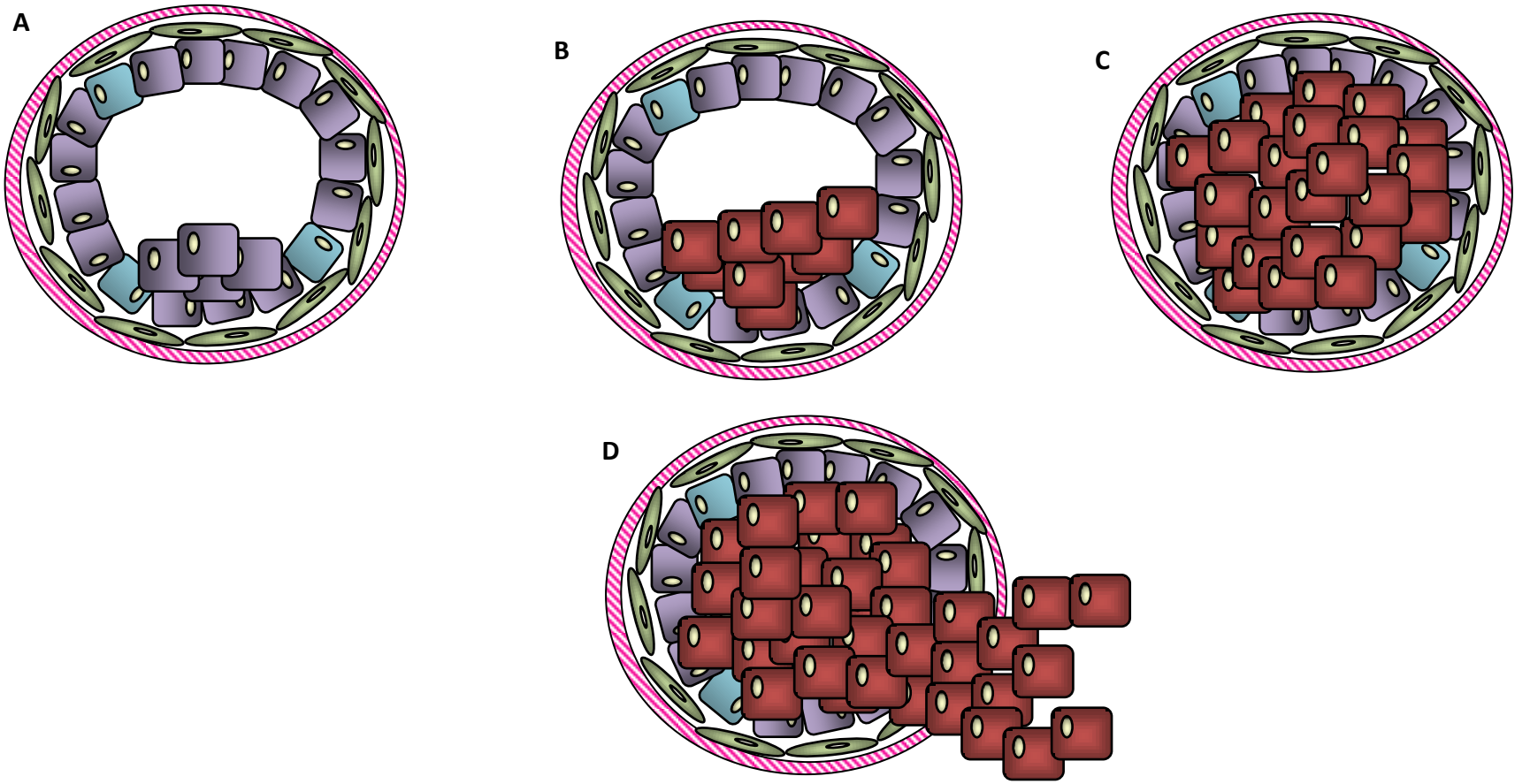

Figure 1.4 Progression of breast cancer. *Epithelial hyperplasia (**A**) can progress to atypical hyperplasia (**B**), which can be followed by ductal carcinoma in situ (**C**). Invasive cancer (**D**) occurs when the abnormal cells penetrate through the basement membrane and invade the surrounding tissue. Cells can then enter the lymphatic or vasculature system and metastasise to other tissues.*

1.2.2.1 Epithelial to mesenchymal transition

To progress from DCIS to invasive breast cancer it is thought that epithelial cells undergo epithelial to mesenchymal transition (EMT) (Choi *et al.* 2013). During EMT epithelial cells lose their apical-basal polarity and acquire mesenchymal characteristics, such as spindle-morphology and increased migration and invasion. The acquisition of these characteristics changes a tumours ability to become invasive and metastatic. To create secondary tumours following metastasis it is thought that these mesenchymal cells then undergo mesenchymal-to-epithelial transition (MET) (Chaffer *et al.* 2006).

EMT is required for processes such as embryogenesis and wound healing and involves the loss of adheren and tight junctions and reorganisation of the cytoskeleton. To achieve mesenchymal transition epithelial cells repress the expression of *CDH1* (epithelial cadherin (E-cadherin)), resulting in the loss of cell-cell junctions, and increase the expression of genes such as *CDH2* (neural cadherin (N-cadherin)) and *VIM* (Vimentin), which make cells more motile and invasive, and also genes such as *MMP2* (metalloproteinase 2) which cause changes to the extracellular matrix (ECM) and increase the invasive potential of the cells (reviewed in (Xu *et al.* 2009)). As well as these differences in gene expression cells undergoing EMT can be characterised by increased expression of EMT-associated transcription factors, such as SNAIL, SLUG, ZEB1/2 and TWIST. The expression of these transcription factors are induced by signalling from transforming growth factor beta 1 (TGF-β1) (Figure 1.5).

TGF-β1 is produced by the tumour microenvironment and binds to a heteromeric complex of two type I and two type II transmembrane serine-threonine kinase receptors. Binding of TGF-β1 to the complex causes the phosphorylation of the type I receptors by the type II receptors, resulting in the subsequent phosphorylation and activation of SMAD2 and SMAD3 by the type I receptors. Phosphorylated SMAD2 and SMAD3 then form trimers with SMAD4, allowing translocation of the complex into the nucleus, where it regulates transcription of target genes.

EMT can also be induced by other pathways such as the Wnt (Yook *et al.* 2005), Notch (Timmerman *et al.* 2004), integrin (Kim *et al.* 2006) and AKT pathways (Grille *et al.* 2003).

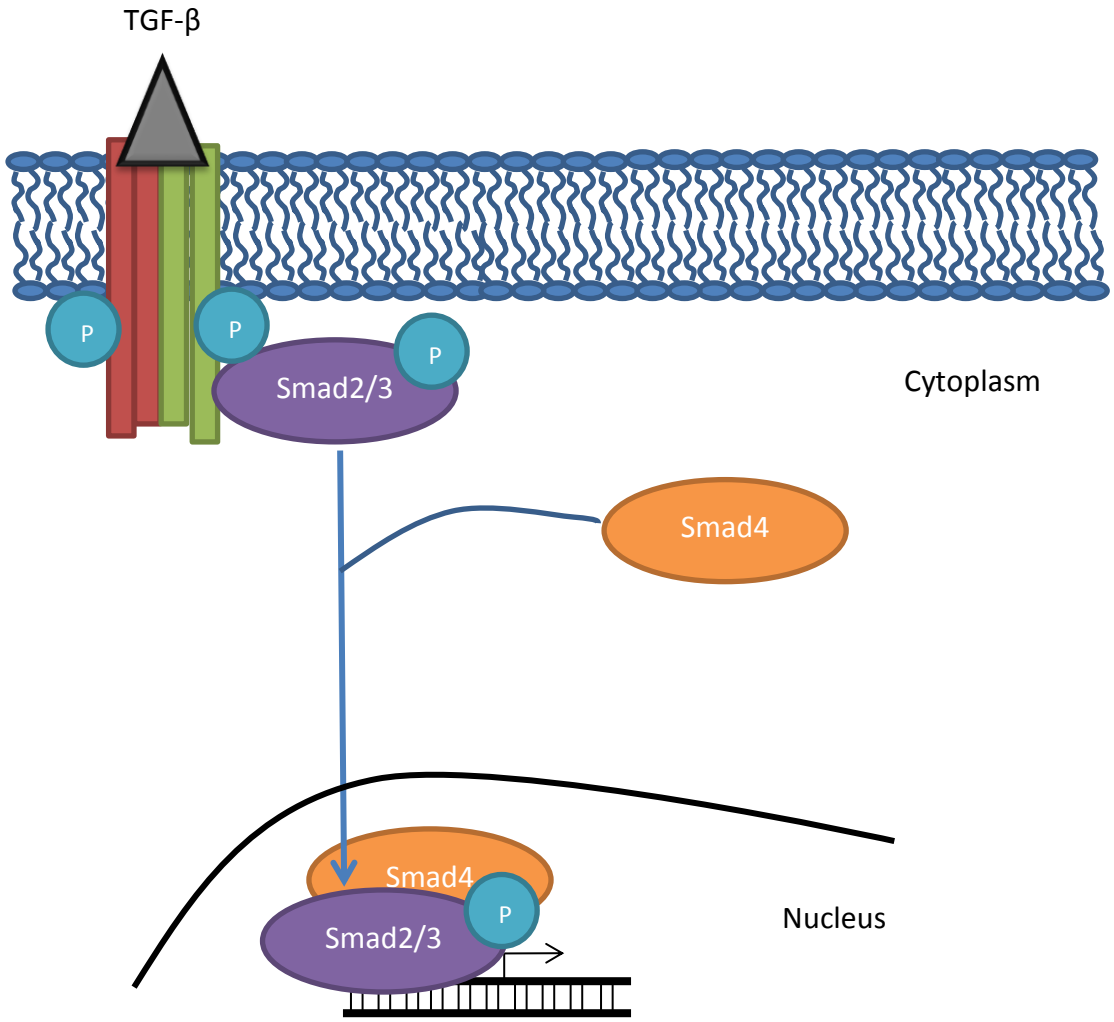

Figure 1.5 TGF-β Signalling. *Binding of TGF-β to the type I (red) and type II (green) receptors causes the phosphorylation and activation of Smad2/3. Smad 4 is then recruited and the complex translocates to the nucleus where it causes changes in target gene expression, for example inducing the expression of Snai1 and Snai2. Figure adapted from Xu et al. 2009.*

1.2.3 Breast cancer heterogeneity

Breast cancer is an extremely heterogeneous disease, with tumours showing inter- and intra-heterogeneity. There are numerous ways to classify breast tumours, ranging from cellular morphology to gene expression. These classification systems help to stratify breast cancers into groups for determination of prognosis and treatment.

1.2.3.1 Histopathological classification

Histopathological classification involves the examination of haematoxylin and eosin (H&E)-stained sections to analyse characteristics and morphological features of the cells within the tumour. There are many different histopathological types of human breast cancer which can be broadly classified into epithelial, mesenchymal and fibroepithelial tumours (Mallon et al. 2000; Lakhani *et al.* 2012). There are numerous subgroups within each of these classifications. In humans invasive breast tumours are predominantly classed as invasive ductal carcinoma of no special type (IDC-NST). These tumours are classified by the exclusion of characteristics which would classify them as other histopathological types; therefore they are a heterogeneous group of tumours. Although mammary tumours from genetically engineered mouse models display a number of differences to those in humans they have shown to have similar molecular and morphological features (Cardiff *et al.* 2000).

1.2.3.2 Grade

The grading system of Bloom and Richardson (Bloom and Richardson 1957) classifies breast tumours into 3 grades, with grade 1 indicating the best prognosis and grade 3 the worst. This grading system comprises of three components that are each given a score from 1-3. The first component is tubule formation, which is indicative of the amount of differentiation within the tumour, with a score of 1 if glandular structures compose over 75% of the tumour, 2 if they make up 10-75% and 3 if they compose less than 10%. The second component is nuclear pleomorphism, with a score of 1 denoting small and regularly shaped nuclei, 2 if there is a moderate change in size and shape, and 3 if there are multinucleated cells with a large variation in size and shape. The final component is mitotic index, which involves counting the number of mitotic cells in 10 high power fields to create an average. If using a 20x objective, a score of 1 is given if 0-9 mitotic nuclei are counted, 2 if 10-19 are counted and 3 if over 19 are counted. The three scores are added together to give a final

total which correlates with the grade: grade 1 corresponds to a score of 3-5, grade 2 to a score of 6-7 and grade 3 to a score of 8-9.

1.2.3.3 Stage

Breast cancers can also be classified into stages, with the most widely used system being the TNM staging system (published by American joint committee on cancer/Union for international cancer control). This involves three components: the size of the tumour and whether it has spread into the surrounding tissues (T), whether it has metastasised to the lymph nodes (N), and whether it has metastasised to distant parts of the body (M). The components are then combined to produce a stage, which are classified as 0-IV.

1.2.3.4 Molecular classification

1.2.3.4.1 Receptor status

Breast tumours can be classified on the expression of three receptors: oestrogen receptor α (ER), the progesterone receptor (PR) and the human epidermal growth factor receptor 2 (HER2). These three receptors are not only used as a classification system, but are also targets for cancer treatment.

Around 75% of human breast cancers are ER positive (+). There are two isoforms of the oestrogen receptor, α and β, which are expressed from two different genes. Currently only the α isoform is used for breast cancer classification. ER is a nuclear transcription factor which is expressed in around a third of luminal cells in the normal mammary gland. Binding of the steroid hormone oestrogen to the receptor causes a conformation change, allowing receptor dimerisation and binding to response elements in DNA resulting in expression of target genes. The ER pathway stimulates growth in normal breast epithelial cells and in tumour cells. The amount of ER positivity within a tumour is predictive of response to endocrine therapy. The PR receptor mediates the effects of the steroid hormone progesterone. There are two isoforms of the receptor which are expressed from the same gene: A and B. PR is expressed in around 65% of human breast cancers. PR is an oestrogen-regulated gene and was originally used in breast cancer as an indicator of an intact ER pathway. Studies have now shown that PR status can also be predictive of therapy, with

ER+/PR+ tumours responding better to a targeted ER therapy than ER+/PR negative (-) tumours (Bardou *et al.* 2003).

HER2 is a member of the epidermal growth factor receptor (EGFR) family. It is a transmembrane receptor which is activated upon ligand binding and causes the activation of the phosphatidylinositol 3-kinase (PI3K) and mitogen-activated protein kinase (MAPK) cascades. 20-30% of human breast cancers overexpress the HER2 receptor, with the majority caused by gene amplification, and these tumours can also express ER and PR. HER2+ tumours tend to be aggressive and patients have a poor prognosis compared to those with HER2- tumours. Tumours that are negative for ER, PR and HER2 are termed triple negative tumours. They account for around 15% of human breast cancers and are associated with a high mitotic index, earlier onset and poor prognosis.

1.2.3.4.2 Gene expression

Breast tumours can be classed into intrinsic subgroups based on their gene expression profiles (Perou *et al.* 2000b; Sorlie *et al.* 2001) and are first classified for ER status.

ER+ breast tumours express genes that are characteristic of luminal cells (for example CK18, CK8 and E-cadherin) and commonly contain epithelial cells which are positive for PR. ER+ breast tumours are the most common intrinsic subgroup of breast cancer (Gusterson *et al.* 1984; Carey *et al.* 2006), accounting for around two thirds of cases, and can be split into two further groups: luminal A and luminal B. Luminal A tumours tend to be PR+/HER2- whereas luminal B tumours tend to be PR+/HER2+. Luminal A is twice as common as luminal B and these two groups can also be distinguished by the expression of proliferation markers, which are more highly expressed in luminal B tumours (Cheang *et al.* 2009). Patients with luminal A tumours have a better prognosis than those with luminal B.

ER- tumours are categorised into four subgroups: HER2+, basal, claudin-low and normal-like. HER2+, ER- breast tumours also tend to be PR-, express low levels of genes characteristic to luminal cells and account for around 5-10% of breast cancers (Carey *et al*. 2006). Basal breast cancers make up 15-20% of breast cancers, express genes that are characteristic to basal cells (for example CK14, CK5, EGFR and p63) and are mainly triple negative (Perou *et al*. 2000b; Sorlie *et al*. 2001).

12-14% of breast tumours are of the claudin-low subtype, which show similar gene expression patterns to basal tumours but are characterised by the low expression of cell-cell adhesion genes (e.g. those that encode claudin 3, 4, 7 and E-cadherin) and high expression of EMT genes (e.g. those that encode vimentin and twist) (Prat *et al.* 2010). They also show high expression of immune response genes, low expression of proliferation markers, high frequency of medullary and metaplastic features and are enriched for stem cell markers and cells with stem-cell-like characteristics (Creighton *et al.* 2009; Hennessy *et al.* 2009; Prat *et al*. 2010).

Normal-like breast tumours show high expression of genes that are characteristic of basal cells, adipose cells and other non-epithelial cells and low expression of luminal genes, although there is controversy over whether this is a genuine subgroup or an artefact of contaminating stromal tissue.

The different intrinsic subgroups of breast cancer are linked to prognosis, with luminal A patients having the best prognosis and those with basal-like or HER2+ tumours having the worst (Sorlie *et al*. 2001).

1.2.3.4.2.1 Origin of intrinsic groups

One hypothesis for the existence of intrinsic subgroups in breast cancer is that tumours arise from different epithelial populations. The clonal evolution theory states that each subgroup is determined by which particular cell along the mammary cell hierarchy the tumour originates from, and that all cells within the tumour are capable of tumour formation (tumour initiating cells). Gene expression analysis studies have suggested that all breast tumours originate from the luminal differentiation hierarchy, with ER+ tumours arising from mature, differentiated luminal cells, HER2+/ER- tumours and basal tumours originating from luminal progenitors and claudin-low tumours arising from the mammary stem cells (Figure 1.6A) (Lim *et al.* 2009; Prat and Perou 2011). In contrast a recent study showed that tumours deriving from the same cell-of-origin in a particular mouse model displayed different molecular features and spanned a broad range of molecular signatures, suggesting that intrinsic subtype does not necessarily reflect its cell-of-origin (Melchor *et al.* 2014).

A criticism of the clonal evolution theory is whether all tumour cells are tumour initiating cells. The cancer stem cell theory states that only a subpopulation of cells within the tumour are tumour initiating cells and that these cells have similar characteristics to mammary stem cells. This theory opens up two hypotheses for intrinsic subgroup origination: either the mammary stem cells are the cells of origin for all the subgroups, or cells along the epithelial differentiation hierarchy acquire stem cell-like characteristics which enable them to initiate tumour development (Figure 1.6B-C).

1.2.3.4.3 Targeted treatments

The presence of intrinsic subgroups of breast cancer suggests that targeted, personalised therapy may be critical for efficient tumour treatment and patient survival. Unlike conventional chemotherapy, which has traditionally targeted any highly proliferative cells, targeted therapy involves the administration of treatments which target a specific signalling pathway, hopefully resulting in low systemic toxicity. An example of a targeted treatment in breast cancer is tamoxifen, a competitive ER inhibitor; which has been very successful in patients with ER+ breast cancers. Following the success of tamoxifen, other therapies that target the ER pathway are also available, including aromatase inhibitors.

Another example of a targeted treatment for breast cancer is the anti-HER2 monoclonal antibody trastuzumab, which perturbs HER2 signalling by targeting the extracellular domain of its receptor and hence is effective in HER2+ breast cancers. It has been shown to increase survival in around 30% of HER2+ breast cancer patients, and response is further increased when used in combination with certain chemotherapeutics (Baselga 2001). However patients can quickly relapse and exhibit resistance. Drugs such as lapatinib, which target multiple members of the EGFR family, are also useful in HER2+ patients.

There are currently no targeted therapies for basal breast cancers. As the majority of basal breast cancers are triple negative, hormone-based therapies, such as tamoxifen and trastuzumab, are ineffective. A potential target for basal breast cancers is the epidermal growth factor receptor (also known as HER1), as it is overexpressed in up to 80% of these tumours. Monoclonal antibodies, such as certuximab, and inhibitors of receptor phosphorylation, for example gefitinib, have been trialled in basal breast cancers to perturb

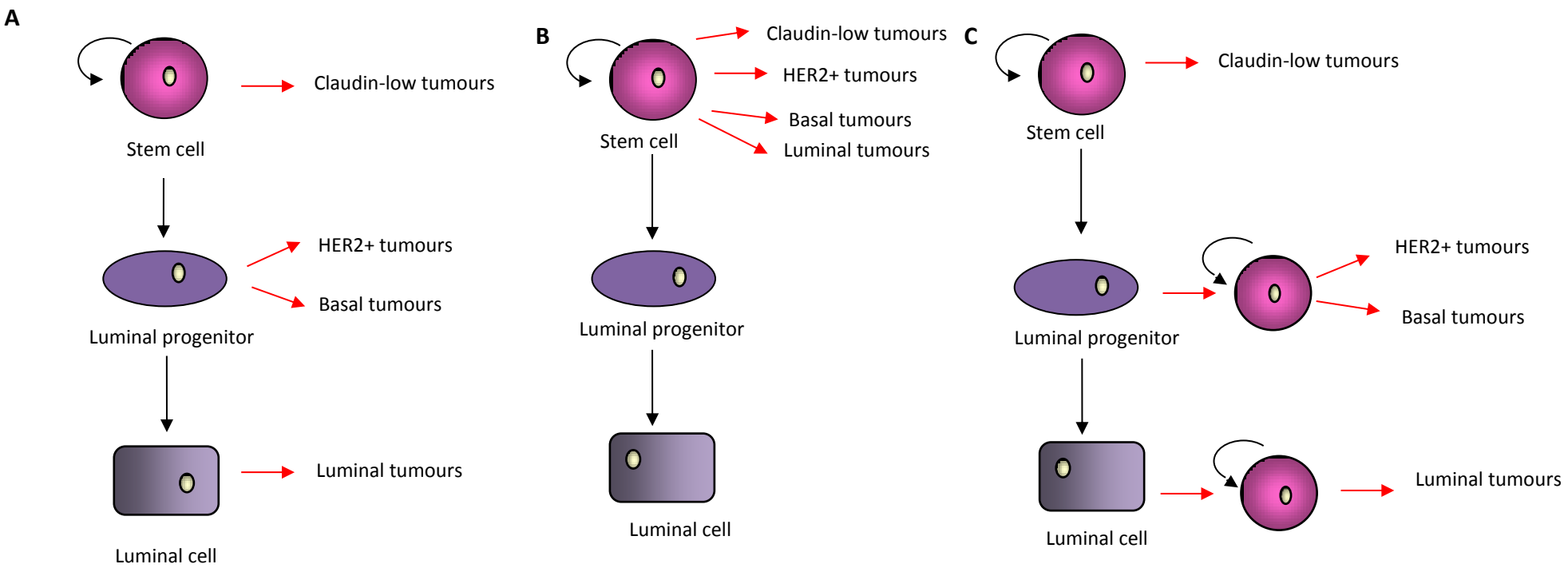

Figure 1.6 Origin of different intrinsic subgroups of breast cancer from cells along the luminal differentiation hierarchy. *(**A**) In the clonal evolution theory each tumour type originates from a different cell type. The cancer stem cell theory states that either (**B**) all tumour types originate from the stem cells, or (**C**) they originate from different cell types that have acquired stem cell characteristics. Figure adapted from Prat and Perou 2011.*

EGFR signalling; however, patients have shown only a modest response (Modi *et al.* 2006; Carey *et al.* 2008; Green *et al.* 2009). It is clear that a better understanding of the molecular processes involved in basal breast cancers is required so that new targets can be discovered.

1.2.4 Drug resistance

A recurring problem with cancer treatment is that of drug resistance, which limits clinical benefit. Hence it is imperative that the mechanisms of drug resistance are discovered and explored to ensure the effectiveness of these important therapies. Tumours can exhibit intrinsic or acquired resistance. 'Classical' resistance mechanisms include rapid metabolism or excretion of the drug, poor absorption and alteration of the drug target (reviewed in (Gottesman 2002; Stewart 2007). Mechanisms can also confer resistance to multiple, unrelated drugs. This is termed multidrug resistance and mechanisms include decreased uptake of drugs into the cell and up-regulation of P-glycoproteins (P-gps), which are energy-dependent drug efflux pumps (reviewed in (Gottesman 2002)).

Studies have shown that tumour cells with stem cell-like characteristics are more resistant to chemotherapy, with characteristics such as high expression of P-gps and anti-apoptotic factors, such as Bcl-2 and sonic hedgehog (Mimeault *et al.* 2008). This small population of cells are termed cancer stem cells (CSCs). It is hypothesised that these cells cause tumour relapse by surviving conventional cancer treatments, therefore therapies that specifically target the CSCs could be a more effective approach to treating cancer (Figure 1.7).

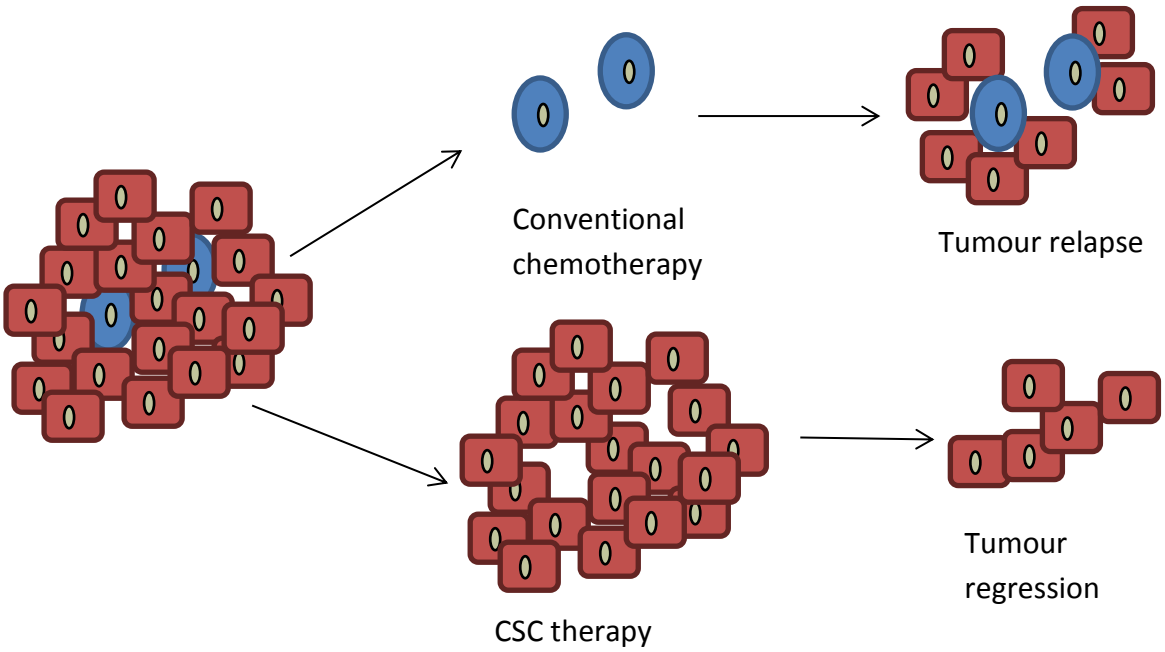

Figure 1.7 Targeting cancer stem cells as a therapeutic strategy. *Cancer stem cells (CSC, blue cells) may be resistant to conventional chemotherapies, allowing tumour relapse. CSC therapies could prevent tumour relapse and cause tumour regression, possible in combination with conventional chemotherapy.*

1.3 Inherited breast cancer

1.3.1 Incidence

Cancer which originates from the inheritance of a mutated gene is termed inherited cancer. Inherited breast cancer is thought to account for around 10% of all breast cancer cases. The most commonly mutated genes in inherited breast cancer are the genes that encode the breast cancer type 1 susceptibility protein (BRCA1) and the breast cancer type 2 susceptibility protein (BRCA2). Patients with a family history of breast cancer can receive genetic screening to search for common mutations in the *BRCA* genes. If the patient is found to carry a *BRCA* mutation then preventive measures are available, including mastectomy which can reduce the risk by approximately 90% (Hartmann *et al.* 1999; Rebbeck *et al.* 2004).

1.3.2 BRCA1 and BRCA2 structure and function

The *BRCA1* and *BRCA2* genes are expressed in the late G2 and S phases of the cell cycle and are located on chromosomes 17q21 and 13q12-13. Both proteins are located in the nucleus and are expressed ubiquitously. BRCA1 is an 1863 amino acid protein with a RING finger domain at its N-terminus and a BRCA1 C-terminal repeat (BRCT) domain at its C-terminus (Figure 1.8). The BRCT domain is composed of a repeated sequence of 100 amino acids and facilitates the binding of BRCA1 to other proteins. BRCA1's DNA binding ability is hypothesised to be facilitated by the BRCT domain, however current studies are conflicting (Yamane *et al.* 2000; Paull *et al.* 2001). The RING finger domain is the binding site for the BRCA1-associated RING domain protein 1 (BARD1). The BRCA1-BARD1 heterodimer is hypothesised to be involved in protein ubiquitination as the dimer possesses ubiquitin ligase activity (Xia *et al.* 2003). BRCA1 also contains a nuclear localisation signal (NLS), and a transcriptional activation domain, which is located close to the BRCT domain (Figure 1.8).

BRCA2 is a 3418 amino acid protein. It contains similar domains to BRCA1 such as a transcriptional activation domain, DNA binding sequences and a NLS; however BRCA1 and BRCA2 have different localisations of these domains within their protein structures (Figure 1.8). BRCA2 contains eight BRC repeats that have variable spacing, such that the repeat region spans around 1000 amino acids, which are vital for its role in DNA repair.

BRCA1 and BRCA2 are unrelated proteins involved in the homologous recombination (HR) pathway of DNA repair. This pathway repairs DNA double stranded breaks (DSBs) using the sister chromatid as a template, enabling an error-free mechanism of DNA repair. *In vitro* and *in vivo* homologous mutants for *Brca1* and *Brca2* show a reduction in HR mediated DNA repair and the human pancreatic adenocarcinomas cell line CAPAN-1, which contains a heterozygous mutation for *BRCA2*, shows a dramatic reduction in HR (Goggins *et al.* 1996); demonstrating that the BRCA proteins are required for efficient HR repair. BRCA1 has two major roles within the HR pathway; (1) it forms part of a multi-protein complex, named the BRCA1-associated genome surveillance complex, which surveys the genome for DNA damage and is involved in the signalling of downstream proteins for repair; (2) it is recruited to sites of DSBs, where its phosphorylation by ataxia telangiectasia mutated protein (ATM) causes the formation of a multi-protein complex including BARD1 and BRCA2, resulting in

the recruitment of BRCA2 to the site of the DNA damage. BRCA2 binds to the DNA recombinase RAD51 via its BRC repeats and functions to recruit and facilitate its loading onto DNA, which is required for the strand invasion step of HR (Yuan *et al.* 1999).

The *BRCA1* and *BRCA2* genes are multifunctional proteins. As well as their roles in HR BRCA1 has been shown to have additional roles in ubiquination, apoptosis, chromatin remodelling and cell cycle checkpoint regulation, whereas BRCA2 has been shown to have roles in cytokinesis and centrosome location (reviewed in (Powell and Kachnic 2003))

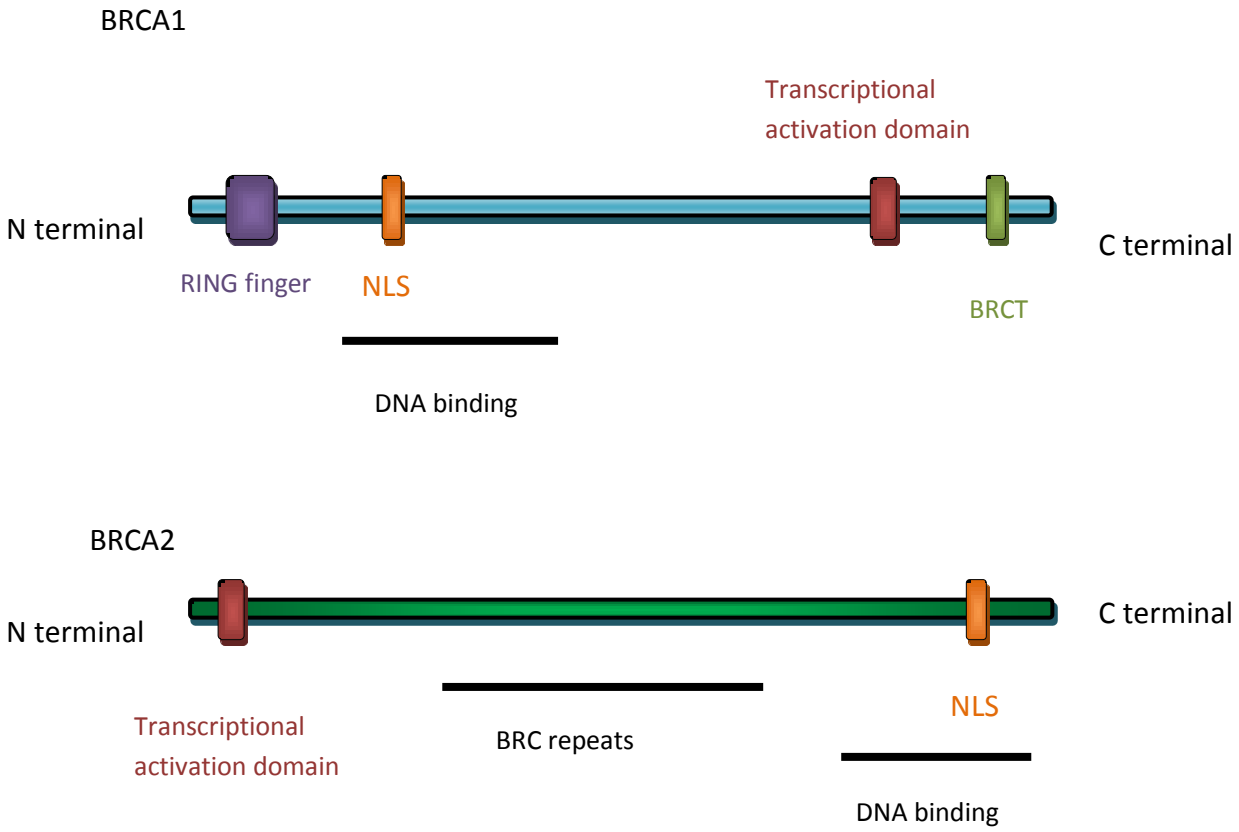

Figure 1.8 Protein structures of BRCA1 and BRCA2*. Both proteins contain a transcriptional activation domain, a nuclear localisation signal (NLS) and a DNA binding domain. BRCA1 contains a RING finger domain at its N terminus and a BRCT domain at the C terminus. BRCA2 contains BRC repeats in the middle of the protein which are essential for its function in the HR pathway. Figure adapted from Powell and Kachnic 2003.*

1.3.3 The Homologous Recombination pathway of DNA repair

DSBs can be caused by reactive oxygen species (ROS) created by cellular metabolism, exogenous components such as ultraviolet light, and unrepaired single stranded breaks (SSBs) in DNA. The HR pathway occurs during the S and G2 phases of the cell cycle and ensures error-free repair of DBSs in DNA by using the sister chromatid as a template (Figure 1.9). The pathway begins with 5'-3' resection of the DNA sequence surrounding the break site by the mitotic recombination 11 (MRE11)-RAD50-Nijmegan breakage syndrome 1(NBS1) (MRN) complex, creating single stranded overhangs. In this process NBS recognises the DSB, and the complex recruits phosphorylated CtBP-interacting protein (CtIP) which activates the exonuclease activity of MRE11. MRE11 then resects the DNA.

BRCA2 is recruited to the site of DNA damage by the multiprotein complex generated by the phosphorylation of BRCA1. Partner and localiser of BRCA2 (PALB2) then stabilises and anchors the protein to the DNA, allowing BRCA2 to facilitate the loading of RAD51 onto the single stranded DNA, by displacing Replication protein A (RPA), a protein that binds to single stranded DNA, thereby preventing RAD51 binding. RAD51 exists as a hexomeric protein ring and polymerises on the single stranded DNA to form a right-handed helical polymer filament, known as a presynaptic filament (Yu *et al.* 2001). This filament holds the DNA in an extended conformation.

Accessory factors such as the SWI/SNF proteins RAD54 and RAD54b aid the invasion of the coated single stranded DNA into the sister chromatid, creating a D-loop structure. Homology in the sister chromatid is searched for by random collisions. Once homology is found the DNA is extended by DNA polymerases. From this point of the HR pathway there are two different models: the double-strand break repair (DSBR) model and the synthesis-dependent strand annealing (SDSA) model. In SDSA the new strand is released from the sister chromatid and anneals to the 3'-end of the DSB. This enables the other strand of DNA to use the new strand as a template for DNA synthesis and complete the DSB repair. In DSBR both DNA strands use the sister chromatid as a template for DNA synthesis. This results in a duplex structure containing two Holliday junctions. These Holliday junctions are then resolved by BLM helicase and topoisomerase IIIα to give either non-crossover or crossover products (Figure 1.9).

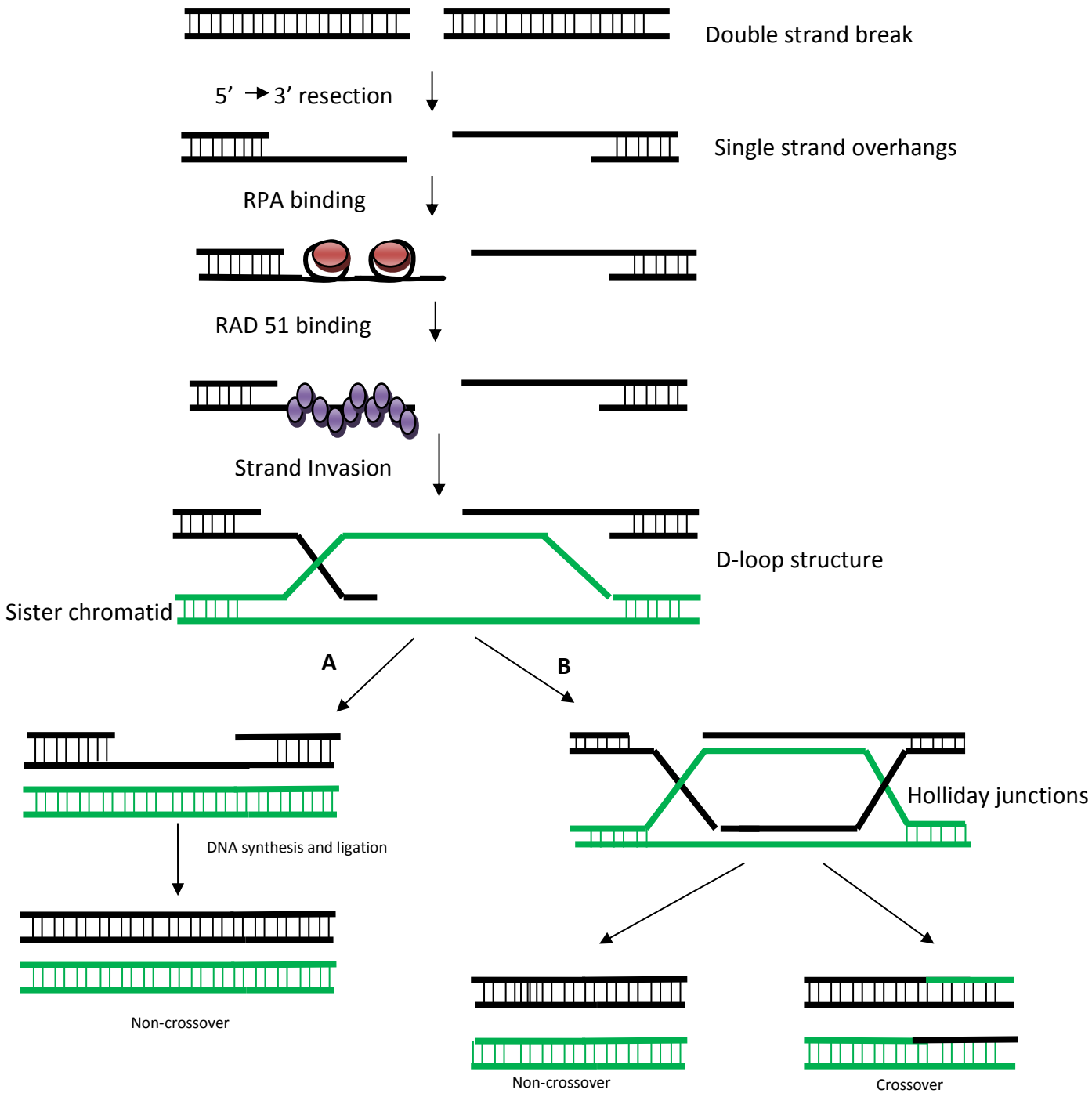

Figure 1.9 The HR pathway. *The pathway begins with 5'-3' resection of the DNA strands to create single strand overhangs. RPA binds to the single stranded DNA and is removed by BRCA2 so that RAD51 can bind to the single strand overhangs and polymerises to form a right-handed helical polymer filament. This filament aids strand invasion into the sister chromatid to form a D-loop structure. DNA extension then begins, using the sister chromatid as a template. From this point the pathway can either use the SDSA model (**A**) or the DSBR*

*model (**B**). The SDSA model only results in non-crossover products whereas the DSBR model produces either non-crossover or crossover products. Figure adapted from (Sung and Klein 2006).*

1.3.4 *BRCA* genes and breast cancer

BRCA mutated breast cancers account for around 25% of inherited breast cancer cases (http://www.cancerresearchuk.org). Mutations in *BRCA1* and *BRCA2* genes results in up to 85% chance of developing breast cancer and also increases the risk of ovarian, prostate and pancreatic cancer. In patients who have inherited mutations in their *BRCA1* or *BRCA2* genes, loss of heterozygosity at the second allele results in a deficiency in the HR pathway, resulting in the cell becoming reliant on error-prone pathways of DNA repair, such as the non-homologous end joining pathway (NHEJ). The NHEJ pathway occurs throughout the cell cycle and ligates the DNA strand together at the site of the break, thereby occasionally causing deletions or mutations. With a deficient HR pathway cells can accumulate further mutations that contribute to the cancer phenotype, eventually causing the cells to become tumourigenic. Patients with *BRCA* mutated breast cancer often also contain mutations in genes that encode proteins involved in cell cycle arrest, for example around 90% of patients have inactivating mutations in *TP53* (p53) (Crook *et al.* 1997; Crook *et al.* 1998). The loss of the cell cycle arrest allows proliferation with the presence of DNA damage, allowing tumour cells to evade cell death.

The majority of *BRCA1* mutated tumours are classified as triple negative basal tumours whereas the majority of *BRCA2* mutated tumours are similar to sporadic ER+ luminal tumours (Laakso *et al.* 2005). Currently all patients with BRCA mutated breast cancer are given the same treatments as patients with sporadic breast cancer.

1.4 Poly(ADP-ribose) polymerase (PARP)

1.4.1 PARP-1

The *Poly (ADP-ribose) polymerase 1 (PARP-1)* gene is located at locus 1q41. PARP-1 is an 113kDa protein which has a nuclear localisation and is expressed in all nucleated cells except neutrophils. PARP-1 consists of three domains; an N-terminal DNA binding domain, a central auto-modification domain and a C-terminal catalytic domain (Figure 1.10). These 3 domains can be further divided into six modules, A-F (Demurcia and Demurcia 1994). Module A is located at the N-terminus of the protein and contains two Cys-Cys-His-Cys zinc fingers. These are the binding sites of DNA and the second has been shown to be important for SSB recognition. Domain B contains a nuclear localisation signal and a caspase 3-cleavage site, which is utilised during apoptosis to prevent the depletion of NAD^+ and ATP^+. Domain C contains a third zinc finger which has a role in enzyme activation. Domain D contains specific glutamate and lysine residues that are the sites of ADP-ribose addition, and a BRCT domain, which is hypothesised to be involved in protein-protein interactions. Domain E contains a WGR domain, which function is currently unknown, and domain F contains the PARP catalytic motif: histidine and tyrosine residues which are important for NAD^+ binding and a glutamate which is needed for enzymatic activity. *PARP-1* knockout mice are viable and show mild phenotypes but have been shown to be sensitive to chemically-induced genomic stress, are susceptible to diet-induced obesity and are resistant to diabetes and inflammation (deMurcia *et al.* 1997; Masutani *et al.* 1999; Shall and de Murcia 2000; Devalaraja-Narashimha and Padanilam 2010).

PARP-1 functions in the base excision repair (BER) pathway, which repairs SSBs in DNA. This pathway uses the complementary strand of DNA as a template and PARP-1 is thought to act as a DNA damage sensor, recruiting proteins involved in the process to the site of the SSB, such as XRCC1 (El-Khamisy *et al.* 2003). The exact role of PARP-1 in this pathway remains controversial. Probably the most widely excepted concept is that the protein functions at the first stages of the pathway, binding to DNA at the site of the SSB, where the enzyme becomes activated and catalyses the addition of poly (ADP-ribose) (PAR) to itself, utilising NAD^+ as a substrate. Studies on whether PARP-1 binds to DNA as a monomer or a dimer are

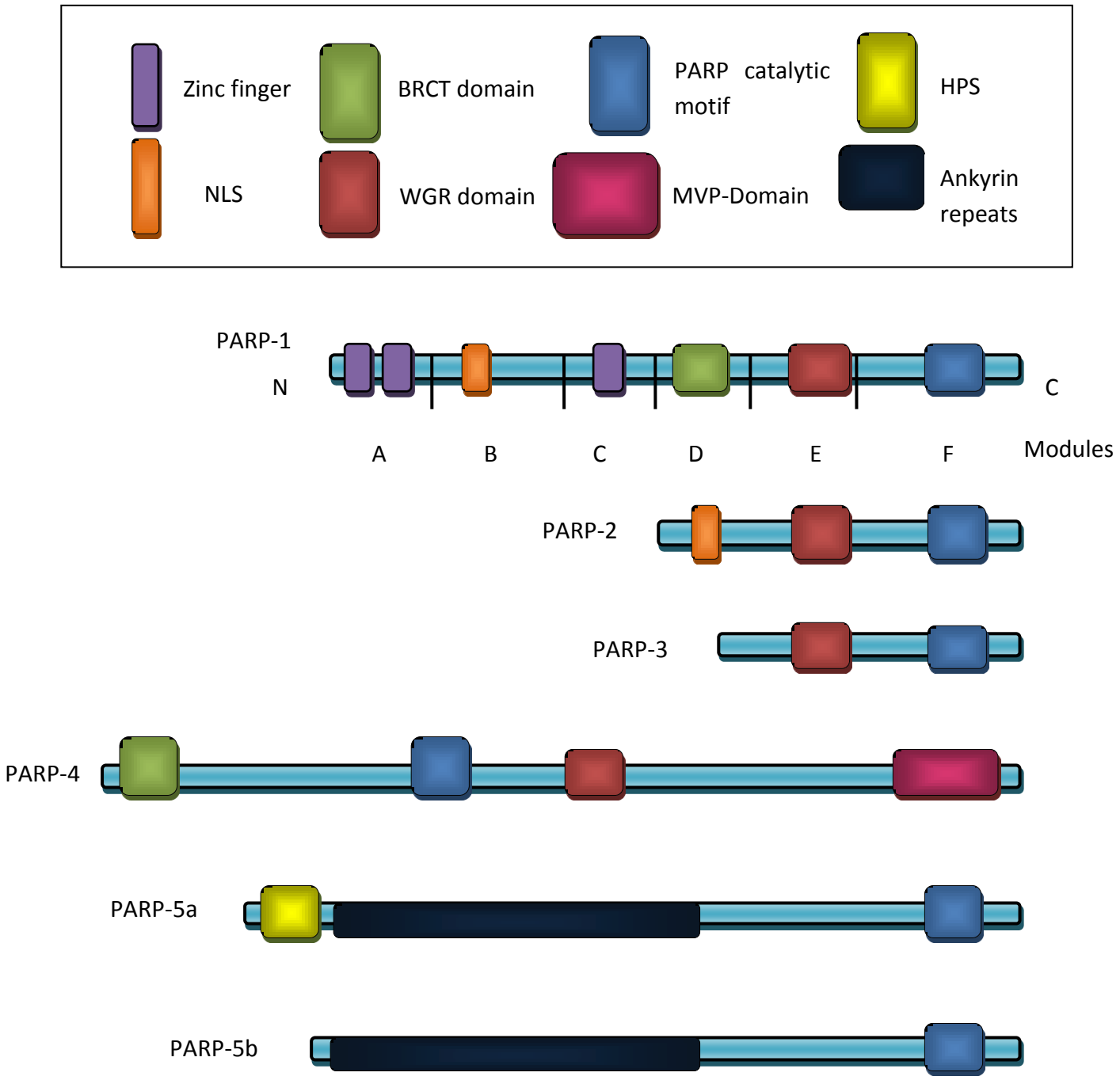

***Figure 1.10 PARP protein structure**. PARP-1 is split into six modules, A-F. PARP-2 and PARP-3 are the smallest of the group and have a similar structure. PARP-4 is the largest of the group and contains an MVP-binding domain which is required for the protein to interact with other VAULT proteins. PARP-5a and PARP-5b have a similar protein structure, both containing ankyrin repeats and the PARP catalytic motif. PARP-5a also contains a His-Pro-Ser rich domain (HPS) at the N terminus. Figure adapted from (Burkle 2005) and (Giansanti et al. 2010).*

conflicting (Eustermann *et al.* 2011; Loeffler *et al.* 2011; Ali *et al.* 2012; Langelier and Pascal 2013). The resulting negative charge created by PAR results in the recruitment of proteins involved in the subsequent steps of the BER pathway, such as XRCC1 and DNA polymerase β. Further addition of PAR to PARP-1 creates a high negative charge, resulting in the protein being repulsed by the DNA. This causes PARP-1 to be released from the SSB site, which then allows recruited DNA repair proteins to access the site. Once PARP-1 has left the SSB, the ADP-ribose polymer chain is rapidly degraded by poly (ADP-ribose) glycohydrolase (PARG). In addition to this role, PARP-1 also causes changes in chromatin structure so that the site of the SSB is exposed for repair by catalysing the addition of ADP-ribose polymers to H1 and H2B histones. Other proposed roles of PARP-1 in BER include producing a source of ATP for the final steps of the pathway (Oei and Ziegler 2000) and the recognition and processing of stalled intermediates (Prasad *et al.* 2001).

As well as its role in SSB repair PARP-1 is also hypothesised to be involved in other DNA processes such as transcription, methylation and DSB repair. Its role in DNA transcription comes from studies showing that PARP-1 can effect chromatin structure, interact with transcription factors such as COX-2 and OCT1, and the presence of PARP-1 at the majority of promoters of actively transcribing genes in MCF-7 cells (Nie *et al.* 1998; Krishnakumar *et al.* 2008; Lin *et al.* 2011). PARP-1 has also been shown to regulate the DNA (cytosine-5)-methyltransferase 1 protein (Dnmt1), by protecting its promoter against epigenetic silencing (Caiafa *et al.* 2009), suggesting a role in DNA methylation. It has also been proposed that PARP-1 may have roles in both the NHEJ and the HR pathways of DSB repair as studies have shown that PARP-1 competitively inhibits NHEJ and promotes the activation of MRE11 and NBS, both of which are involved in the DNA resection step of the HR pathway (Haince *et al.* 2008; Bryant *et al.* 2009). These roles in HR mediated DSB repair however, are not thought to be essential, as PARP null cells *in vitro* do not have drastic defects in the HR pathway (Schultz *et al.* 2003). PARP-1 is also hypothesised to have roles in DNA-independent processes such as inflammation, which is thought to be linked to its coactivator activity for NFκB (Hassa and Hottiger 2002; Hassa *et al.* 2003).

Excessive DNA damage leads to PARP-1 over-activation, resulting in cell death through either NAD^+ depletion or the caspase-independent mechanism of parthanatos. The

parthanatos pathway involves PAR polymers, generated by the over activation of PARP-1, migrating to the cytosol and causing the release of apoptosis-inducing factor (AIF) from mitochondria (Yu *et al.* 2002). AIF then translocates to the nucleus and causes chromatin condensation and large scale DNA fragmentation, resulting in cell death.

PARP-1 has been found to be overexpressed in a number of cancers, for example malignant lymphoma, hepatocellular carcinoma, cervical cancer and colorectal cancer (Fukushima *et al.* 1981; Hirai *et al.* 1983; Tomoda *et al.* 1991; Shiobara *et al.* 2001). In breast cancer, PARP-1 overexpression is more common in high grade basal and triple negative tumours (Goncalves *et al.* 2011; Rojo *et al.* 2012).

1.4.2 BER pathway

The BER pathway occurs in the G1 phase of the cell cycle, and causes removal and replacement of damaged bases within DNA (Figure 1.11). BER is thought to function as a series of independent steps, with a damaged base first recognised from the DNA backbone by DNA glycosylase, due to cleavage of the N-glycosidic bond. The resulting base-less site is termed an abasic or AP site. APE1 endonuclease then cleaves the phosphodiester bond 5' to the AP site, creating a single stranded break. PARP-1 is thought to recognise this single stranded break and recruit the repair proteins XRCC1, DNA polymerase β and DNA ligase III by poly-ribosylating itself. At this point BER may take one of two routes depending on whether DNA polymerase β can remove the 5' sugar phosphate (Figure 1.11). Short patch BER occurs when DNA polymerase β is successful and subsequently adds a new nucleotide, corresponding with the template strand of DNA. The new nucleotide is then sealed into position by DNA ligase III, with XRCC1 acting as a scaffold for these reactions. Long patch BER occurs when DNA polymerase β is unable to remove the 5' sugar phosphate; instead, DNA polymerase δ/ε removes the group and adds a number of nucleotides into the gap, creating a flap. This flap is removed by 5'-flap endonuclease 1 (FEN-1) and DNA ligase I seals the resulting gap in the DNA. If the BER pathway is unsuccessful the SSB will still be present in the S phase of the cell cycle, resulting in the formation of DSBs due to replication fork collapse.

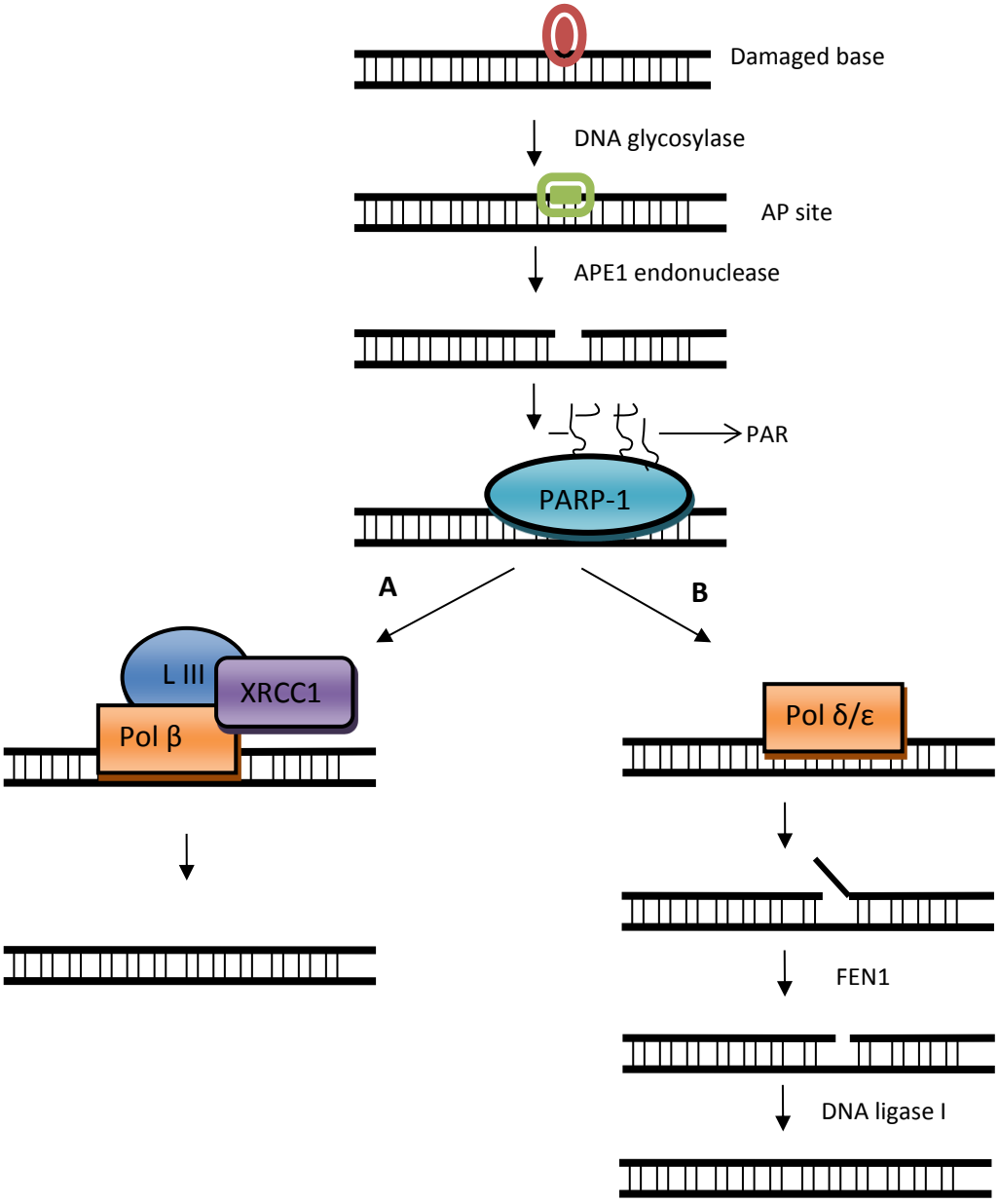

Figure 1.11 The BER pathway. *When a damaged base is identified, DNA glycosylase removes it from the nucleotide to produce an abasic site (AP site). APE1 creates a single stranded break in the DNA by cleaving the phosphosugar backbone. PARP-1 recognises and binds to the single stranded break. PARP-1 adds polymer chains of ADP-ribose to itself which results in the recruitment of XRCC1, DNA polymerase β (pol β) and DNA ligase III (L III). The DNA is either repaired by these proteins (**A**) or by DNA polymerase δ/ε (Pol δ/ε), FEN1 and DNA ligase I (**B**). Figure adapted from (Dianov 2011)*

1.4.3 PARP family

After the discovery of PARP-1 the sequence of its catalytic domain was utilised to search for related proteins; 16 were found, although not all have been shown to have the ability to create PAR, with some members only able to perform mono (ADP-ribose) transfer (Kleine *et al.* 2008). Due to the differences in catalytic function between members of the family, a new nomenclature has been suggested, which would re-name the proteins ADP-ribosyl transferases (Hottiger *et al.* 2010).

PARP-2 is the only other member of the family to share PARP-1's ability to detect SSBs and recruit repair proteins to the sites of damage (Ame *et al.* 1999; Schreiber *et al.* 2002). Its role in SSB repair was discovered due to residual PARP activity in *PARP-1* deficient mice (Ame *et al*. 1999). Whereas *PARP-1* knockout mice show only mild phenotypes *PARP-1*/*PARP-2* double knockout mice are embryonically lethal (de Murcia *et al.* 2003). It is thought that PARP-1 performs around 90% of poly (ADP)-ribosylating activity for DNA repair, with PARP-2 accounting for the remaining 10% (Schreiber *et al*. 2002). *PARP-2* is located at 14q11.2 and alternative splicing results in two isoforms of the protein. The PARP-1 and PARP-2 proteins have 69% similarity in their C terminal catalytic domains; however the DNA binding domain of PARP-2 does not contain any zinc fingers (Figure 1.10) and does not bind as efficiently to single stranded breaks in DNA when compared to PARP-1 (Ame *et al*. 1999; Berghammer *et al.* 1999).

PARP-3 is thought only to perform mono(ADP-ribose) transfer (Loseva *et al.* 2010). Unlike PARP-1 and PARP-2, PARP-3 is not ubiquitously expressed, but limited to certain tissues, e.g. the brain, spinal cord and epithelial cells lining the ducts of the prostate, liver and pancreas. It has a similar protein structure to PARP-2 (Figure 1.10), but has not been shown to be involved in the BER pathway. Its exact roles are unknown but it has been shown to localise to the centrosome and associates with polycomb proteins (Augustin *et al.* 2003; Rouleau *et al.* 2007). PARP-3 has also been implicated in DSB repair, where it is hypothesised to cooperate with PARP-1; however, deletion of PARP-3 does not compromise survival after DNA damage (Boehler *et al.* 2011), suggesting that, like PARP-1, PARP-3's role in DSB repair is not essential.

PARP-4 is the largest member of the family and is a component of the cytoplasmic VAULT complexes, along with major vault protein, telomerase protein component 1 and untranslated RNAs. These large complexes are thought to function in cellular transport (van Zon *et al.* 2003). Due to its inclusion in the VAULT complex, PARP-4 is also termed vPARP. It contains a BRCT domain at the N-terminus, the PARP catalytic motif near the centre of the protein and motifs that allow the formation of multiprotein complexes, such as the major vault protein-binding domain (Figure 1.10).

PARP-5a and PARP-5b are also termed Tankyrase 1 and Tankyrase 2. These proteins are thought to be involved in regulation of telomeres and are components of the human telomeric complex. Tankyrase 1-mediated ADP-ribosylation of telomeric repeat-binding factor 1 (TRF1) has been shown to cause its release from telomeres, resulting in telomere elongation (Smith and de Lange 2000). Due to their similarities in structure (Figure 1.10) Tankyrase 2 is hypothesised that they perform a similar function. The remaining members of the PARP family have not been extensively studied and their functions are currently unknown.

1.4.4 PARP inhibitors

The first generation PARP inhibitors were created in the early 1990s and were based on the benzamide structure of NAD^+ due to its ability to inhibit PARP activity. The majority of PARP inhibitors are designed to competitively inhibit the catalytic domain of PARP-1, preventing the NAD^+ substrate from entering the catalytic site. Second and third generation PARP inhibitors were later designed to improve potency and were based on the structure of tricyclic benzimidaole carboxamides. PARP inhibitors were initially proposed as chemosensitisers, but in 2005 two preclinical papers showed that BRCA deficient cells were highly sensitive to PARP inhibition compared to wild type cells (Bryant *et al.* 2005; Farmer *et al.* 2005). PARP inhibitors selectively cause death in cells that are BRCA deficient through a process known as synthetic lethality; this means that deficiency in either BRCA1/2 or PARP-1 alone is not essential for cell survival, but deficiency in both is lethal (Figure 1.12). Although the exact mechanism is uncertain, the most common theory is following PARP-1 inhibition, unrepaired SSBs result in DSBs due to replication fork collapse, and in BRCA deficient cells these DSBs cannot be repaired efficiently and the accumulation of genomic damage reaches

above the threshold and results in cell death (Bryant *et al*. 2005). In BRCA proficient cells DSBs are repaired by the HR pathway resulting in cell viability. Due to the selectivity of PARP inhibitors for BRCA deficient cells they have the potential of being utilised as a selective, low toxicity, personalised treatment for patients with BRCA mutated cancers.

PARP inhibitors have also been proposed to be suitable for treatment of non-BRCA mutated breast cancers, such as tumours deficient in other components of the HR pathway (McCabe *et al.* 2006) and triple-negative breast cancer. Triple-negative breast cancer contains similar characteristics to BRCA1 mutated cancers, termed BRCAness. Mutations in the *BRCA1* gene are rare in sporadic breast cancers; however, its expression is reduced in around 15% of sporadic breast cancer by hypermethylation of the *BRCA1* promoter (Turner and Reis-Filho 2006), suggesting that the loss of BRCA1, and hence the HR pathway, has a role in cancer development in triple negative breast cancers. Interestingly there is a similar phenomenon with BRCA2 in which the *EMSY* gene, which encodes a suppressor of *BRCA2* expression, is amplified in 13% of sporadic breast cancers (Hughes-Davies *et al.* 2003) This hypothesis suggests that PARP inhibitors may be an effective treatment for triple-negative breast cancers, giving this intrinsic subgroup of breast cancer a selective treatment strategy, of which there are currently none. Indeed the PARP inhibitor iniparib showed promising phase II results when combined with the chemotherapeutic agents gemcitabine and carboplatin in patients with triple-negative breast cancer (O'Shaughnessy *et al.* 2011), but a phase III trial failed to show any difference in progression-free and overall patient survival (Guha 2011). Since then iniparib has been criticised as a PARP inhibitor due to its mechanism of inhibition, which differs from that of other PARP inhibitors, and its failure to inhibit poly(ADP-ribose) polymers *in vitro* (Patel *et al.* 2012). This suggests that there is still a possibility of other PARP inhibitors being utilised to treat patients with triple-negative breast cancer.

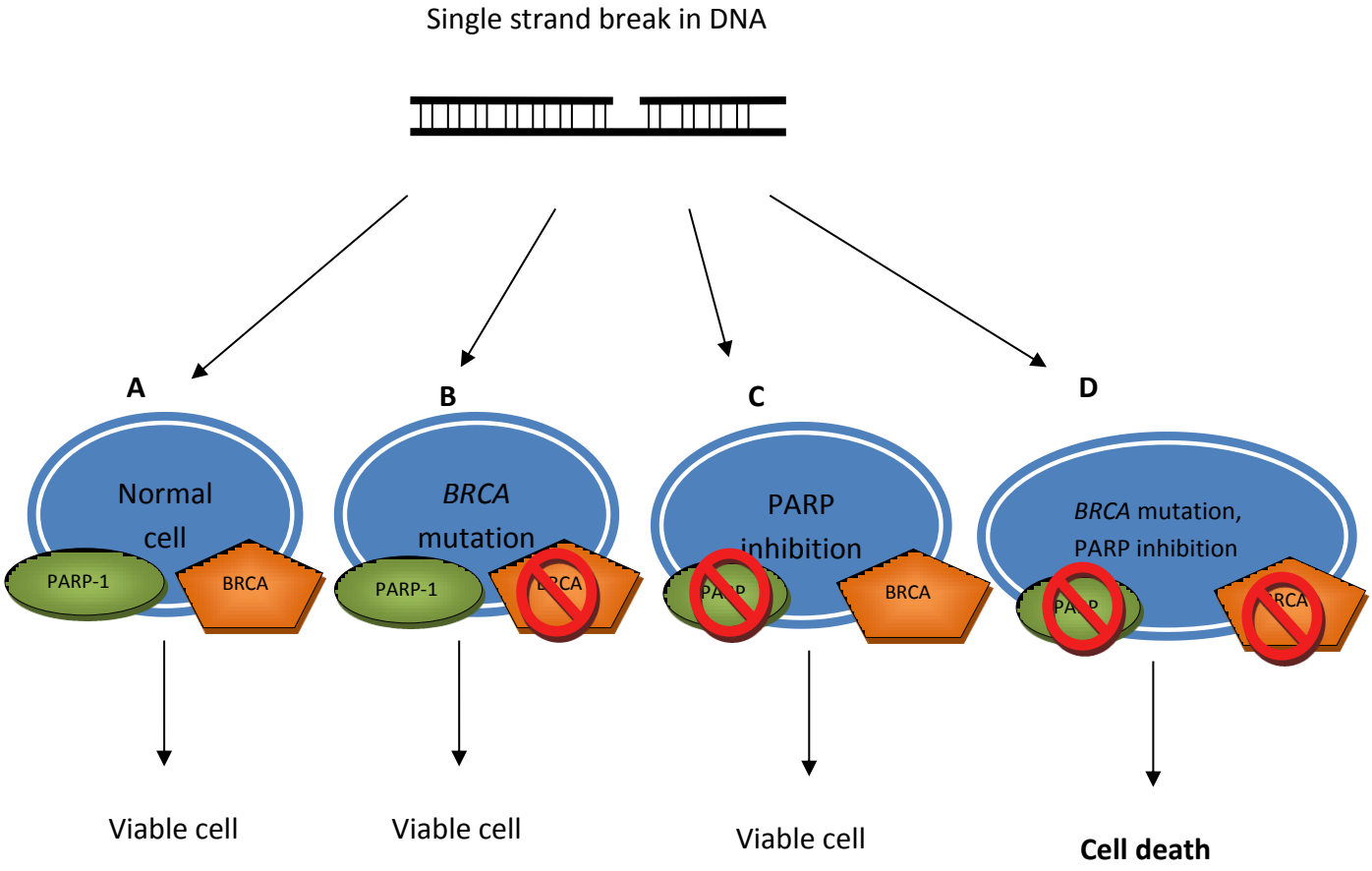

Figure 1.12 Synthetic lethality between BRCA1/2 and PARP-1. *(**A**) In a normal cell in which both PARP-1 and BRCA1/2 (BRCA) are functional, a SSB is repaired efficiently and the cell is viable. (**B**) In a BRCA mutated cell the HR pathway is dysfunctional, but the presence of an active PARP-1 protein keeps the cell viable due to repair via the BER pathway. (**C**) Normal cells that have been treated with PARP inhibitor will have a dysfunctional BER pathway but the HR pathway repairs the DSB so that the cell remains viable. (**D**) Cancer cells with BRCA mutations which have been treated with PARP inhibitors will have dysfunctional HR and BER pathways, meaning their DNA cannot be repaired efficiently, resulting in cell death. Adapted from (Guha 2011).*

PARP inhibitors have also been shown to induce cell death in tumour cells that have no defects in DNA repair, such as *PTEN* mutant cells and HER2+ breast cancer cells (Mendes-Pereira *et al.* 2009; Nowsheen *et al.* 2012), widening the therapeutic potential of these drugs. Currently there are numerous PARP inhibitors in clinical trials, either as a monotherapy or in combination with other chemotherapeutics (Table 1.1).

1.4.4.1 Olaparib

Olaparib (4-(3-4-fluorophenyl) methyl-1(2H)-one) is an oral PARP inhibitor initially developed by KuDOS Pharmaceuticals but since 2006 has been the property of AstraZeneca. It is a competitive inhibitor and has been shown to inhibit PARP-1, -2 and -3 (Menear *et al.* 2008), Oplustilova *et al*, unpublished). Olaparib entered clinical trials in 2005 for breast cancer, and a phase III trial is currently being planned. A phase I trial in which patients were given doses of olaparib ranging from 10mg once daily for two weeks to 600mg twice daily for three weeks showed a 47% response rate in patients with *BRCA*-mutated tumours and no response in patients that did not contain *BRCA* mutations (Fong *et al.* 2009). From the phase I trials the maximum tolerated dose of olaparib was set to 400mg twice daily. A phase II trial of olaparib-monotherapy showed a 41% response rate in patients with *BRCA* mutations that were given 400mg twice daily and 22% with 100mg twice daily (Tutt *et al.* 2010). Toxicity has been mild throughout the trials and reduced in comparison to chemotherapeutics. The most frequent side effect are grade 1 and 2 nausea and fatigue but grade 3 mood alteration, fatigue and somnolence and grade 4 thrombocytopenia have also been reported (grades from the Common Terminology Criteria for Adverse effects). All toxicities resolved after drug discontinuation.

Olaparib is also in clinical trials for ovarian cancer. Phase II clinical trials have shown response rates of 33% in patients with *BRCA* mutated ovarian cancer treated with a PARP inhibitor (Audeh *et al.* 2010) but also 24% in patients without *BRCA* mutations (Gelmon *et al.* 2011). This suggests that olaparib could be used to treat sporadic ovarian cancers. To support this a phase II clinical study in high-grade sporadic serous ovarian cancer showed a 41% response rate in patients who received 400mg olaparib twice daily (Gelmon et al. 2011), suggesting that in ovarian cancer olaparib may be successful in treating both *BRCA*-mutated and non-*BRCA*-mutated tumours.

Table 1.1 Examples of PARP inhibitors currently in clinical trials. Adapted from (Yap *et al.* 2011)

Agent	Company	Route of Administration	Tumour type	Combination studies	Clinical status
AZD2281/ Olaparib	AstraZeneca	Oral	*BRCA* associated breast tumours	-	Phase II-III
				Cisplatin and gemcitabine	Phase II
			BRCA associated ovarian tumours	-	Phase II
				Paclitaxel and Carboplatin	Phase II
ABT888/ Veliparib	Abbott	Oral	Metastatic melanoma	Temozolmide	Phase I
			Leukaemia, pancreatic	-	Phase I
			Glioblastoma	Temozolmide	Phase II-III
			Leukaemia, lymphoma	Cyclophosphamide	Phase I
			BRCA associated breast tumours	Temozolmide	Phase II
BSI-201/ Iniparib	BiPar/Sanofi	Intravenous	Glioblastoma	Temozolmide	Phase I-II
			Breast tumours	Gemcitabine and carboplatin	Phase II
			Lung tumours	Gemcitabine and cisplatin	Phase II
			BRCA associated ovarian tumours	Gemcitabine and carboplatin	Phase III
AG014699	Pfizer	Intravenous	Advanced solid tumours	Temozolmide	Phase I
			BRCA associated breast and ovarian tumours	-	Phase II
MK-4827	Merck	Oral	Ovarian, prostate tumours	-	Phase I
			BRCA associated tumours	-	Phase I
CEP-9722	Cephalon	Oral	Solid tumours	-	Phase I-II
				Temozolmide	Phase I

1.4.4.1.1 Olaparib Resistance

Pre-clinical studies in *Brca1* and *Brca2* conditional knockout mice have shown mammary tumour regression with olaparib treatment; however continual daily treatment resulted in tumour relapse (Rottenberg *et al.* 2008; Hay *et al.* 2009). Clinical resistance has now also been reported (Barber *et al.* 2013). Tumour resistance is highly detrimental in the clinic so it is important to find the mechanism(s) of resistance.

Preclinical studies investigating olaparib resistance have highlighted three possible mechanisms of resistance to olaparib: 1. up-regulation of the drug efflux pumps P-glycoproteins (P-gps), shown in a subset olaparib-resistant tumours from *Brca1* and *Brca2* conditional knockout mice (Rottenberg et al. 2008; Hay et al. 2009); 2. loss of p53-binding protein 1 (53BP1), resulting in reactivation of the HR pathway, shown in a subset of olaparib resistant tumours from *Brca1* conditional knockout mice show (Jaspers *et al.* 2013); and 3. Reactivation of the HR pathway by secondary, activating mutations in the *BRCA*2 gene, shown in BRCA deficient cell lines and in two patients (Edwards *et al.* 2008; Barber et al. 2013).

1.5 Mouse models of Breast Cancer

Mouse models are valuable *in vivo* tools which have greatly enhanced our understanding of breast cancer development and treatment. Mouse models are also critical in drug development and testing, producing analyses of drug efficacy and toxicity. The techniques developed by Capecchi, Evans and Smithies generated mice with targeted disruptions in a gene of interest, resulting in the targeted allele being permanently deleted or disrupted in every cell of the mice (Evans and Kaufman 1981; Doetschman *et al.* 1987; Thomas and Capecchi 1987). These models are termed constitutive knockout models and results in gene inactivation in every tissue and at every stage of development. Some genes involved in carcinogenesis are also required for development, meaning that constitutive knockout can result in embryonic or perinatal lethality. Analysing gene loss in a specific tissue may also be difficult in these mouse models as tumours can arise in other tissues.

To circumvent the drawbacks of constitutive knockout models, conditional knockout systems have also been developed, enabling spatial and temporal control over expression of the gene of interest. The Cre-loxP system enables spatial control by the use of tissue specific

promoters (Figure 1.13). Where expressed, the Cre recombinase causes deletion of DNA sequences between specific recognition sites, termed 'locus of crossover of bacteriophage P1' (loxP) sites. These sites are not found endogenously in the mouse genome, and can therefore be utilised to specifically mutate genes of interest by flanking specific DNA sequences. Using embryonic stem cells two transgenic mice are created: one where the Cre transgene has been inserted into the mouse genome under the control of a tissue specific promoter, and another where the gene(s) of interest are flanked by loxP site. These mice are then used to perform a series of breedings to create mice that contain both the Cre transgene and the flanked gene(s) of interest.

Mouse models of breast cancer utilise mammary-specific promoters, such as the mouse mammary tumour virus-long terminal repeat (MMTV-LTR), whey acidic protein (WAP), Cytokeratin 14 (K14) and β-lactoglobulin (BLG) promoters. These promoters vary in the location and specificity of expression: the WAP promoter is expressed in the alveolar cells of the mammary gland and in other tissues such as the brain, the K14 promoter is expressed in basal mammary cells but also in the skin, whereas the BLG promoter is specifically expressed in the ER- luminal mammary cells (reviewed in (Shen and Brown 2005)). The MMTV, WAP and BLG promoters are hormone-regulated, meaning that their expression increases during pregnancy and lactation. Inducible systems, such as the tetracycline-controlled system, can be utilised to create temporal control; thereby removing the possibility of unwanted effects sometimes seen by constitutively active promoters.

An alternative to genetically modified mice is transplantation of mouse or human cancer cell lines (xenograft). Like genetically modified mouse models, xenografts can be utilised to analyse breast cancer initiation, progression and response to therapy; however, as these mice are immune-compromised, the interaction of the immune system with cancer progression is absent. Due to the absence of one mouse model that completely encapsulates human breast cancer; the type of mouse model chosen for a particular study requires careful consideration.

1.5.1 *Brca2/p53* Conditional knockout mouse model

The *Brca2/p53* conditional knockout mouse models human inherited breast cancer, utilising the CreLoxP system under the control of the BLG promoter, to conditionally knockout *Brca2* and *p53* in the mammary gland. The BLG promoter encodes the whey milk protein β-lactoglobulin, which is expressed preferentially in ER- luminal cells (Molyneux *et al.* 2010) of the mammary gland, thereby ensuring that Cre recombinase activity is specific to these cells (Watson *et al.* 1991). Expression from the BLG promoter is increased by the presence of pregnancy hormones but has also been shown to be active in virgin mice, with *Brca2*$^{fl/f}$, *p53*$^{fl/fl}$ virgin mice developing tumours from six months of age (Hay *et al*. 2009). LoxP sites flank exons 9 and 10 of the *Brca2* gene, truncating the protein before the critical BRC repeats in exon 11, and exons 2-10 of the *p53* gene. These mice develop mammary tumours from 6-15 months of age, with the mean latency of 9 months (Hay *et al*. 2009).

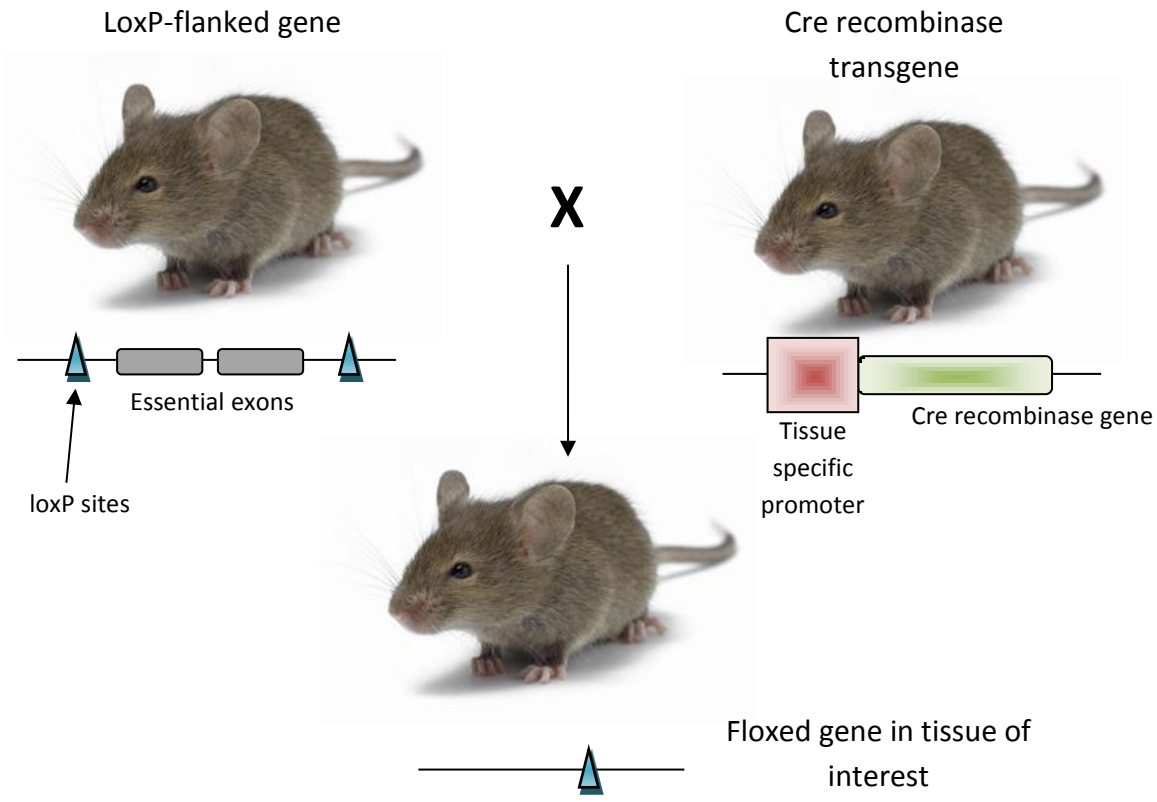

Figure 1.13 Conditional knockout using the Cre loxP system. *A mouse containing loxP sites flanking essential exons of the gene of interest is bred with a mouse that contains the Cre*

recombinase gene under the control of a tissue-specific promoter. In the offspring the Cre recombinase results in the deletion of the DNA sequence flanked by the loxP sites. As the Cre recombinase is placed under a tissue-specific promoter this technology allows spatial control.

1.6 Aims

The two primary objectives of this thesis were to investigate whether different histological mammary tumour types, from a *Brca2/p53* conditional knockout mouse model (section 1.5.1), correlated with different responses to daily olaparib therapy, and to investigate the mechanism(s) of resistance to olaparib in this model.

To address the first objective, untreated tumours from the mouse model were characterised by histopathology to analyse which tumour types were found in this model. Tumours displaying different initial responses to daily olaparib treatment were then classified by histopathology to investigate if tumour type is associated with response. This follows on from a study by Hay *et al* which showed that mammary tumours from *Brca2/p53* conditional knockout mice showed varied initial responses to daily olaparib treatment (Hay et al. 2009).

The rationale behind the second objective also arises from the study by Hay *et al* which showed that Brca2/p53 deficient mouse mammary tumours initially responded well to daily olaparib therapy but relapsed after long term treatment, possibly associated with up-regulation of drug efflux pumps (P-gps) in a proportion of resistant tumours (Hay et al. 2009). The second aim was therefore to use the same mouse model to address this hypothesis by inhibiting the P-gps in resistant tumours. Finally, as the up-regulation of P-gps was only shown in a subset of resistant tumours this suggests that other mechanisms of resistance exist in this mouse model, so other possible mechanisms of resistance were analysed using expression analysis to drive a non-directed approach.

Following on from results obtained from the second objective, which suggested that EMT is involved in olaparib resistance, an additional aim was to analyse the effect of E-cadherin loss on histological tumour type and olaparib therapy. This was achieved by treating a *Brca2/p53/Cdh1* conditional knockout mouse model with daily olaparib therapy, and

comparing the histopathology of untreated and olaparib-resistant tumours to those from the *Brca2/p53* conditional knockout mouse model.

2. Materials and Methods

2.1 Experimental animals

The house mouse (*mus musculus*) was used as an experimental model in this work. All mice used were of outbred background.

2.1.1 Genetic Mouse models

Two different experimental mouse models were used. They were already established in the laboratory, and use Cre loxP technology to conditionally delete genes of interest in the mammary epithelium, using the BLG promoter to drive Cre expression, causing mammary tumour development without the need for induction by pregnancy.

2.1.1.1 *Brca2/p53* conditional knockout mice

In *BlgCre-Brca2*$^{f/f}$*/p53*$^{f/f}$ mice, exons 9-11 of the *Brca2* gene and exons 2-10 of the *p53* gene were flanked by loxP sites (Jonkers *et al.* 2001; Cheung *et al.* 2002).

2.1.1.2 *Brca2/p53/Cdh1* conditional knockout mice

The Brca2/p53/E-cadherin conditional knockout mouse model (*BlgCre-Brca2*$^{f/f}$*/p53*$^{f/f}$*/Cdh1*$^{f/f}$), was created in our laboratory for a currently unpublished study, by crossing *BlgCre-Brca2*$^{f/f}$*/p53*$^{f/f}$ mice with those carrying a *Cdh1* allele, with exons 4-15 flanked by loxP sites, (Derksen *et al.* 2006).

2.1.2 Animal Husbandry

All animals were housed according to UK Home Office Regulations. The mice were fed by Harlan standard diet and water was provided *ab libitum*. All experimental procedures were conducted in accordance with the UK Animals Act 1986 and current UK Home Office regulations.

2.1.3 Experimental cohorts

Mice were monitored weekly for palpable mammary tumours. Once detected, they were allowed to reach a size which would allow measurable growth or regression (around 6mmx6mm), at which point olaparib treatment was initiated. The experimental tumour burden endpoints were if the tumour was close to causing blistering of the skin or starting to impair the animal's movement, or if they became symptomatic of other disease.

2.1.3.1 Mammary tumour measurement

Tumour measurement was initiated on the first day of treatment and was performed twice a week using manual spring-loaded callipers. Tumour volumes were calculated using the following equation: volume = length X (square of width)/2. Relative tumour volumes on each day were calculated by dividing the current tumour volume by the initial volume at the start of treatment.

2.1.3.2 Experimental procedures

All procedures on animals were conducted according to UK Home Office Regulations.

Olaparib was administrated once daily at 100mg/kg by interperitoneal (IP) injection. Tariquidar was administrated IP once daily at 2mg/kg by, five times a week, 30 minutes before olaparib.

2.2 Tissue preparation

2.2.1 Tissue Dissection

Mice were culled via cervical dislocation, according to UK Home Office Regulations. Upon dissection, mice were sprayed with 70% ethanol and mammary tumours were removed from under the skin. The majority of the tumour was used for fixation (section 2.4.2), with a small piece being snap frozen for RNA analysis (section 2.4.3). After the mammary tumours were removed, other organs were also removed from the mouse (liver, kidney, spleen, pancreas and lung) for fixation.

2.2.2 Tissue Fixation

Tissues were immediately placed into cold 10% neutral buffered formalin (Sigma). After 24 hours the tissues were transferred to 70% ethanol at 4°C until paraffin embedding.

2.2.3 Paraffin Embedding and Sectioning

After fixation the tissues were removed from the 70% ethanol and placed in cassette (fisher) and processed using the automatic processor (Leica TP1050). In short, the tissues were dehydrated by incubation in increasing concentrations of ethanol (70% for 1 hour, 95% for 1 hour, 2x 100% for 1 hour 30 minutes, followed by 100% for 2 hours), followed by 2x xylene for 2 hours. They were then placed in liquid paraffin for 1 hour, twice for 2 hours, removed from the cassettes and embedded in paraffin by hand, and left to solidify.

In preparation for histological analysis (section 2.5), sections of embedded tissue were fixed onto slides, by cutting to 5µm using a microtome (Leica RM2135), placing on Poly-L-Lysine coated slides (PLLs) and baking at 58°C for 24 hours.

The paraffin embedding and sectioning was performed by Derek Scarborough and Mark Isaac.

2.2.4 Snap Frozen Tissue

Small pieces of mammary tumour were placed into lockable microtubes, placed in liquid nitrogen until frozen and stored at -80°C until required.

2.3 Histological analysis

2.3.1 Immunohistochemistry

2.3.1.1 Generic Protocol

The generic protocol for immunohistochemistry is described below. For specific conditions for some parts of each immunohistochemistry, please refer to table 2.

2.3.1.1.1 Dewaxing and rehydration of slides.

Paraffin embedded tissue sections on PLL coated slides were dewaxed in xylene (2x 5 min, Fisher Scientific) and rehydrated by washing in decreasing concentrations of ethanol (Fishers Scientific): 2x 3 min in 100% ethanol, 1x 3 min 95% ethanol and 1x 3 min 75% ethanol.

2.3.1.1.2 Antigen retrieval.

Antigen retrieval was carried out to unmask the antigens. Slides were incubated in preheated citrate buffer (99.9°C, pH6 Thermo) in a water bath or pressure cooker for 20 minutes. Slides were then left to cool for 30 min at room temperature.

2.3.1.1.3 Prevention of endogenous staining.

To prevent endogenous background staining, slides were incubated with a peroxidase blocking solution (Table 2.1), which inactivates the endogenous peroxidases, for 15 minutes at room temperature, followed by three 5 minute washes in washing buffer (Table 2.1).

2.3.1.1.4 Serum block.

The slides were blocked with serum diluted in wash buffer (Table 2.1), to block non-specific binding of antibodies, for 45 minutes at room temperature. The serum block was removed

and slides were incubated immediately with the primary antibody in serum/wash buffer. In the case of the 3 antibodies (CK18, CK14 and ERα) that used the mouse-on-mouse kit (MOM kit, Vector labs), the serum block was provided in the kit, and a subsequent blocking step was performed for 30 minutes with Dako protein block (Dako #x0909), before primary antibody incubation.

2.3.1.1.5 Primary antibody.

The slides were incubated overnight at 4°C with the primary antibody at an optimised concentration (Table 2.1). Antibodies were diluted in the same serum solution used in section 2.3.1.1.4. Unbound primary antibody was removed by three 5 minute washes in wash buffer.

2.3.1.1.6 Secondary antibody.

The slides were then incubated for 1 hour at room temperature with the secondary antibody (Table 2.1), followed by three 5 minute washes in wash buffer. Some secondary antibodies were pre-diluted antibodies conjugated to Horse Radish Peroxidase (HRP) (Envision plus kit, DAKO), which catalyses the reaction for signal visualisation, so a signal amplification step was not needed; however, most of the secondary antibodies were biotinylated, so a signal amplification step was required for visualisation (section 2.3.1.1.7). In such cases, the secondary antibody was diluted in the serum solution used in section 2.3.1.1.4.

2.3.1.1.7 Signal amplification.

For protocols that used biotinylated secondary antibodies, the positive signal was amplified by incubating the slides for 30 minutes at room temperature with the Avidin-Biotin Complex (ABC) kit (Vector labs), made up 30 minutes before it was applied. This results in the HRP enzyme being bound to the secondary antibody. The reagent was then removed by 3 x 5 minute washes in wash buffer.

2.3.1.1.8 Visualisation of positivity.

The substrate 3,3'-diaminobenzidine (DAB) was used to visualise the positive signal, due to its HRP-catalysed conversion to a brown colour. This was achieved using the DAB+ Chromogen reagent supplied in the EnVisionTM kit. The reagent was applied to the slides for 10 minutes, and then removed by three 5 minute washes with wash buffer. The slides

were counterstained in haematoxylin for 60 seconds, followed by a wash in running water for 5 minutes. The slides were dehydrated by washing in increasing concentrations of alcohol. Before the slides were mounted they were placed in xylene for 2x 5 minutes.

2.3.1.2 Specific Conditions

Specific conditions for each individual immunohistochemistry are shown in Table 2.1

2.3.2 Analysis of immunohistochemistries

All immunohistochemical stains, apart from Ki67, were scored as described in (Molyneux *et al*. 2010; Melchor *et al*. 2014)

2.3.2.1 Ki67 scoring

Ki67 levels were analysed by counting the number of positive cells per field, using 20X magnification, and finding the percentage from the total number of cells. 3 fields per tumour were counted and an average was calculated for each sample.

2.3.3 Haematoxylin and Eosin staining

To visualise mammary tumours for histopathology sections, nuclei were marked by haematoxylin and cytoplasm by eosin as follows: sections were dewaxed and rehydrated as described in 2.3.1.1.1. before submersion in Haemalum solution (R.A.Lamb) for 45 seconds, followed by a 5 minute wash in running tap water. The sections were placed in 1% Eosin solution (R.A.Lamb) for 5 minutes before two rounds of 15 second washes were performed. Slides were dehydrated and mounted as described in 2.3.1.1.8.

The H&E staining was performed by Derek Scarborough and Mark Isaac.

Table 2.1 Optimised conditions for specific antibodies

Target	P63	Cytokeratin 18	Vimentin	Cytokeratin 14	Oestrogen Receptor α	SMA
Commercial source of primary Ab	Abcam #ab735	Progen #65028	Santa Cruz #SC-7557	Abcam #ab7800	Vector Labs #VP-E613	Abcam #ab5694
Primary Ab raised in	Mouse (mAb)	Mouse (mAb)	Goat (pAb)	Mouse (mAb)	Mouse(mAb)	Rabbit (pAb)
Antigen retrieval	Boiling Citrate buffer, 20 mins	Boiling Citrate buffer, 20 minutes	Boiling citrate buffer, 20 mins	Boiling citrate buffer, 20 mins	Boiling citrate buffer, PC, 20 mins	Boiling citrate buffer, 20 minutes
Peroxidase Block	3% H_2O_2, 15 minutes	1/60 H_2O_2 in methanol, 10 minutes	3% H_2O_2, 15 mins	1/60 H_2O_2 in methanol, 10 minutes	1/60 H_2O_2 in methanol, 10 minutes	3% H_2O_2, 15 minutes
Serum block	10% goat serum, 45 minutes	MOM blocking reagent, 1 hour	10% rabbit serum, 45 mins	MOM blocking reagent, 1 hour	MOM blocking reagent, 1 hour	10% goat serum, 45 mins
Wash buffer	0.1% TBS/Tween	0.1% TBS/Tween	0.1% TBS/Tween	0.1% TBS/Tween	0.1% TBS/Tween	1xPBS
Conditions of primary Ab	1/100, 4°C overnight	1:5, diluted in MOM diluent, 4°C overnight	1/300, 4°C overnight	1/500, diluted in MOM diluent, 4°C overnight	1/500 diluted in MOM diluent, 4°C overnight	1/200, 4°C overnight
Secondary Ab	Anti-mouse labelled polymer-HRP-conjugated (EnVision™ kit)	Anti-mouse (MOM kit)	Anti-goat biotinylated (Dako)	Anti-mouse (MOM kit)	Anti-mouse (MOM kit)	Anti-rabbit biotinylated (Dako)
Conditions of secondary Ab	1 hr, room temp	10 mins, room temp	1/100, 30 mins room temp	10 mins, room temp	10 mins, room temp	1/500, 30 mins room temp
Signal amplification	N/A	ABC kit (Vector labs)	ABC kit (Vector Labs)	ABC kit (Vector labs)	ABC kit (Vector Labs)	N/A

Target	E-cadherin	Twist	Slug	Ki67
Commercial source of primary Ab	BD Transduction #610182	Abcam #ab50887	Cell Signaling #C19G7	Vector Labs
Primary Ab raised in	Mouse	Mouse (mAb)	Rabbit (mAb)	Mouse (mAb)
Antigen retrieval	Boiling Citrate buffer, 20 mins	Boiling Citrate buffer, 20 minutes	Boiling citrate buffer, 20 mins	Boiling citrate buffer, 30 mins
Peroxidase Block	3% H_2O_2, 10 minutes	3% H_2O_2, 10 minutes	3% H_2O_2, 10 minutes	3% H_2O_2, 20 minutes
Serum block	5% goat serum, 30 minutes	5% rabbit serum, 30 minutes	5% goat serum, 30 minutes	20% rabbit serum, 20 minutes
Wash buffer	0.1% TBS/Tween	0.1% TBS/Tween	0.1% TBS/Tween	0.1% TBS/Tween
Conditions of primary Ab	1/300, 4°C overnight	1/500, 4°C overnight	1/100, 4°C overnight	1/20, 4°C overnight
Secondary Ab	Anti-rabbit biotinylated (Dako)	Anti-mouse biotinylated (Dako)	Anti-rabbit biotinylated (Dako)	Anti-mouse biotinylated (Dako)
Conditions of secondary Ab	30 mins room temp	30 mins room temp	30 mins room temp	30 mins room temp
Signal amplification	ABC kit (Vector labs)	ABC kit (Vector labs)	ABC kit (Vector Labs)	ABC kit (Vector labs)

2.4 RNA analysis

Quantitative reverse transcription polymerase chain reaction (qRT-PCR) was used to quantify expression levels of genes in mammary tumours. RNA was extracted from stored frozen tissue, then used as a template to produce cDNA, which was then used to compare expression levels between cohorts (n=4 per cohort).

2.4.1 RNA extraction

Mammary tumour samples were defrosted and placed into homogenising lysing matrix D tubes (MP Biomedicals). 1ml of Trizol (Invitrogen) was added, and the samples were homogenised using a Precellys 24 Homogeniser (Bertin Technologies) at 7000 x g for 2 cycles of 25 seconds. After homogenisation, 200µl of chloroform was added to each sample and they were incubated on ice for 10 minutes, before centrifugation at 9500 x g for 15 minutes at 4°C. The clear supernatant was transferred to a 1.5ml microfuge tube and 600µl of isopropanol (Fisher) was added,mixed well and left on ice for 1 hour to precipitate nucleic acids. Samples were centrifuged at 9500 x g for 15 minutes at 4°C and the supernatants carefully discarded. The remaining pellets were washed with 500µl cold 75% ethanol, before re-centrifugation at 9500 x g for 5 minutes at 4°C. Supernatants were again discarded and the pellets left to air-dry at room temperature for 10 minutes before resuspension in 100µl of diethylprocarbonate (DEPC)-treated water at 65°C for 10 minutes. The samples were then DNase treated (section 2.4.2).

2.4.2 DNase treatment

DNase treatment was performed using the Turbo DNA-free kit (Life technologies). $^{1}/_{10}$ dilution of the buffer and DNase was added to the RNA and incubated at 37°C for 1 hour, before addition of an inactivating agent and further incubation for 10 minutes.

2.4.3 RNA quantification

RNA concentrations were determined by nanodrop analysis using an ND-1000 spectrometer (Labtech, UK).

2.4.4 cDNA synthesis

cDNA was made using superscript III reverse transcriptase (Invitrogen). A master mix was composed so that each sample contained 1µl Random primers (Invitrogen), 2µl 10mM dNTP mix, and 1µg RNA in RNase-free water. The mixtures were placed in nuclease-free

microcentrifuge tubes and incubated at 65°C for 5 minutes followed by 1 minute on ice. Another master mix was composed so that 8µl 5x first-strand buffer, 2µl 0.1M DTT, 2µl RNase-freewater and 1µl superscript III reverse transcriptase was added to each sample and incubated for 5 minutes at room temperature. The samples were then incubated at 50°C for 60 minutes, before inactivation by incubation at 70°C for 15 minutes.

2.4.5 qRT-PCR

2.4.5.1 Taq-Man

The expression of the majority of genes of interest was quantified using TaqMan assays (Applied Biosystems). These use predesigned probes, each containing one forward and one reverse primer for the gene of interest, with a fluorescent molecule and a quencher attached to the 5' end. During thermo-cycling, Taq polymerase cleaves the fluorescent molecule, releasing it from the quencher and enabling fluorescent detection.

Each sample for the qRT-PCR reactions were performed in duplicate, including no cDNA controls, in MicroAmp 96-well PCR plates with 0.1ml wells (Applied Biosystems). Each reaction contained 10ng cDNA, 10µl Taqman universal PCR mastermix (Applied Biosystems), 1µl gene specific assay (Applied Biosystems; Table 2.2) and was made up to 20µl with DEPC-treated water. β-actin was used as an internal control and the reactions carried out using the StepOne Plus Real-Time PCR System (Applied Biosystems), using the following cycling conditions: 50°C for 2 minutes, 95°C for 10 minutes, then 40 cycles of 95°C for 15 seconds (denaturation) and 60°C for 1 minute (annealing/elongation). The data was collected automatically using StepOne software (Applied Biosystems).

2.4.5.2 Syber Green

Quantitation of gene expression of *Grem1* was carried out using Syber Green assays. Using a MicroAmp 96-well PCR plate (Applied Biosystems) each reaction contained 10ng cDNA, 10µl SYBR green fast mix (Invitrogen), 1µl gene specific primers (Table 2.2) and was made up to 20µl with DEPC-treated water. Each sample was performed in duplicate, including no cDNA controls, and β-*actin* was used as an internal control. The reactions were carried out using the StepOne Plus Real-Time PCR System (Applied Biosystems), using the following cycling conditions: 95°C for 20 seconds, then 40 cycles of 95°C for 3 seconds (denaturation) and 60°C for 30 seconds. As with the TaqMan assays, data was collected automatically.

Table 2.2 Primer details for qRT-PCR analysis

SYBER Green	**Forward Primer sequence (5'-3')**	**Reverse primer sequence (5'-3')**
Grem1	GACAAGGCTCAGCACAATGA	ACTCAAGCACCTCCTCTCCA
Taq Man	**Supplier**	
Snail	Applied Biosystems	
Sema3b	Applied Biosystems	
Foxa3	Applied Biosystems	
Sox8	Applied Biosystems	
Pcolce2	Applied Biosystems	
Hmga2	Applied Biosystems	

2.4.5.3 Analysis of data

The data was examined prior to analysis to ensure there was no product in the 'no cDNA' controls, and that the replicates were comparable. Cycle time (C_T) was automatically calculated by the software, and an average of the replicates from each sample was calculated manually. The difference in cycle time (ΔC_T) were calculated manually for each sample, normalising the reaction using the β-*actin* controls, then an average ΔC_T was found for each cohort. The average ΔC_T were then used to calculate the fold change of each gene (fold change = $2^{\Delta\Delta C_T}$) between the different cohorts. The average ΔC_T values were compared statistically to test for significant differences between the cohorts, using the Mann-Whitney U test.

2.5 Pharmacokinetic and Pharmacodynamic analysis

Tumours were removed from mice that were treated with either a single dose of 100mg/kg olaparib or vehicle, and taken 1 and 24 hours later, and from mice that were treated with daily 100mg/kg olaparib until the tumours became resistant. Pieces of mammary tumour were snap frozen (section 2.2.4) then stored at -80°C. The frozen tissue was sent to AstraZeneca, where they analysed the concentrations of olaparib in the samples by mass spectroscopy, as described in Hay *et al*. 2009. To analyse PARP-1 activity, PAR levels were analysed in the same samples by electrochemiluminecense, as described in Hay *et al*. 2009.

2.6 RNA sequencing

Tumours that were either resistant to or responding to daily 100mg/kg olaparib therapy, were removed from mice, snap frozen (section 2.2.4) and sent to AstraZeneca. At AstraZeneca they extracted the RNA from the samples and performed mRNA sequencing (100bp paired-end sequencing) on the Illumina Hi-Seq platform, at 150-fold coverage. The reads were mapped onto the mouse genome using the software Tophat, and counts from the mapped reads were generated using software HTSeq (Anders *et al.* 2014). The differentially-expressed genes were identified using the DESeq R package (http://genomebiology.com/2010/11/10/R106). The output was reads per kilobase of transcript per million mapped reads (R.P.K.M), in which ranges of values correspond with level of expression (0-0.5 represents very low expression, 0.5-8 represents low expression, 8-16 medium expression, 16-128 high expression, and above 128 very high expression).

The genetic profiles of the samples were also compared to an EMT-signature, generated in-house at AstraZeneca, which was composed by comparing cell lines exhibiting epithelial-like expression (e.g. high expression of *CDH1* and low expression of *VIM*) with cell lines exhibiting mesenchymal-like expression (e.g. low *CDH1* expression and high *VIM* expression).

2.7 Mammosphere Assay

The composition of the media used in this assay are shown in Table 2.3.

2.7.1 Digestion and plating of single cells

Following dissection, mammary tumour samples were placed in 15ml digestion media and finely minced in a tissue culture hood using a scalpel and forceps. The minced tumour was then transferred to 9ml heated (37°C) digestion media, mixed with 1ml collagenase solution and incubated at 37°C, with rigorous shaking, for 3 hours. The resulting clumps of cells were broken down to single cells by passing the solution through a 21G needle a number of times, followed by a 25G needle, and finally through 70µm and 40µm cell strainers. The solution was then centrifuged at 10,000 x g for 5 minutes, the supernatant discarded and the pellet resuspended in 5ml of red blood cell lysis buffer (Sigma) and left to incubate at room temperature for 5 minutes. This was followed by a further centrifugation at 10,000 x g for 5 minutes, and once more the supernatant was discarded. The pellet was resuspended in 5ml

digestion media and centrifuged again at 10,000 x g for 5 minutes. Once the supernatant has been discarded, the pellet was resuspended in 5ml digestion media, and the number of cells per ml calculated using Trypan blue stain (Invitrogen) and a haemocytometer.

The cells were seeded to a density of 10,000 cells per well, in sterile 6 well cell culture plates (Cellstar) coated in polyHEMA, with 4ml of heated (37°C) mammosphere growth media in each well. The plates were incubated at 37°C for 7 days, at which point mammospheres larger than 50µm in diameter were counted manually.

2.7.2 Fixation of mammospheres

All tips were rinsed in 0.3% BSA/PBS to prevent mammospheres sticking to them. Medium from the 6 well plates was collected into 50ml unskirted falcon tubes and centrifuged at 7000RPM for 3 minutes. The supernatant were discarded and pellets resuspended in 1ml formalin. The samples were then incubated on ice for 30 minutes followed by a further centrifugation at 7000 x g for 3 minutes and subsequent resuspension of the pellets in 1ml 70% ethanol. After incubation on ice for 30 minutes, the samples were centrifuged at 7000 x g for 3 minutes and the pellest resuspended in 90µl of heated (70°C) Histogel (ThermoScientific). The gel solution was pipetted into a specifically made mould, which was manufactured in the lab, and placed on top of parafilm to enable the gel to set in a 3D sphere. Once set, the sphere was removed from the mould and placed into 70% ethanol prior to paraffin embedding and sectioning (section 2.2.3)

Table 2.3 Details for making the solutions used in the mammosphere assay

Digestion media	**Supplier**
450ml DMEM	Life Technologies
50ml Fetal Bovine Serum	Life Technologies
5ml L-glutamine	Life Technologies
5ml Penecillin Steptomycin	Life Technologies
Mammosphere growth media	
500ml Mammary Epithelial cell growth media	Lonza
2ml of Human Recombinant EGF (100µg/ml)	Sigma
200µl of Gentamycin (50mg/kg)	Sigma
100µl of Hydrocortisone (5mg/ml)	Sigma
500µl of Insulin (5mg/ml)	Sigma
Collagenase solution	
Dissolve collagenase (Sigma) in DMEM media (Life Technologies) to a concentration of 10mg/ml)	
PolyHEMA	
12g polyHEMA (Sigma) dissolved in 1L 95% ethanol. Place 1ml of solution into each well of plate and incubate the plate at 37°C for 48 hours	

2.8 Data analysis

2.8.1 Graphical representation of data

The raw data obtained from scoring, histopathology and qRT-PCR were inputted into Excel spreadsheets (Microsoft). All means, standard deviations and sums were calculated using the calculator functions and the graphical representation of data was produced in Excel.

2.8.2 Comparison of means

Statistical tests were carried out using the Minitab 17 statistical package (Minitab Inc.). To test for normal distribution, the Andersson-Darling normality test was used. As all the data collected was not normally distributed, the comparison of means was tested using the Mann-Whitney U test. Statistical significance was indicated if $p \leq 0.05$.

2.8.3 Survival analysis

Survival data was also analysed using the Minitab 17 statistical package, with Kaplan-Meier plots used to present the data and significance analysed using the Wilcoxon test. Statistical significance was indicated if $p \leq 0.05$.

3. Characterisation of *Brca2/p53*-deficient murine mammary tumours and analysis of initial response to olaparib therapy

3.1 Introduction

Breast cancer is a disease composed of different histological and molecular subtypes, each having distinct clinical behaviours (Perou *et al.* 2000a; Sorlie *et al.* 2003; Reis-Filho and Pusztai 2011). Although human *BRCA2*-mutated mammary tumours display a variety of histological types, the majority are IDC-NSTs that are ER+ and have a luminal gene expression profile (Laakso *et al*. 2005; Larsen *et al.* 2013). The heterogeneity of breast tumours emphasises the need for targeted treatments, such as tamoxifen and herceptin. PARP inhibitors, such as olaparib, show selective toxicity to BRCA-deficient cells (Bryant *et al.* 2005; Farmer *et al*. 2005) and clinical trials have shown that around 40% of patients with *BRCA* mutations respond to daily olaparib treatment (Fong *et al*. 2009; Tutt *et al*. 2010). In accordance with this, a previous study using *BlgCre-Brca2*$^{f/f}$*/p53*$^{f/f}$ mouse model showed that although the vast majority of tumours responded to olaparib monotherapy, the responses were variable (Hay *et al*. 2009), suggesting that further stratification may be required to determine therapeutic relevance.

To investigate whether histological tumour type correlates with response to olaparib treatment, a detailed histopathological analysis of the tumours was performed using previously established criteria (Molyneux *et al*. 2010; Melchor *et al*. 2014) based on human breast tumour classification (Lakhani *et al*. 2012). Immunohistochemistry was used to analyse the luminal (CK18), and basal/myoepithelial (CK14, p63, SMA) cell populations. Vimentin staining was used as a marker of mesenchymal differentiation, its presence thereby indicating the potential occurrence of EMT.

3.2 Results

3.2.1 Presence of four histopathological tumour types in the *BlgCre-Brca2$^{f/f}$/p53$^{f/f}$* mouse model

Examination of a cohort of 20 tumours from untreated mice identified four histopathological tumour types, based on H&E appearance and immunohistochemical staining: IDC-NST, metaplastic spindle cell carcinoma (MSCC), malignant adenomyoepithelioma (AME) and metaplastic adenosquamous carcinoma (ASQC) (Figure 3.1 and Figure 3.2A-E). All IDC-NSTs showed high CK18 expression (60-85% positivity), and the majority showed <1% CK14 expression, with just two showing higher levels. Although the majority were negative for Vimentin, SMA and p63, there was occasional positivity but never more than 1%. AMEs showed high expression of p63 in comparison to IDC-NSTs and MSCCs (Mann-Whitney U test, $p<0.01$) with 20-60% of cells staining positive. They also showed 20-45% positivity for CK18, variable staining for CK14 (1-60%) and Vimentin (1-50%). AMEs showed significantly higher expression of SMA compared to IDC-NSTs (Mann-Whitney U test, $p=0.043$), although staining was variable between tumours (1-55% positivity). ASQCs showed high expression of p63 and CK14 (60-80% positivity), and low expression of CK18 (1-5% positivity), Vimentin (<1% positivity) and SMA (1% positivity). MSCCs showed significantly higher expression of Vimentin compared to IDC-NSTs and AMEs (Mann-Whitney U test, $p=0.011$ and $p<0.01$ respectively), with 70-80% of cells staining positive. Three MSCCs also showed very low levels of CK18 and CK14 expression (<1% of tumour cells) whilst one showed 40% positivity for CK18 and 15% positivity for CK14. All MSCCs had no detectable p63 staining. They also showed significantly higher expression of SMA compared to IDC-NSTs, with 15-45% of cells staining positive (Mann-Whitney U test, $p=0.011$).

All tumours were ERα negative, although ERα positive cells could be observed in normal mammary epithelial ducts around the tumours (Figure 3.1). IDC-NSTs and AMEs were the most prevalent tumour types in this cohort, making up 35% and 40% respectively. MSCCs and ASQCs were less common, making up 15% and 10% respectively (Figure 3.2F).

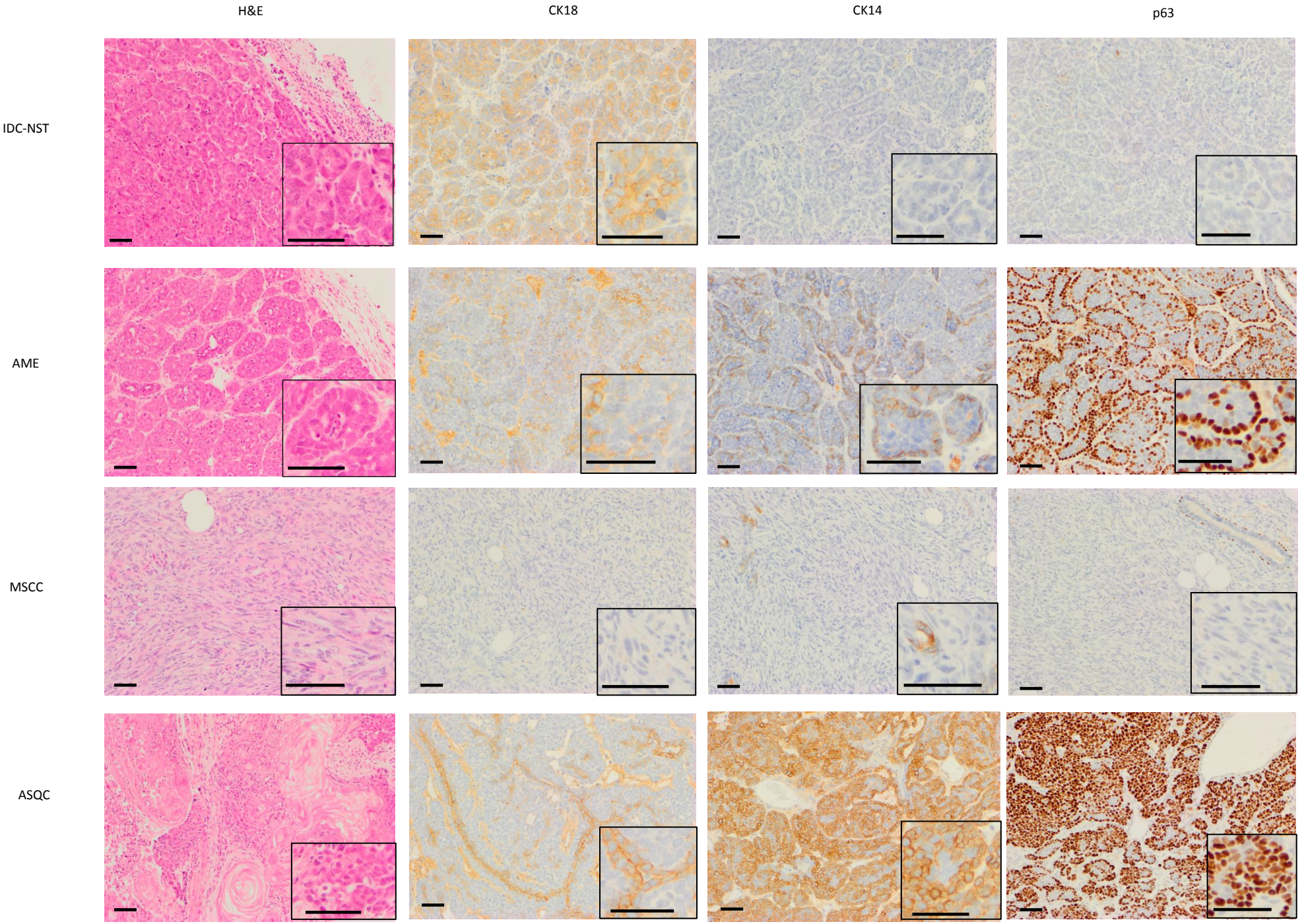
H&E
CK18
CK14
p63
IDC-NST
AME
MSCC
ASQC

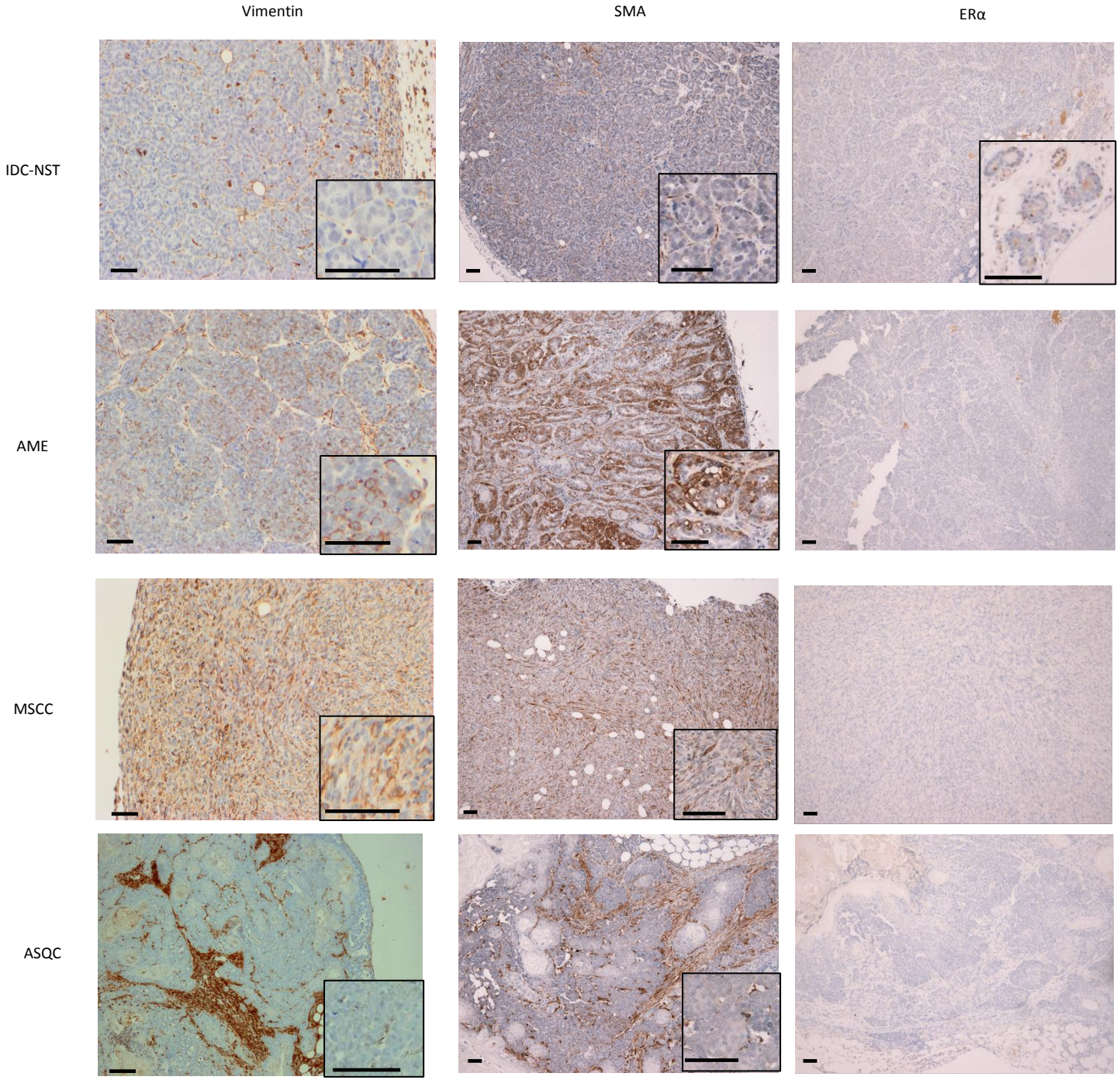

Figure 3.1 Representative pictures of immunohistochemical stains in untreated tumours. *Four different tumour types were identified. H&E staining was used to analyse cellular morphology, CK18 to identify luminal cells, CK14, p63 and SMA to identify basal/myoepithelial cells and Vimentin to identify cells undergoing EMT. All tumours were ER negative, but positive cells were found in the normal mammary tissue (insert). Scale bars represent 50µm.*

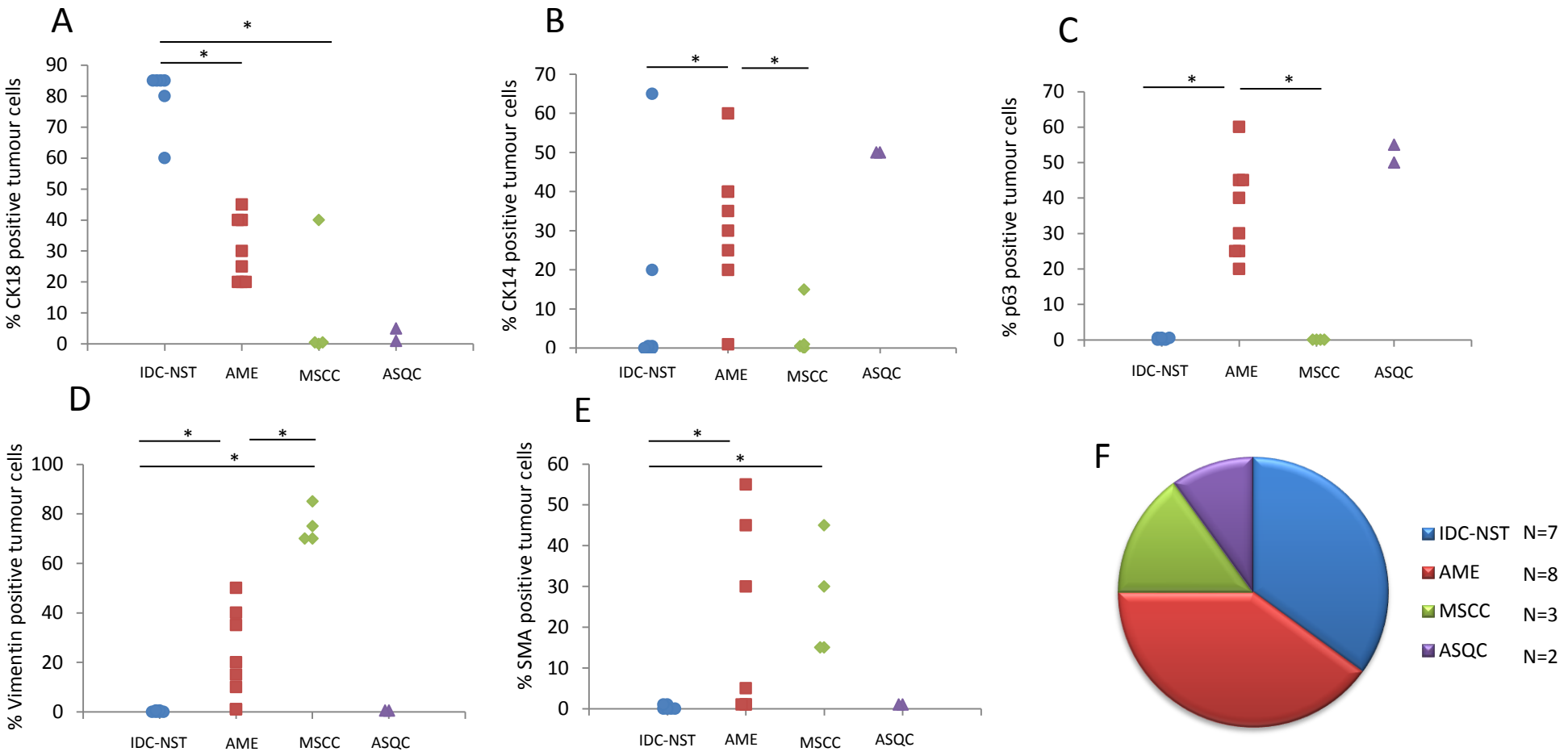

Figure 3.2 Immunohistochemical staining and histopathological tumour proportions of tumours from our BlgCre:Brca2$^{f/f}$/p53$^{f/f}$ mouse model. *Analysis of the percent of tumour cells stained for CK18* ***(A)****, CK14* ***(B)****, and p63* ***(C)****, Vimentin* ***(D)*** *and SMA* ***(E).*** ***(F)*** *Classification of tumours from this model revealed that the most common tumour types were IDC-NSTs and AMEs (n=20). * indicates p≤0.05*

3.2.2 Characterisation of different responses to olaparib treatment

Previous studies have shown that tumours arising in *BlgCre-Brca2$^{f/f}$/p53$^{f/f}$* mice show variable responses to olaparib therapy (Hay et al. 2009). Broadly, three types of responses were observed in these tumours: excellent responders, where the tumours showed a dramatic decrease in size within the first 30 days of treatment; moderate responders, where the tumours stopped growing within the first 30 days but did not decrease dramatically in size; and poor responders where the tumours continued to grow in size throughout treatment (Figure 3.3A). The majority of tumours from mice treated with daily 100mg/kg olaparib therapy show either a moderate (45%) or excellent (34%) response and poor responders are relatively rare (20%) (Figure 3.3B). To investigate whether this variability in response correlated to tumour type mice were treated with daily IP 100mg/kg olaparib and culled 30 days into treatment and tumours were classified by histopathology. Those with poorly-responding tumours were sometimes culled at an earlier time point due to the tumours reaching the designated experimental endpoint.

Analysis of the tumours classified as poor responders showed that they were exclusively MSCCs which were histologically identical to untreated MSCCs (Figure 3.3C and Figure 3.4). Analysis of the tumours classified as moderate responders showed that the majority were either IDC-NSTs or AMEs (both accounting for 38.5%), whilst MSCCs accounted for the remaining 23% (Figure 3.3D). Unlike in the untreated cohort, responding IDC-NSTs showed a significant increase in Vimentin staining, with 20-40% of epithelial cells staining positive (Figure 3.4, Mann-Whitney U test, $p<0.01$). The AMEs in this cohort showed similar p63, CK14 and Vimentin staining to untreated tumours; however, CK18 staining was reduced to less than 1% of the tumours cells. MSCCs from the moderate responder cohort were not composed exclusively of fusiform spindle cells: rather, each contained a small region of epitheloid morphology (Figure 3.4), with the epitheloid sections showing immunostaining patterns similar to those seen in untreated IDC-NSTs, and the spindle cell sections showing similar patterns to untreated MSCCs.

Analysis of the tumours classified as excellent responders showed that the majority were IDC-NSTs, with the remainder being ASQCs (Figure 3.3E). All tumours in this cohort displayed a high proportion of tumour-associated stroma compared to the untreated groups

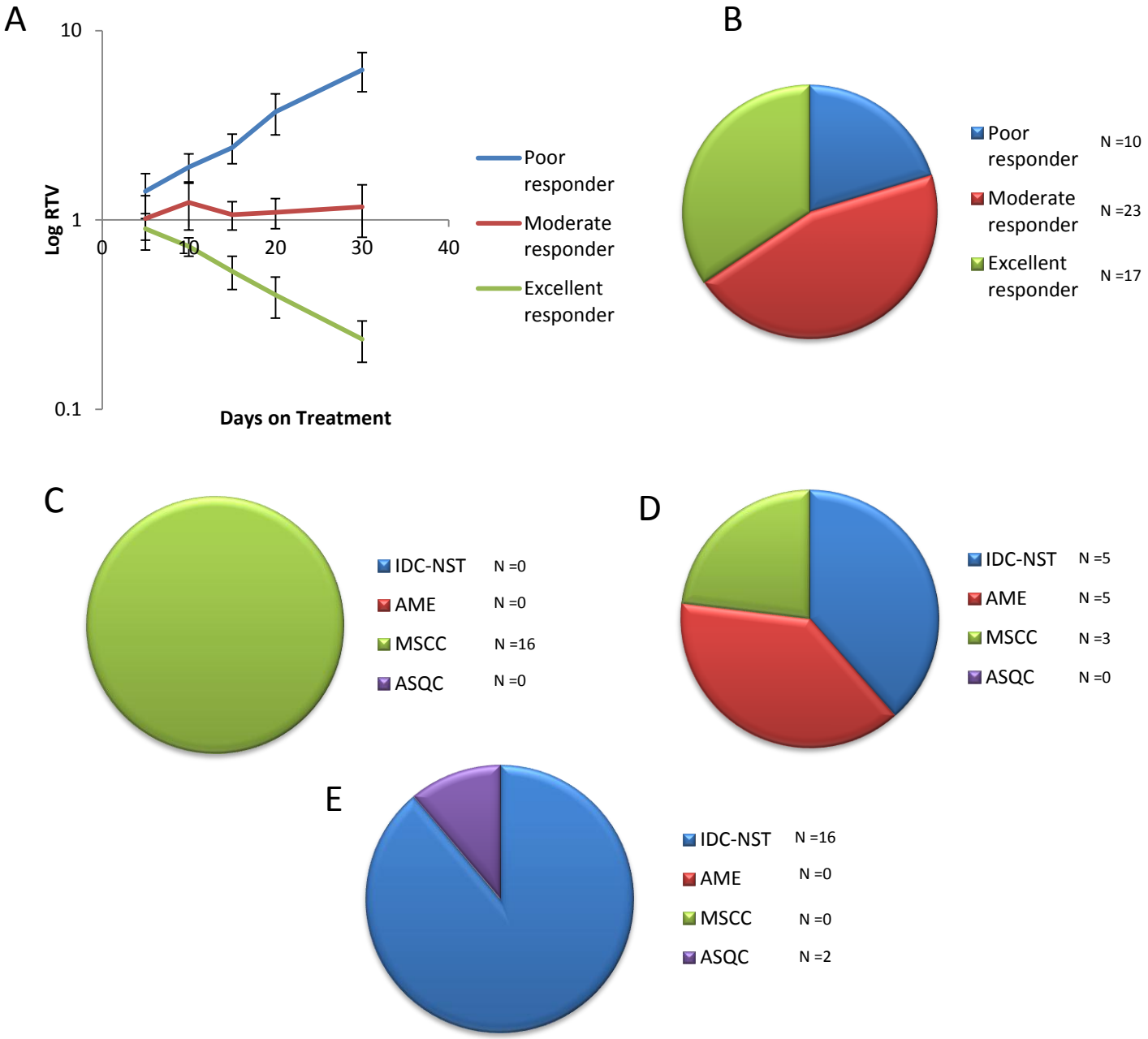

Figure 3.3 Histopathological classification of tumours with different responses to daily 100mg/kg olaparib therapy. (A) *Response to olaparib therapy was classified into three categories shown by the representative RTV graph.* ***(B)*** *Analysis of response showed that moderate and excellent responders were predominant, whilst poor responders were rare.* ***(C)*** *All poor responders were classified as MSCCs (n=16), whilst the majority of moderate responders* ***(D)*** *were either IDC-NSTs (38.5%) or AMEs (38.5%), plus a lower proportion of MSCCs (23%) (n=13).* ***(E)*** *Excellent responders were predominantly IDC-NSTs (89%) with just a few ASQCs (11%) (n=18).*

(Figure 3.4). Immunohistochemical staining showed that the epithelial cells in the treated ASQCs were indistinguishable from untreated ASQCs. However, all of the IDC-NSTs showed an increase in epithelial-like tumour cells staining positive for Vimentin compared to untreated IDC-NSTs (Figure 3.4; Mann-Whitney U test, $p<0.01$).

The presence of only MSCCs in the poor responder cohort, and their absence in the excellent responder cohort, strongly suggests that this tumour type is less sensitive to olaparib therapy in comparison to the other tumour types.

3.2.3 MSCCs show EMT characteristics and low proliferation

The significant increase in Vimentin staining in untreated MSCCs compared to untreated IDC-NSTs and AMEs suggested that cells in this tumour type were undergoing or had undergone EMT. To further investigate this, additional EMT markers (E-cadherin, Twist and Slug) were analysed in the different untreated tumour types by immunohistochemistry. MSCCs showed a significant decrease in the percentage of epithelial cells staining positive for E-cadherin (Mann-Whitney U test, $p=0.02$ and $p=0.011$) and a significant increase in levels of Twist (Mann-Whitney U test, $p=0.014$ and $p<0.01$) compared to IDCNSTs and AMEs (Figure 3.5 and Figure 3.6), which correlate with the increased Vimentin staining. The low number of ASQCs available for analysis did not allow for statistically significant differences in expression to be found; however, E-cadherin and Twist levels in these tumours showed similar levels to those seen in the IDC-NSTs and AMEs (Figure 3.5 and Figure 3.6). Slug expression was significantly higher in AMEs when compared with IDC-NSTs or MSCCs (Figure 3.5; Mann-Whitney U test, $p<0.01$ and $p=0.011$ respectively), with expression in the 2 ASQCs similar to that seen in the AMEs. This suggests that Slug expression may correlate with p63 expression, as Slug staining is seen in the myoepithelial population of both AMEs and ASQCs and in normal mammary gland (Figure 3.6).

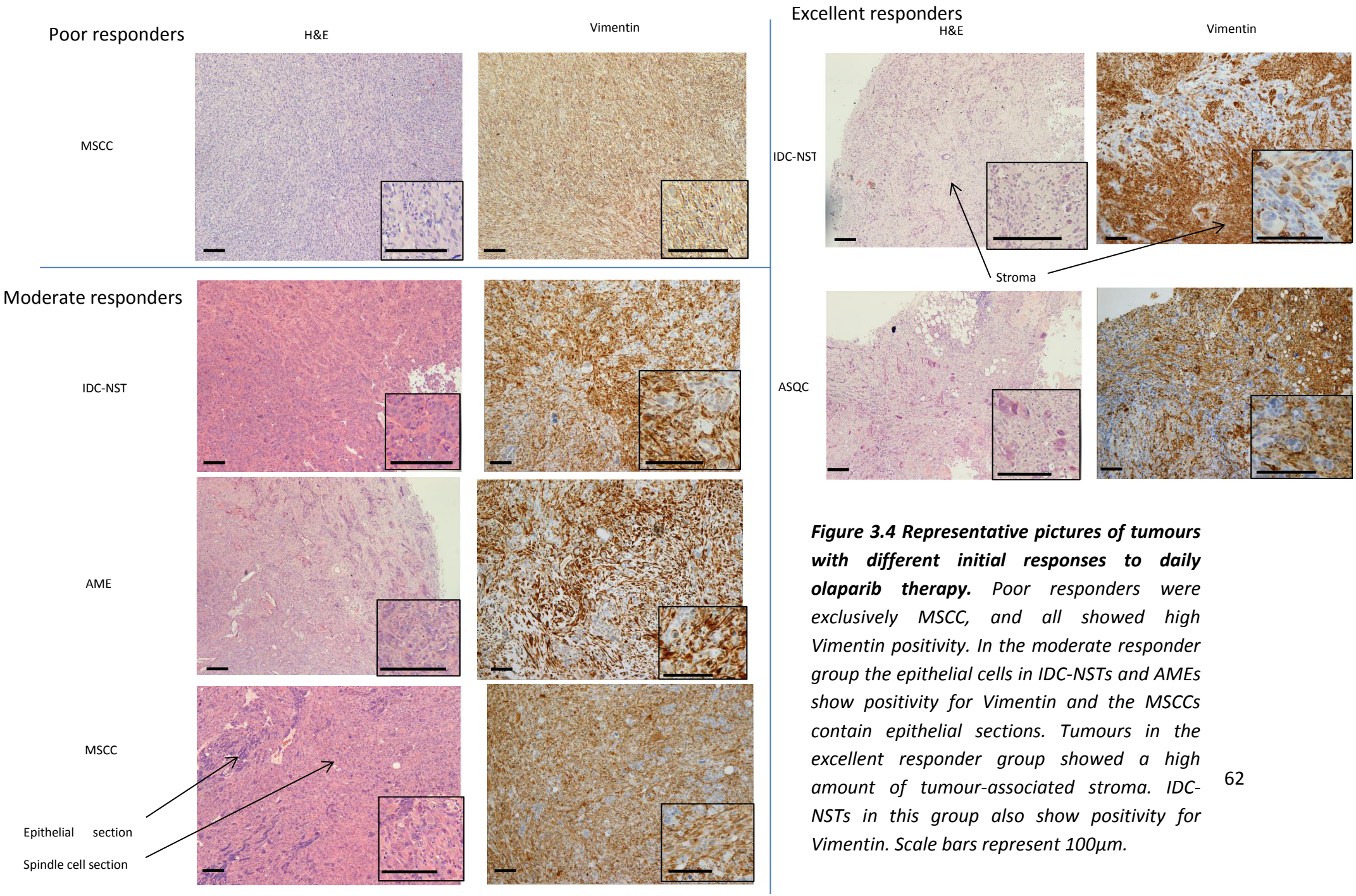

Figure 3.4 Representative pictures of tumours with different initial responses to daily olaparib therapy. *Poor responders were exclusively MSCC, and all showed high Vimentin positivity. In the moderate responder group the epithelial cells in IDC-NSTs and AMEs show positivity for Vimentin and the MSCCs contain epithelial sections. Tumours in the excellent responder group showed a high amount of tumour-associated stroma. IDC-NSTs in this group also show positivity for Vimentin. Scale bars represent 100µm.*

ASQCs showed similar marker expression to AMEs: high levels of E-cadherin and Slug and low levels of Twist. Analysis of Snail expression by qRT-PCR showed no significant differences between IDC-NSTs, AMEs or MSCCs, although there was a trend for an increase of expression in MSCCs (Figure 3.5D). Snail expression was not analysed in ASQCs due to the low numbers of tumours of this type.

Ki67 staining was used to investigate differences in proliferation between the tumour types. Again, ASQCs were not analysed due to the low numbers of tumours of this type. No significant difference was seen between the IDC-NSTs and AMEs; however MSCCs showed a significant decrease in the percentage of cells staining positive for Ki67 (Mann-Whitney U test $p=0.014$ and $p<0.01$, Figure 3.7).

3.2.4 Vimentin staining correlates with response to olaparib

Untreated IDC-NSTs showed very low levels of Vimentin-positive epithelial cells; however, tumours that are responding to olaparib show increased positivity (Figure 3.4). Vimentin staining was compared across IDC-NSTs showing different responses to olaparib and results showed that excellent responders had a significantly lower percentage of positive epithelial cells compared to moderate responders (Figure 3.8A; Mann-Whitney U test $p<0.01$). This suggests that levels of Vimentin staining in IDC-NSTs correspond with response to olaparib. As Vimentin is an EMT marker the same analysis was performed for E-cadherin, Twist and Slug (Figure 3.8B-D, Figure 3.9). Analysis of Slug expression showed no significant differences. E-cadherin expression showed no significant differences between untreated and moderate IDC-NSTs, but did show a significant decrease in moderate responders compared to excellent responders (Mann-Whitney U test, $p=0.038$). Although there were no significant differences in Twist expression between the excellent and moderate responder IDC-NSTs, both groups showed a significant increase compared to untreated IDC-NSTs (Mann-Whitney U test, $p=0.046$ and $p=0.043$ respectively).

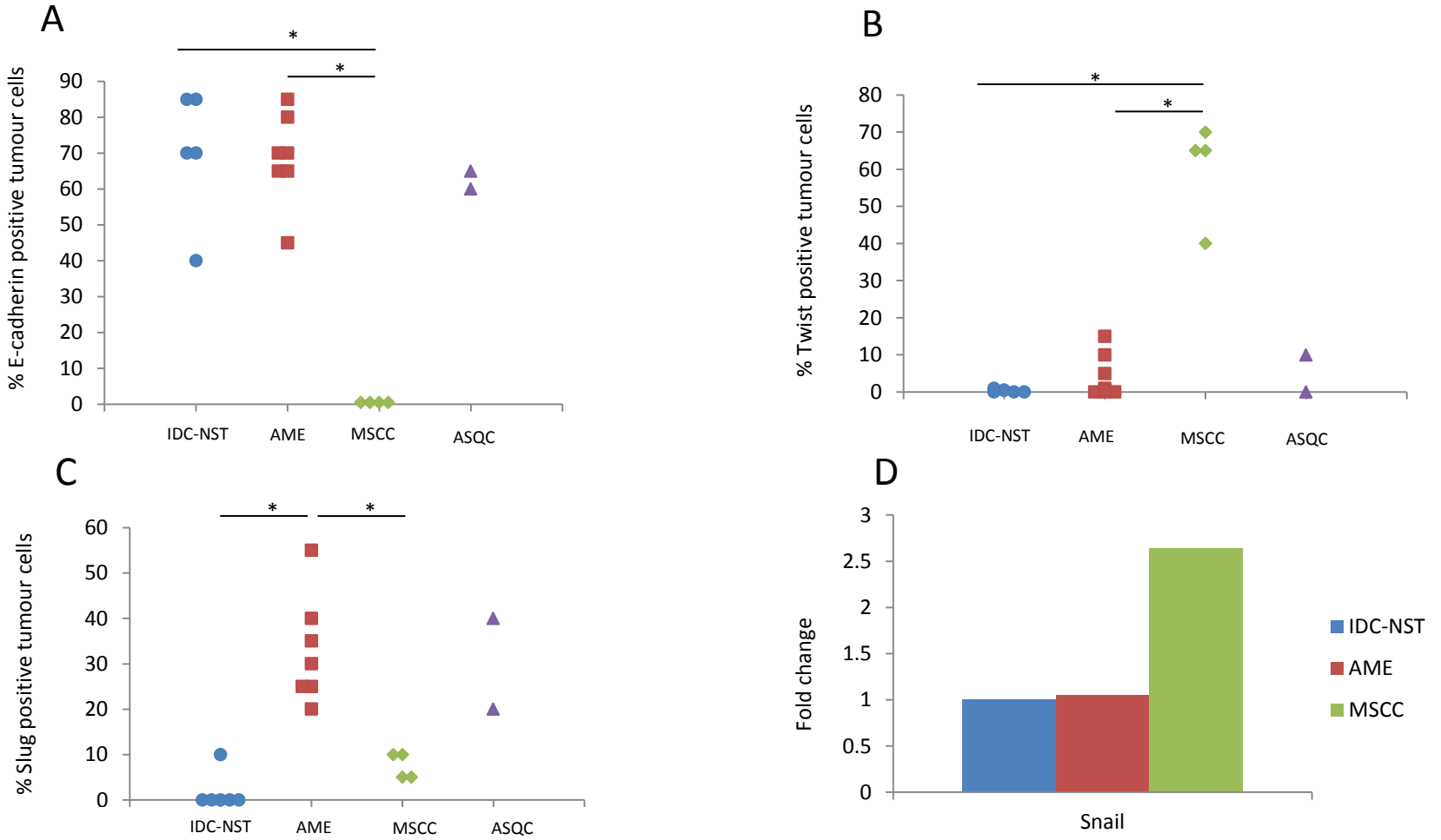

Figure 3.5 EMT marker expression in the different tumour types. *Analysis of the percent of tumour cells positive for E-cadherin* ***(A)****, Twist* ***(B)*** *and Slug* ***(C)****.* ***(D)*** *qRT-PCR showed no significant difference was found in Snail expression between IDC-NSTs, AMEs and MSCCs (n=4 per tumour type.) * indicates p≤0.05*

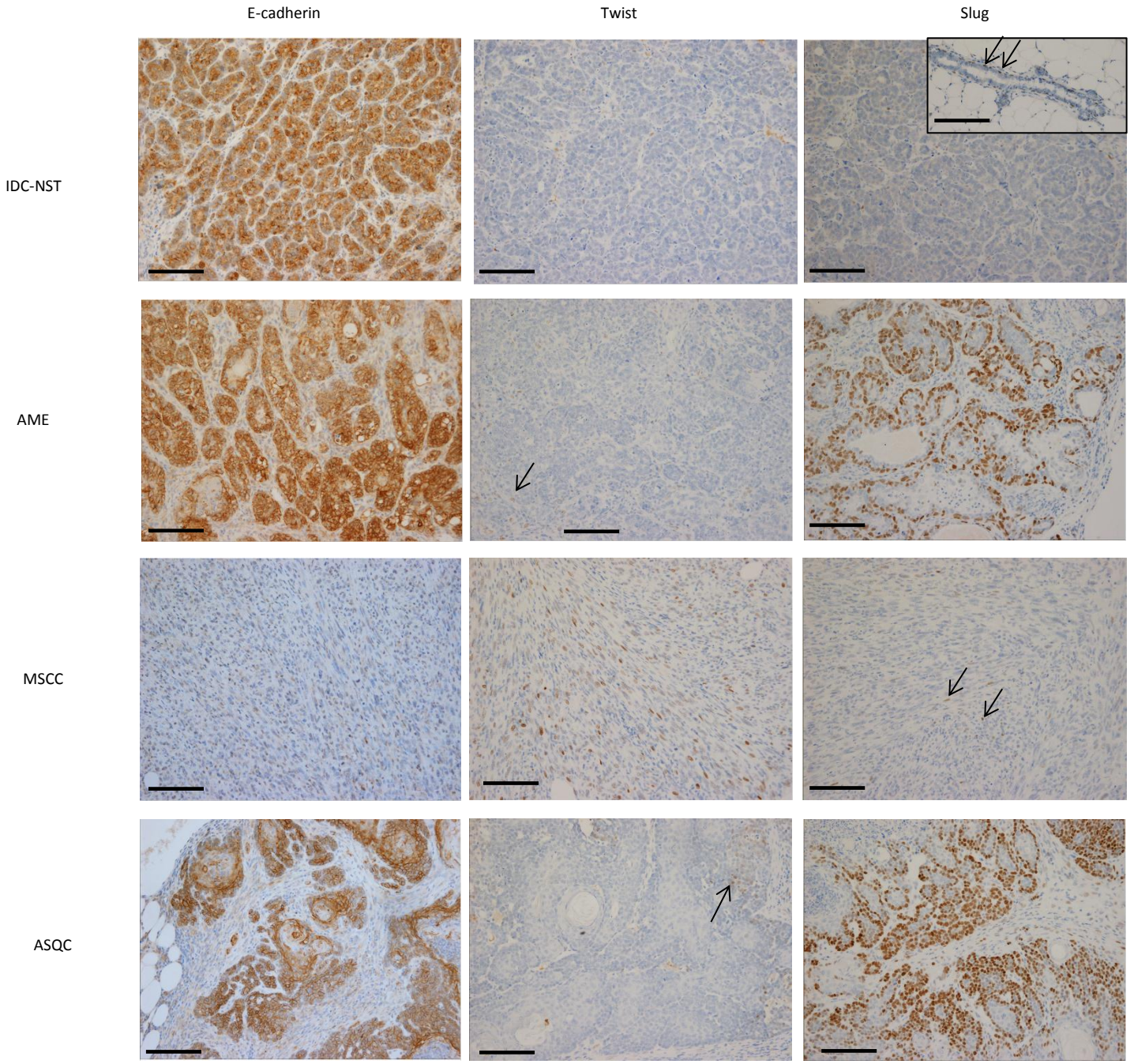

Figure 3.6 Representative pictures of EMT markers in untreated tumour types. *Immunohistochemistry for E-cadherin, Twist and Slug in the different tumour types. Slug expression correlated with myoepithelial cells in the normal mammary tissue (insert). Scale bars represent 50µm.*

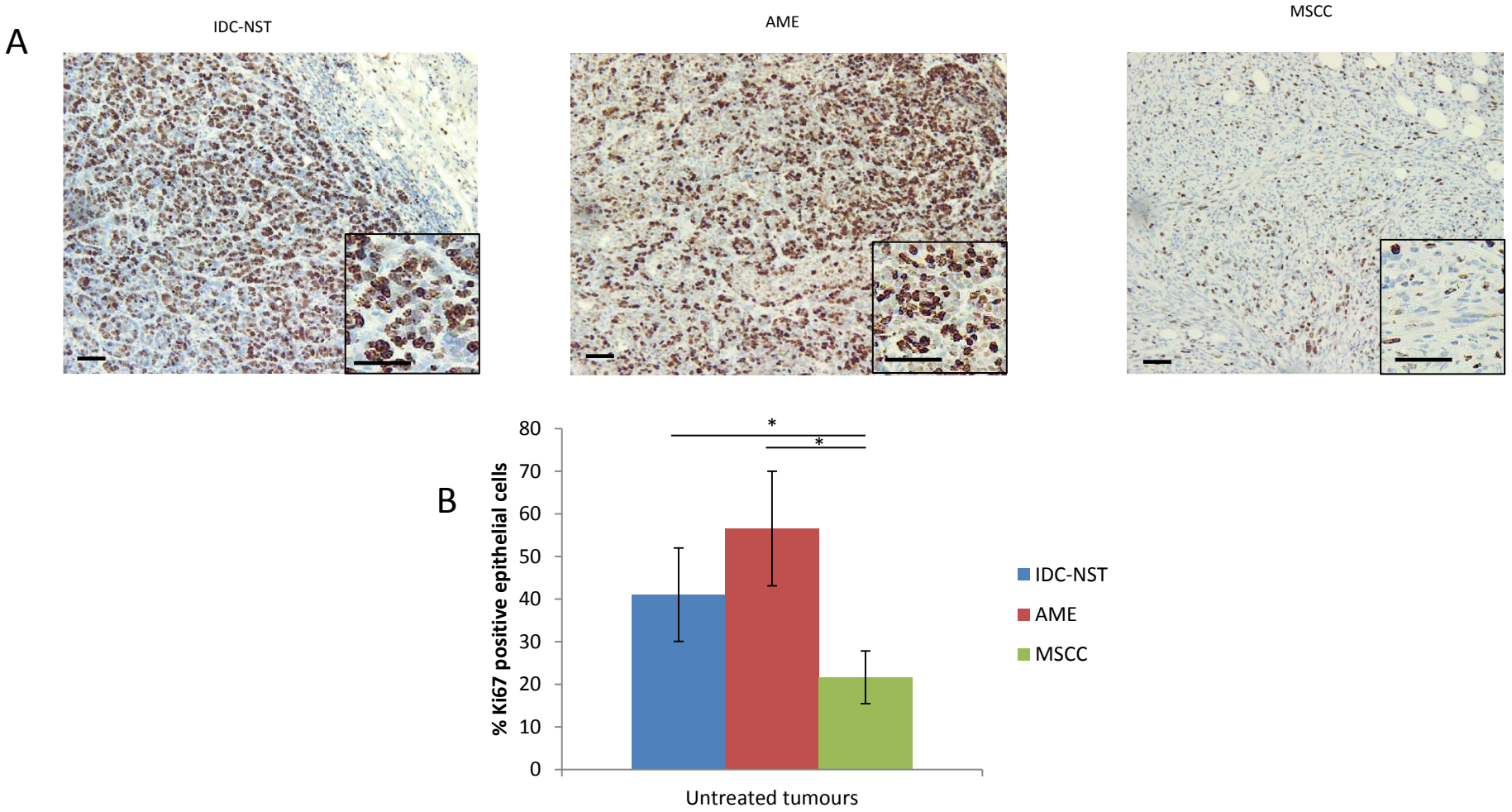

Figure 3.7 Ki67 staining in IDC-NSTs, AMEs and MSCCs. (A) *Representative pictures of Ki67 staining in untreated IDC-NSTs, AMEs and MSCCs. Scale bars represent 100µm.* ***(B)*** *Comparison of % Ki67 positive epithelial cells in the three tumour types (IDC-NSTs n=6, AMEs n=8,and MSCCs n=4). *indicates p<0.05. Error bars indicate standard deviation.*

Vimentin levels across the three different responding tumour groups was also analysed to investigate whether positivity correlates with response to olaparib independently of tumour type. Corresponding with the Vimentin levels in IDC-NSTs, the tumours from the excellent responder cohort were found to have a significantly lower percentage of Vimentin positive epithelial cells when compared to moderate or poor responders, and tumours from the moderate responder cohort also had a significantly lower percentage compared to poor responders (Figure 3.10A; Mann-Whitney U test $p<0.001$ and $p<0.001$). E-cadherin, Twist and Slug levels were also analysed in these tumours (Figure 3.10B-D). Slug expression showed no significant differences between the three cohorts. Twist expression showed similar results to Vimentin expression with a significant increase in expression in poor responders compared to excellent and moderate responders (Mann-Whitney U test, $p<0.01$ and $p<0.01$) but no significant difference between excellent and moderate responders. Levels of E-cadherin showed an inverse pattern to the vimentin staining, with expression being significantly higher in excellent responders compared to moderate and poor responders, and a significantly lower expression in poor responders compared to moderate responders (Mann-Whitney U test, $p<0.01$, $p<0.01$ and $p<0.01$).

To determine whether alterations in vimentin expression in tumours were an early or late response to olaparib treatment, IDC-NSTs were analysed from mice either 1 or 24 hours after a single dose of 100mg/kg olaparib. Results showed that at both time points there was a significant upregulation of Vimentin staining compared to untreated IDC-NSTs (Mann-Whitney U test $p<0.01$ and $p<0.01$, Figure 3.10A, Figure 3.4). No significant difference was found between the 1 and 24 hour treatment groups, although there was a trend for a decrease (Figure 3.10A). Expression of E-cadherin, Twist and Slug were also analysed in IDC-NSTs from mice treated for 1 hour (Figure 3.10B-D and Figure 3.11); results showed no significant difference in E-cadherin and Slug staining but there was a significant increase in Twist staining compared to untreated IDC-NSTs (Mann-Whitney U test, $p=0.028$, Figure 3.10C).

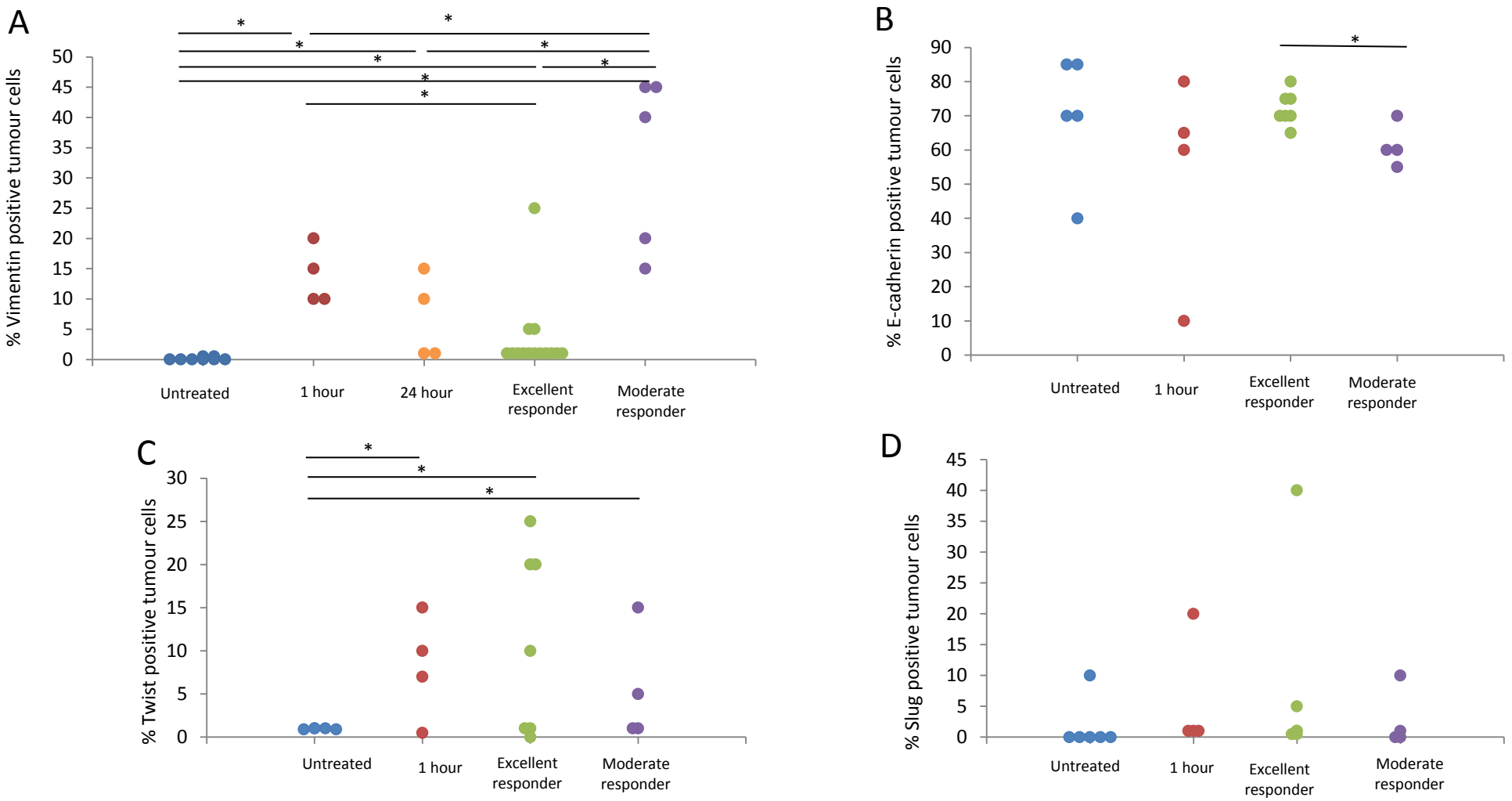

Figure 3.8 EMT markers in IDC-NSTs*. Comparison of the percentage of tumour cells positive for Vimentin* ***(A)****, E-cadherin* ***(B)*** *, Twist* ***(C)*** *and Slug* ***(D)*** *in untreated IDC-NSTs, IDC-NSTs treated with a single dose of 100mg/kg olaparib and taken either 1 hour (1 hour) or 24 hours (24 hour) later and IDC-NSTS showing an excellent or moderate response to daily 100mg/kg olaparib therapy. * indicates p≤0.05.*

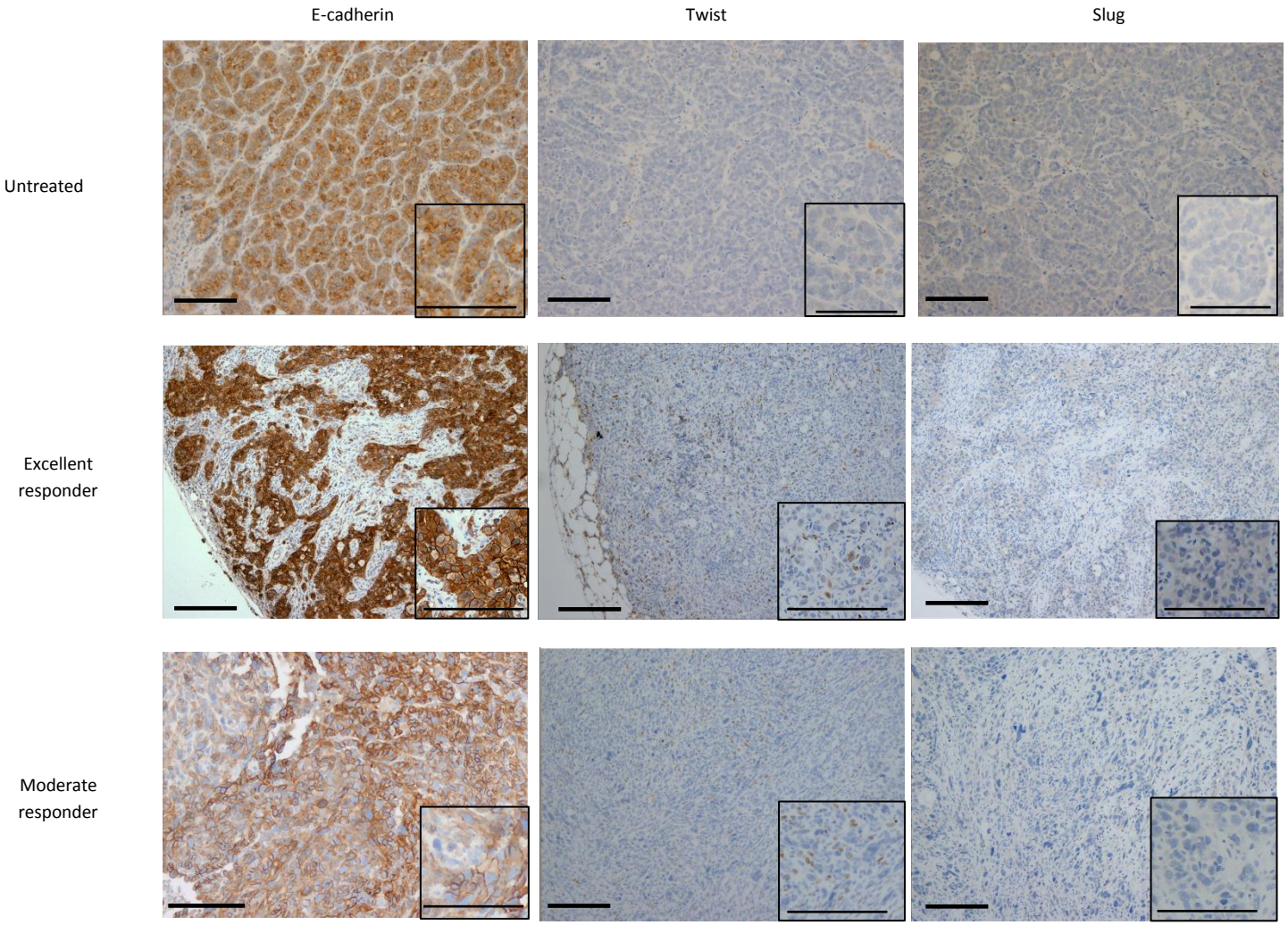

Figure 3.9 Representative pictures of EMT markers in IDC-NSTs. *E-cadherin, Twist and Slug staining in untreated, excellent responders and moderate responders to daily 100mg/kg olaparib therapy classified as IDC-NSTs. Scale bars represent 50μm.*

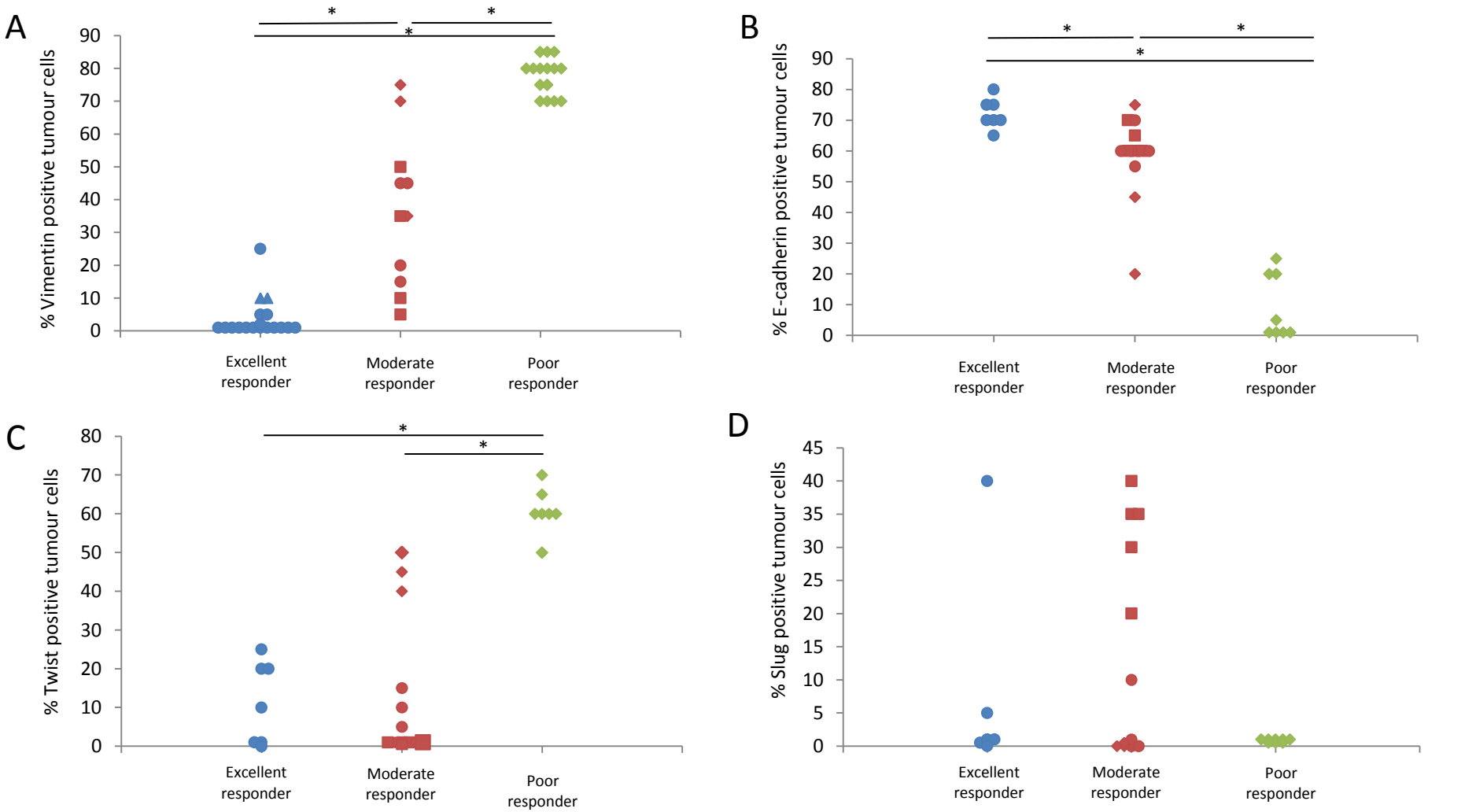

Figure 3.10 EMT marker expression in different initial responses to olaparib therapy. *Comparison of the percentage of tumour cells staining positive for Vimentin* ***(A)****, E-cadherin* ***(B)****, Twist* ***(C)*** *and Slug* ***(D)*** *in tumours showing different responses to daily 100mg/kg olaparib therapy. Circles represent IDC-NSTs, triangles ASQCs, squares AMEs and diamonds MSCCs. * indicates p≤0.05.*

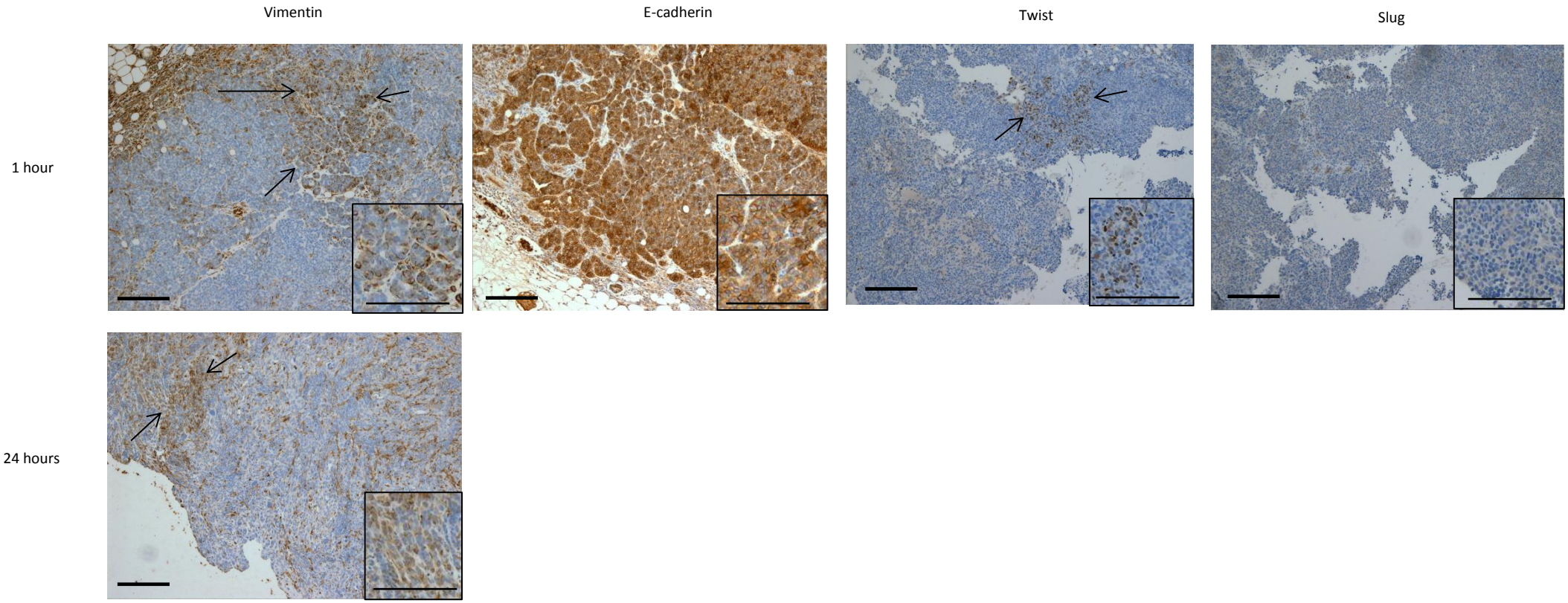

Figure 3.11 Pictures of EMT markers in IDC-NSTs treated with a single dose of 100mg/kg olaparib. *Vimentin staining in IDC-NSTs taken after 1 hour and 24 hours after a single dose of olaparib. IDC-NSTs taken after 1 hour of a single dose also show expression of Twist but retain high E-cadherin staining and low Slug staining. Scale bars represent 50µm.*

3.3 Discussion

3.3.1 Mammary tumours from our *BlgCre-Brca2$^{f/f}$/p53$^{f/f}$* mouse model show similarities in histology and gene expression to human tumours

Characterisation of a cohort of untreated tumours from our *BlgCre-Brca2$^{f/f}$/p53$^{f/f}$* mouse model revealed four different histopathological tumour types. The proportions of these tumour types are similar to those seen in humans, where the majority of breast tumours are classified as IDC-NSTs (60-70%), and metaplastic carcinomas are quite rare (<1%) (Mallon *et al*. 2000; Al Sayed *et al.* 2006). In this study we have observed a high proportion of AMEs, which although rare in humans, are more common in rodent models (Mallon *et al*. 2000). All the tumours from our model were ER-negative. This suggests that, similar to another study in a *BlgCre-Brca2$^{f/f}$/p53$^{f/f}$* mouse model (Melchor *et al*. 2014), these mice are modelling the ER-negative subset of human *BRCA2*-mutated breast cancers, which account for around 13-19% (Melchor and Benitez 2013).

IDC-NSTs from our model showed a similar gene expression profile to luminal tumours (high CK18 and E-cadherin staining and low CK14, p63 staining), corresponding with the majority of human breast tumours (Mallon *et al.* 2000; Lakhani *et al*. 2012). AMEs also correlated with previous studies, showing positivity for luminal and basal markers that were distributed into abluminal and luminal cell layers (Mallon *et al*. 2000; Melchor *et al*. 2014). In agreement with previous studies, this work shows that the MSCCs generated in the model show similarities with claudin-low tumours with respect to expression of a number of proteins, including low expression of E-cadherin and Ki67 and high expression of EMT-associated proteins such as Vimentin and Twist (Hennessy *et al*. 2009; Weigelt *et al.* 2009; Taube *et al.* 2010; Melchor *et al.* 2014). As metaplastic carcinomas are so rare in humans they tend to be grouped together; however, this work shows that MSCCs and ASQCs have differences in biological characteristics and clinical behaviour, suggesting that this heterogeneous group of tumours should be stratified for cancer treatment.

3.3.2 MSCCs may have intrinsic resistance to olaparib therapy

Clinical trials with olaparib in *BRCA*-mutated breast cancers have shown around 40% response rate (Fong *et al*. 2009; Tutt *et al*. 2010). In this study, analysis of tumours with different initial responses to olaparib therapy showed that poorly-responding tumours were

exclusively MSCCs. This correlates with human metaplastic breast carcinoma patients having a poor prognosis (Al Sayed *et al*. 2006; Hennessy *et al*. 2009) and is therefore of clinical relevance. These MSCCs were morphologically and immunohistochemically identical to untreated MSCCs, suggesting that patients with this tumour type would not benefit from olaparib therapy. One reason for this could be the low percentage of proliferating cells in the MSCCs, as PARP inhibitors have been shown to be more effective in the S phase of the cell cycle, suggesting that rapidly dividing tumours are more susceptible to these agents (Noel *et al.* 2006). Tumours that showed a moderate response to daily 100mg/kg olaparib therapy show higher percentages of Vimentin positive epithelial cells compared to tumours responding excellently, suggesting that the proportion of Vimentin-expressing epithelial cells within the tumour is indicative of the response to olaparib therapy. Analysis of other EMT markers showed no significant difference in Slug or Twist expression between moderate and excellent responders; however, moderate responders do show significantly lower expression of E-cadherin compared to excellent responders. Taken with the Vimentin levels, this may mean that some mesenchymal-characteristics affect olaparib response. Other studies have also shown a correlation between EMT markers, such as Vimentin, and response to cancer therapy, for example non-small cell lung cancer carcinoma (NSCLC) cell lines that express Vimentin were shown to be insensitive to EGFR kinase inhibition (Thomson *et al.* 2005). This study, together with the data presented here, suggests that cells that have undergone/undergoing EMT have mechanisms that confer resistance to multiple, unrelated drugs. To support this, a study investigating Adriamycin treatment on breast cancer cell lines found that, in a subpopulation of cells, treatment induced EMT, and that these cells displayed up-regulation of P-gps, multidrug resistance to chemotherapeutic agents and increased invasion (Li *et al.* 2009). This suggests that the mechanism of multidrug resistance could be the up-regulation of P-gps.

The MSCCs in the moderate responder cohort differed from untreated MSCCs in that they also contained epitheloid sections, suggesting that these tumours may be going through a change in tumour type. This would correspond with the study by Li *et al.*, which showed that epithelial cells treated *in vitro* with Adriamycin showed mesenchymal morphology, decreased expression of E-cadherin and up-regulation of Vimentin, suggesting that cells

under treatment are undergoing EMT (Li *et al*. 2009); therefore changing into mesenchymal cells, and could lead to the formation of MSCCs during treatment.

3.3.3 Vimentin expression is induced at an early time point following olaparib treatment

In comparison to an untreated cohort, a significantly higher percentage of Vimentin positive epithelial cells were seen in IDC-NSTs 1 hour after a single dose of 100mg/kg olaparib, suggesting that olaparib treatment induces its expression. Although there was no significant difference in positivity in IDC-NSTs 24 hours after a single dose, compared to 1 hour, there was a trend for a decrease, suggesting that Vimentin expression may reduce after an initial peak of expression. Another study analysing PARP-1 in endothelial cells showed that PARP inhibition *in vitro* resulted in a down-regulation of Vimentin (Isabel Rodriguez *et al.* 2013), suggesting that PARP inhibition has different effects in different cell types.

Slug expression was not shown to differ in the various responses to olaparib, or at the early (1 hour and 24 hour) time points, suggesting that other EMT transcription factors are involved. IDC-NSTs treated with a single dose of olaparib and taken 1 hour later showed significantly higher percentage of Twist positive cells, but no significant difference in E-cadherin. This suggests that Twist expression is also induced following olaparib treatment, and that changes in E-cadherin expression occurs at later time points. This work suggests for the first time that olaparib treatment in mammary tumours induces EMT at a very early time point. Other studies have shown treatment-induced EMT, for example cisplatin treatment in ovarian cancer cell lines (Ahmed *et al.* 2010; Latifi *et al.* 2011), suggesting that other cancer therapeutics also induce EMT. A study in breast epithelial cells showed that PARP-1 knockdown *in vitro* promoted EMT upon TGF-β stimulation, and suggested that PARP-1 regulates Smad-mediated transcription (Lonn *et al.* 2010), correlating with the increase in Vimentin seen upon olaparib treatment in the *BlgCre-Brca2*$^{f/f}$*/p53*$^{f/f}$ mouse model. In contrast other *in vitro* studies suggest that PARP inhibition decreases the expression of EMT markers (McPhee *et al.* 2008; Rodriguez *et al.* 2011), meaning that, although the existing studies are conflicting, these studies suggest that PARP-1 has a role in regulating EMT, and therefore treatment with PARP inhibitors will also effect EMT.

3.4 Summary

Mammary tumours arising from our *BlgCre-Brca2$^{f/f}$/p53$^{f/f}$* mouse model show similar proportions and immunohistochemical staining to human breast tumours. Response to daily olaparib therapy may be influenced by mesenchymal-characteristics, with MSCCs having an intrinsic resistance. Olaparib treatment may induce early stages of EMT.

3.5 Further Work

Further investigation into the different responses to olaparib therapy may shed some light as to why not all patients with *BRCA*-mutated breast cancers respond to olaparib therapy. It would be interesting to investigate whether Vimentin is part of the mechanisms that govern response. It would also be useful to further analyse the effect of olaparib treatment at the very early time points to understand the initial response.

As this work suggests that MSCCs have an intrinsic resistance to olaparib it would be interesting to investigate the mechanism(s) that govern this. Discovering the mechanism(s) may give insight into how these tumours can be effectively treated or sensitised to therapy. This would have implications in the clinic as MSCCs have a poor prognosis. As metaplastic breast tumours and mesenchymal cells have been shown to be resistant to chemotherapies (Hennessy *et al.* 2006; Sayan *et al.* 2009) the next step in this project was to investigate whether olaparib-resistant tumours have MSCC/mesenchymal characteristics (chapter 4).

4. Investigating the mechanism of resistance to olaparib in *BlgCre-Brca2$^{f/f}$/p53$^{f/f}$* tumours

4.1 Introduction

Resistance is a recurring problem with targeted treatments in cancer, and is highly detrimental in the clinic, causing tumour relapse and rendering drugs ineffective, therefore emphasising the importance of discovering the mechanisms involved. Common mechanisms of resistance include increased expulsion of the drug from the cell, prevention of the drug entering the cell, modification of the drug target, increased cellular metabolism of the drug and compensation by changes in cellular signalling (reviewed in Gottesman 2002; Stewart 2007). Although clinical trials have shown that olaparib can provide clinical benefit to some patients with *BRCA*-mutated breast cancer, resistance has been reported in preclinical mouse models (Rottenberg *et al*. 2008; Hay *et al*. 2009) and in two patients (Barber *et al*. 2013).

Currently there are three proposed mechanisms of resistance to olaparib that have been published. The first involves restoration of the HR pathway by secondary activating mutations in the *BRCA2* gene, as reported in *in vitro* studies and also in two patients that became resistant to olaparib (Edwards *et al*. 2008; Barber *et al*. 2013). The second is the loss of 53BP1, as a study in *Brca1*-deficient tumours showed that a subset of tumours that became resistant to olaparib showed partial restoration of the HR pathway by loss of this protein (Jaspers *et al*. 2013). The third proposed mechanism of resistance is the upregulation of P-gps, which are transmembrane, energy-dependent pumps that efflux drugs out of the cell. Preclinical studies in both *Brca1/p53* and *Brca2/p53* conditional knockout mice showed upregulation of a number of P-gps in olaparib-resistant tumours compared to untreated tumours (Rottenberg *et al*. 2008; Hay *et al*. 2009), and inhibition of P-gps in the *Brca1/p53* conditional knockout mouse model was shown to cause re-sensitisation to olaparib (Rottenberg *et al*. 2008). The study in the *Brca2/p53* mouse model showed that out of numerous multidrug resistance proteins, P-gps were the only ones found to be up-regulated in resistant tumours.

To further investigate the third proposed mechanism, studies have been performed where *Brca1*- and *Brca2*-deficient tumours were treated with a novel PARP inhibitor AZD2461, which has a lower affinity for P-gps compared to olaparib (Jaspers *et al.* 2013; Hay *et al.* unpublished; Oplustilova *et al*. unpublished). *BlgCre-Brca2*$^{f/f}$*/p53*$^{f/f}$ tumour-bearing mice were initially treated with daily IP 100mg/kg olaparib, and when the tumours became resistant they were switched to 100mg/kg AZD2461 for five days per week by oral gavage. Results showed no effect on tumour relapse (Figure 4.1, Hay *et al*. unpublished data). To ensure that AZD2461 was effective as a first line therapy for these tumours, mice were treated with 100mg/kg AZD2461 by oral gavage five days per week and results showed that the tumours responded well, although long-term treatment again resulted in resistance on a similar timescale to that seen when mice were treated with daily IP 100mg/kg olaparib (Figure 4.1, Hay *et al*. unpublished data). In comparison *Brca1/p53* conditional knockout mice showed an increased survival with AZD2461 treatment compared to olaparib; however, resistance still occurred with long term therapy (Jaspers *et al*. 2013).

To further investigate if the upregulation of P-gps is contributing to the resistance to olaparib in *BlgCre-Brca2*$^{f/f}$*/p53*$^{f/f}$ tumours, the P-gp inhibitor Tariquidar was administered in combination with olaparib in mice with such tumours.

To investigate whether olaparib-resistant tumours show differences in tumour type and immunohistochemical staining compared to untreated tumours, they were classified by histopathology using the same set of criteria outlined in chapter 3.

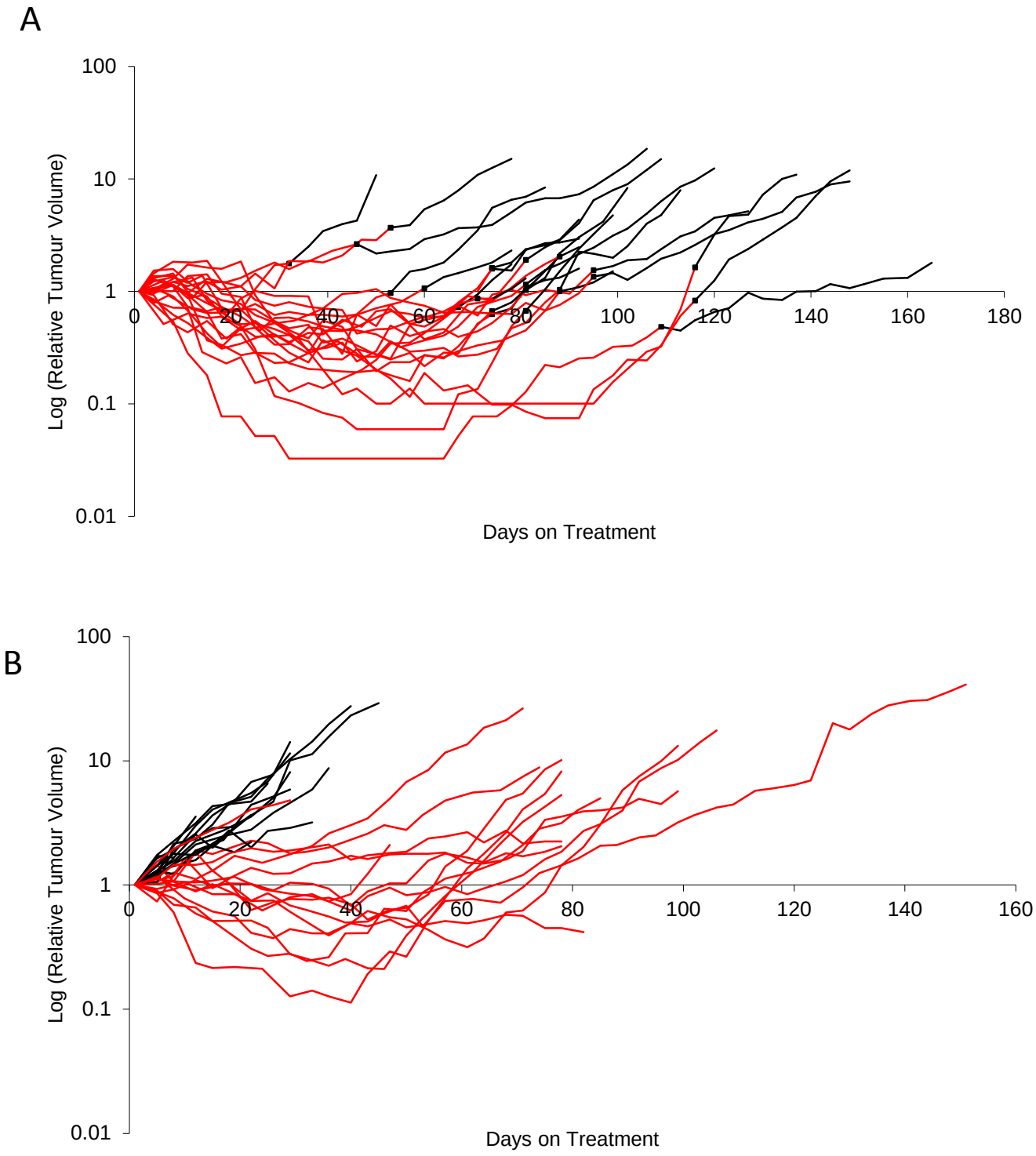

Figure 4.1 Brca2/p53-deficient tumours treated with AZD2461. (A) *Mice were initially treated with daily 100mg/kg olaparib (red lines), then once tumours became resistant mice were switched to a follow-up therapy of oral 100mg/kg AZD2461, 5 days per week (black lines).* ***(B)*** *Mice were treated with 100mg/kg AZD2461 5 days per week (red lines) and compared to vehicle treatment (black lines). Experiment performed by Dr Trevor Hay.*

4.2 Results

4.2.1 Inhibition of P-gps has no effect on tumour relapse

Previous studies involving mouse *Brca2/p53* and *Brca1/p53* breast cancer models hypothesised that upregulation of P-gps may at least partly contribute to olaparib resistance in such cancers (Rottenberg *et al*. 2008; Hay *et al*. 2009). Unpublished data from our laboratory showed that the novel PARP inhibitor AZD2461 had no effect on tumour relapse in *BlgCre-Brca2$^{f/f}$/p53$^{f/f}$* mice. To further investigate the involvement of P-gps in resistance, the P-gp inhibitor Tariquidar was administered to mice with olaparib-resistant tumours. Tariquidar is a specific, non-competitive inhibitor of P-gps and studies in a *Brca1/p53* conditional knockout model have shown that olaparib-resistant tumours in these mice regained sensitivity to olaparib when combined with Tariquidar (Rottenberg *et al*. 2008). *BlgCre-Brca2$^{f/f}$/p53$^{f/f}$* mice were treated with 100mg/kg daily olaparib until the tumours became resistant, where they were then placed on a combination treatment of daily 100mg/kg olaparib with 2mg/kg Tariquidar (given half hour before the olaparib) five days per week. Results show that the addition of Tariquidar had no effect on tumour relapse in any of the tumours tested (Figure 4.2), adding further weight to the theory that up-regulation of P-gps in this model is a consequence of treatment in a subset of tumours, but not a mechanism of resistance.

4.2.2 Resistant tumours show a shift in histopathological phenotype

Tumours from *BlgCre-Brca2$^{f/f}$/p53$^{f/f}$* mice that had become resistant to olaparib were classified by histopathology. These 51 tumours initially responded to daily IP 100mg/kg olaparib treatment but then relapsed until tumour burden made it necessary to cull the mice. Resistant tumours showed the presence of the same four tumour types as seen in the untreated cohort (Figure 4.3), but there was a dramatic change in their relative proportions (Figure 4.4; Chi squared test, p=0.05), with an increase in the proportion of MSCCs from 11% to 53%, and a reduction in the proportions of the other three tumour types compared to the untreated group.

Although the same four tumour types were present in both cohorts, immunohistochemical analysis showed some differences in staining patterns (Figure 4.3, Figure 4.4 and Figure 4.5).

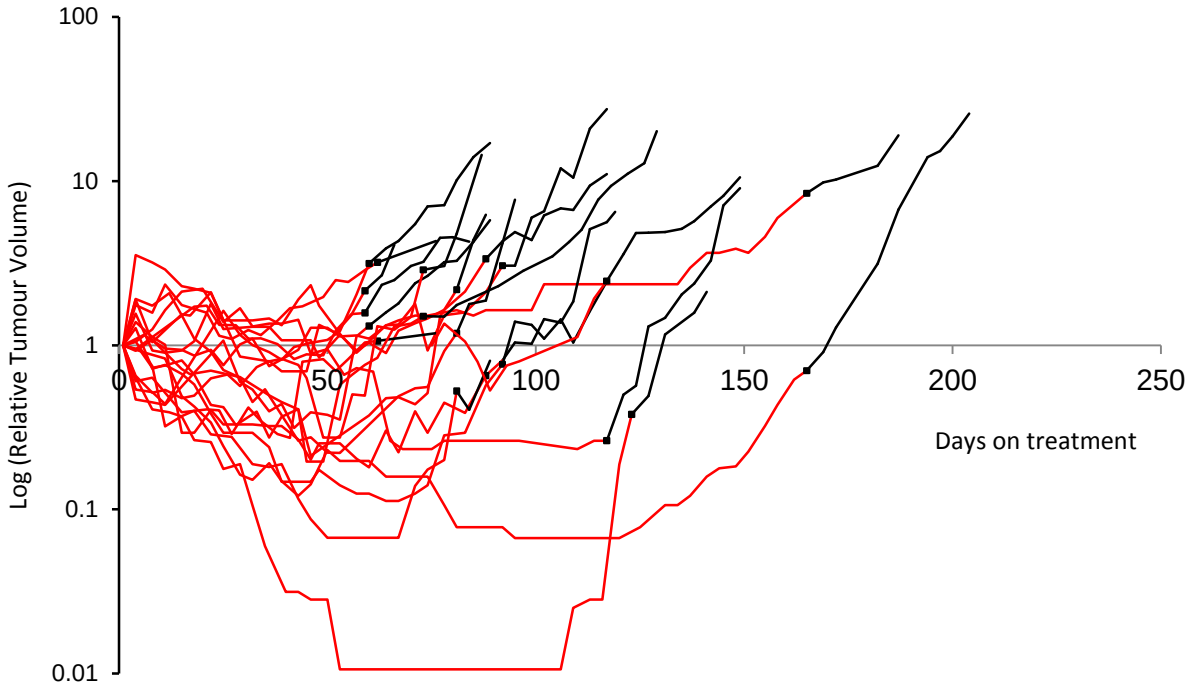

Figure 4.2 Analysis of tumours treated with Tariquidar. *Mice were initially treated with daily 100mg/kg olaparib (red line) until tumours became resistant where they were switched to a combination follow-up therapy of 2mg/kg Tariquidar, administered 30 minutes before 100mg/kg olaparib (black line).*

Resistant IDC-NSTs showed a significantly higher expression of Vimentin and CK14 and a significantly lower expression of CK18 compared to untreated IDC-NSTs (Mann-Whitney U test, $p<0.01$, $p=0.039$ and $p=0.039$, respectively). These tumours showed no significant differences in SMA or p63 staining. Resistant AMEs showed no significant difference in CK18, CK14, p63 or SMA staining but did show a significant increase in Vimentin positive cells compared to untreated AMEs (Mann-Whitney U test, $p=0.041$). Resistant MSCCs retained the same levels of Vimentin, SMA and p63 expression but similar to the MSCCs in the moderate responder cohort (see chapter 3), these tumours contained small regions with histopathological features similar to IDC-NSTs or AMEs. Compared to untreated MSCCs, resistant MSCCs showed a significantly higher expression of CK18 (Mann-Whitney U test, $p=0.045$) and a subset showed higher levels of CK14 staining, which may be due to the IDC-NST and AME regions, but the spindle cells themselves also showed cytokeratin positivity. The one ASQC tumour showed similar staining patterns to the untreated ASQCs (Figure 4.3). Like untreated tumours, all tumours were shown to be ERα negative (Figure 4.3).

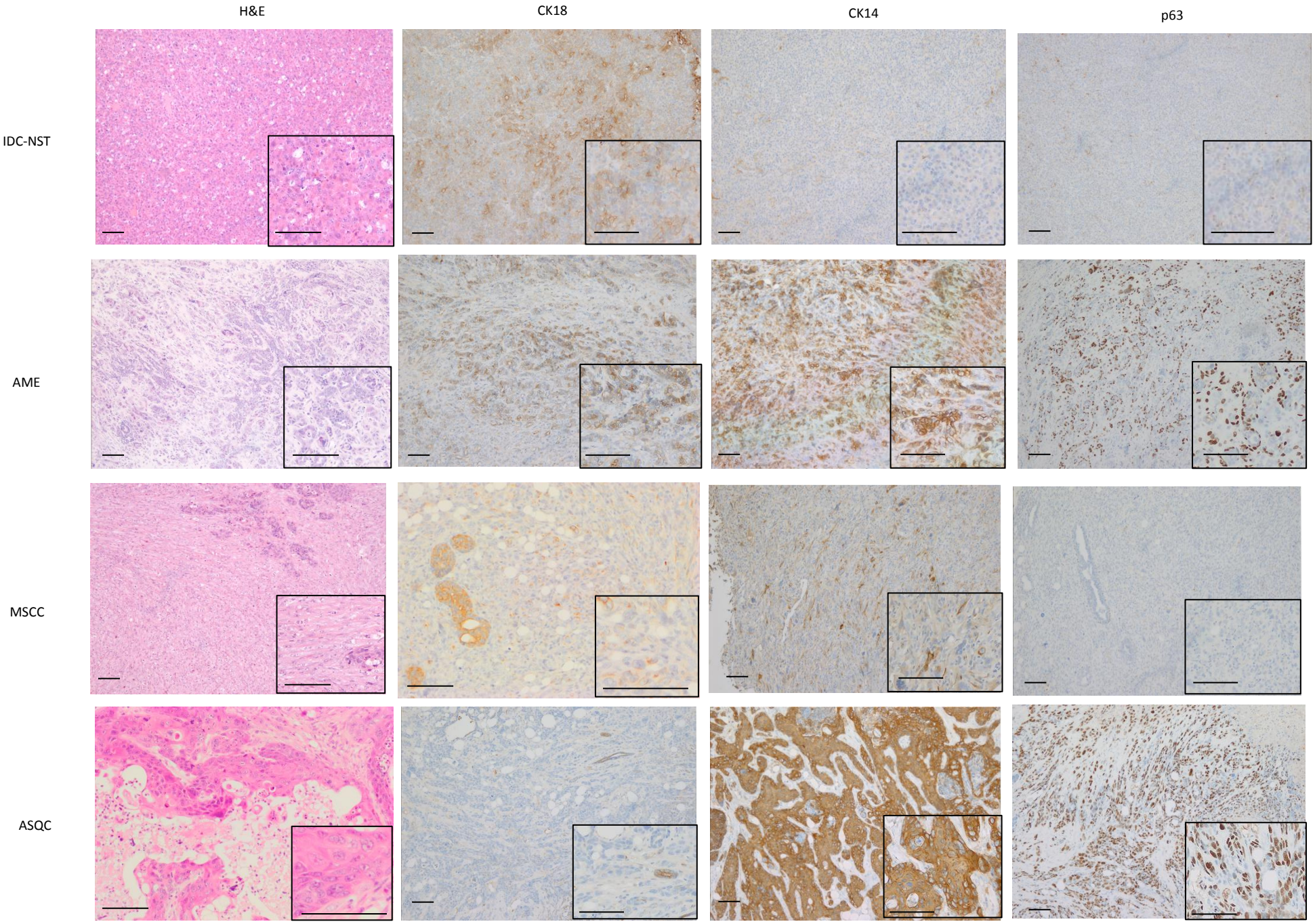
H&E
CK18
CK14
p63
IDC-NST
AME
MSCC
ASQC

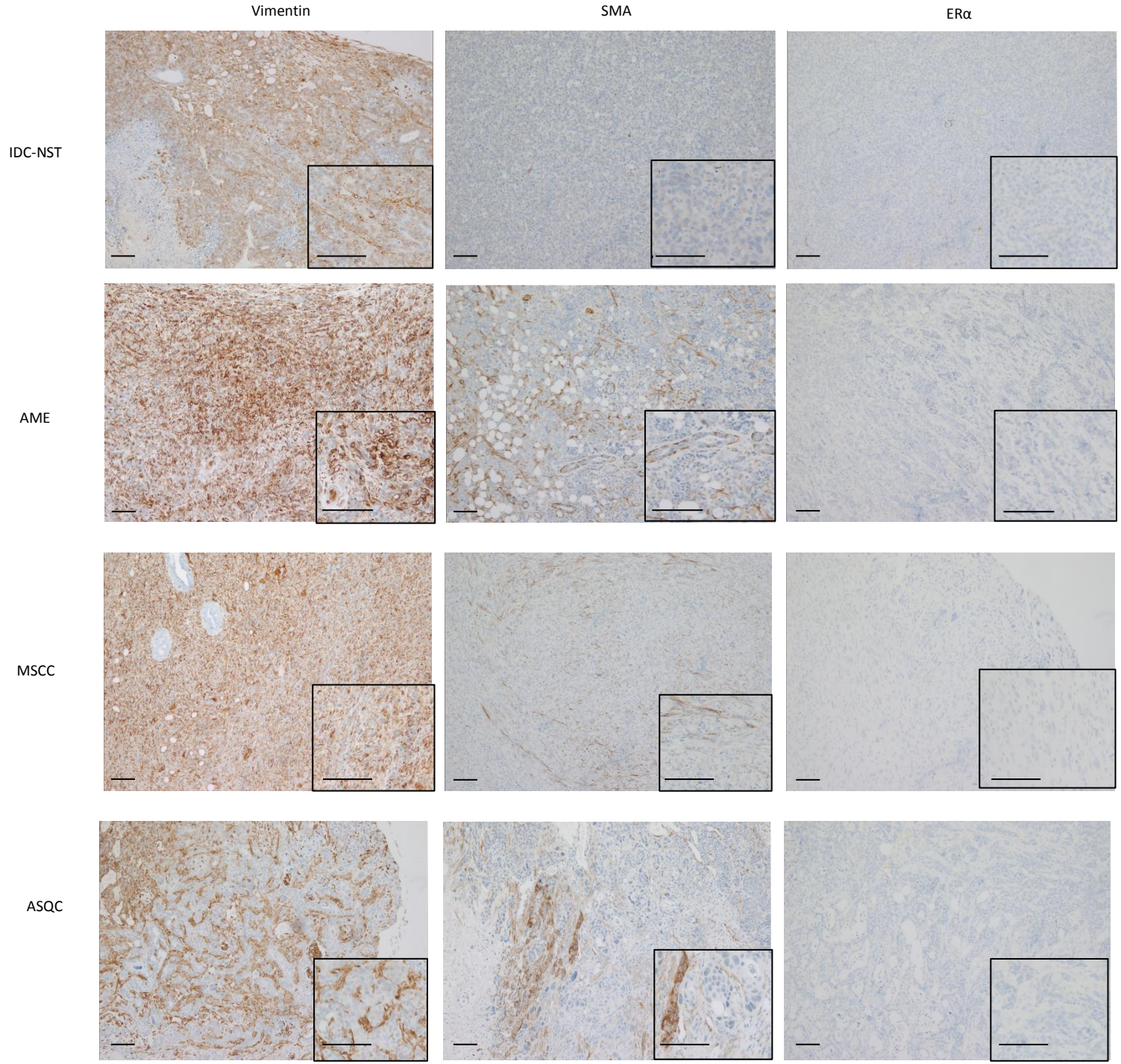

Figure 4.3 Representative pictures of immunohistochemical stains in olaparib-resistant tumours. *Olaparib-resistant tumours were classified by histopathology. H&E stains were performed to analyse cell morphology, whilst CK18, CK14, p63 and SMA were used to characterise different cell populations. Vimentin positivity marks mesenchymal cells and the ERα stain was performed to analyse ER receptor expression. Scale bars show 100µm.*

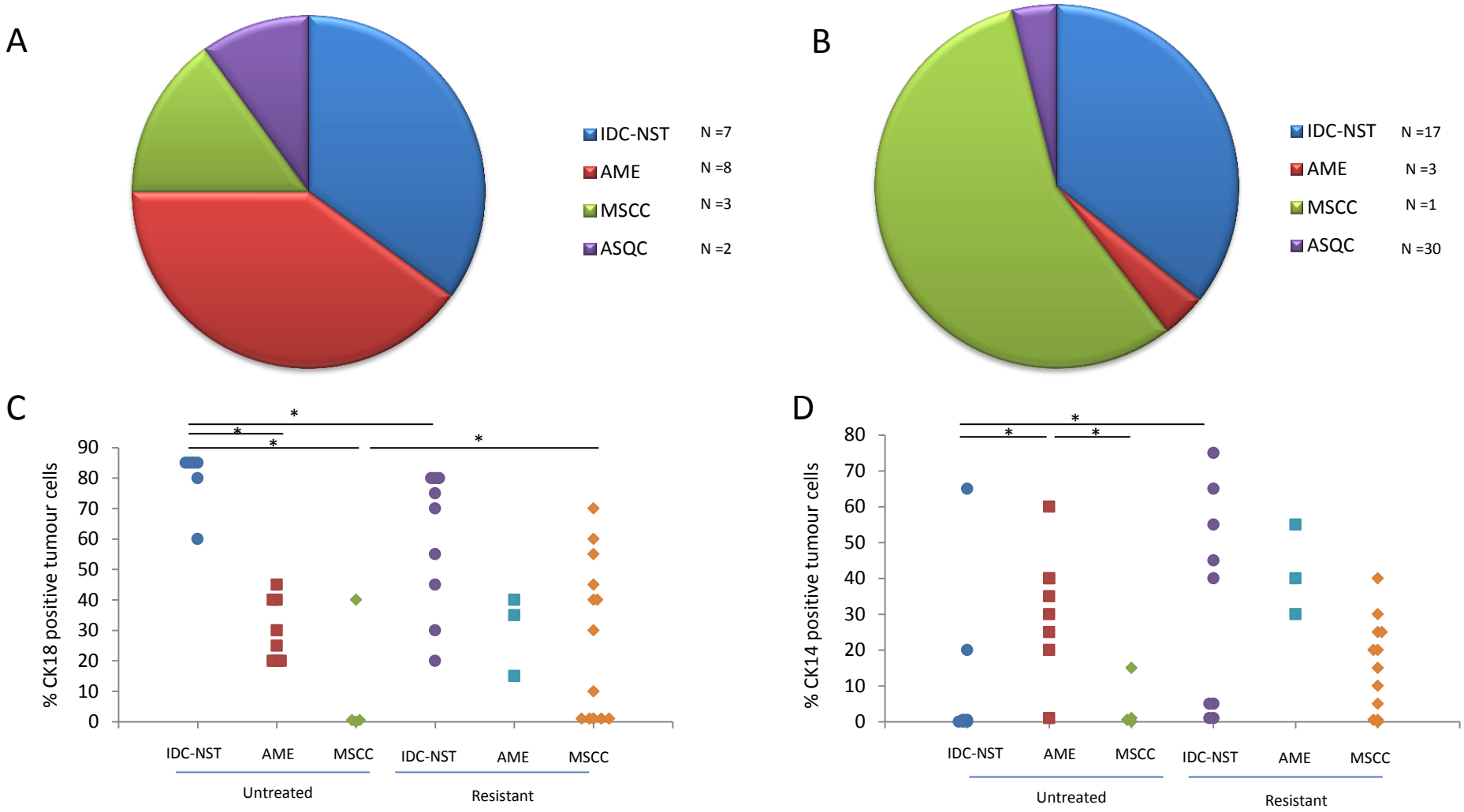

Figure 4.4 Comparison of untreated and olaparib-resistant tumours. *Histopathological classification showed untreated tumours **(A)** have a significant difference in proportions compared to olaparib-resistant tumours **(B).** Analysis of immunohistochemistry for CK18 **(C)** and CK14 **(D)**, showing percentage of positive tumour cells, comparing untreated and resistant tumour types. *p≤0.05*

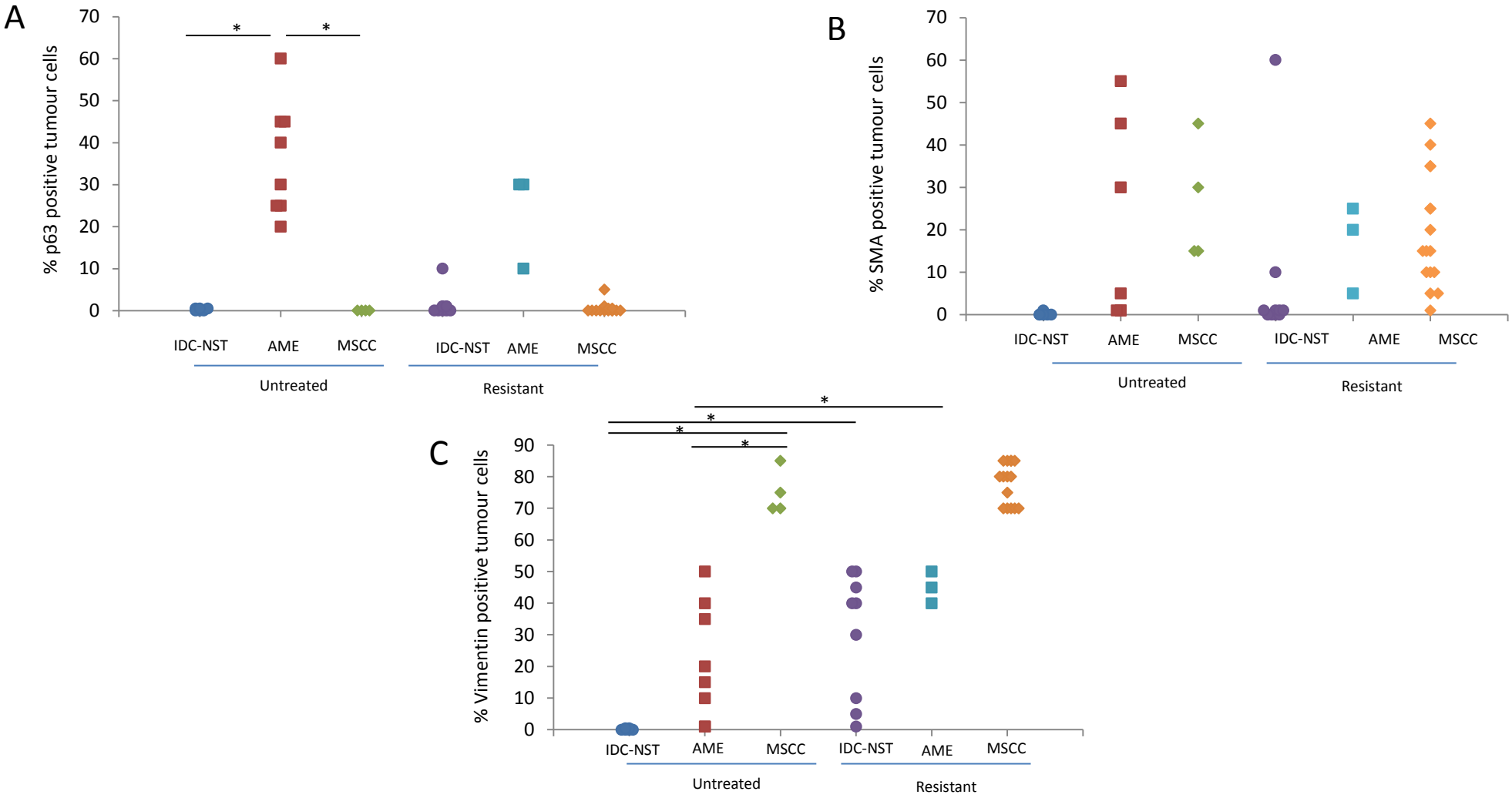

Figure 4.5 p63, Vimentin and SMA positivity in olaparib-resistant tumours. *Analysis of p63 (**A**), SMA (**B**) and Vimentin (**C**) positivity in untreated and olaparib-resistant tumours. *p≤0.05*

Tumours treated with AZD2461 monotherapy (n=15) and olaparib-resistant tumours which were followed up with either AZD2461 (n=25) or the Tariquidar/olaparib combination (n=27) were classified by histopathology to see if they were similar to olaparib-resistant tumours. Analysis of all three cohorts showed that the same tumour types were present in very similar proportions in all cohorts, with MSCCs predominating (Figure 4.6), and showed similar staining patterns to tumours that had become resistant to olaparib monotherapy.

Proliferation in resistant tumours was analysed by Ki67 staining. Resistant IDC-NSTs (n=9) and AMEs (n=3) showed no significant difference in percentage of Ki67 positive cells compared to untreated tumours; however, resistant MSCCs (n=16) showed a significant increase in positivity (Mann-Whitney U test, p=0.009, Figure 4.7), resulting in no significant difference in Ki67 positivity between the different tumour types in the resistant cohort.

4.2.3 Reduced olaparib concentration in resistant tumours does not correlate with high PAR levels.

To investigate whether the mechanism of resistance to olaparib involves the reduction in concentration of the drug, olaparib levels were analysed in tumours from three cohorts: (1) 1 hour after a single dose of 100mg/kg olaparib, (2) 24 hours after a single dose of 100mg/kg olaparib, and (3) 1 hour after the final dose of 100mg/kg olaparib in resistant tumours (Figure 4.8). Olaparib levels in tumours from mice treated with a single dose of olaparib and taken 1 hour later ranged from 0.6-0.93 μM, while those from mice treated with a single dose and taken 24 hours later were substantially lower (<0.007 μM, Mann-Whitney U test p=0.03), corroborating a previous study in our laboratory, which showed that olaparib is rapidly removed from tumours (Hay *et al*. 2009). The levels of inhibitor in resistant tumours 1 hour after their final dose were highly variable (0.01-0.63μM) and were significantly lower than in tumours 1 hour after a single dose, but significantly higher than in the tumours taken 24 hours after a single dose (Mann-Whitney U test, $p<0.01$ and $p<0.01$ respectively). Histopathology of the resistant tumours could not distinguish between tumours which contained a low olaparib concentration and those with a high concentration (Figure 4.8), suggesting that tumour type does not affect olaparib concentration in resistant tumours.

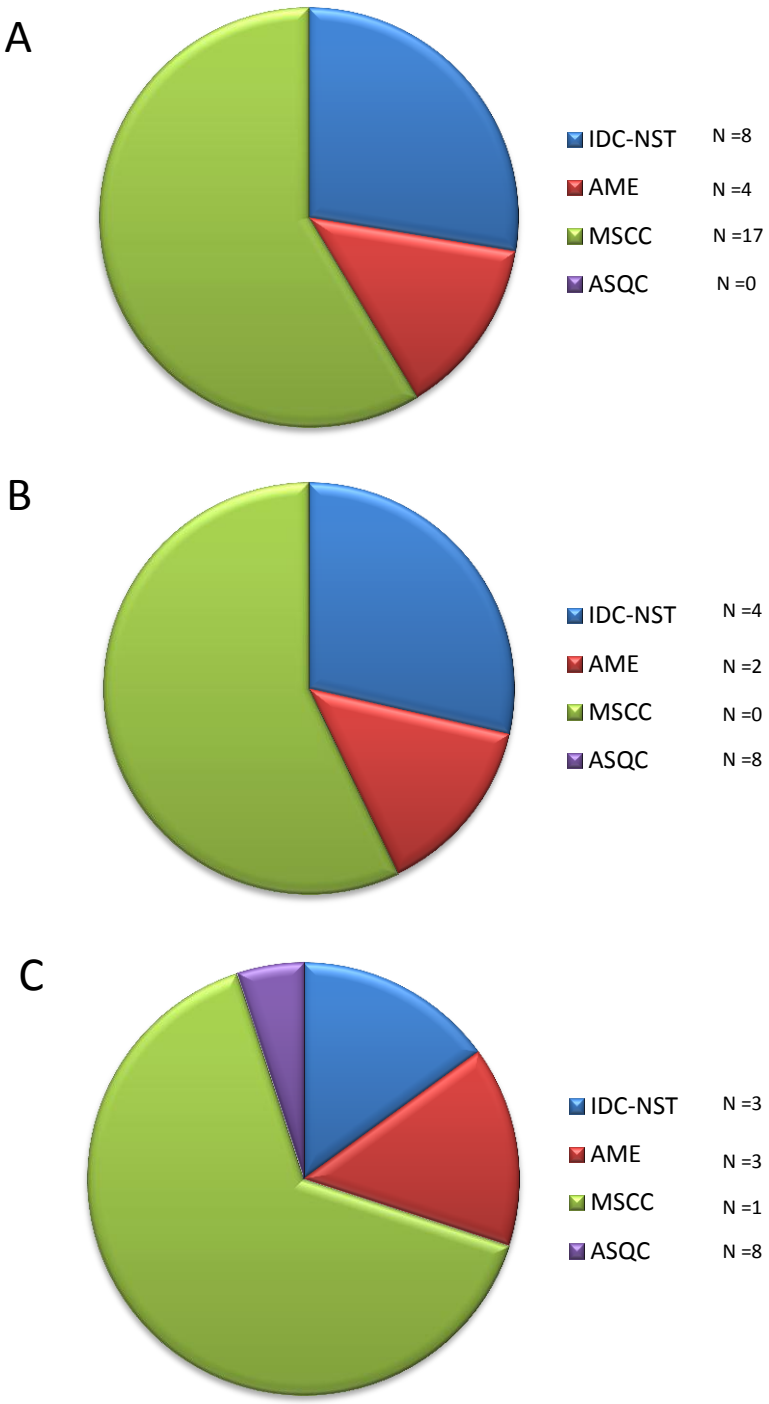

Figure 4.6 Histopathology of tumours treated with Tariquidar or AZD2461. *Histopathological analysis of olaparib-resistant tumours treated with either Tariquidar* ***(A)****, AZD2461* ***(B)*** *or AZD2461-resistant tumours* ***(C)****.*

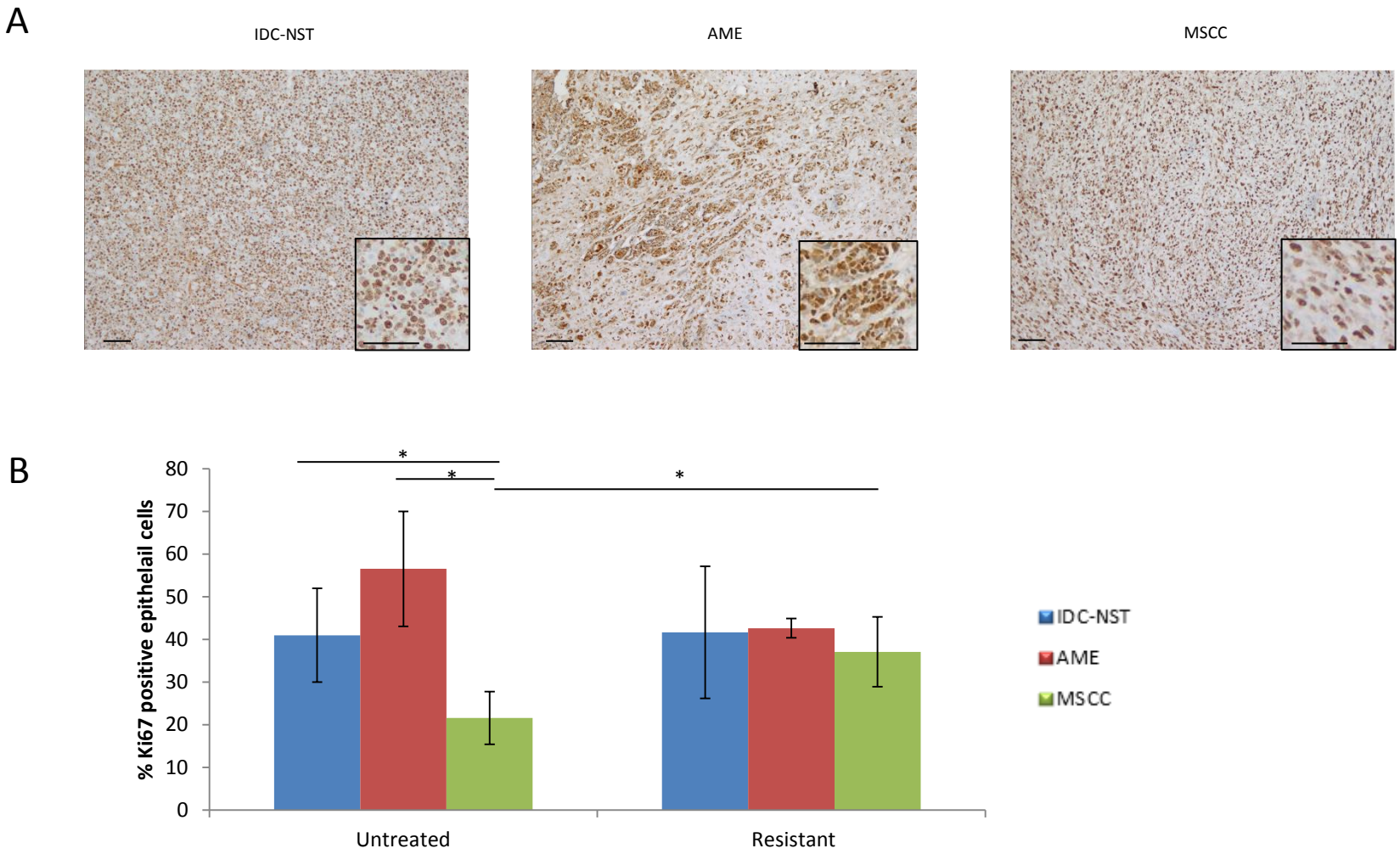

Figure 4.7 Ki67 positivity in olaparib-resistant tumours. (A) *Representative pictures of Ki67 staining in resistant IDC-NSTs, AMEs and MSCCs.* ***(B)*** *Comparison of percentage of positive Ki67 cells in untreated and olaparib-resistant tumour types. *p≤0.05*

PAR is a product of PARP activity and as such the amount of PAR within a tumour can be indicative of the level of PARP activity. PAR levels were analysed in the same set of tumours discussed above, as well as from tumours 1 hour and 24 hours after a single dose of vehicle for olaparib (Figure 4.8). Levels of PAR in tumours from mice treated with vehicle showed wide variability, ranging from 15.1-139.9pg/ml, with no significant difference between the 1 hr and 24 hr cohorts (shown in Figure 4.8 as one cohort). Tumours from mice treated with a single dose of olaparib and taken 1 hour later showed a significantly reduced PAR level compared to the overall vehicle group (Mann-Whitney U test, $p<0.01$) and those from mice treated with a single dose of olaparib and taken 24 hours later showed a significant increase in PAR compared to those taken 1 hour later (Mann-Whitney U test, $p=0.03$), correlating with the olaparib concentration seen in these tumours. PAR levels in olaparib-resistant tumours taken one hour after their final dose were significantly lower compared to the vehicle group and in tumours 24 hours after a single dose (Mann-Whitney U test, $p<0.001$ and $p=0.025$ respectively) and were similar to PAR levels in tumours 1 hour after a single dose. This suggests that PARP activity is still low in resistant tumours, despite the variable concentrations of olaparib found within these tumours.

The variation in PAR levels in the vehicle cohort suggests variable endogenous level of PARP activity within untreated tumours. Histopathological analysis of the tumours revealed that those with the highest PAR levels were IDC-NSTs (n=5), whilst those with the lowest levels were either AMEs (n=2) or MSCC (n=1) (Figure 4.8), suggesting that tumour type may affect PARP activity levels.

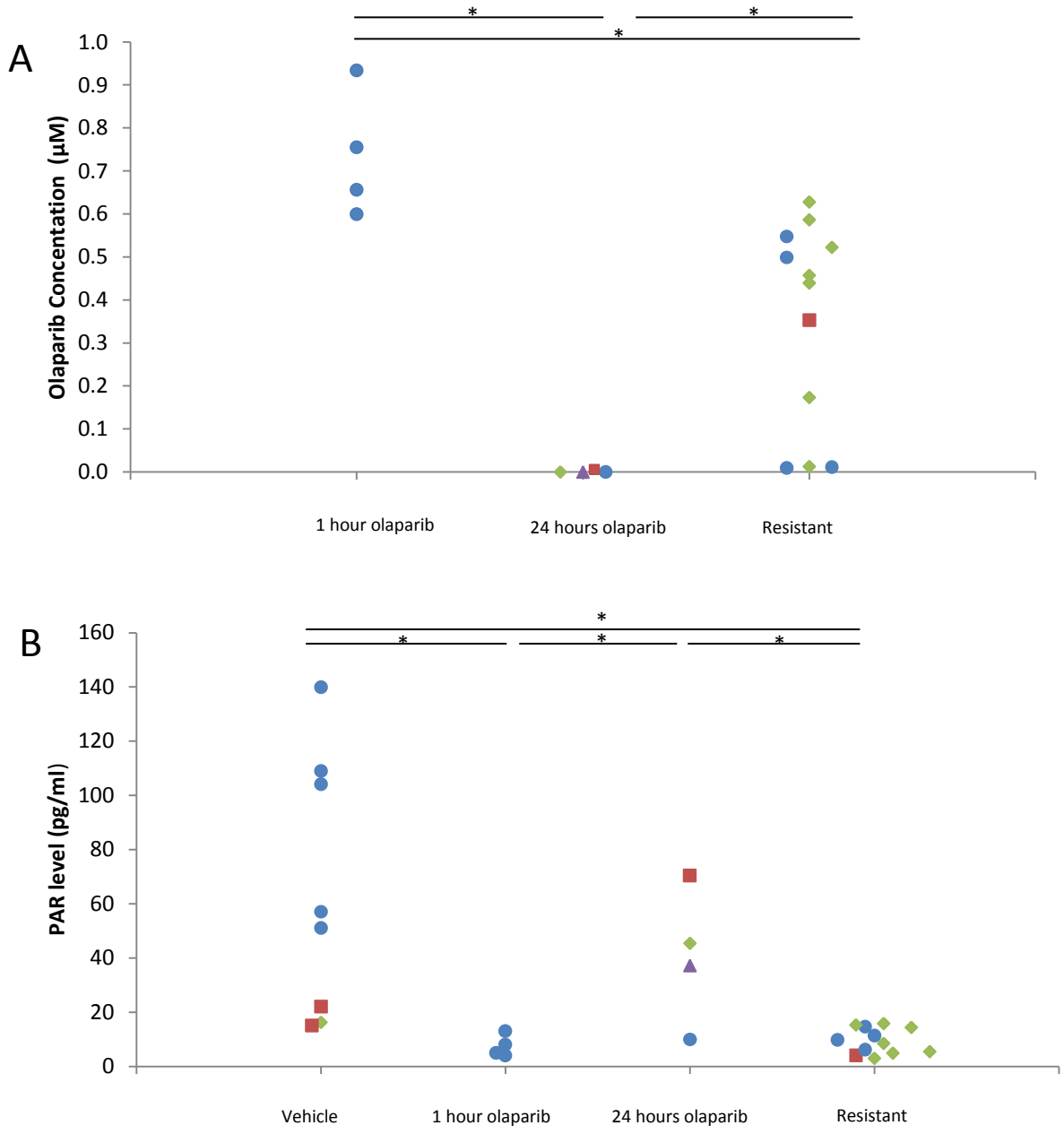

Figure 4.8 Analysis of olaparib concentration and poly(ADP-ribose) (PAR) levels in olaparib-resistant tumours. (A) *Olaparib concentration in tumours from mice treated with a single dose of 100mg/kg olaparib and taken 1 hour later (1 hour olaparib) and 24 hours later (24 hours olaparib) were compared to those in olaparib-resistant tumours (resistant).* ***(B)*** *PAR levels were analysed and compared in the same tumours and also compared to levels in tumours treated with a single dose of vehicle (vehicle). Circles represent IDC-NSTs, triangles ASQCs, squares AMEs and diamonds MSCCs. *p≤0.05. Analysis was performed by AstraZeneca.*

4.2.4 A subset of resistant tumours have EMT characteristics.

Resistant IDC-NST and AMEs show significantly higher expression of Vimentin compared to untreated tumours, suggesting that the cells are undergoing EMT. Analysis of EMT markers in resistant IDC-NSTs showed no significant differences in E-cadherin, Twist or Slug levels compared to untreated tumours, although a subset of these tumours did show reduced E-cadherin expression (2/6) and increased Twist expression (3/6) (Figure 4.9 and Figure 4.10). Resistant AMEs showed similar levels of E-cadherin and Slug to untreated AMEs, with a significant increase in Twist levels (Mann-Whitney U test, $p=0.041$; Figure 4.9 and Figure 4.10). Resistant MSCCs showed no significant difference in positivity for any of the EMT markers compared to untreated MSCCs, retaining the high expression of Twist and low expression of E-cadherin (Figure 4.9 and Figure 4.10). The one ASQC also showed similar expression of EMT markers compared to untreated tumours (Figure 4.9 and Figure 4.10). qRT-PCR analysis of *Snail* expression in resistant IDC-NSTs and MSCCs showed no significant difference to untreated tumours, although resistant MSCCs did show a trend for an increase in *Snail* expression compared to untreated MSCCs (Figure 4.10D).

This suggests that even though some resistant IDC-NSTs and AMEs look morphologically similar to untreated tumours, they show increases in some EMT features, which are characteristically high in MSCCs.

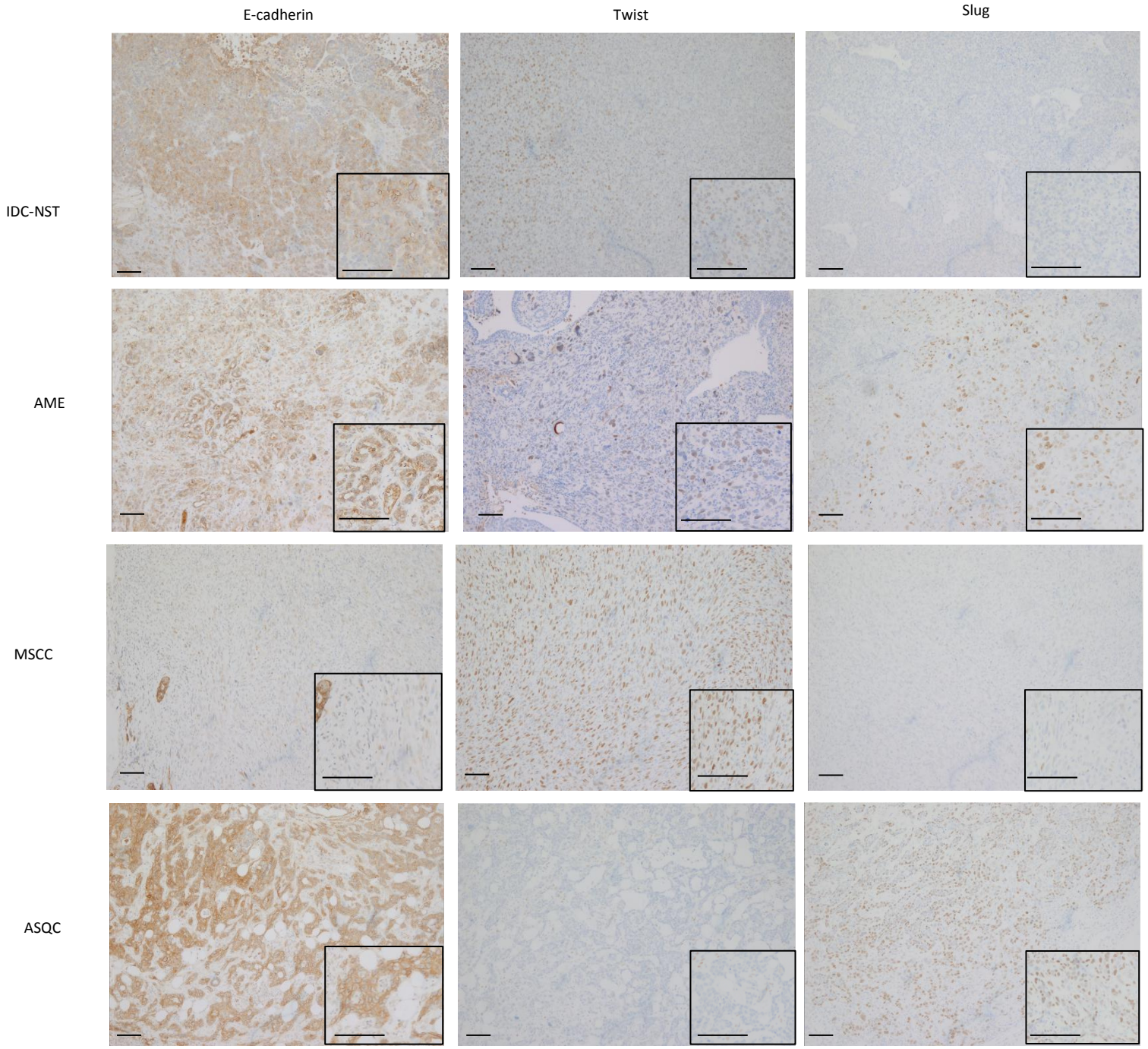

Figure 4.9 Representative pictures of EMT markers in resistant tumour types. *Immunohistochemistries were performed for E-cadherin, Twist and Slug to analyse EMT in the different tumour types within the resistant cohort. Scale bars show 100µm.*

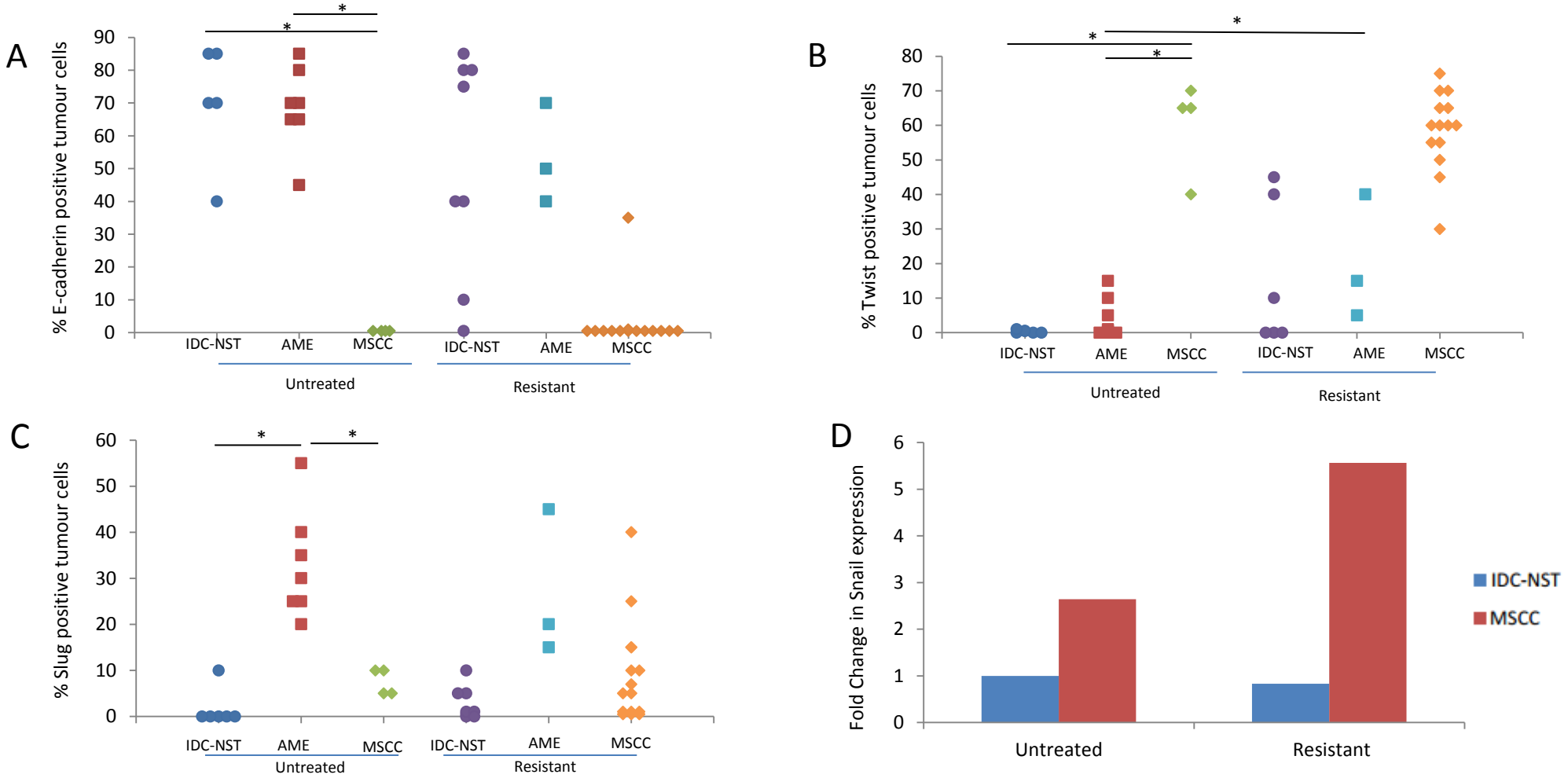

Figure 4.10 EMT markers in olaparib-resistant tumours. *Analysis of E-cadherin* ***(A),*** *Twist* ***(B)*** *and Slug* ***(C)*** *immunohistochemistries, showing the percentage of positive tumour cells, comparing untreated and resistant tumour types.* ***(D)*** *qRT-PCR analysis of Snail expression in untreated and resistant IDC-NSTs and MSCCs. *p≤0.05.*

4.2.5 Resistant IDC-NSTs show genetic similarities to MSCCs

A study from Dr Matthew Smalley's group performed a microarray to compare gene expression between different histopathological tumour types from mouse models of breast cancer (unpublished data). This data is suggestive of the genes that are characteristic for the different histological tumour types. qRT-PCR analysis of the expression of six of these genes were carried out in untreated tumours from *BlgCre-Brca2*$^{f/f}$*/p53*$^{f/f}$ mice and were compared to the expression levels in resistant tumours. As there were not enough AMEs and ASQCs to generate statistically significant data, these tumours were excluded from the analysis.

Using the microarray data, three genes that were characteristic for IDC-NSTs were chosen; *Sema3b, Foxa3* and *Sox8* (Figure 4.11). Results showed that untreated IDC-NSTs (n=4) showed a significant upregulation of all three genes compared to untreated MSCCs (n=4, Mann-Whitney U test; p=0.02, p=0.03 and p=0.03, respectively) which corresponds with the microarray data. Interestingly, resistant IDC-NSTs (n=4) showed a significant down-regulation in all three genes compared to untreated IDCNSTs (Mann-Whitney U test, p=0.03, p=0.03 and p=0.03, respectively). No significant differences were seen between untreated MSCCs and resistant MSCCs (n=4). This suggests that there are differences in gene expression between untreated and resistant IDC-NSTs.

Three genes that were shown to be characteristic for MSCCs were chosen from the microarray and analysed in the same samples as above (Figure 4.11). Corresponding with the microarray, the expression levels of *Grem1, Pcolce2* and *Hmga2* were shown to be significantly up-regulated in untreated MSCCs compared to untreated IDC-NSTs (Mann-Whitney U test, p=0.03, p=0.03 and p=0.03, respectively). No significant differences were seen between untreated MSCCs and resistant MSCCs. Resistant IDC-NSTs showed no significant difference in expression of *Pcolce2* compared to untreated tumours but they did show a significant upregulation of *Grem1* (Mann-Whitney U test, p=0.03) and a trend for higher expression of *Hmga2*, suggesting that resistant IDC-NSTs contain some genetic similarities to MSCCs.

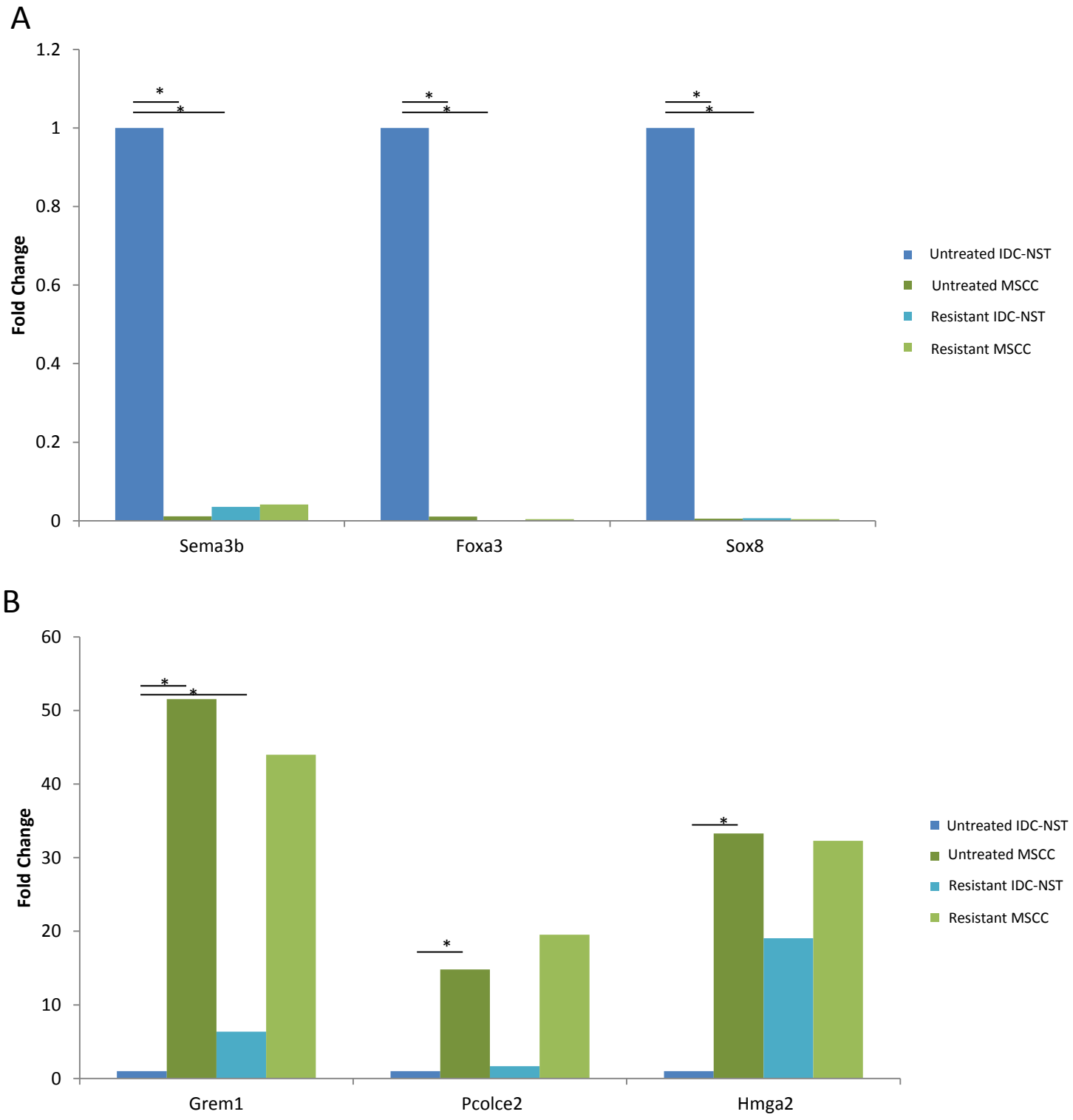

Figure 4.11 Comparison of IDC-NST and MSCC characteristic gene expression in untreated and resistant tumours. *qRT-PCR analysis of IDC-NST characteristic genes Sema3b, Foxa3 and Sox8* ***(A)*** *and MSCC characteristic genes Grem1, Pcolce2 and Hmga2* ***(B)****, comparing untreated and resistant IDC-NSTs and MSCCs. *p≤0.05*

4.2.6 Responding and resistant tumours show a mesenchymal signature

Results in this project suggest that an EMT-like process correlates with resistance to PARP inhibitors; however, it is unclear whether this EMT-like program is limited to a small number of markers coupled with morphological changes or whether broad changes are occurring in the transcriptional programmes of tumour cells. mRNA expression levels were compared from tumours that were either responding well to olaparib (n=7) or had become resistant to treatment (n=20). All mice had been treated with daily 100mg/kg olaparib and culled one hour after their final dose. Histopathological analysis showed that the responding cohort consisted of 6 IDC-NSTs and 1 ASQC, whereas the resistant cohort was made up of 12 MSCCs, 6 IDC-NSTs and 2 AMEs, with both cohorts showed similar staining patterns as other excellent responders and resistant tumours, as described previously.

Expression of genes were individually compared in the responding and resistant cohorts for differential expression, and network analysis showed that the main networks of genes were involved in development and function of the haematological system, control of the cell cycle, DNA replication, recombination and repair and inflammatory response (Appendix I); however, as of yet, I have not had the opportunity to follow-up these results.

Analysis of Brca2 and p53 expression showed low expression in resistant and responding tumours (Figure 4.12A), with no significant difference in p53 expression between the two cohorts. Resistant tumours did show a significant increase in Brca2 expression compared to responding tumours (Mann-Whitney U test, $p=0.004$), although the expression was still low. A similar pattern was also seen in Brca1 expression between the two cohorts (Mann-Whitney U test, $p<0.001$; Figure 4.12A). Expression levels of 53BP1 were also analysed, and there was found to be no difference in expression between the two cohorts (Figure 4.12A), suggesting that loss of this protein in not a mechanism of resistance to olaparib in *Brca2*-deficient mammary tumours, as has been shown in previously in a model of olaparib-resistant *Brca1/p53*-deficient breast cancer (Jaspers et al, 2013).

Principle component analysis of this expression data showed that the olaparib-resistant tumours cluster separately from the responding tumours, but also that those classified as resistant MSCCs clustered separately from the other resistant tumour types (Figure 4.12B), so we then compared gene expression between the different histopathological tumour

types. Compared to the resistant IDC-NSTs, resistant MSCCs showed up-regulation of the genes that encode Vimentin, Zeb1, and Zeb2 (Mann-Whitney U test $p<0.001$, $p<0.001$, $p<0.001$ respectively) and down-regulation of those that encode E-cadherin, CK18, Claudin 3, Claudin 4 and Claudin 7 (Figure 4.13; Mann-Whitney U test $p=0.002$, $p<0.001$, $p<0.001$, $p<0.001$ respectively), corresponding with previous data that these tumours have a similar expression profile to claudin-low tumours.

The responding and resistant IDC-NSTs also clustered separately in the principle component analysis, suggesting that even though they have the same morphology, differences in gene expression exist between the two cohorts. Compared to responding IDC-NSTs, resistant IDC-NSTs showed up-regulation of the genes that encode Twist, Brca1, CD44 and β-catenin (Figure 4.14; Mann-Whitney U test, $p=0.008$, $p=0.005$, p-0.013 and $p=0.005$ respectively). Interestingly both responding and resistant IDC-NSTs showed a mesenchymal gene signature (Figure 4.15), which correlates with previous data in this project which suggests that resistant IDC-NSTs have mesenchymal characteristics. In responding IDC-NSTs this mesenchymal signature may be due to the high proportion of stroma seen in these tumours, rather than in the epithelial cells themselves; however immunohistochemical analysis has shown a significant upregulation of Vimentin and Twist in epithelial cells compared to untreated IDC-NSTs (chapter 3).

4.2.7 Resistant tumours show a reduction in mammosphere forming units

Studies have shown that Claudin-low tumours have enrichment for cells with stem cell characteristics (Creighton *et al.* 2009; Hennessy *et al*. 2009). To investigate if olaparib-resistant tumours show a similar enrichment we compared the mammosphere-forming ability of these tumours (n=8) to that of untreated tumours (n=9) (Figure 4.16).

The percentage of mammosphere forming units (MFUs) was calculated by dividing the number of mammospheres formed by the number of cells seeded. In the untreated cohort there was a degree of variability, with MFUs ranging between 0.3-3.6% (Figure 4.16). Histopathological analysis of these tumours revealed that the majority (7/9) were IDC-NSTs with just 2 MSCCs, which accounted for two of the three lowest values of %MFUs (Figure 4.16). Resistant tumours showed a significant decrease in the %MFUs, ranging from 0.04-

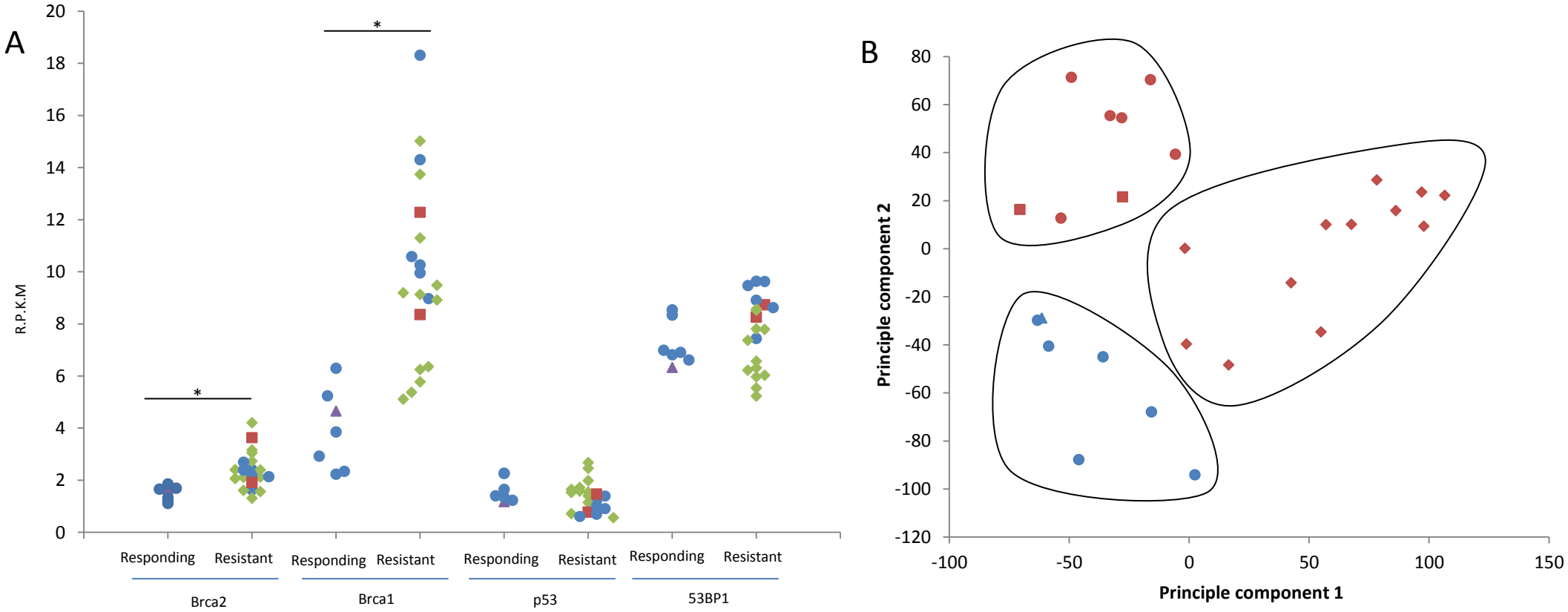

Figure 4.12 Comparison of RNA expression levels in responding and resistant tumours. (A) *RNA seq analysis compared the expression of Brca2, Brca1, p53 and 53BP1 in responding and resistant tumours. R.P.K.M=reads per kilobase of transcript per million mapped reads. Values for R.P.K.M – 0-0.5 represents very low expression, 0.5-8 represents low expression, 8-16 represents medium expression, 16-128 represents high expression, and above 128 represents very high expression. *p≤0.05.* ***(B)*** *Principle component analysis comparing responding (blue) and resistant (red) tumour types. Circles represent IDC-NSTs, triangles ASQCs, squares AMEs and diamonds MSCCs. Analysis was performed by AstraZeneca.*

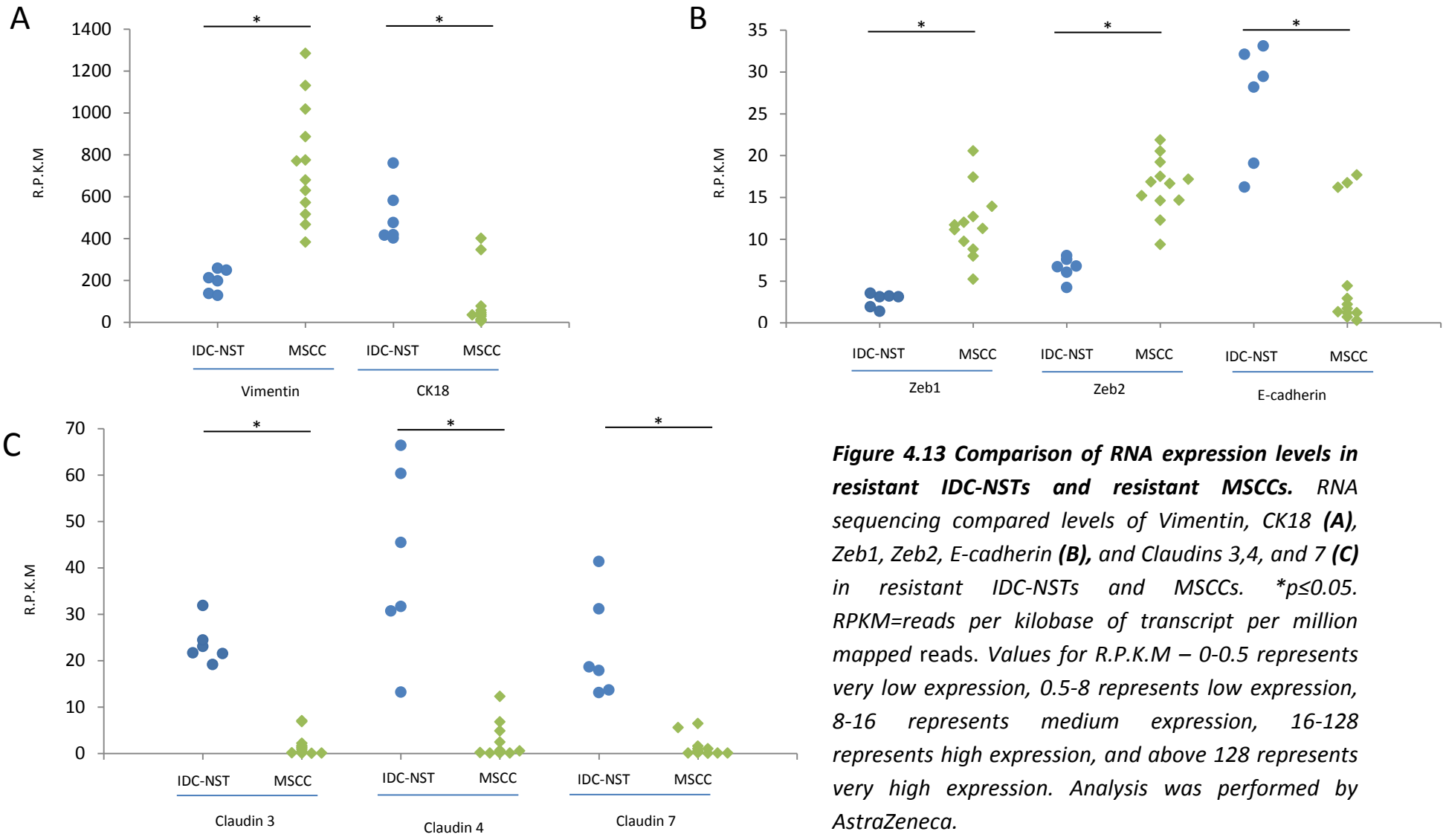

Figure 4.13 Comparison of RNA expression levels in resistant IDC-NSTs and resistant MSCCs. *RNA sequencing compared levels of Vimentin, CK18* ***(A)****, Zeb1, Zeb2, E-cadherin* ***(B),*** *and Claudins 3,4, and 7* ***(C)*** *in resistant IDC-NSTs and MSCCs. *p≤0.05. RPKM=reads per kilobase of transcript per million mapped* reads. *Values for R.P.K.M – 0-0.5 represents very low expression, 0.5-8 represents low expression, 8-16 represents medium expression, 16-128 represents high expression, and above 128 represents very high expression. Analysis was performed by AstraZeneca.*

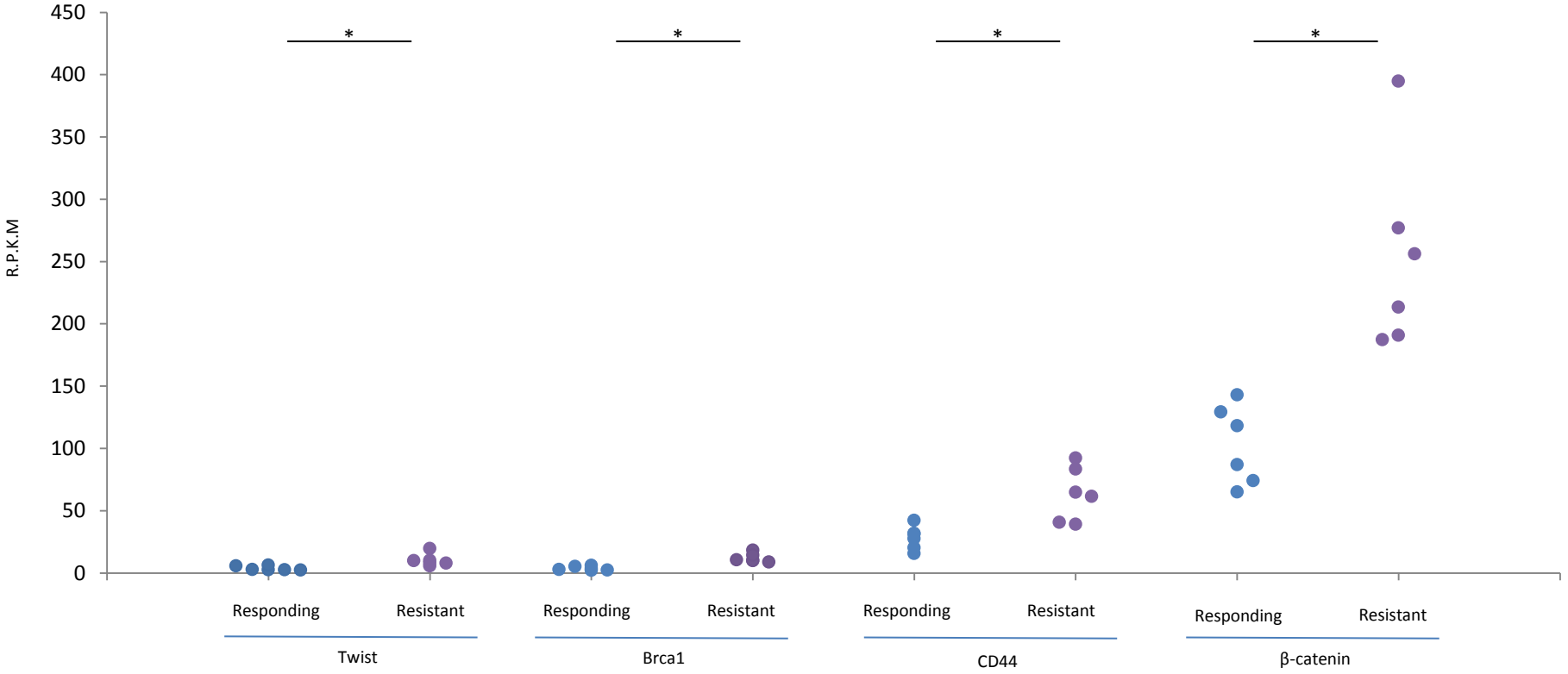

Figure 4.14 Comparison of RNA expression levels in responding and resistant IDC-NSTs. *RNA sequencing compared levels of Twist, Brca1, CD44, β-catenin and CK18 in responding and resistant IDC-NSTs. *p≤0.05. RPKM=reads per kilobase of transcript per million mapped reads. Values for R.P.K.M – 0-0.5 represents very low expression, 0.5-8 represents low expression, 8-16 represents medium expression, 16-128 represents high expression, and above 128 represents very high expression. Analysis was performed by AstraZeneca.*

Figure 4.15 Analysing EMT signature of responding and resistant tumours. *RNA expression profiles were compared to an in-house EMT signature, where positive values are associated with an epithelial profile and negative values are associated with a mesenchymal profile. Circles represent IDC-NSTs, triangles ASQCs, squares AMEs and diamonds MSCCs. Analysis was performed by AstraZeneca.*

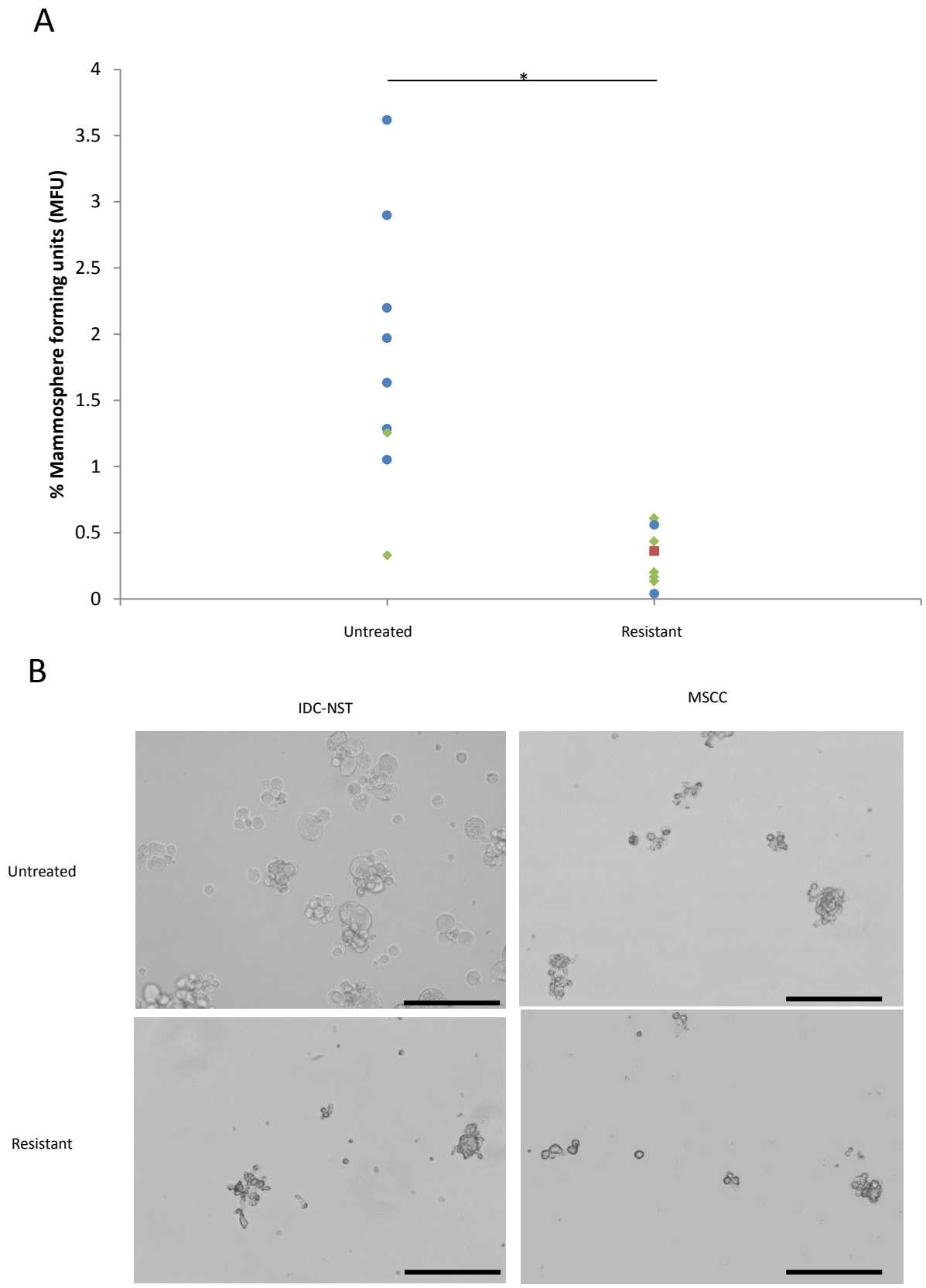

Figure 4.16 Mammosphere forming units in untreated and resistant tumours. (A) *Comparison of %MFUs in untreated and resistant tumours. Circles represent IDC-NSTs, triangles ASQCs, squares AMEs and diamonds MSCCs. *p≤0.05* ***(B)*** *Representative pictures of*

mammospheres from untreated and resistant IDC-NSTs and MSCCs. Scale bar represents 200µm.

0.6% (Mann-Whitney U test, $p<0.01$). Resistant tumours were characterised as 5 MSCCs, 2 IDC-NSTs and 1 AME, with all tumour types showing similar %MFUs. This suggests that olaparib-resistant tumours have a lower number of mammosphere-producing cells than untreated tumours. Mammospheres were fixed and embedded in paraffin wax to allow for H&E and immunohistochemical staining. Immunohistochemistry on mammospheres from the untreated cohort revealed that they had similar staining patterns to the tumour type they originated from (Figure 4.17), with those from IDC-NSTs showing high CK18 and E-cadherin levels and low CK14 and p63 levels. Those from MSCCs showing high Vimentin levels and low levels of CK18, CK14, p63 and E-cadherin. However, mammospheres from IDC-NSTs did show an higher levels of Vimentin staining, with variable staining between different samples (ranging from 1-60% of positive cells, Figure 4.17), compared to untreated tumours (<1%). Mammospheres from the resistant cohort also showed similarities in staining to the corresponding tumour type, with those from MSCCs showing high Vimentin and variable expression of CK18, CK14 and p63, those from IDC-NSTs showing high CK18 and E-cadherin levels and low levels of CK14 and p63, and those from the AME showing high Vimentin and E-cadherin positivity (Figure 4.18). In contrast to the corresponding tumour type, mammospheres from resistant MSCCs showed higher E-cadherin levels, those from resistant IDC-NSTs showed low Vimentin expression and those from the AME showed low levels of CK18, CK14 and p63 (Figure 4.18). This data suggests that mammospheres formed from different tumour types retain some of their characteristic staining patterns, but that they may not be truly reflective of the tumour types from which they originated.

4.2.8 Carboplatin-resistant tumours show similarities to olaparib-resistant tumours

Other studies have shown that the acquisition of EMT features is associated with therapeutic resistance (Li *et al.* 2008; Creighton *et al*. 2009), suggesting that the results seen in olaparib-resistant tumours may also occur in those resistant to other drugs. To investigate this, tumours from *BlgCre-Brca2$^{f/f}$/p53$^{f/f}$* mice that were treated with IP 50mg/kg Carboplatin once every four weeks until tumours relapsed (n=15, performed by Dr Trevor

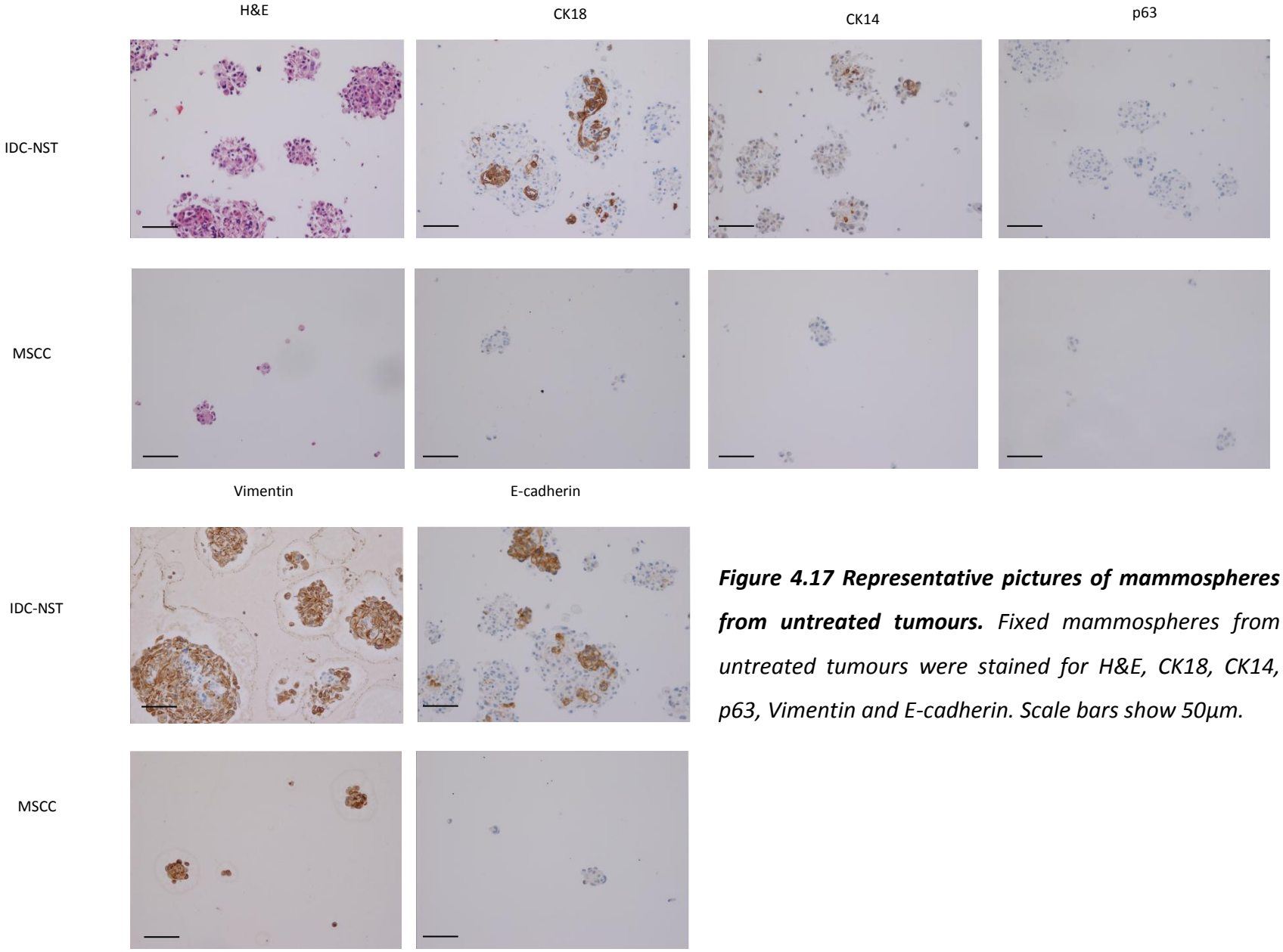

Figure 4.17 Representative pictures of mammospheres from untreated tumours. *Fixed mammospheres from untreated tumours were stained for H&E, CK18, CK14, p63, Vimentin and E-cadherin. Scale bars show 50µm.*

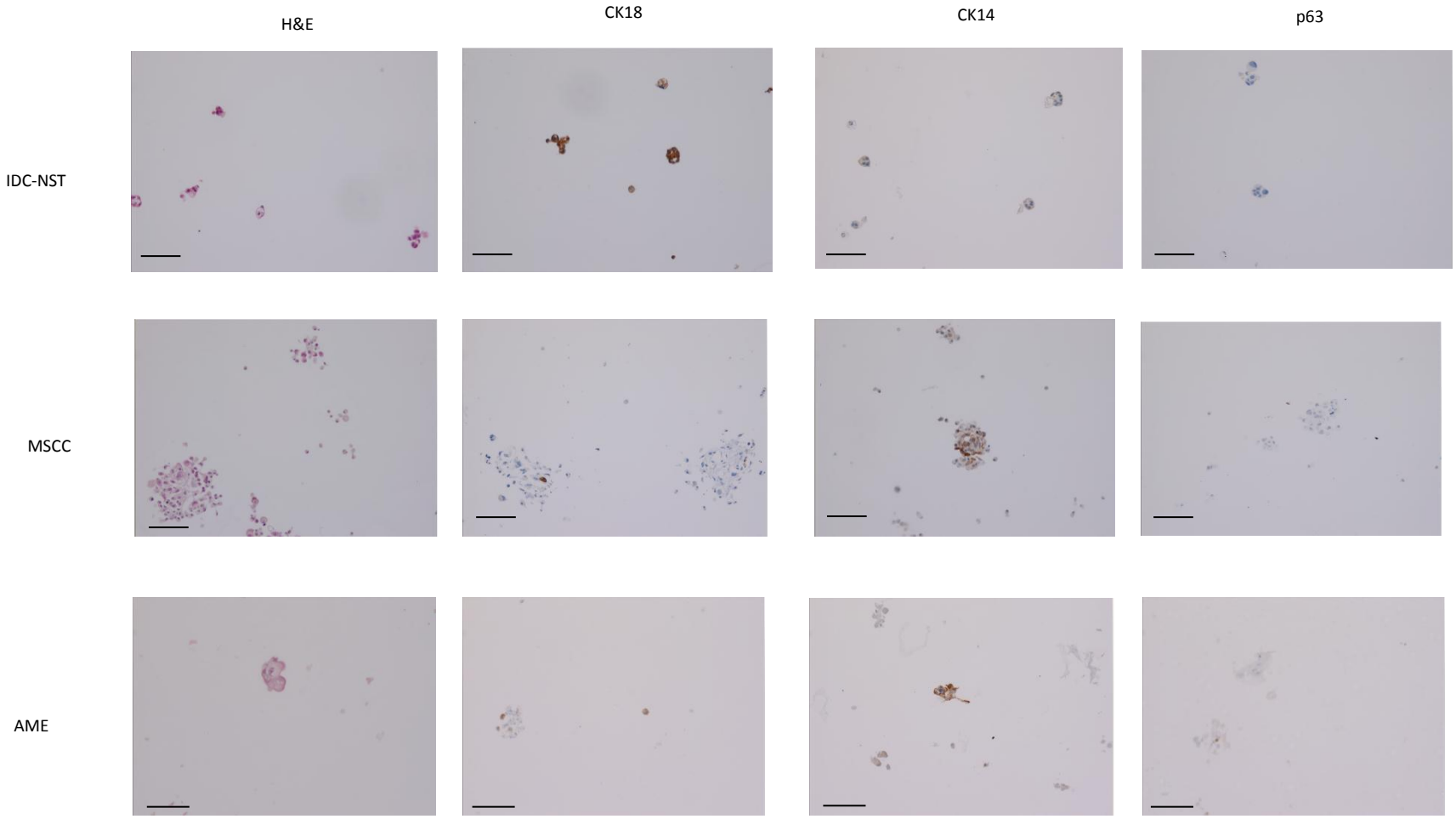
H&E
CK18
CK14
p63
IDC-NST
MSCC
AME

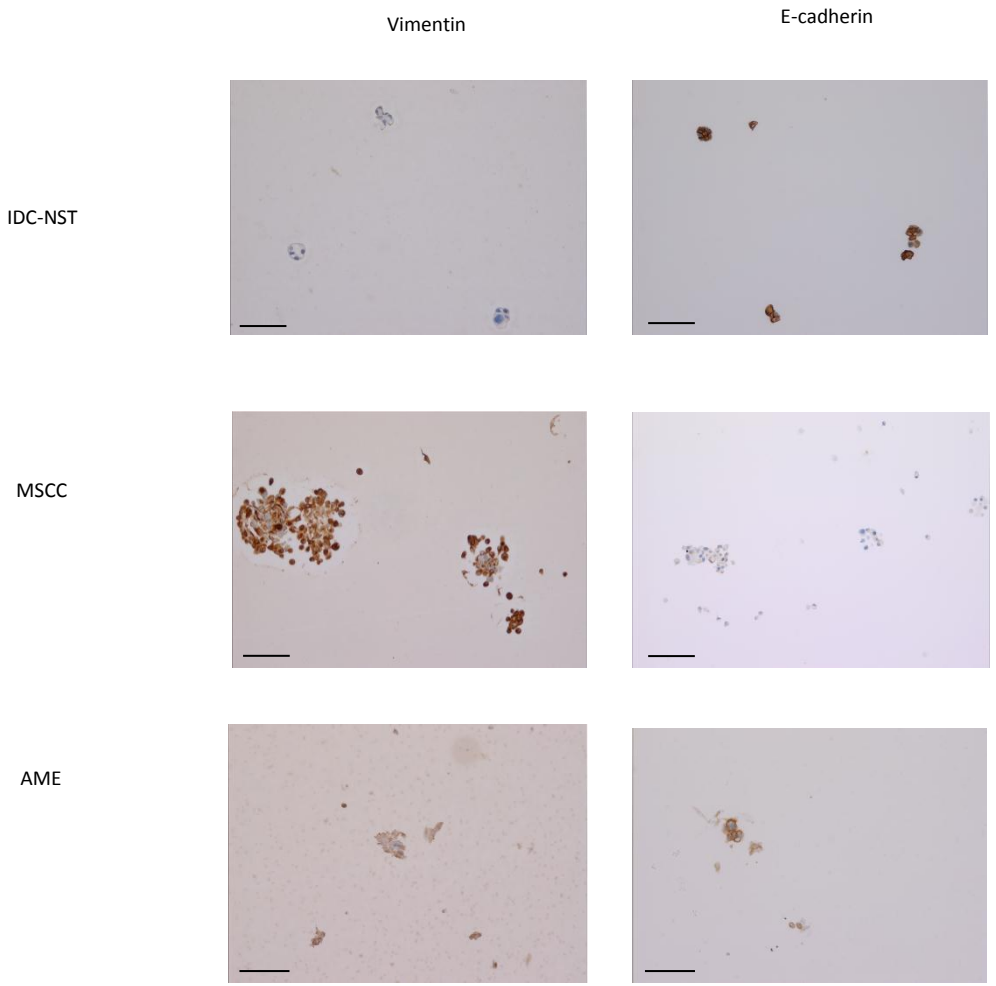

Figure 4.18 Representative pictures of mammospheres from olaparib-resistant tumours. *Fixed mammospheres from resistant tumours were stained for H&E, CK18, CK14, p63, Vimentin and E-cadherin. Scale bars show 50µm.*

Hay), were analysed histopathologically and for the expression of EMT markers Vimentin and Twist.

The majority (67%) of carboplatin-resistant tumours were found to be IDC-NSTs, with MSCCs accounting for 26% and AMEs 7%, resulting in a significant difference in proportions compared to untreated tumours (Chi Squared, p=0.05; Figure 4.20), with a higher proportion of IDC-NSTs and MSCCs and a lower proportion of AMEs. These proportions are also significantly different to those seen in olaparib-resistant tumours (Chi Squared, p=0.05; Figure 4.20), which have a higher proportion of MSCCs and a lower proportion of IDC-NSTs. This suggests that although there is an increase in MSCCs in carboplatin-resistant tumours there are differences between the two therapies.

Compared to untreated IDC-NSTs, those in the carboplatin-resistant cohort showed a significant reduction in CK18 staining and an increase in Vimentin and Twist staining (Mann-Whitney U test, p=0.02, p<0.01 and p=0.026 respectively), whilst they maintained variable expression of CK14 (1-65%) and low expression of p63 (<1%, Figure 4.19, Figure 4.20, Figure 4.21). These are similar staining patterns to olaparib-resistant IDC-NSTs (Figure 4.22), which also show a decrease in CK18 staining and an increase in Vimentin staining, with a subset showing an increase in Twist staining, compared to untreated tumours.

The one AME in this cohort showed a similar staining pattern to untreated AMEs, with a high level of CK14 (75%) and p63 (65%), a low level of Vimentin (1%) and Twist (<1%), and 15% positivity for CK18 (Figure 4.19, Figure 4.20, and Figure 4.21). The expression patterns differ to those seen in olaparib-resistant AMEs (Figure 4.22), as these show higher levels of positivity for Vimentin (40-50%) and Twist (5-40%).

The MSCCs in this cohort showed variable CK18 staining, with 2 tumours showing an increase compared to untreated MSCCs, while retaining low expression of CK14 and p63 (<1%, Figure 4.19 Figure 4.20 and Figure 4.21). The majority showed high Vimentin (65-80%) and Twist staining (40-70%), similar to the levels seen in untreated MSCCs (Figure 4.19 and Figure 4.21), although one tumour showed a low level of Twist (10%). MSCCs in this cohort showed similar CK18, p63, Vimentin and Twist staining, and a trend for a decrease in CK14 staining compared to olaparib-resistant MSCCs (Figure 4.22).

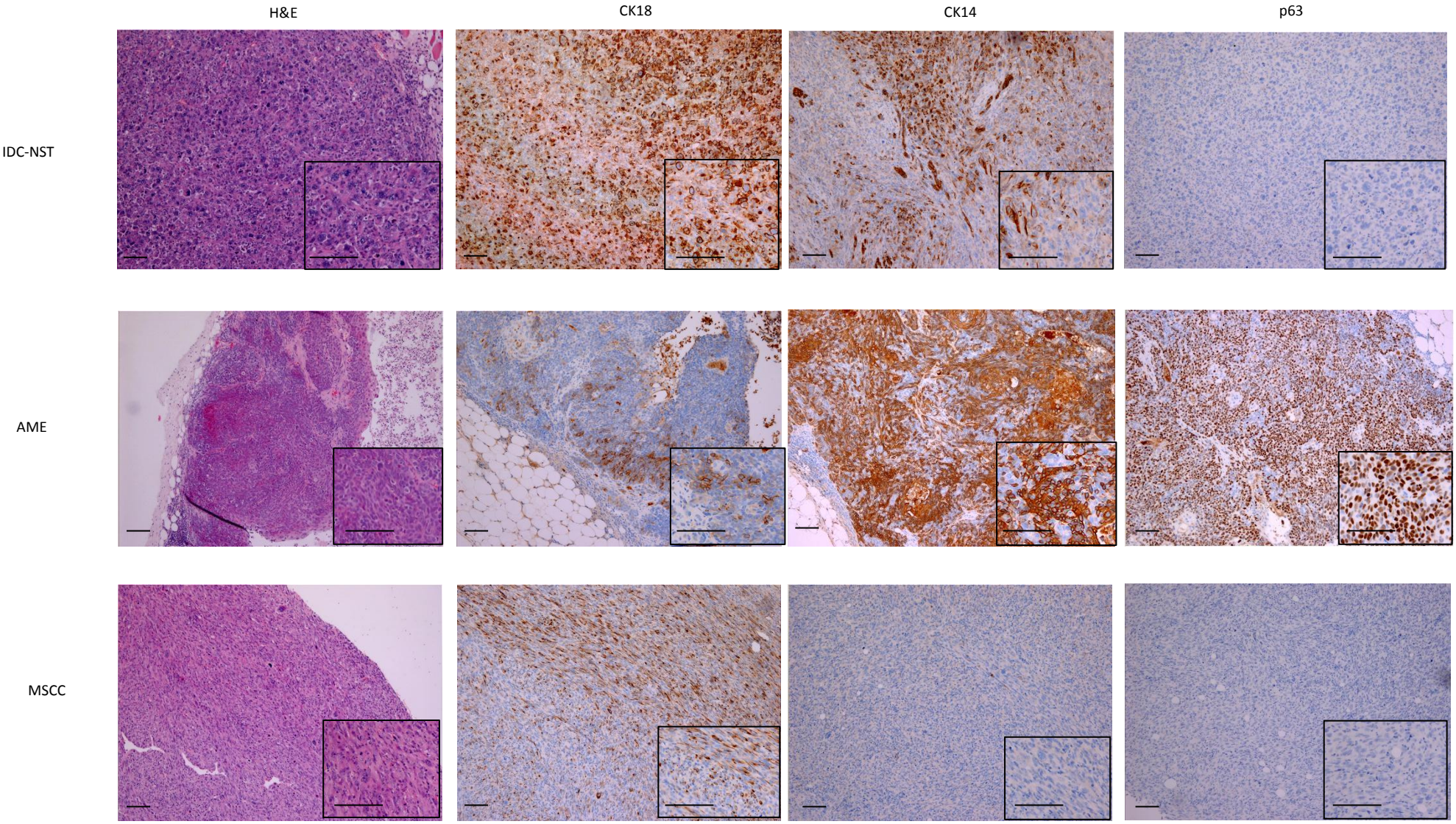
H&E
CK18
CK14
p63
IDC-NST
AME
MSCC

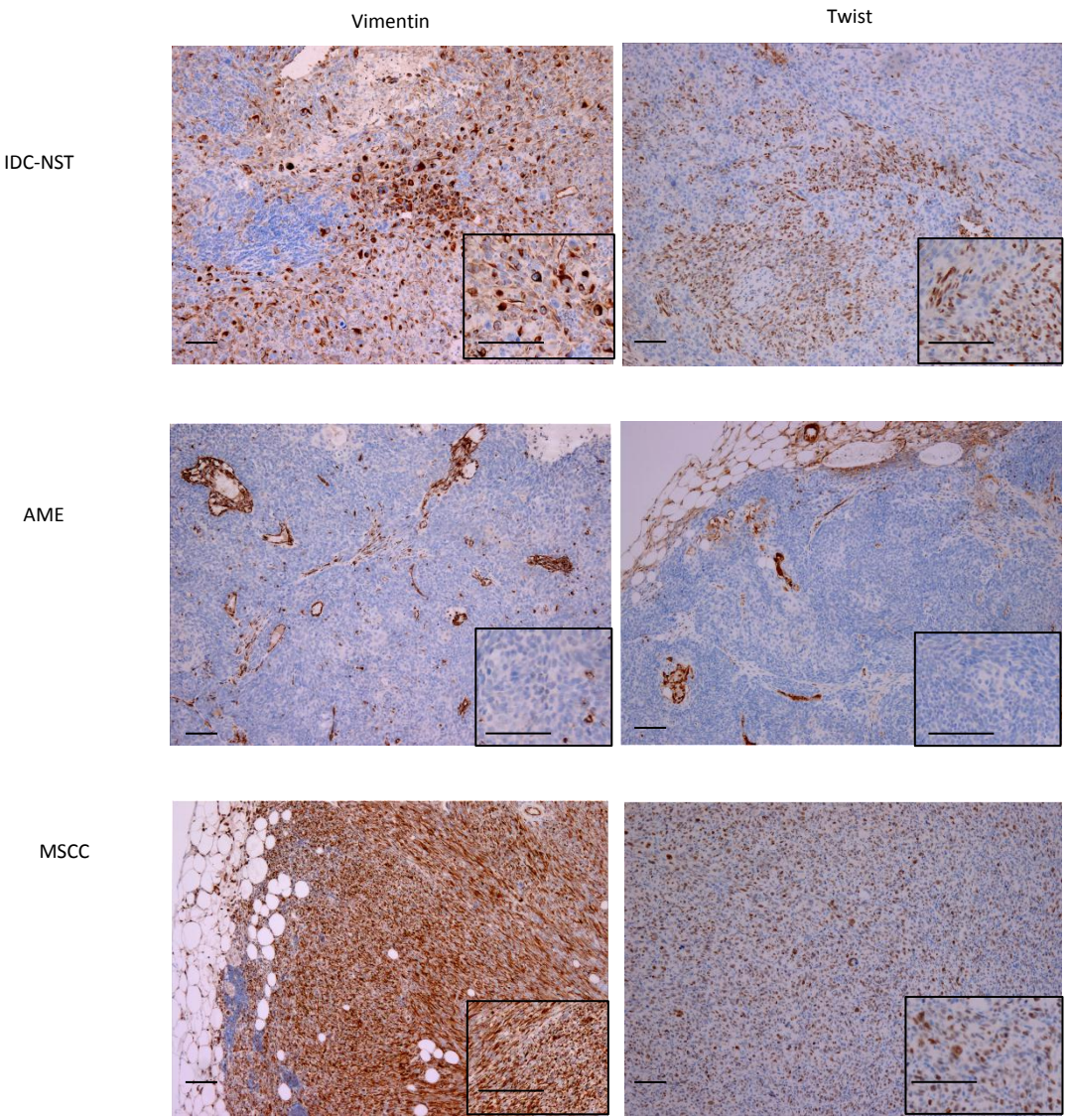

Figure 4.19 Representative pictures of immunohistochemical stains in Carboplatin-resistant tumours. *Carboplatin-resistant were classified by histopathology, with H&E staining used to analyse cell morphology. The different tumour types were analysed for Ck18, Ck14, p63, Vimentin and Twist positivity. Scale bars show 100µm.*

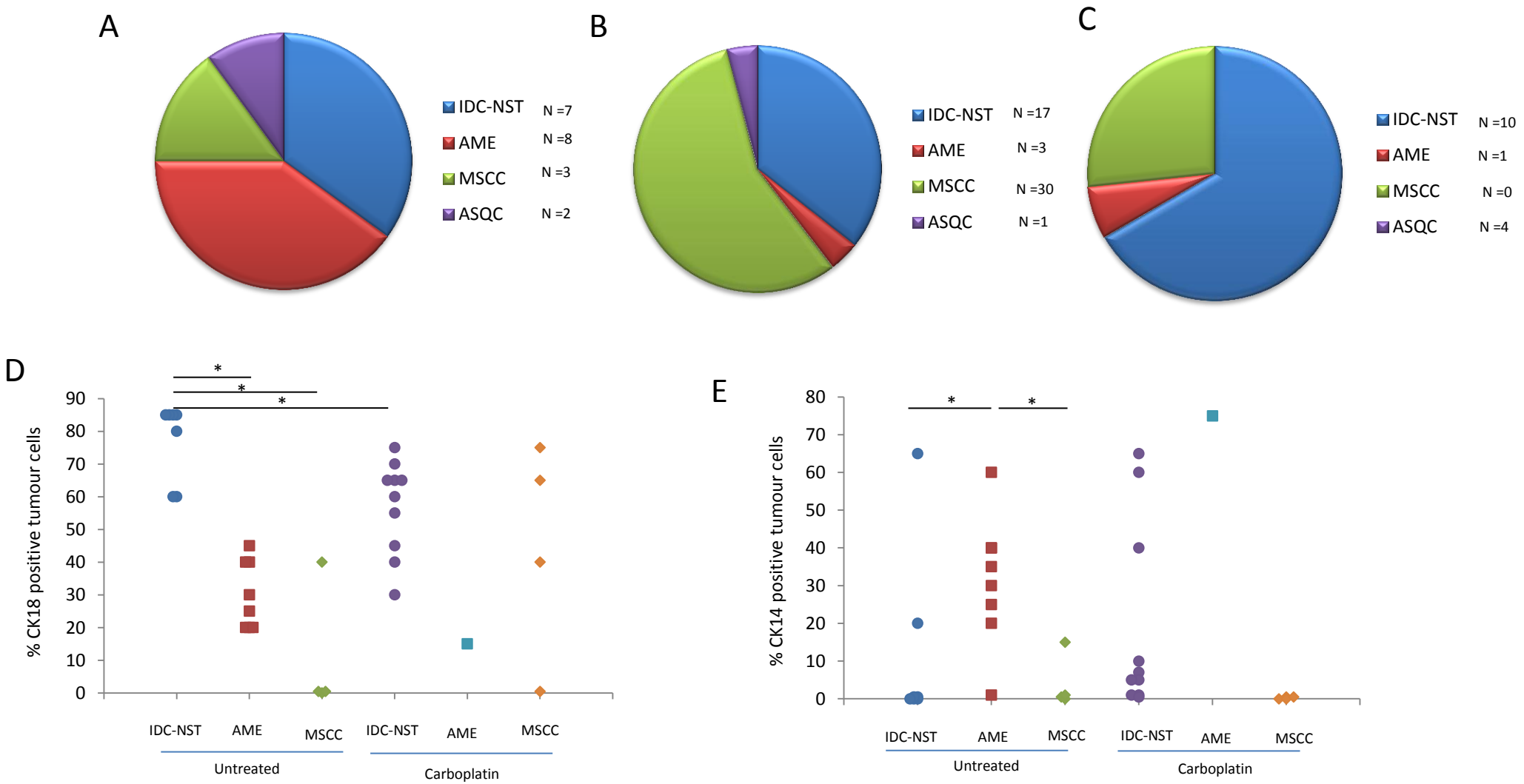

Figure 4.20 Proportions of Carboplatin-resistant tumours compared to untreated and olaparib-resistant cohorts. *Carboplatin- resistant tumours were classified by histopathology* ***(C)*** *and the proportions were compared to those from untreated* ***(A)*** *and olaparib-resistant cohorts* ***(B)****. Carboplatin-resistant tumours were analysed for CK18* ***(D)*** *and CK14* ***(E)*** *positivity, and compared to untreated tumours. *p≤0.05*

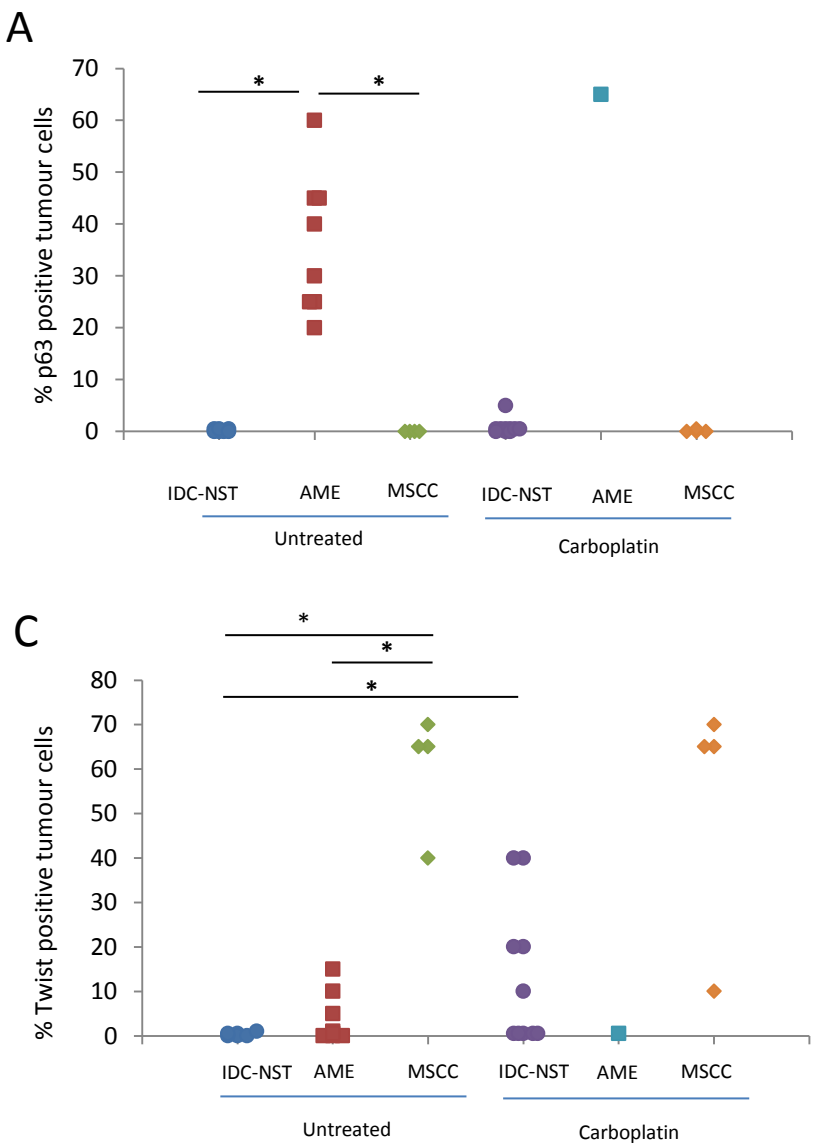

Figure 4.21 Comparison of Carboplatin-resistant tumours to untreated tumours. *Positivity for p63* ***(A),*** *Vimentin* ***(B)*** *and Twist* ***(C)*** *was analysed in carboplatin-resistant tumours, and compared to levels in untreated tumours. *p≤0.05*

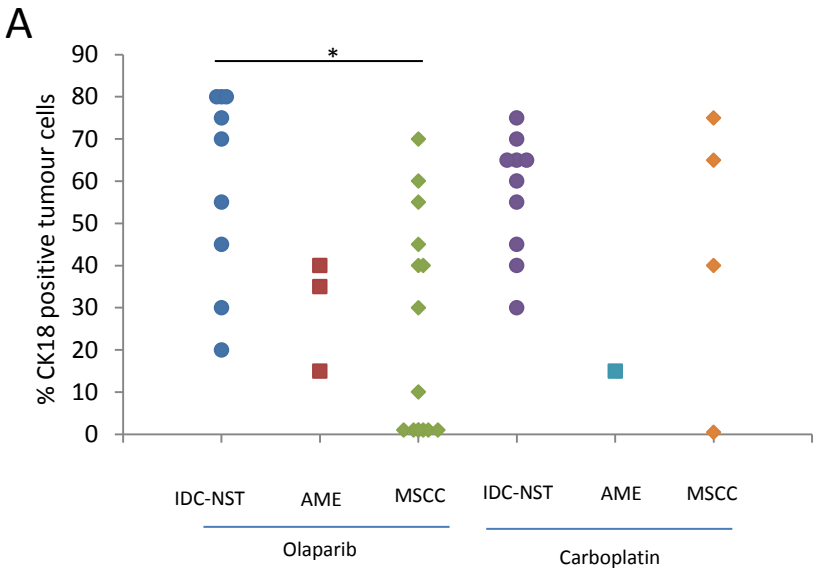
A
% CK18 positive tumour cells
90
80
70
60
50
40
30
20
10
0
*
IDC-NST
AME
MSCC
IDC-NST
AME
MSCC
Olaparib
Carboplatin

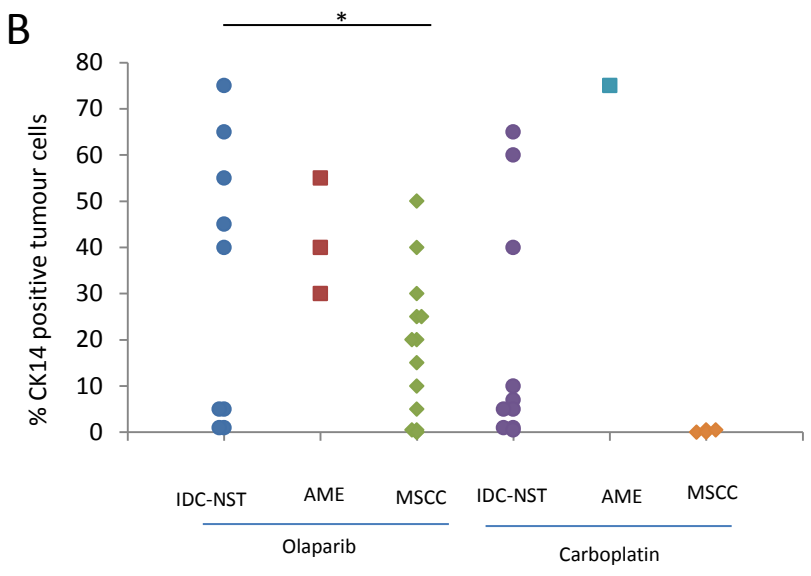
B
% CK14 positive tumour cells
80
70
60
50
40
30
20
10
0
*
IDC-NST
AME
MSCC
IDC-NST
AME
MSCC
Olaparib
Carboplatin

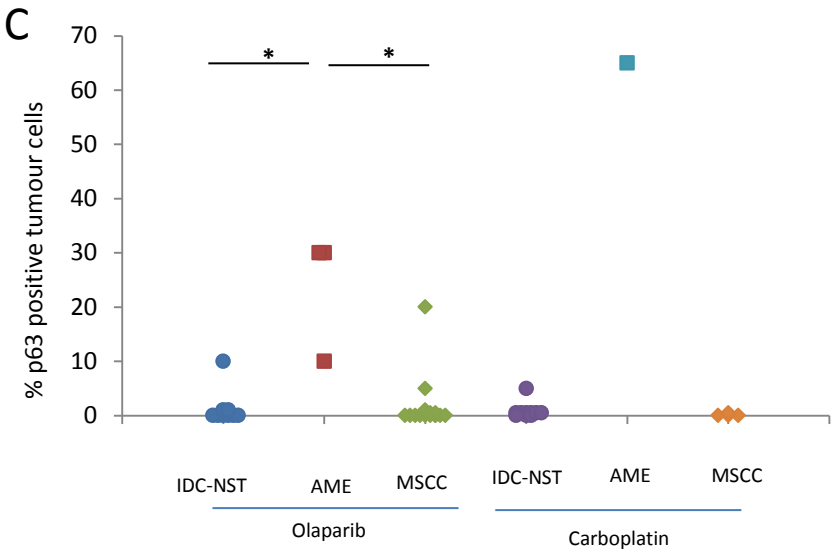
C
% p63 positive tumour cells
70
60
50
40
30
20
10
0
*
*
IDC-NST
AME
MSCC
IDC-NST
AME
MSCC
Olaparib
Carboplatin

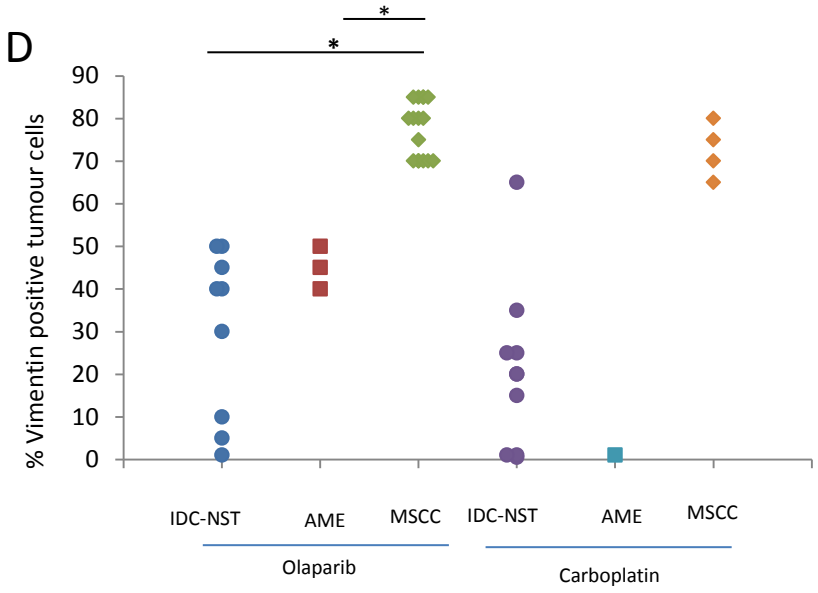
D
% Vimentin positive tumour cells
90
80
70
60
50
40
30
20
10
0
*
*
IDC-NST
AME
MSCC
IDC-NST
AME
MSCC
Olaparib
Carboplatin

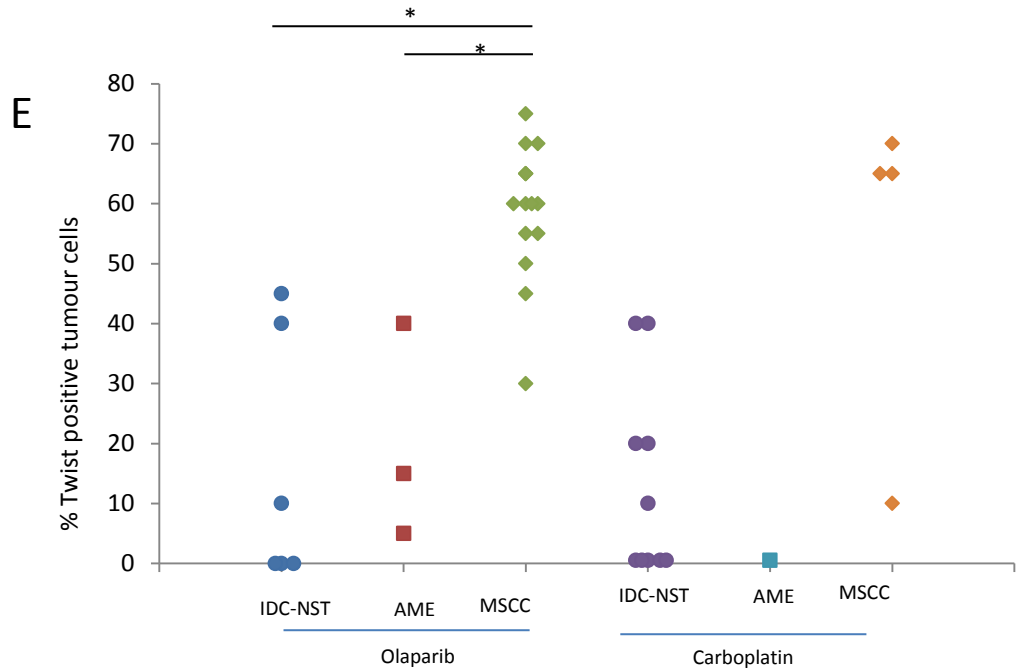

Figure 4.22 Comparison between Olaparib- and Carboplatin-resistant tumours. *Levels of CK18* ***(A)****, CK14* ***(B)****, p63* ***(C)****, Vimentin* ***(D)*** *and Twist* ***(E)*** *positivity in carboplatin-resistant tumours (carboplatin) were compared to those seen in olaparib-resistant tumours (olaparib). *p≤0.05*

These results suggest, as with olaparib-resistant tumours, that the majority of carboplatin-resistant tumours show mesenchymal features, either by the presence of morphologically-recognisable spindle cells or by changes in various protein levels.

4.3 Discussion

4.3.1 Tumours from *BlgCre-Brca2$^{f/f}$/p53$^{f/f}$* mice are showing a novel mechanism of olaparib resistance

Results from the work described in this chapter suggest that the three currently proposed mechanisms of resistance to PARP inhibitors in HR-deficient cancers do not account for the resistance to olaparib seen in our *BlgCre-Brca2$^{f/f}$/p53$^{f/f}$* breast cancer model.

The first of these involves up-regulation of P-gps, which are members of the multi-drug resistance protein (MDR) family and are transmembrane protein pumps that actively efflux drugs. It is well established that over-expression of MDRs are involved in resistance to a number of drugs (reviewed in Gottesman 2002), for example a study in a mouse model of *BRCA1*-mutated breast cancer showed that resistance to doxorubicin was due to upregulation of P-gps (Pajic *et al.* 2009). Previous studies in *Brca2*- and *Brca1*-deficient mammary tumours that became resistant to olaparib in a subset of tumours was associated with a significant up-regulation of P-gps compared to untreated tumours, suggesting that this may be a mechanism of olaparib resistance (Rottenberg *et al*. 2008; Hay *et al*. 2009). Here, it has been shown that the addition of the P-gp inhibitor Tariquidar to mice with olaparib-resistant tumours had no effect on tumour relapse, correlating with unpublished data from our group, in which resistant tumours were treated with the novel PARP inhibitor AZD2461, which has a lower affinity for P-gps, and also showed no effect on tumour relapse (Hay *et al.* unpublished). These two pieces of experimental data suggest that the previously reported up-regulation of P-gps is simply a characteristic of resistant tumours, rather than a mechanism of resistance. This differs from studies in a mouse model of *Brca1/p53* mutant breast cancer, where sensitivity to olaparib was at least partially restored upon inhibition of P-gps with Tariquidar or by treatment with AZD2461 (Rottenberg *et al*. 2008; Jaspers *et al*. 2013). however tumours from a similar mouse model, which contained additional P-gp null alleles, were treated with olaparib and eventually developed relapsed, showing that olaparib resistance can develop in the absence of P-pgs (Jaspers *et al*. 2013).

These results suggest that there may be differences in the mechanisms of resistance to PARP inhibition between the Brca1- and Brca2-deficient mouse models and clearly there are important clinical implications if such differences were replicated in *BRCA1*- and *BRCA2*-mutated human breast cancers.

Analysis of olaparib concentration in olaparib-resistant tumours show a significant reduction 1 hour after the final treatment compared to tumours 1 hour after a single dose, suggesting that the up-regulation of P-gps may be having an effect on olaparib levels. However, in these same tumours PARP activity is still suppressed, which would explain why inhibition of the P-gps in these tumours had no effect on tumour relapse. In this study results showed that tumours treated with a single dose of vehicle showed variable levels of PARP activity, and that the variability correlated with tumour type. Other studies have shown that PARP expression is heterogeneous in human breast tumours and that certain molecular subtypes show increased levels compared to others (Goncalves *et al*. 2011; Prat and Perou 2011). This suggests that different tumour types have different endogenous levels of PAR, which may contribute to the differences in response to olaparib therapy (chapter 3), and therefore has clinical implications.

The second proposed mechanism of resistance involves the protein 53BP1. In a subset of olaparib-resistant tumours from a *Brca1*-deficient mouse model it was shown that loss of 53BP1 leads to restoration of the HR pathway (Jaspers *et al*. 2013). RNA expression data from tumours from the *BlgCre-Brca2*$^{f/f}$*/p53*$^{f/f}$ model showed no significant difference in 53BP1 levels between responding and resistant tumours. Taken together with the fact that 53BP1 is known to interact with BRCA1 but not BRCA2 (Bouwman *et al.* 2010), it therefore seems unlikely that modulation of 53BP1 levels is a mechanism of resistance in *BRCA2*-mutated breast cancer.

The third established mechanism of resistance involves secondary activating mutations in the BRCA2 gene. Preclinical and clinical studies have shown that olaparib-resistant tumours contain such mutations, resulting in the re-activation of the protein and restoration of the HR pathway (Edwards *et al*. 2008; Barber *et al*. 2013). Similar results have been seen in tumours that become resistant to carboplatin and cisplatin (Edwards *et al*. 2008; Sakai *et al.*

2008). Analysis of Brca2 mRNA levels in *BlgCre-Brca2$^{f/f}$/p53$^{f/f}$* mice showed a significant increase in resistant tumours compared to responding tumours, although expression was still low, and Brca1 mRNA levels were also shown to be significantly increased in resistant tumours. This suggests that resistant tumours may be trying to up-regulate genes involved in the HR pathway to overcome the synthetic lethality; however, given the large deletion of the *Brca2* coding sequence upon Blg-Cre activated recombination, we hypothesis that the HR pathway is inactive in these tumours, suggesting that the differences in Brca levels do not have a role in olaparib resistance.

It therefore seems clear that resistance to olaparib in our model falls out with the current proposed pre-clinical and clinical mechanisms and that there must be other novel mechanisms which account for the tumour relapse seen in our tumours.

4.3.2 Olaparib-resistant tumours have mesenchymal features

Following extensive histopathological and immunohistochemical analysis described in this chapter, olaparib-resistant tumours in our model were shown to be predominantly MSCCs, which make up a much smaller proportion of untreated tumours. Results from chapter 3 suggest that these tumours are similar to claudin-low tumours, and mRNA analysis in this chapter supports this suggestion, by showing up-regulation of *Vim, Zeb1,* and *Zeb2,* and down-regulation of *Cdh1*, *CK18* and the genes that encode Claudins 3, 4 and 7. RNA analysis also showed that MSCCs arising in this *BlgCre-Brca2$^{f/f}$/p53$^{f/f}$* mouse model have similar expression to MSCCs from other mouse models by showing a significant up-regulation of *Grem1, Pcolce2* and *Hmga2* and a down-regulation of the IDC-NST associated genes *Sema3b, Foxa3* and *Sox8* (Smalley *et al.* unpublished) compared to untreated IDC-NSTs. The Grem1 and Hmga2 proteins are hypothesised to play a role in EMT (Carvajal *et al.* 2008; Thuault *et al.* 2008), and Pcolce2 is involved in the cleavage of pro-collagen (Steiglitz *et al.* 2002), possibly explaining why these genes are specific to this mesenchymal-like tumour type. Currently there are no studies explaining the link between the three IDC-NST associated genes and breast cancer, although Foxa3's family member Foxa1 has been shown to be a luminal lineage-specific gene (Yamaguchi *et al.* 2008), corresponding with the luminal genetic profile of these tumours.

The high proportion of MSCCs in the resistant cohort correlates with other studies that suggest that metaplastic carcinomas are associated with treatment resistance (Al Sayed *et al*. 2006; Hennessy *et al*. 2009). Olaparib-resistant tumours treated with either AZD2461 or Tariquidar and AZD2461-resistant tumours showed similar proportions to olaparib-resistant tumours, adding weight to the suggestion that olaparib resistance in a BRCA2 setting may occur following spindle cell metaplasia to generate spindle cell carcinomas which are refractory to PARP inhibitor therapy. It is not really surprising that the tumours which were given the follow-up therapies are so similar, as initial treatment regimes were identical and the follow-up had no effect in either case, but it is interesting to note that treatment with the alternative PARP inhibitor had the same effect as treatment with olaparib. Currently there are no extensive studies that show that olaparib-resistant *Brca1*-deficient mammary tumours show an increase in MSCCs; however, one such AZD2461-resistant tumour was shown to have an EMT phenotype (Jaspers *et al*. 2013), suggesting that EMT may be associated with resistance to PARP inhibitors in both *Brca1*- and *Brca2*-deficient tumours.

Resistant tumours characterised as IDC-NSTs show an EMT gene signature, including increased expression of EMT markers/associated genes Vimentin, Twist and *Grem1,* and a decreased expression of IDC-NST/luminal genes CK18, *Sema3b, Fox3a* and *Sox8,* compared to untreated IDC-NSTs. This suggests that even though olaparib-resistant tumours show different morphologies they all show EMT characteristics, which correlates with other studies where the acquisition of EMT features has been associated with therapeutic resistance (Creighton *et al*. 2009; Liu *et al.* 2013). RNA analysis also showed that resistant IDC-NSTs have a significant increase in the β-catenin and CD44 mRNA expression compared to responding IDC-NSTs, suggesting that these tumours have an increase in Wnt signalling. Wnt signalling has been shown to induce EMT, through the regulation of Snail (Yook *et al*. 2005), suggesting a role for this pathway in olaparib resistance. CD44, as well as being a Wnt target gene, is also a cancer stem cell marker in human mammary tumours. Stem-like cells from breast cancer cells can be sorted from mixed populations in humans by the $CD44^{+}/CD24^{-/low}$ markers (Al-Hajj *et al.* 2003), suggesting that resistant IDC-NSTs may contain more cells with stem-cell characteristics, however, the mammosphere experiment

in this chapter showed a decrease in MFUs compared to untreated tumours, so the increased expression of CD44 may be due to Wnt signalling.

Resistant MSCCs show very similar immunohistochemical staining patterns and gene expression to untreated MSCCs; however, they do show a significant increase in CK18 positive cells and a significant increase in proliferating cells, resulting in a proliferation rate that is similar to the other tumour types, suggesting that they have some luminal characteristics. Some of them also contain epithelial sections which show characteristic staining patterns of IDC-NSTs or AMEs, which is similar to what is seen in moderately-responding MSCCs on daily olaparib therapy at 30 days into treatment. The presence of epithelial sections and spindle cells that are CK18-positive in MSCCs, and epithelial tumour types with EMT features, suggest that resistant tumours result from olaparib therapy either by cellular conversion or clonal expansion (Figure 4.23). The former would suggest that epithelial cells acquire mesenchymal characteristics (through EMT) during olaparib therapy, resulting in resistance to the drug. This could be linked to cancer stem cells as studies have shown that the induction of EMT in mammary epithelial cells *in vitro* results in the expression of stem cell markers (Mani *et al.* 2008) and that non-cancer stem cells can convert to cancer stem cells by the induction of ZEB1 expression (Chaffer *et al.* 2013). Other studies have shown treatment-induced EMT, with cisplatin treatment in ovarian cancer cell lines (Ahmed *et al*. 2010; Latifi *et al*. 2011), cyclosporine A treatment in renal proximal tubular epithelial cells (McMorrow *et al.* 2005), and Adriamycin treatment in a breast cancer cell line (Li *et al*. 2009), suggesting that EMT conversion may occur in response to a variety of different drugs. The clonal expansion theory would suggest that cells which are intrinsically resistant to olaparib, possibly those with EMT features and/or stem cell-like properties, would remain during treatment, with their outgrowth resulting in tumour relapse. A study by Li and colleagues suggests that cancer stem cells are resistant to conventional cancer therapies, as they showed in patients that have undergone 12 weeks of chemotherapy, that there is an increase in the percentage of cells with stem cell markers and stem cell-like properties (Li *et al*. 2008), so these cells may also be resistant to other

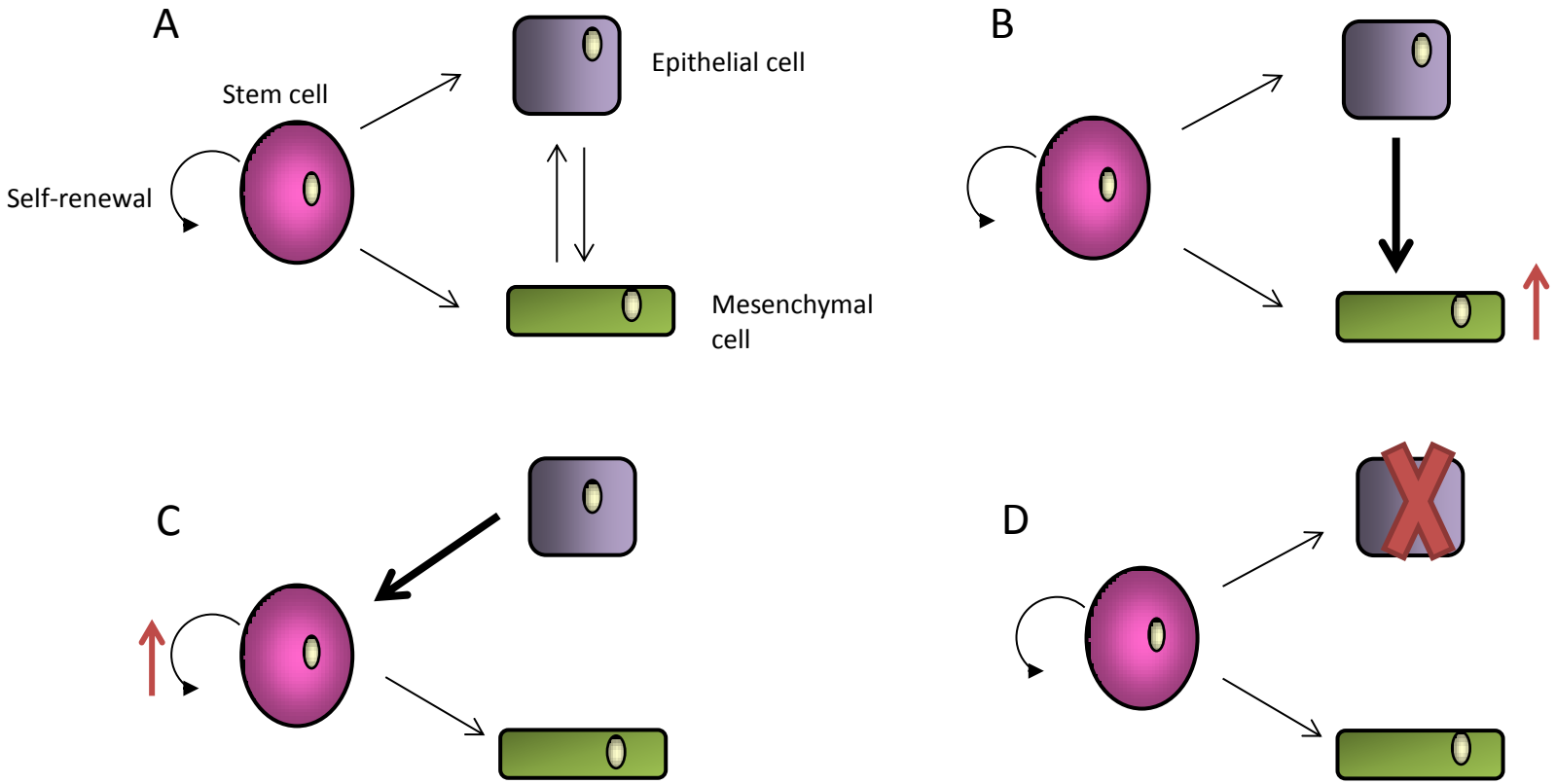

Figure 4.23 Clonal expansion and cellular conversion theory of olaparib resistance. ***(A)*** *In mammary tumours both epithelial and spindle cells exist, and are able to interconvert through EMT and MET. During olaparib therapy epithelial cells are placed under selective pressure, resulting in* ***(B)*** *the conversion to mesenchymal-like cells or* ***(C)*** *to stem-like cells, which both have EMT features.* ***(D)*** *Another possibility is that the epithelial cells are depleted, whilst the mesenchymal-like cells survive, resulting in clonal expansion and tumour relapse.*

cancer treatments such as olaparib. This theory would also correlate with other studies that show that cells with EMT features are resistant to treatment, for example studies by Arumugam *et al*. and Tryndak *et al*., showed that pancreatic cancer cell lines with high Zeb-1 and low E-cadherin expression were resistant to gemcitabine and cisplatin (Arumugam *et al.* 2009), and that ZEB-1 disruption in breast cancer cell lines increased sensitivity to doxorubicin (Tryndyak *et al.* 2010).

4.3.3 EMT phenotype did not correlate with an increase in mammosphere forming units

Previous studies have shown that Claudin-low tumours show an increase in stem-cell markers in comparison to other tumour types, suggesting that they may be enriched for cancer stem cells (Creighton *et al*. 2009; Hennessy *et al*. 2009). The mammosphere assay is an *in vitro* technique that is used to measure stem cell/progenitor cell frequency in a mixed population (Ponti *et al.* 2005; Liao *et al.* 2007). Single cells are cultured in suspension and stem cells survive, developing into 3D, non-adherent, multicellular structures.

As MSCCs have a similar gene expression profile to Claudin-low tumours, and given that an EMT signature is associated with cancer stem cells (Mani *et al*. 2008; Creighton *et al*. 2009; Prat *et al*. 2010), this suggested that olaparib-resistant tumours may have an increase in MFUs compared to untreated tumours. In contrast to this theory, results showed that resistant tumours show a significant decrease in MFUs, suggesting that they contain fewer cells with stem-cell properties. Another explanation could be the difference in proliferative activity of the stem cells. Results from a study by Liu et al. suggested that breast cancer stem cells that were characterised as mesenchymal-like were quiescent, whilst those that were epithelial-like were proliferative (Liu *et al.* 2014), suggesting that the higher number of MFUs in the untreated IDC-NSTs could be due to an epithelial phenotype, whereas the reduction of MFUs in resistant tumours could be due to mesenchymal characteristics. Further studies need to be performed to analyse the self-renewal capacity of the mammospheres formed from these tumours, which can be assessed by serial passage.

As there was no clear difference in MFUs between the different tumour types in the resistant cohort, this is further evidence that olaparib-resistant tumours exhibit characteristics that are independent of morphology.

4.3.4 Carboplatin-resistant tumours also show mesenchymal characteristics

Correlating with other studies that show that metaplastic tumours and tumours with EMT features are associated with treatment resistance (Al Sayed *et al*. 2006; Li *et al*. 2008; Creighton *et al*. 2009; Hennessy *et al*. 2009), carboplatin-resistant tumours from *BlgCre-Brca2$^{f/f}$/p53$^{f/f}$* mice show an increase in proportion of MSCCs, as well as IDC-NSTs with significantly higher levels of Vimentin and Twist staining, suggestive of EMT. These staining patterns are similar to those seen in olaparib-resistant tumours, suggesting that mesenchymal-like tumours may be involved in resistance to multiple drugs, and therefore may have broader clinical implications. In support of this another study also showed an association between EMT and carboplatin resistance, by finding that biopsies from resistant epithelial ovarian tumours had an EMT phenotype (Marchini *et al.* 2013).

4.4 Summary

In conclusion these results suggest that resistance to olaparib in a *BlgCre-Brca2$^{f/f}$/p53$^{f/f}$* mouse model is not caused by any of the currently proposed mechanisms for PARP inhibitor resistance, but instead it may be due to a dramatic shift in phenotype to mesenchymal-like tumours.

4.5 Further work

4.5.1 Investigate HR re-activation

Two of the proposed mechanisms of resistance to olaparib involve re-activation of the HR pathway. To investigate if the increased levels of Brca2 and Brca1 in resistant tumours has an effect on the HR pathway it would be interesting to analyse the HR pathway in these tumours. This could be performed by analysing Rad51 foci formation and γH2AX levels in resistant tumours.

4.5.2 Confirmation of Tariquidar inhibition

To ensure that the administration of Tariquidar has no effect on tumour relapse experiments need to be performed to confirm that the drug is inhibiting P-gps in the tumours from this mouse model. A previous experiment, using drug resistant cell lines, confirmed the action of Tariquidar by measuring the efflux of a fluorescent substrate (Mistry *et al.* 2001). A similar experiment could be performed using 2D cultured primary cells from tumour from *BlgCre-Brca2$^{f/f}$/p53$^{f/f}$* mice.

4.5.3 Analyse PARP-1 levels in tumours

Results show that resistant tumours have low PAR levels, suggesting that PARP-1 is still inhibited in these tumours. Another theory could be that resistant tumours have reduced *PARP-1* expression. A study showed that *in vitro* PARP-1-deficient cells are resistant to olaparib (Pettitt *et al.* 2013) so it would be interesting to analyse PARP-1 levels in resistant tumours and compare them to levels in untreated tumours.

The variation in PAR levels in the vehicle cohort suggests that PARP-1 activity varies between different tumour types, and could explain the different responses of *Brca2*-deficient tumours to olaparib therapy. It would therefore be interesting to also analyse PARP-1 levels in the different tumour types.

4.5.4 Change in tumour type due to conversion or clonal expansion

Olaparib-resistant tumours show an increase in MSCCs; however it is not yet clear whether this occurs by cellular conversion or clonal expansion. This could be investigated by producing specific fluorescent reporters for spindle cells and epithelial cells (using data from Dr Matthew Smalley's microarray) and transfecting primary cells *in vitro* where changes in morphology and reporter expression could be analysed by time-lapse microscopy, after the addition of olaparib. These fluorescent reporters could also be utilised *in vivo* to create a mouse model to be used for intravital imaging (Kedrin *et al.* 2008), which would enable real-time visualisation of the effect of olaparib treatment.

4.5.5 Target mesenchymal tumours

This work suggests that EMT/mesenchymal features may be involved in resistance to olaparib. It would be interesting to treat olaparib-resistant tumours with an anti-spindle cell or anti-mesenchymal cell therapy and analyse the effect on tumour relapse. It will also be important to identify which of these features is important for resistance in order to target the resistance. The effect of the loss of E-cadherin in *Brca2*-deficient tumours and olaparib treatment is investigated in chapter 5.

4.5.6 Investigate the roles of fibroblasts in resistance

This study has concentrated on analysing the epithelial cells within the mammary tumours. Other studies are now showing the importance of the interactions between the epithelial cells and the tumour-associated stroma in tumourigenesis. Cancer-associated fibroblasts

can be analysed by the expression of SMA, and release TGF-β, which activates TGF-β signalling in adjacent epithelial cells, suggesting that these cells could be contributing to the EMT phenotype seen in the resistant tumours, therefore it would be interesting to see if there is a difference in these cells in untreated and resistant tumour types.

4.5.7 Investigate other mechanisms of resistance

There are also other common mechanisms of drug resistance that could be investigated. Other pathways of DNA repair could be involved in olaparib resistance, for example the NHEJ pathway. These could be investigated by analysing the expression of the genes involved in the pathways, or analysing the repair of DSBs. A decrease in vascularisation within the tumours, resulting in hypoxia, can lead to a decrease in drug concentration. Vascularisation of olaparib-tumours could be analysed by staining for endothelial markers (e.g. CD31), and compared to untreated tumours. These other mechanisms could also be investigated by further analysis of the RNA sequencing study, which compared responding and resistant tumours, which could be complimented by exome sequencing and proteomic analysis.

5. Investigating the effect of E-cadherin loss in *Brca2/p53*-deficient tumours

5.1 Introduction

The maintenance of epithelial layers is accomplished by cell-cell and cell-matrix contacts. Adheren junctions, tight junctions and desmosomes are the three major types of contacts that mediate cellular layer integrity. In the mammary gland, cell-cell contacts give stability to the ductal structure and maintain cellular polarity of the luminal cells. Adheren junctions are mediated by E-cadherin, a single-pass, transmembrane glycoprotein (reviewed in Harstock and Nelson 2008). E-cadherin forms Ca^{2+}-dependent homo-dimers with E-cadherin molecules on neighbouring cells in the intercellular space. The cytoplasmic domain of E-cadherin binds to β-catenin and p120-catenin, which links to the actin cytoskeleton through interaction with α-catenin. Deletion of E-cadherin has been shown to promote invasive and metastatic behaviour in tumours from mouse models of breast and pancreatic cancer (Perl *et al.* 1998; Derksen *et al*. 2006), suggesting that the loss of E-cadherin leads to a mesenchymal phenotype, thereby making it easier for cells to detach from the primary tumour and metastasise.

The loss of E-cadherin is thought to be a hallmark of EMT, resulting in cytoskeletal reorganisation, breakdown of adheren junctions, and acquisition of mesenchymal characteristics, suggesting that it is an important caretaker of the epithelial phenotype (reviewed in Christiansen and Rajasekaran 2006). An EMT gene signature associates with Claudin-low and metaplastic breast tumours in humans and certain genes within this cluster are correlated with poor survival (Taube *et al*. 2010). Previous results in this study suggest that MSCCs have a poor response to olaparib therapy and may be involved in olaparib resistance. These tumours have EMT characteristics, with mesenchymal morphology, high levels of Vimentin and Twist expression and very low percentage of E-cadherin positive epithelial cells. As loss of E-cadherin is thought to be a critical step in EMT, we hypothesize that a high proportion of tumours that originate from cells that have enforced loss of E-cadherin expression will be MSCCs, and therefore not respond well to olaparib therapy.

To investigate whether loss of E-cadherin drives EMT, and thereby affects histological tumour type, tumours from conditional *Brca2/p53/Cdh1* floxed mice (Reed *et al*, unpublished) were classified by histopathology. Mice harbouring such tumours were also treated with the daily 100mg/kg olaparib therapy to investigate whether loss of E-cadherin had any effect on tumour response.

5.2 Results

5.2.1 *BlgCre-Brca2$^{f/f}$/p53$^{f/f}$/Cdh1$^{f/f}$* untreated tumours show differences in tumour proportion and characteristic staining patterns compared to *BlgCre-Brca2$^{f/f}$/p53$^{f/f}$* tumours

Although no metastatic sites were observed in organ samples *BlgCre-Brca2$^{f/f}$/p53$^{f/f}$/Cdh1$^{f/f}$* tumour-bearing mice, they did show a significantly earlier age of tumour onset compared to *BlgCre-Brca2$^{f/f}$/p53$^{f/f}$* mice, with a median age of 246 days compared to 290 days (Wilcoxon, p=0.009; Figure 5.1), suggesting that loss of E-cadherin promotes initiation of mammary tumour growth, rather than metastasis, in this mouse model.

Examination of a cohort of 15 untreated tumours from *BlgCre-Brca2$^{f/f}$/p53$^{f/f}$/Cdh1$^{f/f}$* mice revealed the presence of three histological types (Figure 5.2). The majority (13) were IDC-NSTs with 1 AME and 1 ASQC, resulting in a significant difference in proportions compared to untreated tumours from *BlgCre-Brca2$^{f/f}$/p53$^{f/f}$* mice (Chi Squared, p=0.05; Figure 5.3A-B). Compared to IDC-NSTs from *BlgCre-Brca2$^{f/f}$/p53$^{f/f}$* mice, those in this cohort showed a significant up-regulation of CK14 and p63 and a significant down-regulation of CK18 (Mann-Whitney U test, p=0.037, p=0.045 and p<0.01 respectively; Figure 5.2 and Figure 5.3C-D). The AME and ASQC in this cohort showed similar staining patterns to the same tumour types from BlgCre-Brca2$^{f/f}$/p53$^{f/f}$ mice, with high expression of p63 and CK14; however, the AME had a low level of CK18 staining (Figure 5.2 and Figure 5.3C-D). As with the BlgCre-Brca2$^{f/f}$/p53$^{f/f}$ mouse model, all tumours were ERα negative (Figure 5.4).

Immunohistochemical analysis of E-cadherin in untreated *BlgCre-Brca2$^{f/f}$/p53$^{f/f}$/Cdh1$^{f/f}$* tumours showed low levels of expression, with the majority showing up to 10% positivity and 1 at 30% (Figure 5.5). IDC-NSTs from this cohort showed 0-30% positivity, which is a significant reduction from IDC-NSTs in *BlgCre-Brca2$^{f/f}$/p53$^{f/f}$* mice, which show 40-85%

(Mann-Whitney U test, $p<0.01$). The AME and ASQC in this cohort both showed low (<1%) levels of E-cadherin staining compared to tumours from *BlgCre-Brca2$^{f/f}$/p53$^{f/f}$* mice (45-85% and 60-65% respectively).

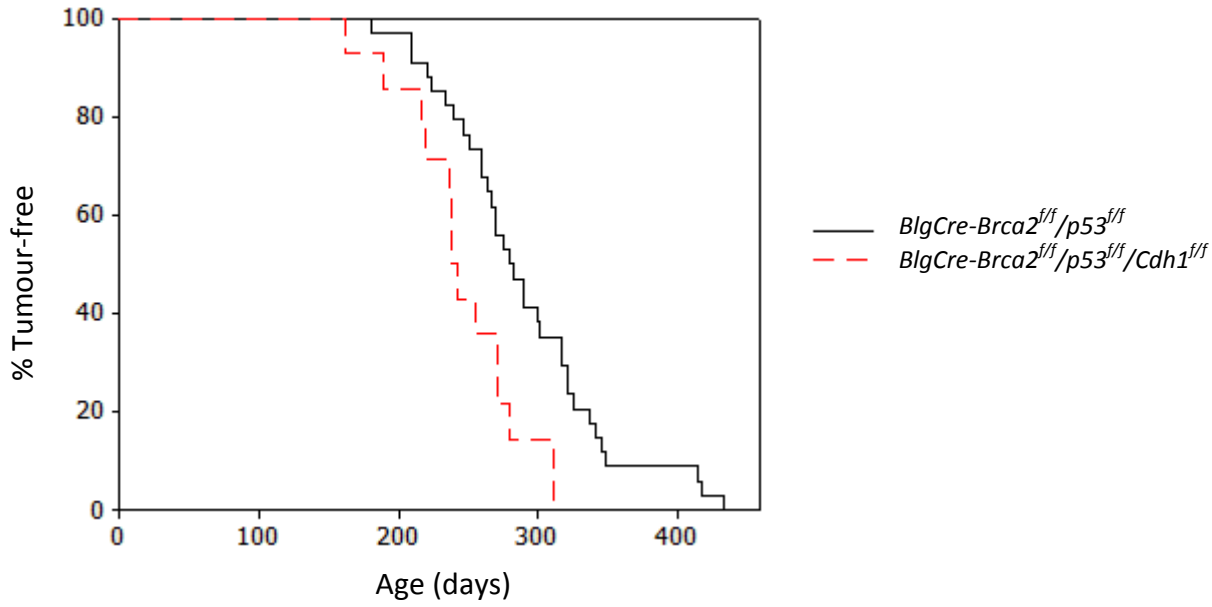

Figure 5.1 Loss of E-cadherin promotes tumour initiation in Blg-cre Brca2$^{f/f}$ p53$^{f/f}$ model. *Ages of tumour onset in BlgCre-Brca2$^{f/f}$/p53$^{f/f}$/Cdh1$^{f/f}$ mice and BlgCre-Brca2$^{f/f}$/p53$^{f/f}$ mice.*

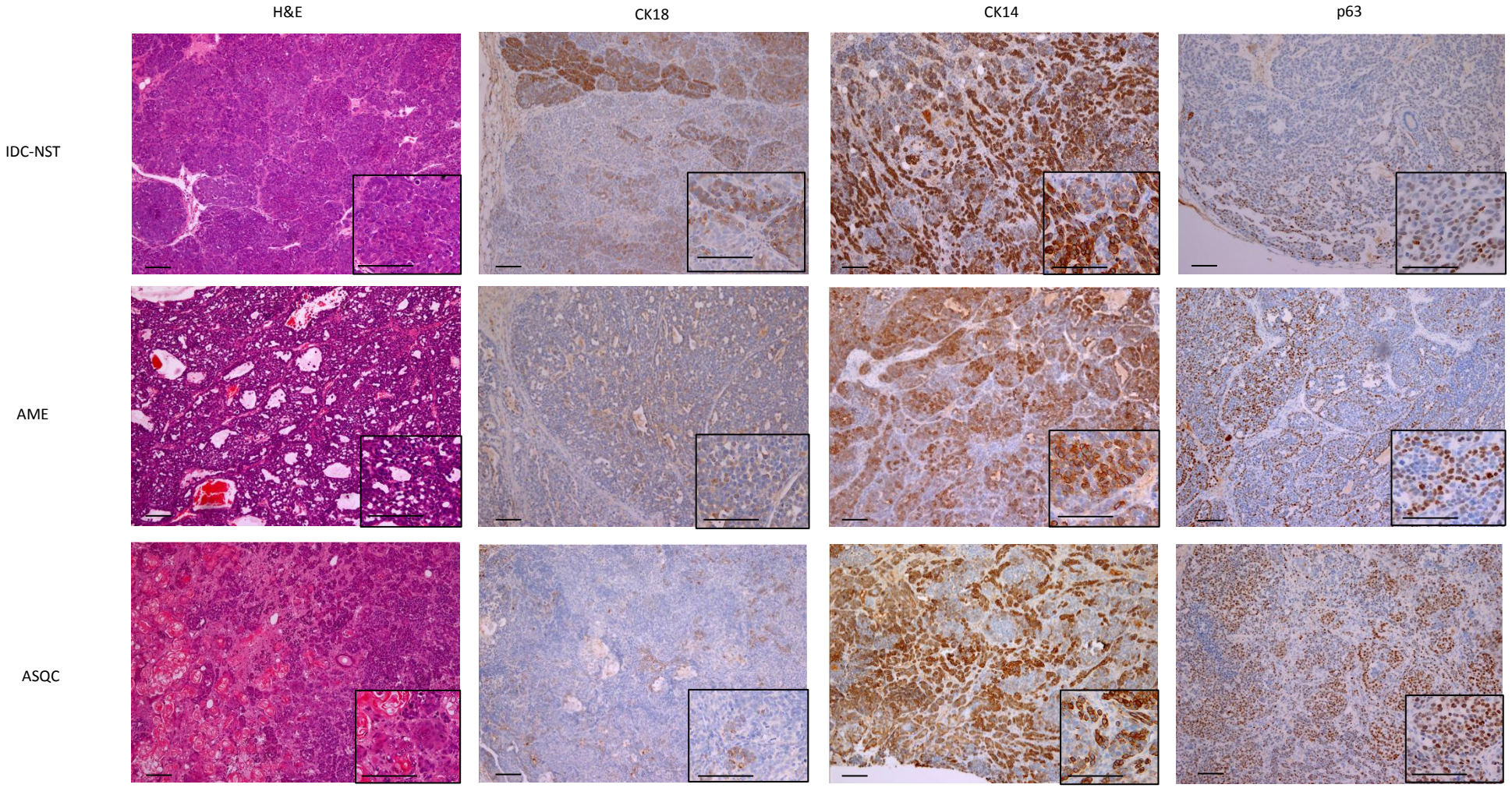

Figure 5.2 Representative pictures of untreated tumours from BlgCre-Brca2$^{f/f}$/p53$^{f/f}$/Cdh1$^{f/f}$ mice. *Tumours were stained with H&E to analyse cell morphology, and CK18, CK14 and p63 to analyse the luminal and basal populations.*

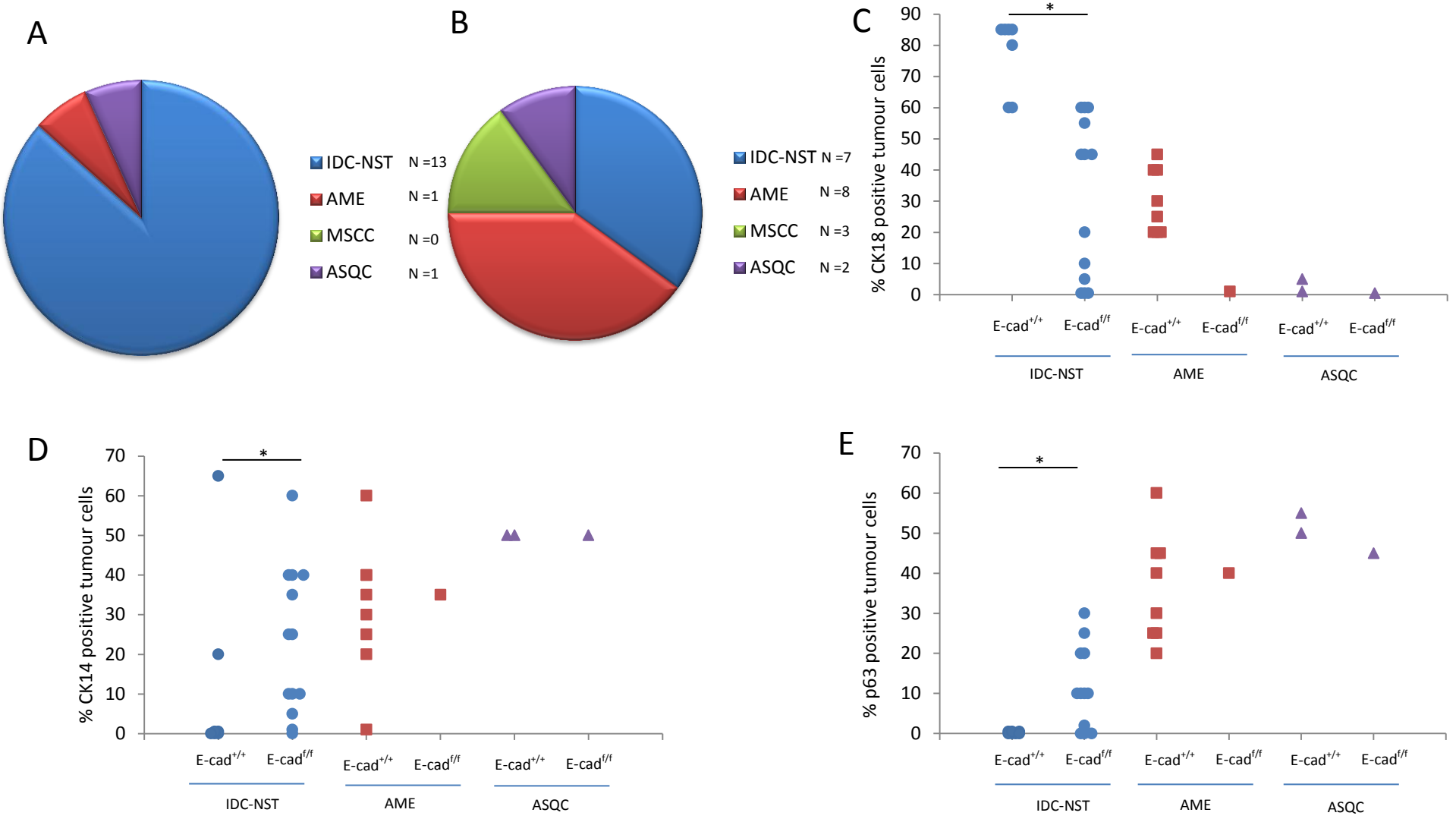

Figure 5.3 Histopathology of tumours from BlgCre-Brca2$^{f/f}$/p53$^{f/f}$/Cdh1$^{f/f}$ mice*. Proportions of histopathological tumour types in BlgCre-Brca2$^{f/f}$/p53$^{f/f}$/Cdh1$^{f/f}$ (E-cad$^{f/f}$) mice* ***(A)*** *and BlgCre-Brca2$^{f/f}$/p53$^{f/f}$ mice (E-cad$^{+/+}$)* ***(B).*** *Tumours were analysed for CK18* ***(C),*** *CK14* ***(D)*** *and p63* ***(E)****. * p≤0.05*

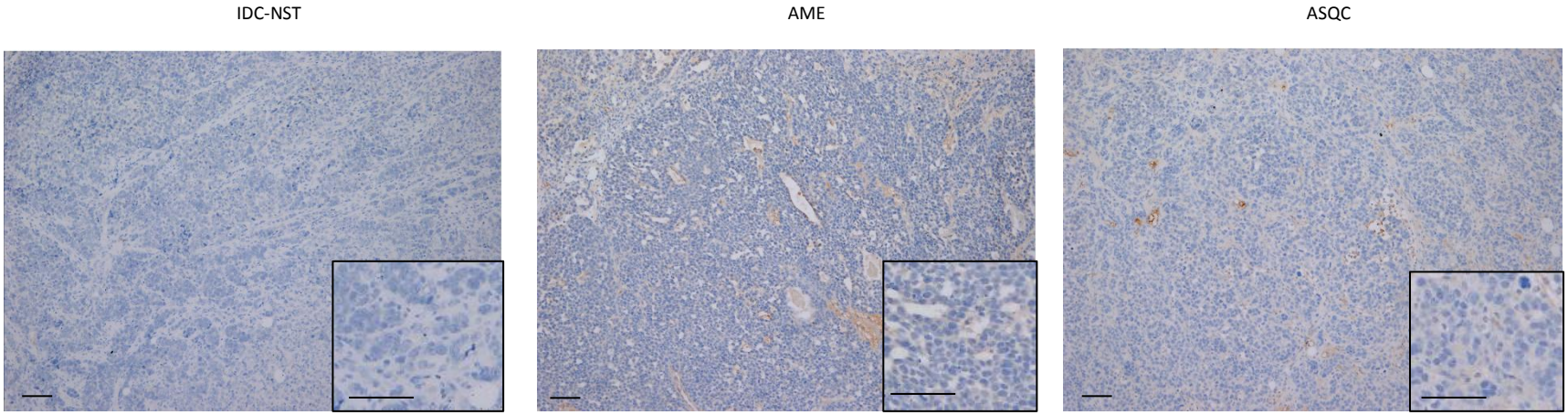

Figure 5.4 Representative pictures of ERα positivity in tumours from BlgCre-Brca2$^{f/f}$/p53$^{f/f}$/Cdh1$^{f/f}$ mice. *Immunohistochemistry for ERα in tumours from BlgCre-Brca2$^{f/f}$/p53$^{f/f}$/Cdh1$^{f/f}$ mice. Immunohistochemistry performed by Jarrad Jenkins.*

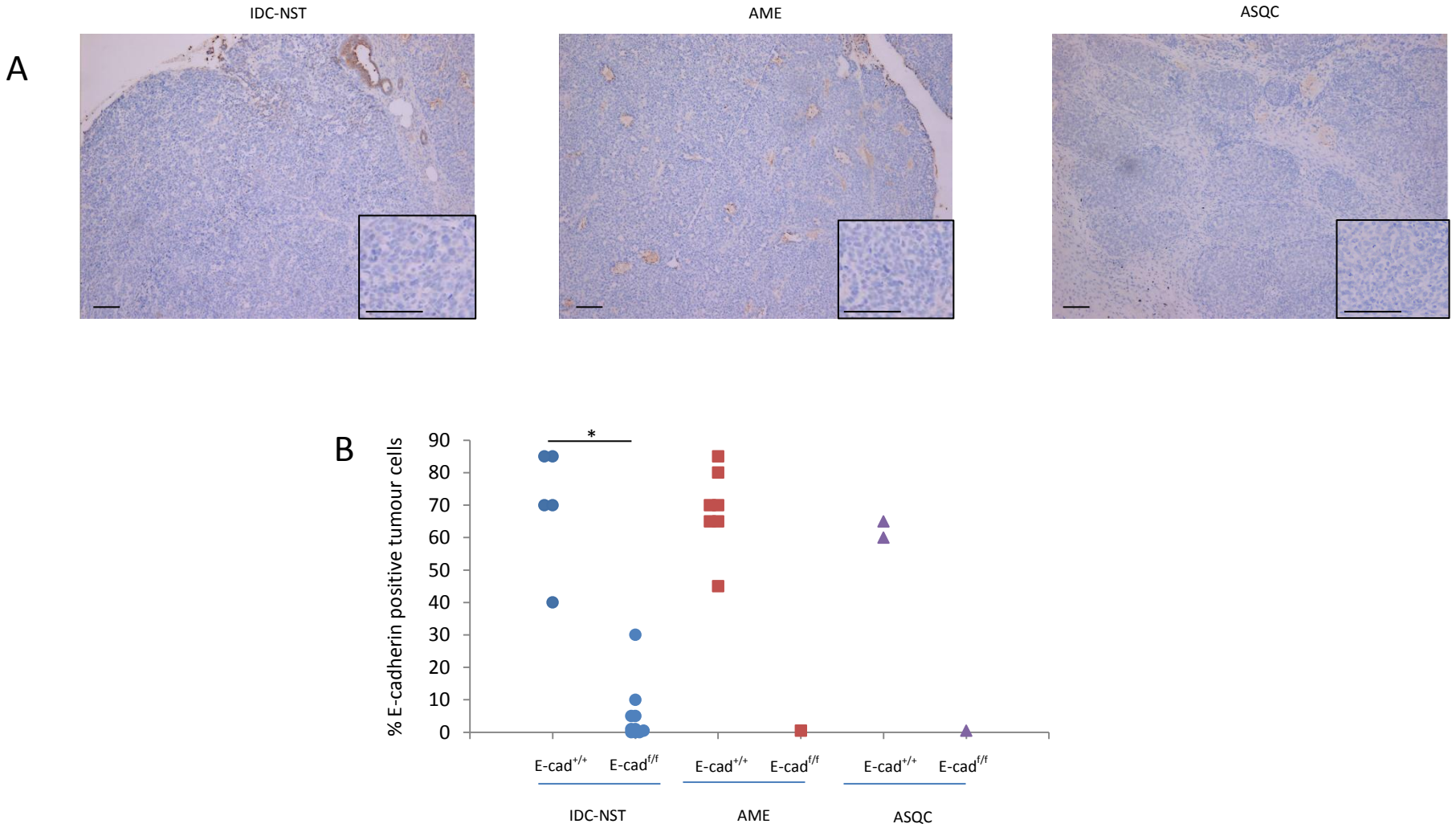

Figure 5.5 E-cadherin levels in tumours from BlgCre-Brca2$^{f/f}$/p53$^{f/f}$/Cdh1$^{f/f}$ mice. (A) *Representative pictures of E-cadherin staining in the different tumour types.* ***(B)*** *Tumours from BlgCre-Brca2$^{f/f}$/p53$^{f/f}$/Cdh1$^{f/f}$ mice (E-cad$^{f/f}$) were analysed for E-cadherin positivity and compared to those from BlgCre-Brca2$^{f/f}$/p53$^{f/f}$ mice (E-cad$^{+/+}$). * p≤0.05. E-cadherin immunohistochemistry performed by Jarrad Jenkins.*

5.2.2 Loss of E-cadherin does not lead to an increase in EMT markers

As the loss of E-cadherin is thought to be an important step in EMT, EMT markers were analysed in tumours from *BlgCre-Brca2$^{f/f}$/p53$^{f/f}$/Cdh1$^{f/f}$* mice (Figure 5.6 and Figure 5.7). IDC-NSTs showed a significant increase in Slug positivity (Mann-Whitney U test, p=0.04), a trend for an increase in Vimentin staining (<1-20% compared to 0-<1%), and no significant difference in Twist levels compared to IDC-NSTs from BlgCre-Brca2$^{f/f}$/p53$^{f/f}$ mice. qRT-PCR analysis of Snail expression showed no significant difference between IDC-NSTs from the two mouse models (Figure 5.7D). The AME and ASQC showed no differences in EMT marker expression compared to tumours from *BlgCre-Brca2$^{f/f}$/p53$^{f/f}$* mice, retaining the low expression of Twist and Vimentin and high expression of Slug. These results show that tumours from *BlgCre-Brca2$^{f/f}$/p53$^{f/f}$/Cdh1$^{f/f}$* mice have low expression of Twist and Vimentin and high expression of Slug.

5.2.3 *BlgCre-Brca2$^{f/f}$/p53$^{f/f}$/Cdh1$^{f/f}$* olaparib-resistant tumours show similarities to *BlgCre-Brca2$^{f/f}$/p53$^{f/f}$* resistant tumours

To investigate the effect of E-cadherin loss on response to olaparib therapy, 13 tumour-bearing *BlgCre-Brca2$^{f/f}$/p53$^{f/f}$/Cdh1$^{f/f}$* mice were treated with daily IP 100mg/kg olaparib and tumour volumes were measured bi-weekly during treatment (Figure 5.8A). The same range of responses was seen as in tumours from *BlgCre-Brca2$^{f/f}$/p53$^{f/f}$* mice, with the majority showing a moderate or excellent response, and tumours that initially responded well relapsing with long-term treatment (Figure 5.8B-C).

Histopathological analysis of olaparib-resistant *BlgCre-Brca2$^{f/f}$/p53$^{f/f}$/Cdh1$^{f/f}$* tumours (n=12) showed the presence of three of the same tumour types as in the *BlgCre-Brca2$^{f/f}$/p53$^{f/f}$* mice, with the majority (58%) being IDC-NSTs, 25% MSCCs and 17% AMEs, resulting in a significant difference in proportions compared to untreated tumours, where there is a higher proportion of IDC-NSTs and ASQCs, a lower proportion of AMEs and the absence of MSCCs (Chi Squared, p=0.05; Figure 5.8D-E). The proportions are also significantly different compared to resistant tumours from *BlgCre-Brca2$^{f/f}$/p53$^{f/f}$* mice, which show higher proportions of MSCCs and ASQCs, and lower proportions of IDC-NSTs and AMEs (Chi Squared, p=0.05; Figure 5.8F).

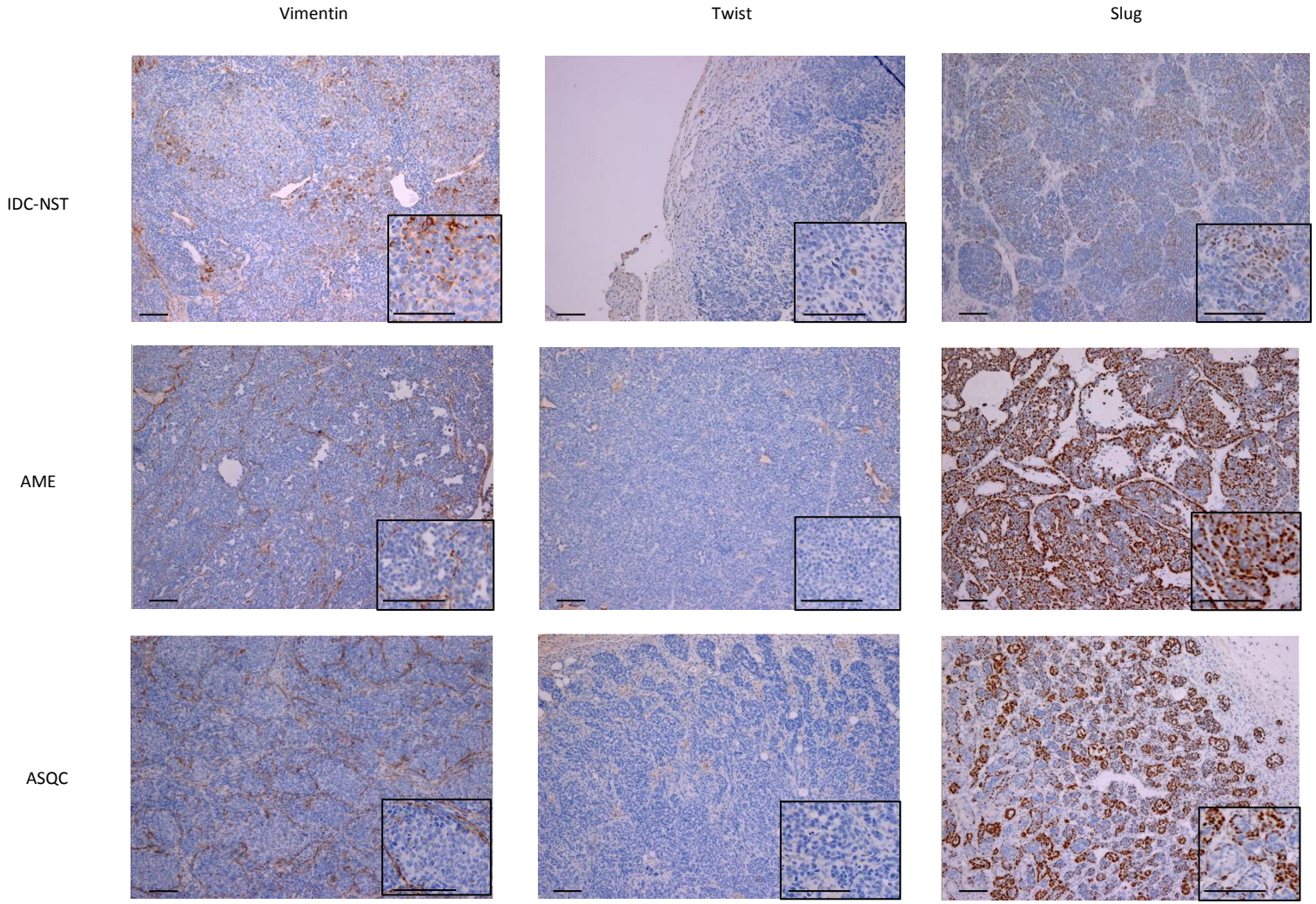

Figure 5.6 Representative pictures of EMT markers in untreated tumours from BlgCre-Brca2$^{f/f}$/p53$^{f/f}$/Cdh1$^{f/f}$ mice. *Tumours were stained for EMT markers Vimentin, Twist and Slug.*

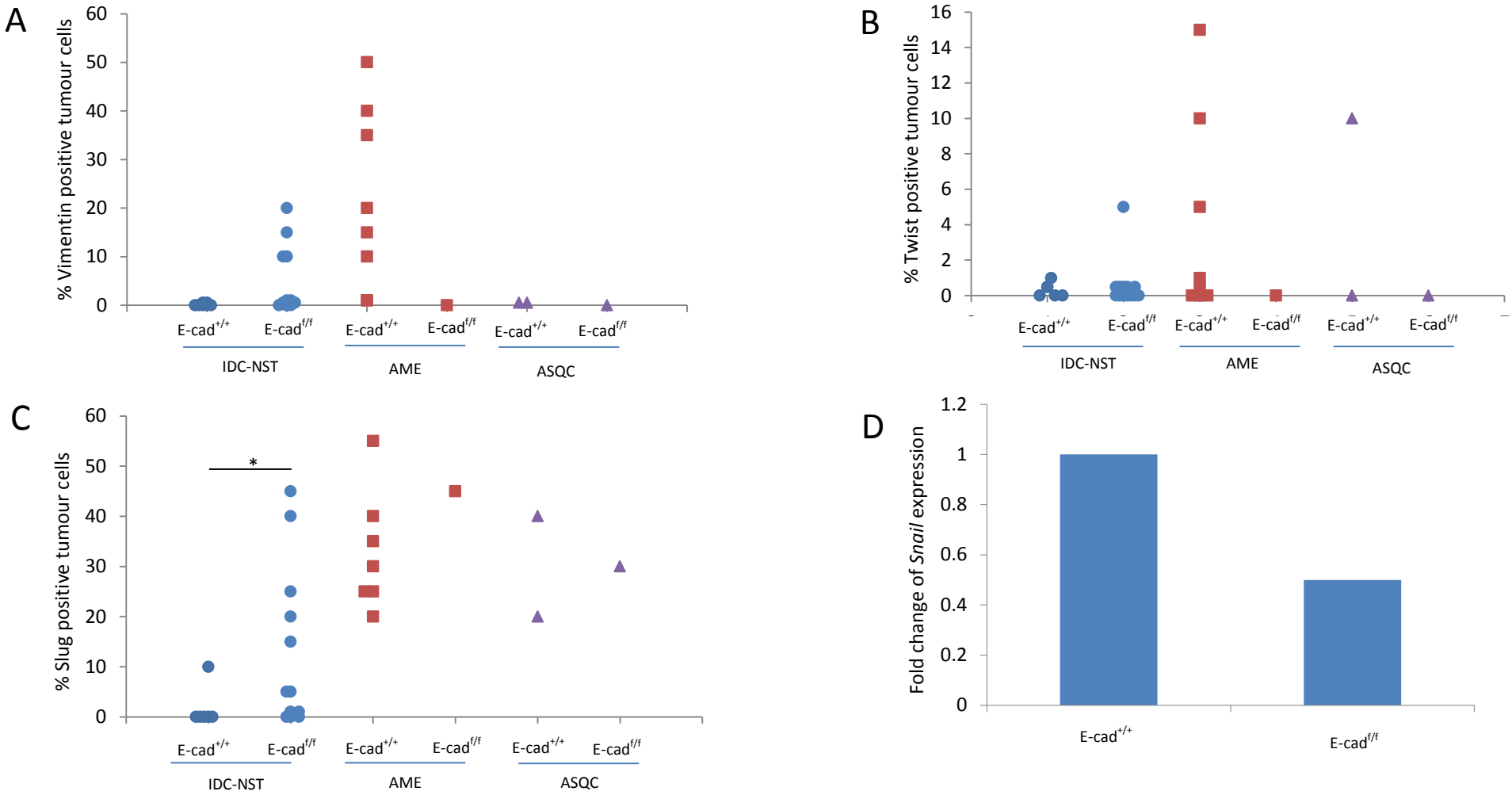

Figure 5.7 EMT markers in tumours from BlgCre-Brca2$^{f/f}$/p53$^{f/f}$/Cdh1$^{f/f}$ mice. *Vimentin* ***(A)****,Twist* ***(B)*** *and Slug* ***(C)*** *expression were analysed in tumours from BlgCre-Brca2$^{f/f}$/p53$^{f/f}$/Cdh1$^{f/f}$ mice (E-cad$^{f/f}$) and compared to tumours from BlgCre-Brca2$^{f/f}$/p53$^{f/f}$ mice (E-cad$^{+/+}$).* ***(D)*** *Snail expression was analysed by qRT-PCR in IDC-NSTs from the two mouse models. qRT-PCR performed by Jarrad Jenkins. * p≤0.05.*

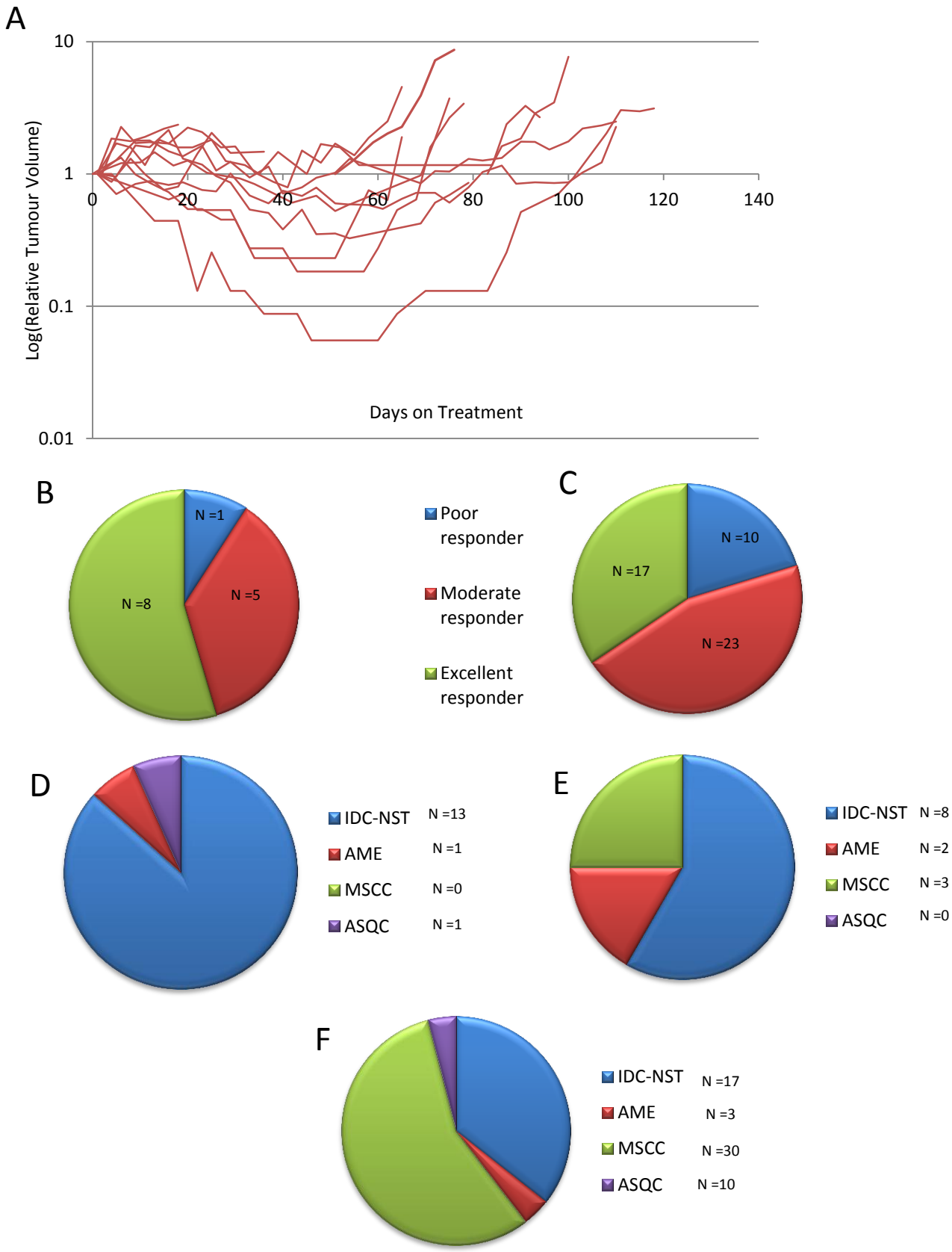

Figure 5.8 The effect of E-cadherin loss on olaparib therapy. (A) *BlgCre-Brca2$^{f/f}$/p53$^{f/f}$/Cdh1$^{f/f}$ mice were treated with daily 100mg/kg olaparib therapy and tumours (n=14) showed similar range of responses compared to tumours from BlgCre-Brca2$^{f/f}$/p53$^{f/f}$*

mice, and long-term treatment resulted in tumour relapse. Response to therapy in BlgCre-Brca2$^{f/f}$/p53$^{f/f}$/Cdh1$^{f/f}$ mice ***(B)*** *and BlgCre-Brca2$^{f/f}$/p53$^{f/f}$ mice* ***(C)*** *was classified into three groups: poor, moderate and excellent. Olaparib-resistant tumours from BlgCre-Brca2$^{f/f}$/p53$^{f/f}$/Cdh1$^{f/f}$ mice were classified by histopathology* ***(E)*** *and the proportions were compared to untreated tumours* ***(D)****, and olaparib-resistant tumours from BlgCre-Brca2$^{f/f}$/p53$^{f/f}$ mice* ***(F)****.*

IDC-NSTs from the resistant cohort (n=7) show a significant reduction in p63 staining compared to untreated IDC-NSTs (Mann-Whitney U test, p=0.04), while retaining variable expression of CK14 and CK18 (Figure 5.9 and Figure 5.10). Resistant AMEs (n=2) showed similar staining to the 1 untreated AME, with high p63 and CK14 expression and low CK18 expression (Figure 5.9 and Figure 5.10), although the low numbers of this tumour type in both cohorts make it difficult to draw any firm conclusions. Comparison of staining patterns in resistant tumours from either the E-cadherin^{+} or E-cadherin^{-} models showed that IDC-NSTs in the BlgCre-Brca2$^{f/f}$/p53$^{f/f}$/Cdh1$^{f/f}$ cohort had a significant reduction in CK18 expression (Mann-Whitney U test, p=0.03), and similar p63 and CK14 levels (Figure 5.11). Resistant AMEs also showed a reduction in CK18 staining compared to those from BlgCre-Brca2$^{f/f}$/p53$^{f/f}$ mice, although again the low number of tumours means that statistical significance was not reached (Figure 5.11). Resistant MSCCs from both cohorts showed similar staining for all three markers (Figure 5.9 and Figure 5.11) and as before these tumours contained epithelial sections that showed staining patterns similar to IDC-NSTs or AMEs, with AME sections showing p63 and CK14 positivity and IDC-NST sections showing CK18 positivity.

All resistant IDC-NSTs and AMEs showed low levels of E-cadherin staining (0-10%; untreated tumours. Resistant MSCCs showed <30% E-cadherin positivity (Figure 5.12), which correlated with the epithelial sections.

Analysis of EMT markers in resistant tumours showed that IDC-NSTs had a significant increase in Vimentin and Twist staining compared to untreated IDC-NSTs (Mann-Whitney U test, p=0.04 and p=0.01 respectively), and the 2 resistant AMEs also showed higher levels of Vimentin staining over the 1 untreated AME (Figure 5.13 and Figure 5.14). These results are similar to resistant IDC-NSTs and AMEs from BlgCre-Brca2$^{f/f}$/p53$^{f/f}$ mice which also show

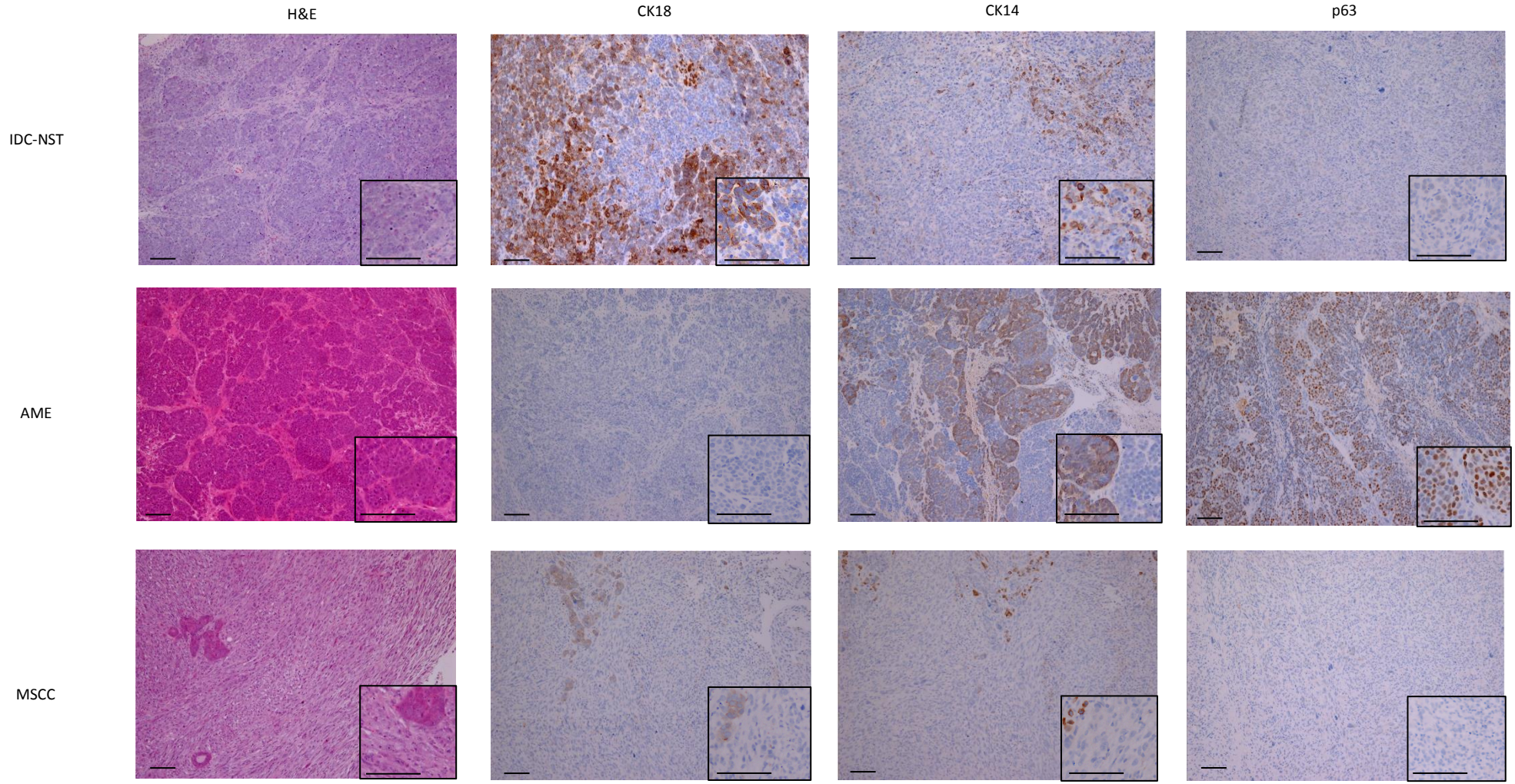

Figure 5.9 Representative pictures of olaparib-resistant tumours from BlgCre-Brca2$^{f/f}$/p53$^{f/f}$/Cdh1$^{f/f}$ mice. *Resistant tumours were stained with H&E and immunohistochemistries for CK18, CK14 and p63 were performed.*

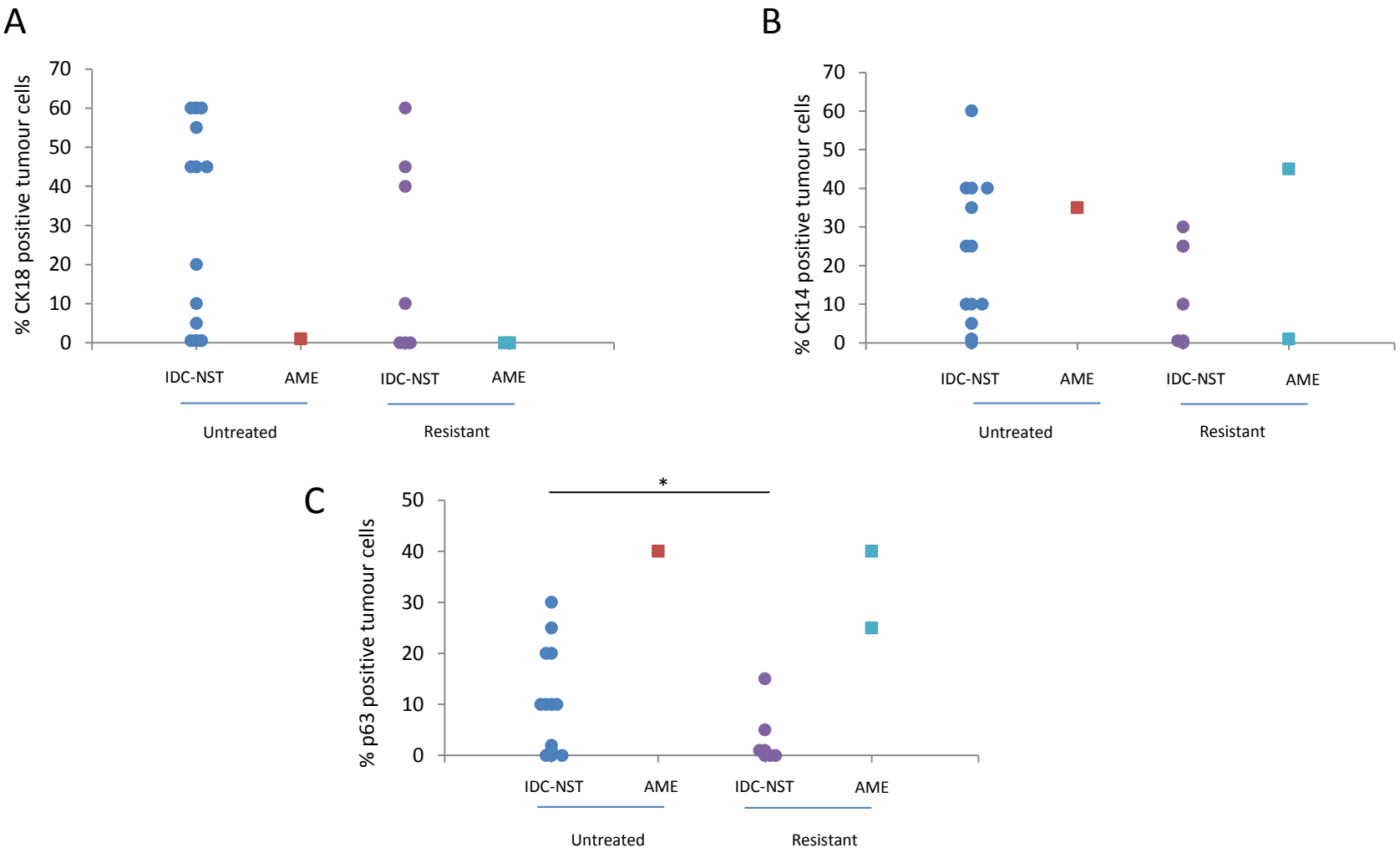

Figure 5.10 Comparison of luminal and basal marker expression in untreated and olaparib-resistant tumours from BlgCre-Brca2$^{f/f}$/p53$^{f/f}$/Cdh1$^{f/f}$ mice. *Tumours were analysed for expression of CK18* ***(A),*** *CK14* ***(B)*** *and p63* ***(C).*** ** p≤0.05*

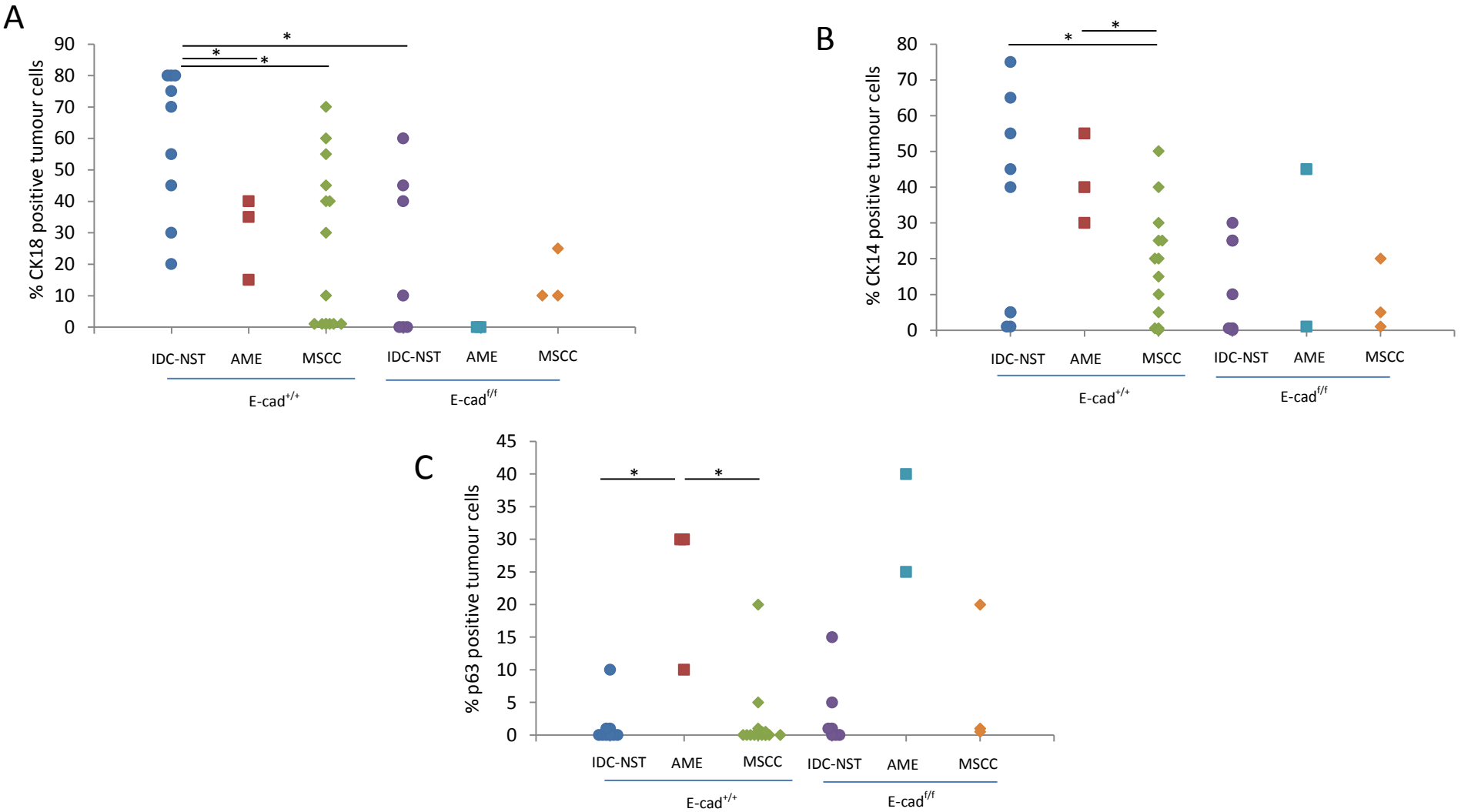

Figure 5.11 Comparison of luminal and basal markers between olaparib-resistant tumours from BlgCre-Brca2$^{f/f}$/p53$^{f/f}$/Cdh1$^{f/f}$ mice (E-cad$^{f/f}$) and BlgCre-Brca2$^{f/f}$/p53$^{f/f}$ mice (E-cad$^{+/+}$). *Tumours were analysed for CK18* ***(A),*** *CK14* ***(B)*** *and p63* ***(C)****. * p≤0.05.*

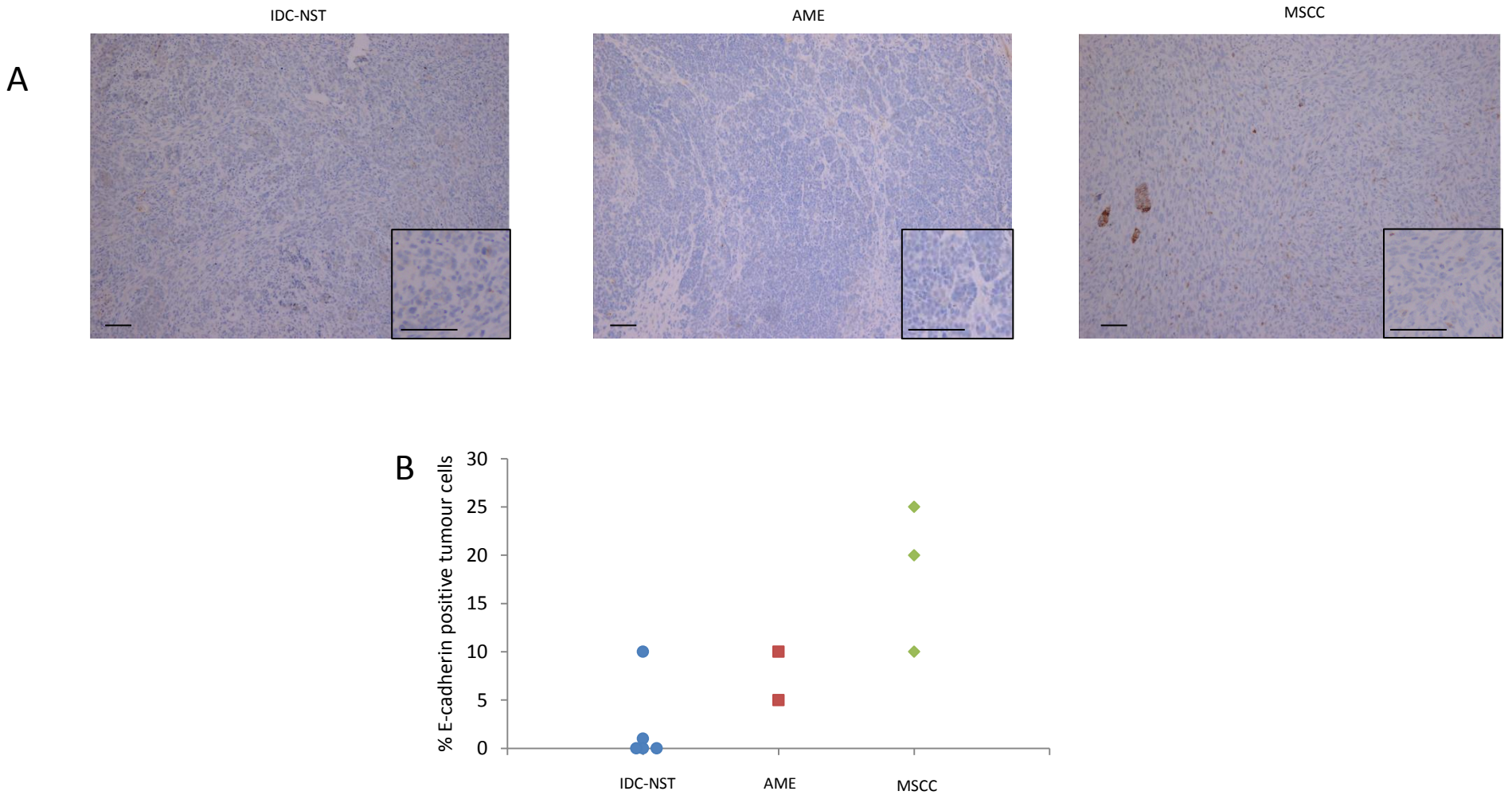

Figure 5.12 E-cadherin levels in olaparib-resistant tumours from BlgCre-Brca2$^{f/f}$/p53$^{f/f}$/Cdh1$^{f/f}$ mice. (A) *Representative pictures of E-cadherin staining in the olaparib-resistant tumour types.* ***(B)*** *E-cadherin positivity in resistant tumours from BlgCre-Brca2$^{f/f}$/p53$^{f/f}$/Cdh1$^{f/f}$ mice.*

higher levels of Vimentin and Twist positivity compared to untreated tumours (chapter 4), adding weight to the suggestion that olaparib-resistant tumours with epithelial morphology have mesenchymal-like gene expression. The IDC-NSTs and AME also showed a trend for a decrease in Slug staining, compared to untreated tumours (Figure 5.14). The MSCCs showed high levels of all three EMT markers (Figure 5.13 and Figure 5.15). Comparison between *BlgCre-Brca2$^{f/f}$/p53$^{f/f}$/Cdh1$^{f/f}$* resistant tumours and *BlgCre-Brca2$^{f/f}$/p53$^{f/f}$* resistant tumours showed that the MSCCs and IDC-NSTs had similar staining patterns for Vimentin, Twist and Slug (Figure 5.15). Resistant AMEs from BlgCre-Brca2$^{f/f}$/p53$^{f/f}$/Cdh1$^{f/f}$ mice showed a decrease in Vimentin and Twist expression compared to BlgCre-Brca2$^{f/f}$/p53$^{f/f}$ resistant AME tumours (Figure 5.15), although again this may be due to the low numbers in these cohorts.

5.2.4 Characterisation of initial response to olaparib therapy

Of 15 tumours that received daily IP 100mg/kg olaparib therapy, 13 became resistant following either an excellent or moderate response, 1 had a poor response and continued growing, and one was harvested during a moderate response due to resistance in a second tumour on the same mouse. The poor responder was classified as an AME, which had similar staining patterns to the untreated AME from the same mouse model, with high expression of p63, CK14 and Slug, and low expression of Vimentin, CK18 and Twist; however, it showed a high level of E-cadherin staining in comparison to the 1 untreated AME (45% compared to <1%; Figure 5.16 and Figure 5.17). As only one tumour has been analysed, firm conclusions cannot be made, but it is interesting that it differs to the *BlgCre-Brca2$^{f/f}$/p53$^{f/f}$* model, in which tumours that had a poor response to olaparib therapy were all classified as MSCCs (n=16, chapter 3).

The moderate responder was classified as an IDC-NST, which had similar staining patterns to untreated IDC-NSTs from the same mouse model, apart from showing an increase in E-cadherin staining (60% compared to 0-30%; Figure 5.16 and Figure 5.17). In the *BlgCre-Brca2$^{f/f}$/p53$^{f/f}$* model, IDC-NSTs that are responding moderately to daily olaparib therapy show an increase in Vimentin and Twist expression compared to untreated IDC-NSTs; however, this IDC-NST retained the low expression of Vimentin and Twist seen in the untreated tumours.

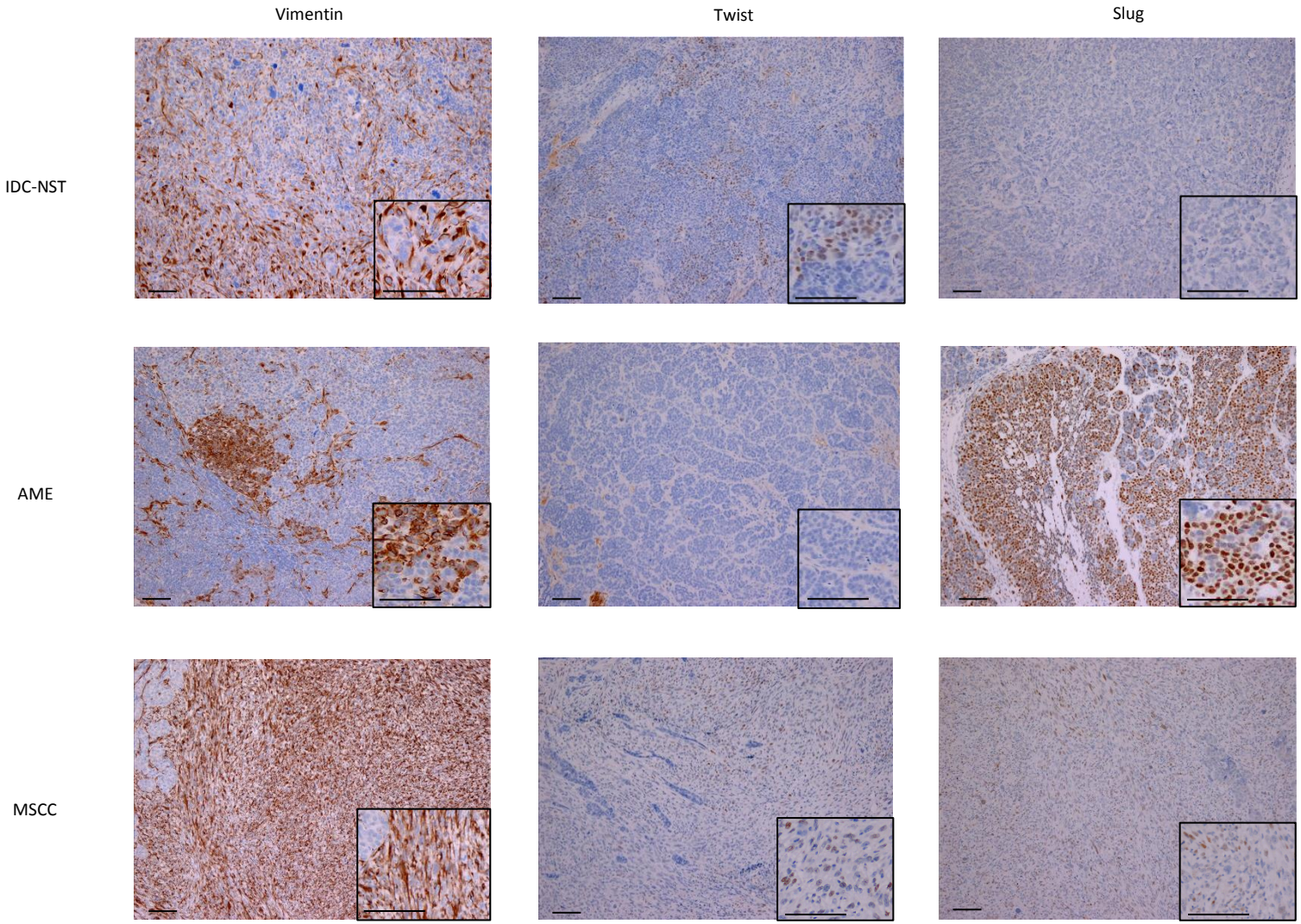

Figure 5.13 Representative pictures of EMT markers in olaparib-resistant tumours from BlgCre-Brca2$^{f/f}$/p53$^{f/f}$/Cdh1$^{f/f}$ mice. *Resistant tumours were stained for Vimentin, Twist and Slug to analyse EMT.*

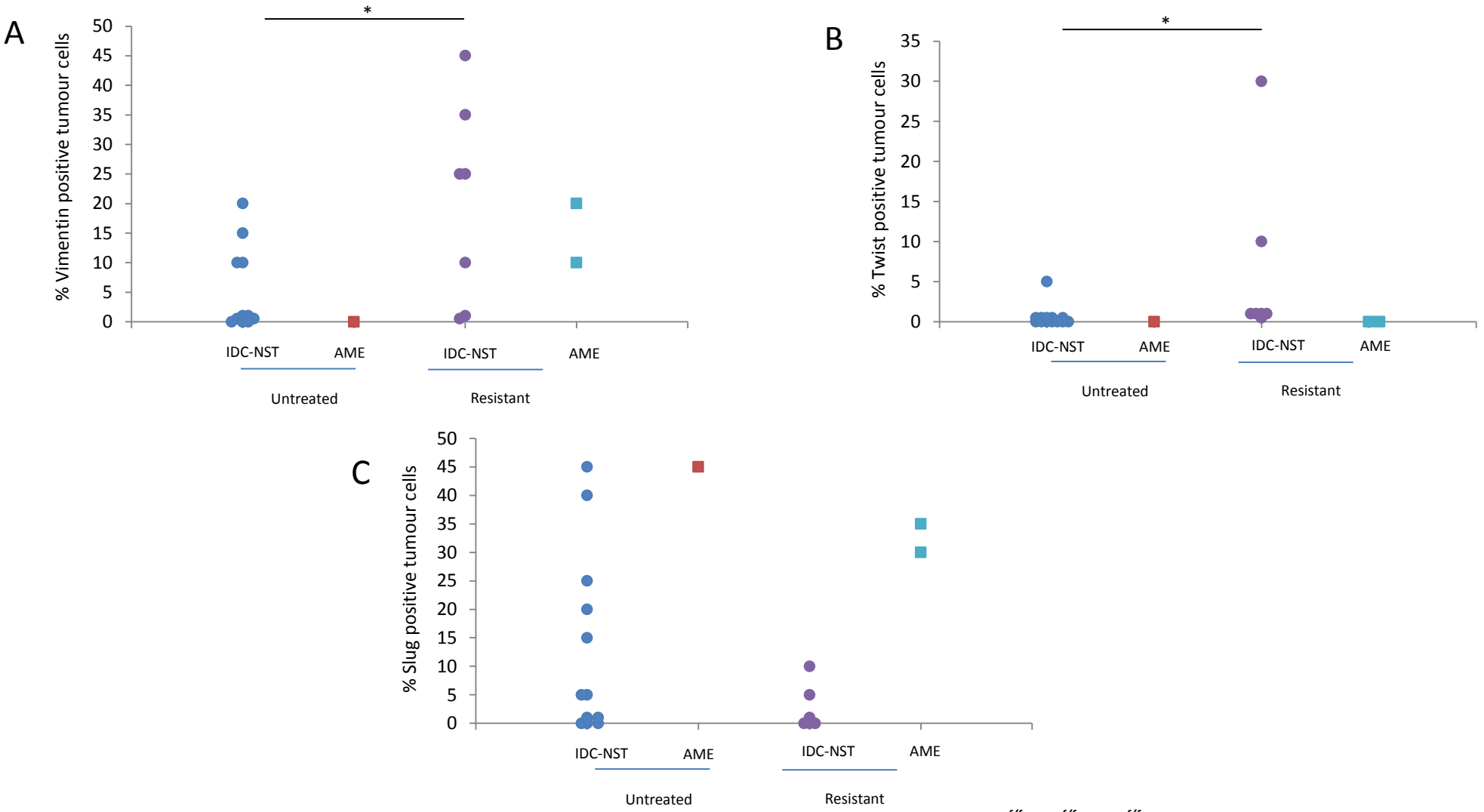

Figure 5.14 Comparison of EMT markers between untreated and olaparib-resistant tumours from BlgCre-Brca2$^{f/f}$/p53$^{f/f}$/Cdh1$^{f/f}$ mice. *Vimentin **(A)**, Twist **(B)** and Slug **(C)** positivity in resistant tumours, compared to untreated tumours. * p≤0.05.*

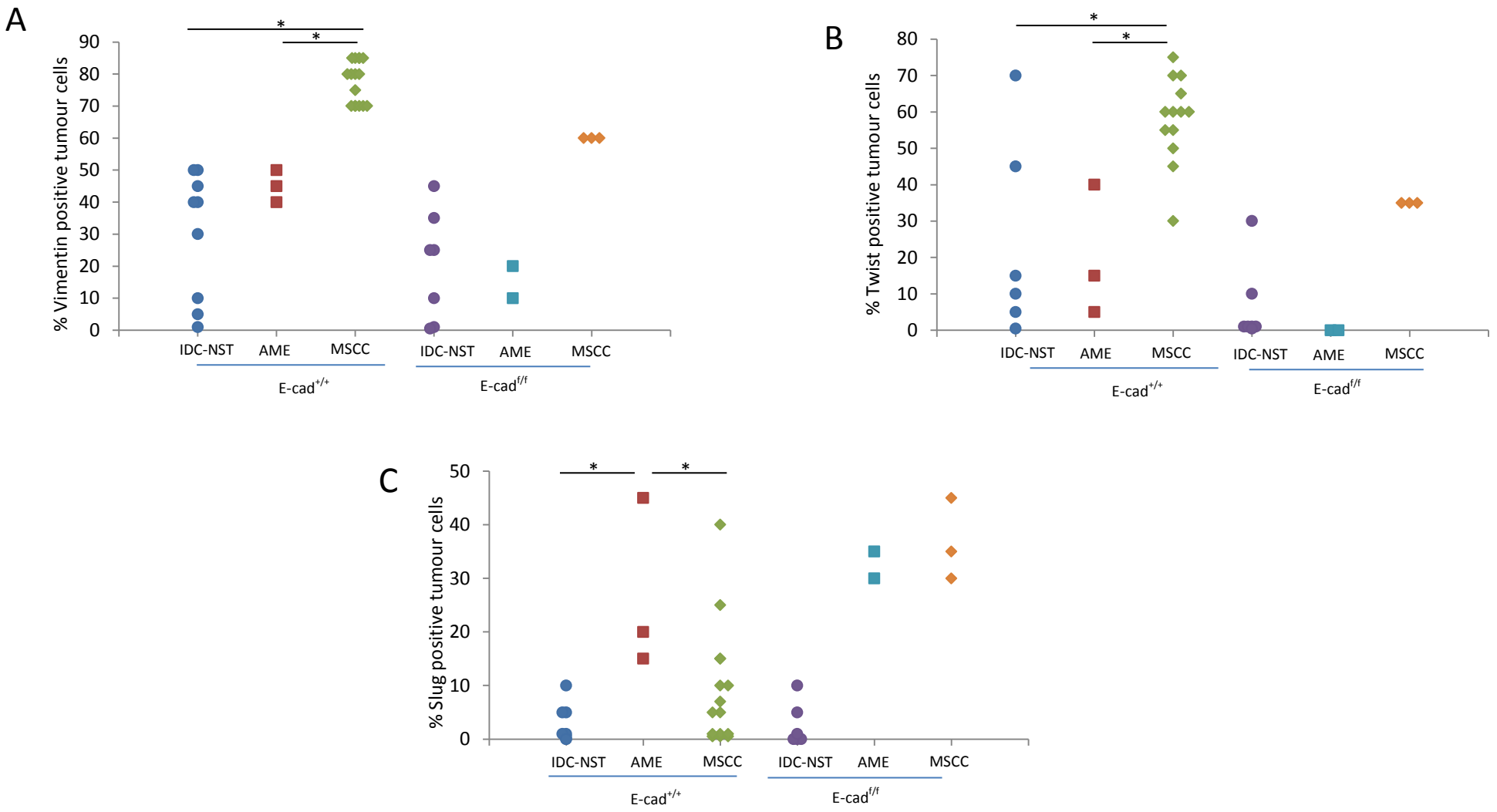

Figure 5.15 Comparison of EMT markers between olaparib-resistant tumours from BlgCre-Brca2$^{f/f}$/p53$^{f/f}$/Cdh1$^{f/f}$ mice (E-cad$^{f/f}$) and BlgCre-Brca2$^{f/f}$/p53$^{f/f}$ mice (E-cad$^{+/+}$). *Vimentin **(A)**, Twist **(B)** and Slug **(C)** positivity in resistant E-cad$^{f/f}$ tumours, compared to resistant E-cad$^{+/+}$ tumours. * p≤0.05.*

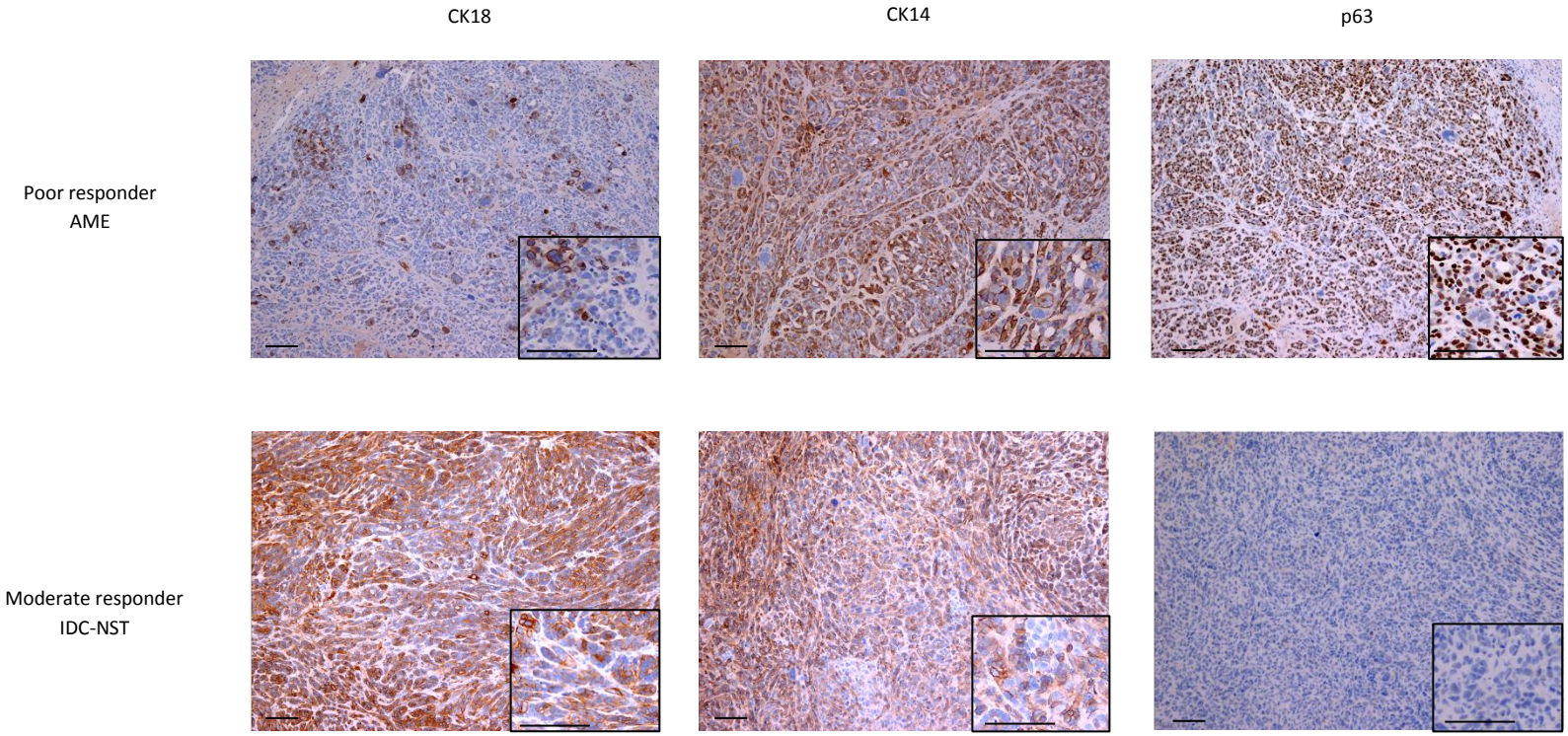

Figure 5.16 Representative pictures of a poor and moderate responder to daily olaparib therapy. *The poor and moderate responder to daily 100mg/kg olaparib treatment from BlgCre-Brca2$^{f/f}$/p53$^{f/f}$/Cdh1$^{f/f}$ mice were characterised by staining for CK18, CK14 and p63.*

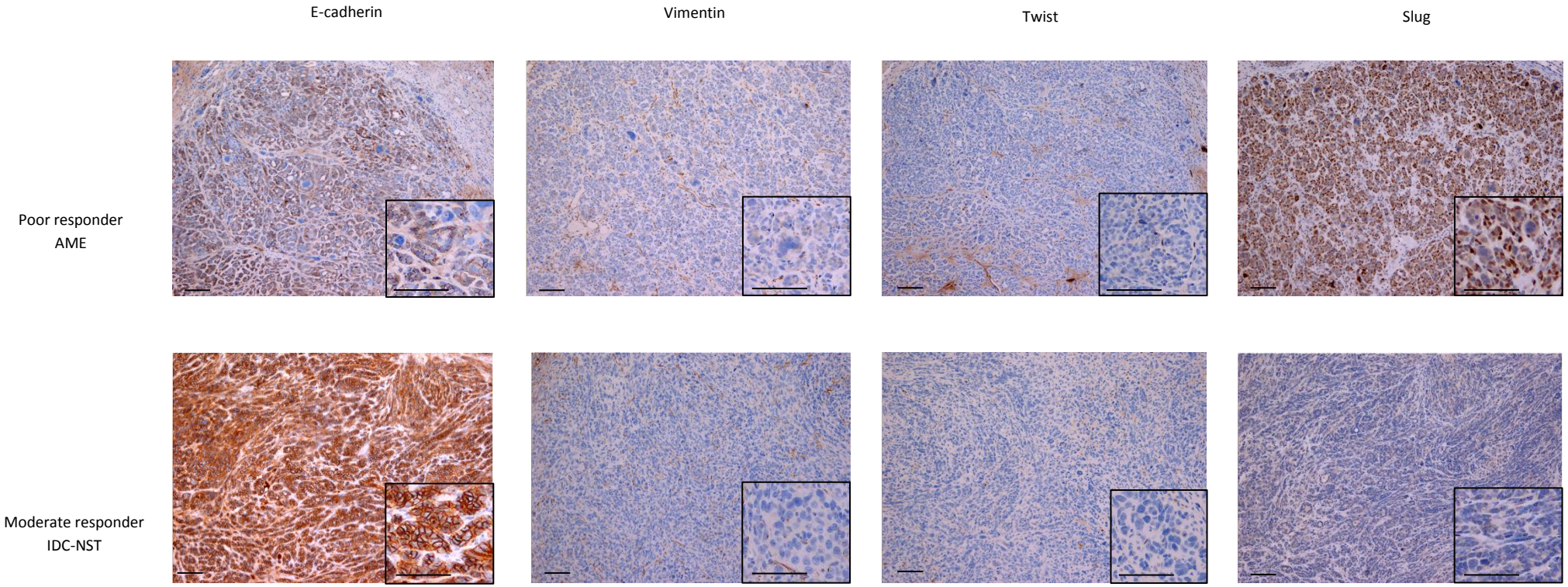

Figure 5.17 Representative pictures of EMT markers in a poor and moderate responder to daily olaparib therapy. *The poor and moderate responder to daily 100mg/kg olaparib treatment from BlgCre-Brca2$^{f/f}$/p53$^{f/f}$/Cdh1$^{f/f}$ mice were analysed for EMT by staining for E-cadherin, Vimentin, Twist and Slug.*

5.3 Discussion

5.3.1 Loss of E-cadherin in *Brca2/p53*-deficient mammary tumours leads to earlier age of tumour onset

Previous studies have shown that loss of E-cadherin in mouse models of breast and prostate cancer promotes cancer progression (Perl *et al*. 1998; Derksen *et al*. 2006). In this study, *BlgCre-Brca2$^{f/f}$/p53$^{f/f}$/Cdh1$^{f/f}$* mice showed a significantly earlier age of tumour onset compared to *BlgCre-Brca2$^{f/f}$/p53$^{f/f}$* mice. Correlating with this, a study in *K14Cre;Cdh1$^{f/f}$/p53$^{f/f}$* mouse model suggested that loss of E-cadherin gives a selective advantage during tumour initiation (Derksen *et al*. 2006). This suggests that the loss of E-cadherin may promote the growth of mammary tumours in these mouse models, possibly by producing a more tumour permissive environment, allowing neoplastic cells to grow out and form tumours at earlier time points.

Other studies investigating E-cadherin loss in mammary tumours, using the *K14Cre*, have shown that it leads to metastasis, with the presence of CK18/CK14 positive epithelial cells in a number of organs (Derksen *et al*. 2006; Derksen *et al.* 2011). No secondary lesions were observed during the dissection and histological analysis of organs from mammary-tumour-bearing *BlgCre-Brca2$^{f/f}$/p53$^{f/f}$/Cdh1$^{f/f}$* mice in this study. This could be due to differences in the mouse models, for example the different promoters for Cre expression, or the inclusion of *Brca2$^{f/f}$* in our model; however, it would be interesting to investigate whether any CK18/CK14 positive cells are present in the organs described in the previous reports.

5.3.2 Loss of E-cadherin does not result in high proportions of MSCCs

MSCC tumours from the *BlgCre-Brca2$^{f/f}$/p53$^{f/f}$* model show EMT features, with mesenchymal morphology, high Vimentin and Twist staining and low E-cadherin expression. As loss of E-cadherin is thought to be critical in EMT, it was hypothesised that additional deletion of E-cadherin in *Brca2/p53*-deficient mammary tumours would lead to an increase in the proportion of MSCCs; however this study showed the absence of MSCCs in these mice, with the majority of tumours being IDC-NSTs. A cohort of tumours from *BlgCre-Brca2$^{f/f}$/p53$^{f/f}$/Cdh1$^{f/f}$* mice did show differences in the relative proportions of tumour types compared to those from the *BlgCre-Brca2$^{f/f}$/p53$^{f/f}$* model, with an increase in IDC-NSTs, a decrease in AMEs and the absence of MSCCs. The absence of MSCCs suggests therefore that

loss of E-cadherin is not a driving step in the formation of MSCC tumours in the *BlgCre-Brca2$^{f/f}$/p53$^{f/f}$* model, and that it is possibly the other roles of the transcription factors that regulate EMT that are critical for the initiation of the process. This corresponds with a study by Derksen and colleagues, where mammary tumours from *K14Cre-Cdh1$^{f/f}$/p53$^{f/f}$* mice were found to be mainly invasive lobular carcinomas, which express the luminal marker CK8, have variable expression of CK14 and are negative for Vimentin (Derksen *et al*. 2006). An interesting study by Lombaerts and colleagues investigated the effects of different mechanisms of loss of E-cadherin expression in a panel of human mammary cell lines and showed that cells with rounded morphology and luminal characteristics contained *Cdh1* gene mutations, whilst cells with mesenchymal morphology and EMT characteristics had methylation of the E-cadherin promoter (Lombaerts *et al.* 2006). This may explain the absence of MSCCs in the cohort of tumours from the *BlgCre-Brca2$^{f/f}$/p53$^{f/f}$/Cdh1$^{f/f}$* mice and suggests that MSCCs from the *BlgCre-Brca2$^{f/f}$/p53$^{f/f}$* model and olaparib-resistant tumours have low E-cadherin expression due to promoter methylation rather than gene mutation.

Although three of the same tumour types that are present in the *BlgCre-Brca2$^{f/f}$/p53$^{f/f}$* model were observed, tumours showed differences in staining patterns. The IDC-NSTs showed a significant down-regulation of CK18 and up-regulation of p63 and CK14, and, although there were low numbers of AMEs and ASQCs, they also showed a reduction in CK18 staining, suggesting that although loss of E-cadherin does not lead to changes in morphology, it results in changes in gene expression, with tumours showing a reduction in luminal markers and an increase in basal markers. This correlates with other studies that have also shown that reduction of E-cadherin is associated with a basal phenotype, for example an investigation in human invasive breast carcinomas showed that a reduction in E-cadherin was associated with CK5/6 and CK17 positivity and triple negative phenotypes (Mahler-Araujo *et al.* 2008), and analysis of different types of human breast tumours showed that EMT, including reduction of E-cadherin, related to basal-like tumours (Sarrio *et al.* 2008).

5.3.3 Loss of E-cadherin does not drive EMT in *Brca2/p53*-deficient tumours

Transcriptional repression of E-cadherin is thought to be a critical step in EMT. To investigate if the loss of E-cadherin expression drives this process in the *BlgCre-*

Brca2$^{f/f}$*/p53*$^{f/f}$ model, EMT markers were analysed in tumours from *BlgCre-Brca2*$^{f/f}$*/p53*$^{f/f}$*/Cdh1*$^{f/f}$ mice. The majority of tumours showed ≥1% positivity for Vimentin and Twist, with levels no different to those observed in *BlgCre-Brca2*$^{f/f}$*/p53*$^{f/f}$ tumours. The majority also showed high levels of Slug staining, which is characteristic for AMEs and ASQCs, but low levels are observed in IDC-NSTs from *BlgCre-Brca2*$^{f/f}$*/p53*$^{f/f}$ mice. This high level of Slug staining corresponds with high p63 staining, which correlates with previous observations in this study (chapter 3). This data suggests that loss of E-cadherin does not drive tumour cells to undergo EMT, corresponding with the absence of mesenchymal morphology in these tumours. Although some reports indicate that transcriptional repression of E-cadherin can induce EMT (Cano *et al.* 2000; Bolos *et al.* 2003), others have shown that loss of E-cadherin alone is not essential for EMT; for example, a study by Hollestelle and colleagues analysed the loss of E-cadherin expression in different breast cancer cell lines and found that not all that had undergone EMT showed loss of E-cadherin (Hollestelle *et al.* 2013). They also investigated the effect of re-introducing E-cadherin cDNA into a spindle breast cancer cell line, where they showed no changes in expression and that the cells retained their spindle-cell morphology, suggesting that loss of E-cadherin is not a critical step in EMT. An *in vitro* study by Maeda *et al* (Maeda *et al.* 2005) induced EMT in mammary epithelial cell lines showed that the morphological changes of EMT preceded the down-regulation of E-cadherin, again suggesting that loss of E-cadherin is not essential for mesenchymal morphology, which could explain why the genetic loss of E-cadherin alone in mammary tumours from *BlgCre-Brca2*$^{f/f}$*/p53*$^{f/f}$ mice does not result in mesenchymal morphology.

5.3.4 Loss of E-cadherin has no effect on olaparib treatment and resistance

We hypothesised that as loss of E-cadherin would lead to a high proportion of MSCCs, therefore a poor response to olaparib therapy, as these tumours have been implicated in both poor response and resistance to olaparib (chapters 3 and 4). In contrast this study showed an absence of MSCCs in these mice, which correlated with daily olaparib treatment in tumours from *BlgCre-Brca2*$^{f/f}$*/p53*$^{f/f}$*/Cdh1*$^{f/f}$ mice showing similar initial responses to those seen in *BlgCre-Brca2*$^{f/f}$*/p53*$^{f/f}$ tumours, with the majority showing either an excellent or moderate response, with poor response being rare, suggesting that loss of E-cadherin has

little or no effect on the initial response to olaparib therapy. Long-term olaparib treatment also resulted in tumour relapse, on a similar timescale to that seen in mice with *BlgCre-Brca2$^{f/f}$/p53$^{f/f}$* tumours. This contrasts with studies in human bladder and pancreatic cancers which show that tumours with reduced E-cadherin expression have worse progression free survival and overall survival (Fondrevelle *et al.* 2009; Hong *et al.* 2011). A study investigating E-cadherin expression in human gastric carcinomas, did show that there was no relation to response to chemotherapy; however patients with reduced expression did show worse survival (Graziano *et al.* 2004b).

As seen in resistant tumours from *BlgCre-Brca2$^{f/f}$/p53$^{f/f}$* mice, olaparib-resistant *BlgCre-Brca2$^{f/f}$/p53$^{f/f}$/Cdh1$^{f/f}$* tumours showed an increase in the proportion of MSCCs (25%) compared to the untreated cohort (0%), re-enforcing the idea that this tumour type is involved in the process of olaparib resistance in *Brca2*-deficient breast cancer. However, the predominant tumour type was still found to be IDC-NST, as seen in the untreated cohort. Analysis of luminal and basal markers in resistant AMEs showed no significant differences to untreated tumours, retaining the low expression of CK18 and high expression of CK14 and p63, although due to the low numbers in these cohorts no firm conclusions can be made. Resistant IDC-NSTs showed similar CK18 expression to untreated tumours, but showed a significant reduction in p63 staining and a trend for a decrease in CK14 staining, suggesting that they have lower expression of basal-like genes. As such, they show similar levels of basal markers to olaparib-resistant IDC-NSTs from *BlgCre-Brca2$^{f/f}$/p53$^{f/f}$* mice. Taken together with the analysis of resistant MSCCs in this mouse model, which showed similar expression of CK18, CK14 and p63 compared to resistant MSCCs from *BlgCre-Brca2$^{f/f}$/p53$^{f/f}$* mice, this suggests that loss of E-cadherin does not affect levels of these histological markers in olaparib-resistant tumours.

Resistant IDC-NSTs and AMEs from *BlgCre-Brca2$^{f/f}$/p53$^{f/f}$* mice show similarities in EMT marker expression to MSCCs, with an increase in Vimentin and Twist staining. The resistant MSCCs from *BlgCre-Brca2$^{f/f}$/p53$^{f/f}$/Cdh1$^{f/f}$* mice also had high Vimentin (60-80%) and Twist (35-45%) levels, showing that MSCCs from the two mouse models have similar EMT expression patterns. Resistant IDC-NSTs from *BlgCre-Brca2$^{f/f}$/p53$^{f/f}$/Cdh1$^{f/f}$* mice showed a significant increase in both Vimentin and Twist levels and resistant AMEs also showed

increased levels of Vimentin compared to untreated tumours, suggesting that additional loss of E-cadherin does not alter the mesenchymal-like gene expression of olaparib-resistant *BlgCre-Brca2$^{f/f}$/p53$^{f/f}$* tumours.

Two of the tumours treated with daily olaparib did not become resistant as they had to be taken at earlier time points. One showed a poor response to olaparib therapy, and was characterised as an AME, which differs to the results from *BlgCre-Brca2$^{f/f}$/p53$^{f/f}$* tumours, where it was shown poor responders were exclusively MSCCs, suggesting that this tumour type has an intrinsic resistance (chapter 3). This resistant AME showed low levels of the EMT markers Vimentin and Twist, suggesting that it did not have MSCC characteristics, and showed similar staining patterns to the untreated AME from the same mouse model, apart from a higher level of E-cadherin staining (45% compared to <1%). This suggests that there may be other factors involved in the poor response to olaparib therapy.

The high expression of E-cadherin in this AME was unusual, as all other untreated and resistant tumours analysed showed low expression (0-30%). Interestingly, analysis of a moderately-responding *BlgCre-Brca2$^{f/f}$/p53$^{f/f}$/Cdh1$^{f/f}$* tumour also showed high expression of E-cadherin (60%). This tumour was classified as an IDC-NST, which showed similar staining patterns to untreated IDC-NSTs from the same mouse model, but did not show an increase in Vimentin and Twist staining as seen in moderately responding IDC-NSTs from *BlgCre-Brca2$^{f/f}$/p53$^{f/f}$* mice, suggesting that in the E-cadherin^{-} model, olaparib therapy may not induce Vimentin and Twist expression. These results suggest that further investigation into the early responses to olaparib therapy is needed in this mouse model, as there may be clinically significant differences from those seen in tumours from *BlgCre-Brca2$^{f/f}$/p53$^{f/f}$* mice.

5.4 Summary

Results presented in this chapter suggest that the additional genetic loss of E-cadherin in *BlgCre-Brca2$^{f/f}$/p53$^{f/f}$* tumours does not drive EMT and increase the number of MSCCs. In contrast, tumours show a reduction in the luminal marker CK18 and high expression of basal markers. In addition, loss of E-cadherin did not markedly alter the response to olaparib treatment or the development of resistance. Results also give further evidence that EMT/mesenchymal characteristics are involved in resistance to olaparib, with resistant

tumour cohorts showing an increase in the proportion of MSCCs and other resistant tumour types showing an increase in at least some EMT markers.

5.5 Further Work

Work presented in this chapter has investigated the effect of additional genetic loss of E-cadherin in *BlgCre-Brca2$^{f/f}$/p53$^{f/f}$* tumours. It would be interesting to also investigate the effect of perturbing expression of other EMT markers in these tumours and analysing tumour histology and formation, as well as response and resistance to olaparib. This could be done *in vivo,* by creating new mouse models, or *in vitro*, using primary cell culture. Of particular interest would be loss of Vimentin, as analysis of expression in tumours from *BlgCre-Brca2$^{f/f}$/p53$^{f/f}$* mice suggest that it is induced by olaparib treatment, resistant tumours show high expression, and MSCCs, which have shown to have a poor response to olaparib therapy (chapter 3), show high levels of vimentin staining.

As mentioned previously, as other studies have suggested that loss of E-cadherin in mammary tumours leads to metastasis (Derksen *et al*. 2006; Derksen *et al*. 2011), it would be interesting to investigate if tumours cells have metastasised in *BlgCre-Brca2$^{f/f}$/p53$^{f/f}$/Cdh1$^{f/f}$* mice, by observing if there are CK18/CK14 positive cells in other organs.

It would also be interesting to carry out a more in-depth analysis of the initial responses of *BlgCre-Brca2$^{f/f}$/p53$^{f/f}$/Cdh1$^{f/f}$* tumours to olaparib therapy. This could be done by analysing tumours at early time points during olaparib therapy, for example 1 hour and 24 hours after a single dose, and tumours showing different responses to daily olaparib therapy after around 30 days, similar to the study on *BlgCre-Brca2$^{f/f}$/p53$^{f/f}$* tumours performed in chapter 3, thereby allowing comparison of early response between the two genetically-distinct tumour types.

6. General Discussion

6.1 Analysing initial response to olaparib

Breast cancer is the most common cancer in the UK and, despite increases in survival rates, is still the second most common cause of cancer death in women in the UK, (http://www.cancerresearchuk.org). Conventional chemotherapies target highly proliferating cells, resulting in systemic toxicity, particularly at sites such as hair follicles and the small intestine. In order to try to reduce this toxicity in cancer patients, a plethora of targeted therapies are in various stages of development, which are designed such that they target specific signalling pathways, thereby causing selective death of cancer cells. As breast cancer is such a heterogeneous disease, with multiple classification systems and intrinsic subgroups, targeted therapies may be critical in the treatment of this disease, thereby allowing for personalised therapy to be developed, which is where the patient receives a specific tailored treatment based on the genetic/signalling perturbations in their particular cancer.

One strategy for targeted therapy is that of synthetic lethality. First proposed by Theodore Dobzhansky in the 1940's, this is a process where a cell can survive with a deficiency in either of two specific proteins, but will die if both are absent (Dobzhansky 1946). PARP inhibitors harness the synthetic lethality between deficiencies in the HR pathway (such as the BRCA proteins) and deficiency in PARP-1. They cause selective toxicity to BRCA-deficient cells (Bryant *et al*. 2005; Farmer *et al*. 2005), resulting in low systemic toxicity, making them an excellent potential personalised therapy for patients with *BRCA* mutations that cause breast, ovarian and other types of cancers (Audeh *et al*. 2010; Gelmon *et al*. 2011). Other studies have also suggested that their therapeutic potential may be broadened to other subgroups of breast cancer, such as triple-negative breast cancer (Turner and Reis-Filho 2006).

As breast cancer is a very heterogeneous disease, precise stratification will be essential for patients selected for targeted therapies. PARP inhibitors have been shown to cause selective toxicity to BRCA-deficient cells (Bryant *et al*. 2005; Farmer *et al*. 2005); however,

clinical trials have shown that not all patients with BRCA-deficient breast tumours respond to olaparib treatment. A phase I trial in which patients were given doses of olaparib ranging from 10mg once daily for two weeks to 600mg twice daily for three weeks, showed a 47% response rate in patients with BRCA-mutated tumours (Fong *et al*. 2009), and a follow-up phase II trial showed a 41% response rate in patients with BRCA mutations that were given 400mg twice daily (Tutt *et al*. 2010). Preclinical studies in *BlgCre-Brca2*$^{f/f}$*/p53*$^{f/f}$ mice have also shown a range of responses to daily olaparib therapy (Hay *et al*. 2009).

6.1.1 Investigating if tumour type correlates with different responses to olaparib

The aim of the work presented in the first chapter of this thesis was to conduct the first *in vivo* study to investigate if tumour type is associated with response to olaparib therapy in a *BRCA2*-mutant setting. Tumour-bearing *BlgCre-Brca2*$^{f/f}$*/p53*$^{f/f}$ mice were treated with daily 100mg/kg olaparib for 30 days. The responses to olaparib were classified into three groups: poor, moderate and excellent, and the tumours classified by histopathology.

Previous studies have shown that different tumour types have different clinical behaviours (Perou *et al*. 2000a; Sorlie *et al*. 2003; Reis-Filho and Pusztai 2011), and the presence of four different histopathological tumour types in this model indicates that tumour type may stratify the response to olaparib therapy. The majority of tumours showed either an excellent or a moderate response, with only 20% showing a poor response. Tumours showing an excellent response were characterised as ASQCs and IDC-NSTs, whilst moderate responders were either AMEs, MSCCs or IDC-NSTs, and poor/non- responders were exclusively MSCCs. This variation in responses between the different types of tumours suggests that there is indeed a correlation between tumour type and response to olaparib therapy. This is important for the clinic, as it suggests that further stratification will be needed to determine maximum patient benefit.

The presence of IDC-NSTs in two different response groups may be explained by the significant differences in vimentin staining seen between the groups. Those in the moderate responder cohort showed higher levels of vimentin staining, suggesting that vimentin levels may be indicative of response. This was also shown to be true independent of tumour type, with the tumours in the excellent responder cohort showing low levels of Vimentin-positive epithelial cells, whilst moderate responders contained significantly higher levels when

compared to excellent responders. In addition, poor responders showed significantly higher levels than moderate responders. Other studies have also shown correlations between Vimentin expression and sensitivity to therapy, for example gefitinib-resistant cell lines of head and neck squamous cell carcinoma and NSCLC were found to express Vimentin, as well as other EMT markers, whilst expression was absent in sensitive lines (Frederick *et al.* 2007). Untreated IDC-NSTs show very low levels of Vimentin staining, suggesting that Vimentin expression is induced during olaparib treatment. This is supported by the significant increase in Vimentin positive cells in IDC-NSTs treated with a single dose of olaparib and taken 1 hour later, compared to untreated tumours. The study by Li *et al.* showed that Adriamycin treatment on MCF7 cells induced EMT in a subpopulation (Li *et al*. 2009), suggesting that other cancer therapeutics also induce EMT.

The significant increase of Vimentin positive cells in IDC-NSTs 1 hour after a single dose of olaparib suggests that it has a secondary role of driving EMT/mesenchymal phenotype in these tumours. A study analysing olaparib therapy in breast cancer cells *in vitro* showed that treatment induced expression of phosphorylated ERK (Shimo *et al.* 2014), and they conclude that cell death is induced by this pathway. The ERK pathway has also shown to induce ZEB1 and TWIST expression, suggesting that in a subset of cells olaparib induces EMT via the expression of ZEB1 and/or TWIST. This would correlate with the increase in Twist positive cells in IDC-NSTs 1 hour after a single dose of olaparib seen in this study. This induction could then drive plasticity to eventually form olaparib resistance, resulting in tumour relapse. This mechanism may have a broader relevance for cancer therapy, as cisplatin has also been shown to induce EMT in ovarian cancer cell lines (Ahmed *et al.* 2010) and carboplatin-resistant tumours in this study classified as IDC-NSTs show a significant increase in Vimentin- and Twist-positive cells.

MSCCs were also found in two different response groups: moderate and poor. Those in the poor responder group showed identical morphological and immunohistochemical staining patterns to untreated MSCCs, but those in the moderate responder group contained small regions of epitheloid morphology, which had similar immunohistochemical staining to IDC-NSTs or AMEs. This feature was also seen in resistant MSCCs, suggesting that at 30 days of treatment, tumours may be starting to show signs of resistance.

In contrast, 2 tumours taken between 18 and 40 days of olaparib therapy from *BlgCre-Brca2$^{f/f}$/p53$^{f/f}$/Cdh1$^{f/f}$* mice showed differences to *BlgCre-Brca2$^{f/f}$/p53$^{f/f}$* mice, with a poor responder characterised as an AME, and a moderate responder characterised as an IDC-NST, with both tumours showing low Vimentin positivity. Because there were only 2 tumours, no firm conclusions can be formed, but it suggests that there may be differences between the two models which may warrant further investigation.

6.1.2 MSCCs may be intrinsically resistant

Poor responders were found to be exclusively MSCCs, showing identical morphology and immunohistochemical staining patterns as untreated MSCCs. This suggests that this tumour type may have an intrinsic resistance to PARP inhibition, and correlates with studies in human breast tumours, which show that metaplastic carcinomas have a poor prognosis (Al Sayed *et al*. 2006; Hennessy *et al*. 2009). This is interesting as the majority of tumours in our model which became resistance during treatment are also MSCCs, or display MSCC characteristics, suggesting that the endpoint of acquired resistance in many tumours may be the same as those which are intrinsically resistant, or that the tumours which initially responded had a low level of intrinsically-resistant cells at treatment outset, which survived and were selected for during therapy. EMT features are also associated with resistance to other drugs, such as gemcitabine and cisplatin (Arumugam *et al*. 2009).

The possibility that MSCCs have an intrinsic resistance to olaparib is very important for the clinic, as it suggests that patients with this tumour type will not benefit from olaparib therapy, thereby suggesting that the histopathology of tumours should be taken into account when stratifying patients for olaparib treatment. Although MSCCs are very rare in humans, the intrinsic resistance may also apply to tumours with MSCC features, for example the presence of mesenchymal morphology or those with similar expression profiles, therefore widening the clinical implications.

6.2 Investigating the mechanism of resistance to olaparib

Unfortunately, a recurring problem with cancer treatment is that of drug resistance. Pre-clinical studies with the PARP inhibitor olaparib in *Brca1* and *Brca2* conditional knockout mice have shown that long-term treatment invariably results in tumour relapse (Rottenberg *et al*. 2008; Hay *et al*. 2009), and clinical resistance has also been reported (Barber *et al*.

2013). Tumour resistance is highly detrimental in the clinic, hence it is imperative that the mechanisms of drug resistance are discovered and explored to ensure the effectiveness of cancer drugs.

The main objective of the work presented in chapter 4 was to discover the mechanism(s) of olaparib resistance in a *Brca2* conditional knockout mouse model. Olaparib resistance has been investigated by other laboratories *in vitro* and in a *Brca1* conditional knockout mouse model, making this the first study of an *in vivo* investigation in a mutant *Brca2* setting. Two strategies were taken to investigate the mechanism of resistance; firstly by analysing the current proposed mechanisms, and secondly by assessing whether histopathological tumour type impacts on resistance.

6.2.1 Investigating proposed mechanisms of resistance

The rationale behind utilising the P-gp inhibitor Tariquidar in combination with olaparib on relapsed tumours from olaparib-treated *BlgCre-Brca2$^{f/f}$/p53$^{f/f}$* mice came from previous work in which such olaparib-resistant tumours showed a significant up-regulation of these efflux pumps in comparison to untreated tumours (Hay *et al*. 2009), suggesting that it was likely to be a major mechanism of resistance. However, the addition of Tariquidar to olaparib-resistant tumours had no effect on tumour relapse and resistant tumours retained low PAR levels 1 hour after treatment, suggesting that PARP-1 is still effectively inhibited in resistant tumours, despite the up-regulation of P-gps. In addition, it corroborates previous work in this model with the AstraZeneca PARP inhibitor AZD2461, which was designed to be a lower substrate for P-gps, which found that resistant tumours did not respond to this follow-up therapy either (Hay *et al.* unpublished). This differs from studies in a mouse model of *Brca1/p53* mutant breast cancer, where sensitivity to olaparib was at least partially restored upon inhibition of P-gps with Tariquidar or by treatment with AZD2461 (Rottenberg *et al*. 2008; Jaspers *et al*. 2013). Tariquidar has also been shown to reverse the resistant phenotype of *Brca1*-deficient mouse mammary tumours to doxorubicin (Pajic *et al*. 2009).

Analysis of 53BP1 levels in resistant tumours showed no significant difference to tumours that were responding to daily olaparib treatment, suggesting that, unlike in *Brca1*-deficient tumours (Jaspers *et al*. 2013), loss of this protein is not involved in olaparib resistance.

These results show that there are differences in the mechanisms of resistance to PARP inhibition between these two genetically distinct mouse models and this will have important clinical implications if such differences are replicated in *BRCA1*- and *BRCA2*-mutated human cancers. Consequently, this would suggest that targeting of resistant tumours from patients with *BRCA1*- and *BRCA2*-mutated breast cancers will require different therapeutic strategies; therefore further studies are needed to investigate the reasons behind the differences. It would be interesting to investigate if a similar phenomenon is seen with resistance to other drugs, such as carboplatin and cisplatin.

Results from *in vitro* and clinical studies investigating olaparib resistance in a *BRCA2* setting have suggested that secondary mutations in the gene, causing the re-activation of the HR pathway, is a mechanism of resistance (Edwards *et al*. 2008; Barber *et al*. 2013). Analysis of *Brca2* expression in resistant tumours in this study showed low expression, suggesting that the re-activation of the protein does not occur in this mouse model. However, to fully investigate this possibility, sequencing of the *Brca2* gene should be performed in resistant tumours and re-activation of the HR pathway should be analysed in more detail.

This is the first study to suggest that olaparib-resistance in a mutant *BRCA2* setting is not due to these already proposed mechanisms, therefore a novel mechanism or mechanisms must be involved.

6.2.2 Analysing olaparib-resistant tumour types

The rationale behind analysing olaparib-resistant tumours by histopathology was due to previous studies suggesting that certain breast tumour subtypes are resistance to traditional chemotherapeutics (Al Sayed *et al*. 2006; Hennessy *et al*. 2009). The majority of olaparib-resistant *Brca2*/*p53*-mutant tumours in this study were characterised as MSCCs, which only account for a small proportion of untreated tumours. They are mesenchymal tumours, with spindle morphology and high expression of EMT genes such as Vimentin and Twist. Interestingly, although other types of resistant tumours showed epitheloid morphology, they also exhibited similar expression profiles to MSCCs, with increased expression of EMT markers and a decrease in luminal characteristics. This suggests that the mesenchymal/EMT features may be important in causing resistance to olaparib in this model, correlating with

other studies that show that EMT features are associated with resistance to chemotherapeutics (Creighton *et al*. 2009; Liu *et al*. 2013). The presence of resistant tumours with epitheloid morphology suggests that mesenchymal morphology is not necessary for olaparib resistance, rather it is down to the genetic changes, which could be termed as partial EMT, and this is the first *in vivo* study to suggest this. Histological analysis of human olaparib-resistant tumours will be critical to see if the results seen in the mouse model are recapitulated in humans. This work has important implications for research into olaparib therapy as it suggests that relapsed tumours in patients may have EMT features, and therefore further studies are needed to investigate whether these features are critical for resistance. It will also be important to investigate the processes that lead to the EMT features, so that therapies can be developed to prevent resistance to PARP inhibitors. Current theories include clonal expansion of cells with intrinsic resistance, or conversion of epitheloid cells to more mesenchymal-like cells (Figure 4.23), possibly through partial or full EMT. To further this study it would have been beneficial to analyse matched, sequential biopsies of initially sensitive and subsequently resistant tumours from the mouse model. This would have allowed us to analyse if the same tumour has changed histopathological type during treatment. Unfortunately this is impractical in the mouse model due to Home Office regulations, the small amount of tumour material that is available in these models, and the wound response may also impact the results.

One further possible hypothesis for the mechanism of resistance is loss of *PARP-1* expression. A previous study has shown that *in vitro PARP-1*-deficient cells are resistant to olaparib (Pettitt *et al*. 2013), and work in this thesis has shown that PAR levels in resistant tumours were low, indicating low PARP activity, which could be due to the loss of *PARP-1* expression. This would correlate with the theory that PARP inhibitors trap PARP-1 at sites of damaged DNA, which is cytotoxic to the cell, resulting in cell death (Murai *et al.* 2012), therefore the loss of PARP-1 would prevent the toxicity. As mentioned previously, MSCCs may have an intrinsic resistance to olaparib. 2 MSCCs that were treated with vehicle showed lower PAR levels compared to IDC-NSTs, suggesting that these tumours have lower PARP-1 expression, which could lead to intrinsic resistance.

6.2.3 Role of E-cadherin

To further investigate if/which EMT characteristics are important for resistance to olaparib, the response to olaparib therapy and tumour histopathology was analysed in tumours from *BlgCre-Brca2$^{f/f}$/p53$^{f/f}$/Cdh1$^{f/f}$* mice. Histopathological analysis of untreated tumours showed that the majority had high expression of basal markers and low expression of luminal markers, but no difference in EMT associated genes or the presence of mesenchymal morphology, suggesting that the genetic loss of E-cadherin does not drive EMT and the formation of MSCCs. These results are comparable to those in previous studies performed in a similar mouse model (Derksen *et al*. 2006) and in human breast tumours (Mahler-Araujo *et al*. 2008). Daily olaparib treatment also showed no clear differences compared to *BlgCre-Brca2$^{f/f}$/p53$^{f/f}$* mice, with the same range of initial responses and relapse with long term treatment. This may be because genetic loss of E-cadherin does not seem to drive EMT in this model. Resistant tumours showed similar morphological and expression profiles to those in *BlgCre-Brca2$^{f/f}$/p53$^{f/f}$* mice, suggesting that EMT is involved in olaparib resistance and that the loss of E-cadherin is not critical for resistance. This is probably not surprising as resistant IDC-NSTs and AMEs from *BlgCre-Brca2$^{f/f}$/p53$^{f/f}$* mice do not show loss of E-cadherin. This is important as it eliminates genetic loss of E-cadherin as a possible target for therapeutic intervention of olaparib resistance; however other studies suggest that mesenchymal morphology correlates with loss of E-cadherin by methylation of the promoter (Lombaerts *et al*. 2006), suggesting that methylation, rather than mutations are important for EMT and mesenchymal characteristics. This would correlate with a study in human gastric carcinomas which showed that hypermethylation of *CDH1* was associated with worse prognosis and reduced 5-year survival rate (Graziano *et al.* 2004a) This means that loss of E-cadherin by methylation may be important for olaparib resistance, and requires further investigation.

6.3 Summary of olaparib therapy in a mouse model of *BRCA2*-mutated breast cancer

Daily olaparib therapy has shown to cause regression of BRCA-deficient tumours in preclinical studies (Rottenberg *et al*. 2008; Hay *et al*. 2009) and clinical trials (Fong *et al*. 2009; Tutt *et al*. 2010); however these studies have also shown that not all BRCA-deficient

tumours respond to the treatment. The work in this thesis suggests that tumours with mesenchymal features have an intrinsic resistance to olaparib therapy, which would mean that further patient stratification is required when deciding on whether this therapy may be suitable, and may explain why not all patients with *BRCA*-mutated breast cancer have benefitted from olaparib therapy in current clinical trials.

Investigating resistance to olaparib therapy in this thesis suggests that tumours which initially respond to olaparib therapy harness or acquire certain mesenchymal characteristics in order to develop resistance during treatment. This is a novel mechanism of resistance to olaparib therapy, and requires further investigation into the specific mechanisms and molecular pathways involved in order to target resistance, and prolong clinical benefit. The presence of mesenchymal characteristics in carboplatin-resistant tumours from the same mouse model suggests that this mechanism could be involved in resistance to other cancer treatments, therefore widening the potential benefit of targeting this mechanism.

Although it is difficult to calculate precisely how many cancer patients will be impacted by this research, it has the potential to further stratify *BRCA*-mutated patients for olaparib therapy, thereby impacting patients with tumours that do not have mesenchymal features, which the percentage of breast cancer cases is currently unknown.. Tumours with mesenchymal features have shown here to have a poorer response to olaparib therapy, this suggests that histology, or Vimentin expression in the tumours, could be used to further stratify patients for treatment. This work also allows future research to focus on discovering the mechanisms that govern this poorer response in order to re-sensitise these tumours, therefore potentially improving patient responses. Pre-clinical studies have shown that all BRCA-deficient tumours on continuous olaparib therapy relapse, suggesting that a similar effect will be seen in humans. This work suggests that majority of these relapsed tumours will have mesenchymal features. By discovering the mechanisms of this, and investigating if they are critical for tumour relapse, will provide the clinic with a way of combating olaparib resistance, therefore possibly impacting the majority of patients with *BRCA2*- mutated breast cancer, that have initially responded to olaparib.

Biblography

Ahmed, N., Abubaker, K., Findlay, J. and Quinn, M. (2010). Epithelial Mesenchymal Transition and Cancer Stem Cell-Like Phenotypes Facilitate Chemoresistance in Recurrent Ovarian Cancer. *Current Cancer Drug Targets* **10:**268-278.

Al-Hajj, M., Wicha, M. S., Benito-Hernandez, A., Morrison, S. J. and Clarke, M. F. (2003). Prospective identification of tumorigenic breast cancer cells. *Proceedings of the National Academy of Sciences of the United States of America* **100:**3983-3988.

Al Sayed, A. D., El Weshi, A. N., Tulbah, A. M., Rahal, M. M. and Ezzat, A. A. (2006). Metaplastic carcinoma of the breast Clinical presentation, treatment results and prognostic factors. *Acta Oncologica* **45:**188-195.

Ali, A. A. E., Timinszky, G., Arribas-Bosacoma, R., Kozlowski, M., Hassa, P. O., Hassler, M., Ladurner, A. G. *et al.* (2012). The zinc-finger domains of PARP1 cooperate to recognize DNA strand breaks. *Nature Structural & Molecular Biology* **19:**685-+.

Ame, J. C., Rolli, V., Schreiber, V., Niedergang, C., Apiou, F., Decker, P., Muller, S. *et al.* (1999). PARP-2, a novel mammalian DNA damage-dependent poly(ADP-ribose) polymerase. *Journal of Biological Chemistry* **274:**17860-17868.

Anders, S., Pyl, P. T. and Huber, W. (2014). HTSeq — A Python framework to work with high-throughput sequencing data. *bioRxiv*.

Arumugam, T., Ramachandran, V., Fournier, K. F., Wang, H., Marquis, L., Abbruzzese, J. L., Gallick, G. E. *et al.* (2009). Epithelial to Mesenchymal Transition Contributes to Drug Resistance in Pancreatic Cancer. *Cancer Research* **69:**5820-5828.

Audeh, M. W., Carmichael, J., Penson, R. T., Friedlander, M., Powell, B., Bell-McGuinn, K. M., Scott, C. *et al.* (2010). Oral poly(ADP-ribose) polymerase inhibitor olaparib in patients with BRCA1 or BRCA2 mutations and recurrent ovarian cancer: a proof-of-concept trial. *Lancet* **376:**245-251.

Augustin, A., Spenlehauer, C., Dumond, H., Murcia, J. M. D., Piel, M., Schmit, A. C., Apiou, F. *et al.* (2003). PARP-3 localizes preferentially to the daughter centriole and interferes with the G1/S cell cycle progression. *Journal of Cell Science* **116:**1551-1562.

Barber, L. J., Sandhu, S., Chen, L., Campbell, J., Kozarewa, I., Fenwick, K., Assiotis, I. *et al.* (2013). Secondary mutations in BRCA2 associated with clinical resistance to a PARP inhibitor. *Journal of Pathology* **229:**422-429.

Bardou, V. J., Arpino, G., Elledge, R. M., Osborne, C. K. and Clark, G. M. (2003). Progesterone receptor status significantly improves outcome prediction over estrogen receptor status alone for adjuvant endocrine therapy in two large breast cancer databases. *Journal of Clinical Oncology* **21:**1973-1979.

Baselga, J. (2001). Herceptin((R)) alone or in combination with chemotherapy in the treatment of HER2-positive metastatic breast cancer: Pivotal trials. *Oncology* **61:**14-21.

Beral, V., Bull, D., Doll, R., Peto, R., Reeves, G., La Vecchia, C., Magnusson, C. *et al.* (2002). Breast cancer and breastfeeding: collaborative reanalysis of individual data from 47 epidemiological studies in 30 countries, including 50 302 women with breast cancer and 96 973 women without the disease. *Lancet* **360:**187-195.

Berghammer, H., Ebner, M., Marksteiner, R. and Auer, B. (1999). pADPRT-2: a novel mammalian polymerizing(ADP-ribosyl)transferase gene related to truncated pADPRT homologues in plants and Caenorhabditis elegans. *Febs Letters* **449:**259-263.

Bloom, H. J. G. and Richardson, W. W. (1957). HISTOLOGICAL GRADING AND PROGNOSIS IN BREAST CANCER - A STUDY OF 1409 CASES OF WHICH 359 HAVE BEEN FOLLOWED FOR 15 YEARS. *British Journal of Cancer* **11:**359-&.

Boehler, C., Gauthier, L. R., Mortusewicz, O., Biard, D. S., Saliou, J.-M., Bresson, A., Sanglier-Cianferani, S. *et al.* (2011). Poly(ADP-ribose) polymerase 3 (PARP3), a newcomer in cellular response to DNA damage and mitotic progression. *Proceedings of the National Academy of Sciences of the United States of America* **108:**2783-2788.

Bolos, V., Peinado, H., Perez-Moreno, M. A., Fraga, M. F., Esteller, M. and Cano, A. (2003). The transcription factor Slug represses E-cadherin expression and induces epithelial to mesenchymal transitions: a comparison with Snail and E47 repressors. *Journal of Cell Science* **116:**499-511.

Bouwman, P., Aly, A., Escandell, J. M., Pieterse, M., Bartkova, J., van der Gulden, H., Hiddingh, S. *et al.* (2010). 53BP1 loss rescues BRCA1 deficiency and is associated with triple-negative and BRCA-mutated breast cancers. *Nature Structural & Molecular Biology* **17:**688-U656.

Bryant, H. E., Petermann, E., Schultz, N., Jemth, A.-S., Loseva, O., Issaeva, N., Johansson, F. *et al.* (2009). PARP is activated at stalled forks to mediate Mre11-dependent replication restart and recombination. *Embo Journal* **28:**2601-2615.

Bryant, H. E., Schultz, N., Thomas, H. D., Parker, K. M., Flower, D., Lopez, E., Kyle, S. *et al.* (2005). Specific killing of BRCA2-deficient tumours with inhibitors of poly(ADP-ribose) polymerase. *Nature* **434:**913-917.

Burkle, A. (2005). Poly(ADP-ribose) - The most elaborate metabolite of NAD. *Febs Journal* **272:**4576-4589.

Caiafa, P., Guastafierro, T. and Zampieri, M. (2009). Epigenetics: poly(ADP-ribosyl)ation of PARP-1 regulates genomic methylation patterns. *Faseb Journal* **23:**672-678.

Cano, A., Perez-Moreno, M. A., Rodrigo, I., Locascio, A., Blanco, M. J., del Barrio, M. G., Portillo, F. *et al.* (2000). The transcription factor Snail controls epithelial-mesenchymal transitions by repressing E-cadherin expression. *Nature Cell Biology* **2:**76-83.

Cardiff, R. D., Anver, M. R., Gusterson, B. A., Hennighausen, L., Jensen, R. A., Merino, M. J., Rehm, S. *et al.* (2000). The mammary tumor pathology of genetically engineered mice: A consensus classification among veterinary and medical pathologists. *Toxicologic Pathology* **28:**858-858.

Carey, L. A., Perou, C. M., Livasy, C. A., Dressler, L. G., Cowan, D., Conway, K., Karaca, G. *et al.* (2006). Race, breast cancer subtypes, and survival in the Carolina Breast Cancer Study. *Jama-Journal of the American Medical Association* **295:**2492-2502.

Carey, L. A., Rugo, H. S., Marcom, P. K., Irvin, W., Jr., Ferraro, M., Burrows, E., He, X. *et al.* (2008). TBCRC 001: EGFR inhibition with cetuximab added to carboplatin in metastatic triple-negative (basal-like) breast cancer. *Journal of Clinical Oncology* **26**.

Carvajal, G., Droguett, A., Burgos, M. E., Aros, C., Ardiles, L., Flores, C., Carpio, D. *et al.* (2008). Gremlin: A novel mediator of epithelial mesenchymal transition and fibrosis in chronic allograft nephropathy. *Transplantation Proceedings* **40:**734-739.

Chaffer, C. L., Brennan, J. P., Slavin, J. L., Blick, T., Thompson, E. W. and Williams, E. D. (2006). Mesenchymal-to-epithelial transition facilitates bladder cancer metastasis: Role of fibroblast growth factor receptor-2. *Cancer Research* **66:**11271-11278.

Chaffer, C. L., Marjanovic, N. D., Lee, T., Bell, G., Kleer, C. G., Reinhardt, F., D'Alessio, A. C. *et al.* (2013). Poised Chromatin at the ZEB1 Promoter Enables Breast Cancer Cell Plasticity and Enhances Tumorigenicity. *Cell* **154:**61-74.

Cheang, M. C. U., Chia, S. K., Voduc, D., Gao, D., Leung, S., Snider, J., Watson, M. *et al.* (2009). Ki67 Index, HER2 Status, and Prognosis of Patients With Luminal B Breast Cancer. *Journal of the National Cancer Institute* **101:**736-750.

Cheung, A. M. Y., Hande, M. P., Jalali, F., Tsao, M. S., Skinnider, B., Hirao, A., McPherson, J. P. *et al.* (2002). Loss of Brca2 and p53 synergistically promotes genomic instability and deregulation of T-cell apoptosis. *Cancer Research* **62:**6194-6204.

Choi, Y., Lee, H. J., Jang, M. H., Gwak, J. M., Lee, K. S., Kim, E. J., Kim, H. J. *et al.* (2013). Epithelial-mesenchymal transition increases during the progression of in situ to invasive basal-like breast cancer. *Human Pathology* **44:**2581-2589.

Christiansen, J. J. and Rajasekaran, A. K. (2006). Reassessing epithelial to mesenchymal transition as a prerequisite for carcinoma invasion and metastasis. *Cancer Research* **66:**8319-8326.

Creighton, C. J., Li, X., Landis, M., Dixon, J. M., Neumeister, V. M., Sjolund, A., Rimm, D. L. *et al.* (2009). Residual breast cancers after conventional therapy display mesenchymal as well as tumor-initiating features. *Proceedings of the National Academy of Sciences of the United States of America* **106:**13820-13825.

Crook, T., Brooks, L. A., Crossland, S., Osin, P., Barker, K. T., Waller, J., Philp, E. *et al.* (1998). p53 mutation with frequent novel codons but not a mutator phenotype in BRCA1- and BRCA2-associated breast tumours. *Oncogene* **17:**1681-1689.

Crook, T., Crossland, S., Crompton, M. R., Osin, P. and Gusterson, B. A. (1997). p53 mutations in BRCA1-associated familial breast cancer. *Lancet* **350:**638-639.

de Murcia, J. M. N., Ricoul, M., Tartier, L., Niedergang, C., Huber, A., Dantzer, F., Schreiber, V. *et al.* (2003). Functional interaction between PARP-1 and PARP-2 in chromosome stability and embryonic development in mouse. *Embo Journal* **22:**2255-2263.

Demurcia, G. and Demurcia, J. M. (1994). POLY(ADP-RIBOSE) POLYMERASE - A MOLECULAR NICK-SENSOR. *Trends in Biochemical Sciences* **19:**172-176.

deMurcia, J. M., Niedergang, C., Trucco, C., Ricoul, M., Dutrillaux, B., Mark, M., Oliver, F. J. *et al.* (1997). Requirement of poly(ADP-ribose) polymerase in recovery from DNA damage in mice and in cells. *Proceedings of the National Academy of Sciences of the United States of America* **94:**7303-7307.

Derksen, P. W. B., Braumuller, T. M., van der Burg, E., Hornsveld, M., Mesman, E., Wesseling, J., Krimpenfort, P. *et al.* (2011). Mammary-specific inactivation of E-cadherin and p53 impairs functional gland development and leads to pleomorphic invasive lobular carcinoma in mice. *Disease Models & Mechanisms* **4:**347-358.

Derksen, P. W. B., Liu, X., Saridin, F., van der Gulden, H., Zevenhoven, J., Evers, B., van Beijnum, J. R. *et al.* (2006). Somatic inactivation of E-cadherin and p53 in mice leads to metastatic lobular mammary carcinoma through induction of anoikis resistance and angiogenesis. *Cancer Cell* **10:**437-449.

Devalaraja-Narashimha, K. and Padanilam, B. J. (2010). PARP1 deficiency exacerbates diet-induced obesity in mice. *Journal of Endocrinology* **205:**242-251.

Dianov, G. L. (2011). Base excision repair targets for cancer therapy. *American Journal of Cancer Research* **1:**845-851.

Dobzhansky, T. (1946). GENETICS OF NATURAL POPULATIONS .13. RECOMBINATION AND VARIABILITY IN POPULATIONS OF DROSOPHILA-PSEUDOOBSCURA. *Genetics* **31:**269-290.

Doetschman, T., Gregg, R. G., Maeda, N., Hooper, M. L., Melton, D. W., Thompson, S. and Smithies, O. (1987). TARGETED CORRECTION OF A MUTANT HPRT GENE IN MOUSE EMBRYONIC STEM-CELLS. *Nature* **330:**576-578.

Edwards, S. L., Brough, R., Lord, C. J., Natrajan, R., Vatcheva, R., Levine, D. A., Boyd, J. *et al.* (2008). Resistance to therapy caused by intragenic deletion in BRCA2. *Nature* **451:**1111-U1118.

El-Khamisy, S. F., Masutani, M., Suzuki, H. and Caldecott, K. W. (2003). A requirement for PARP-1 for the assembly or stability of XRCC1 nuclear foci at sites of oxidative DNA damage. *Nucleic Acids Research* **31:**5526-5533.

Eustermann, S., Videler, H., Yang, J.-C., Cole, P. T., Gruszka, D., Veprintsev, D. and Neuhaus, D. (2011). The DNA-Binding Domain of Human PARP-1 Interacts with DNA Single-Strand Breaks as a Monomer through Its Second Zinc Finger. *Journal of Molecular Biology* **407:**149-170.

Evans, M. J. and Kaufman, M. H. (1981). ESTABLISHMENT IN CULTURE OF PLURIPOTENTIAL CELLS FROM MOUSE EMBRYOS. *Nature* **292:**154-156.

Farmer, H., McCabe, N., Lord, C. J., Tutt, A. N. J., Johnson, D. A., Richardson, T. B., Santarosa, M. *et al.* (2005). Targeting the DNA repair defect in BRCA mutant cells as a therapeutic strategy. *Nature* **434:**917-921.

Fondrevelle, M. E., Kantelip, B., Reiter, R. E., Chopin, D. K., Thiery, J. P., Monnien, F., Bittard, H. *et al.* (2009). The expression of Twist has an impact on survival in human bladder cancer and is influenced by the smoking status. *Urologic Oncology-Seminars and Original Investigations* **27:**268-276.

Fong, P. C., Boss, D. S., Yap, T. A., Tutt, A., Wu, P., Mergui-Roelvink, M., Mortimer, P. *et al.* (2009). Inhibition of Poly(ADP-Ribose) Polymerase in Tumors from BRCA Mutation Carriers. *New England Journal of Medicine* **361:**123-134.

Frederick, B. A., Helfrich, B. A., Coldren, C. D., Zheng, D., Chan, D., Bunn, P. A., Jr. and Raben, D. (2007). Epithelial to mesenchymal transition predicts gefitinib resistance in cell lines of head and neck squamous cell carcinoma and non-small cell lung carcinoma. *Molecular Cancer Therapeutics* **6:**1683-1691.

Fukushima, M., Kuzuya, K., Ota, K. and Ikai, K. (1981). POLY(ADP-RIBOSE) SYNTHESIS IN HUMAN CERVICAL-CANCER CELL - DIAGNOSTIC CYTOLOGICAL USEFULNESS. *Cancer Letters* **14:**227-236.

Gelmon, K. A., Tischkowitz, M., Mackay, H., Swenerton, K., Robidoux, A., Tonkin, K., Hirte, H. *et al.* (2011). Olaparib in patients with recurrent high-grade serous or poorly differentiated ovarian carcinoma or triple-negative breast cancer: a phase 2, multicentre, open-label, non-randomised study. *Lancet Oncology* **12:**852-861.

Giansanti, V., Dona, F., Tillhon, M. and Scovassi, A. I. (2010). PARP inhibitors: New tools to protect from inflammation. *Biochemical Pharmacology* **80:**1869-1877.

Goggins, M., Schutte, M., Lu, J., Moskaluk, C. A., Weinstein, C. L., Petersen, G. M., Yeo, C. J. *et al.* (1996). Germline BRCA2 gene mutations in patients with apparently sporadic pancreatic carcinomas. *Cancer Research* **56:**5360-5364.

Goncalves, A., Finetti, P., Sabatier, R., Gilabert, M., Adelaide, J., Borg, J.-P., Chaffanet, M. *et al.* (2011). Poly(ADP-ribose) polymerase-1 mRNA expression in human breast cancer: a meta-analysis. *Breast Cancer Research and Treatment* **127:**273-281.

Gottesman, M. M. (2002). Mechanisms of cancer drug resistance. *Annual Review of Medicine* **53:**615-627.

Graziano, F., Arduini, F., Ruzzo, A., Bearzi, I., Humar, B., More, H., Silva, R. *et al.* (2004a). Prognostic analysis of E-cadherin gene promoter hypermethylation in patients with surgically resected, node-positive, diffuse gastric cancer. *Clinical Cancer Research* **10:**2784-2789.

Graziano, F., Mandolesi, A., Ruzzo, A., Bearzi, I., Testa, E., Arduini, F., Silva, R. *et al.* (2004b). Predictive and prognostic role of E-cadherin protein expression in patients with advanced gastric carcinomas treated with palliative chemotherapy. *Tumor Biology* **25:**106-110.

Green, M. D., Francis, P. A., Gebski, V., Harvey, V., Karapetis, C., Chan, A., Snyder, R. *et al.* (2009). Gefitinib treatment in hormone-resistant and hormone receptor-negative advanced breast cancer. *Annals of Oncology* **20:**1813-1817.

Grille, S. J., Bellacosa, A., Upson, J., Klein-Szanto, A. J., van Roy, F., Lee-Kwon, W., Donowitz, M. *et al.* (2003). The protein kinase Akt induces epithelial mesenchymal transition and promotes enhanced motility and invasiveness of squamous cell carcinoma lines. *Cancer Research* **63:**2172-2178.

Guha, M. (2011). PARP inhibitors stumble in breast cancer. *Nature Biotechnology* **29:**373-374.

Gusterson, B. A., Warburton, M. J., Monaghan, P., Foster, C., Edwards, P., Kraft, N., Smith, C. *et al.* (1984). The use of immunohistochemical probes in the study of benign and malignant breast disease. *Behring Institute Mitteilungen* 39-48.

Haince, J.-F., McDonald, D., Rodrigue, A., Dery, U., Masson, J.-Y., Hendzel, M. J. and Poirier, G. G. (2008). PARP1-dependent kinetics of recruitment of MRE11 and NBS1 proteins to multiple DNA damage sites. *Journal of Biological Chemistry* **283:**1197-1208.

Hartmann, L. C., Schaid, D. J., Woods, J. E., Crotty, T. P., Myers, J. L., Arnold, P. G., Petty, P. M. *et al.* (1999). Efficacy of bilateral prophylactic mastectomy in women with a family history of breast cancer. *New England Journal of Medicine* **340:**77-84.

Hartsock, A. and Nelson, W. J. (2008). Adherens and tight junctions: Structure, function and connections to the actin cytoskeleton. *Biochimica Et Biophysica Acta-Biomembranes* **1778:**660-669.

Hassa, P. O., Buerki, C., Lombardi, C., Imhof, R. and Hottiger, M. O. (2003). Transcriptional coactivation of nuclear factor-kappa B-dependent gene expression by p300 is regulated by poly(ADP)-ribose polymerase-1. *Journal of Biological Chemistry* **278:**45145-45153.

Hassa, P. O. and Hottiger, M. O. (2002). The functional role of poly(ADP-ribose)polymerase 1 as novel coactivator of NF-kappa B in inflammatory disorders. *Cellular and Molecular Life Sciences* **59:**1534-1553.

Hay, T., Matthews, J. R., Pietzka, L., Lau, A., Cranston, A., Nygren, A. O. H., Douglas-Jones, A. *et al.* (2009). Poly(ADP-Ribose) Polymerase-1 Inhibitor Treatment Regresses Autochthonous Brca2/p53-Mutant Mammary Tumors In vivo and Delays Tumor Relapse in Combination with Carboplatin. *Cancer Research* **69:**3850-3855.

Hennessy, B. T., Giordano, S., Broglio, K., Duan, Z., Trent, J., Buchholz, T. A., Babiera, G. *et al.* (2006). Biphasic metaplastic sarcomatoid carcinoma of the breast. *Annals of Oncology* **17:**605-613.

Hennessy, B. T., Gonzalez-Angulo, A.-M., Stemke-Hale, K., Gilcrease, M. Z., Krishnamurthy, S., Lee, J.-S., Fridlyand, J. *et al.* (2009). Characterization of a Naturally Occurring Breast Cancer Subset Enriched in Epithelial-to-Mesenchymal Transition and Stem Cell Characteristics. *Cancer Research* **69:**4116-4124.

Hennighausen, L. and Robinson, G. W. (2005). Information networks in the mammary gland. *Nature Reviews Molecular Cell Biology* **6:**715-725.

Hirai, K., Ueda, K. and Hayaishi, O. (1983). ABERRATION OF POLY(ADENOSINE DIPHOSPHATE-RIBOSE) METABOLISM IN HUMAN-COLON ADENOMATOUS POLYPS AND CANCERS. *Cancer Research* **43:**3441-3446.

Hollestelle, A., Peeters, J. K., Smid, M., Timmermans, M., Verhoog, L. C., Westenend, P. J., Heine, A. A. J. *et al.* (2013). Loss of E-cadherin is not a necessity for epithelial to mesenchymal transition in human breast cancer. *Breast Cancer Research and Treatment* **138:**47-57.

Hong, S.-M., Li, A., Olino, K., Wolfgang, C. L., Herman, J. M., Schulick, R. D., Iacobuzio-Donahue, C. *et al.* (2011). Loss of E-cadherin expression and outcome among patients with resectable pancreatic adenocarcinomas. *Modern Pathology* **24:**1237-1247.

Hottiger, M. O., Hassa, P. O., Luscher, B., Schuler, H. and Koch-Nolte, F. (2010). Toward a unified nomenclature for mammalian ADP-ribosyltransferases. *Trends in Biochemical Sciences* **35:**208-219.

Hovey, R. C., Trott, J. F. and Vonderhaar, B. K. (2002). Establishing a framework for the functional mammary gland: From endocrinology to morphology. *Journal of Mammary Gland Biology and Neoplasia* **7:**17-38.

Howard, B. A. and Gusterson, B. A. (2000). Human breast development. *Journal of Mammary Gland Biology and Neoplasia* **5:**119-137.

Hughes-Davies, L., Huntsman, D., Ruas, M., Fuks, F., Bye, J., Chin, S. F., Milner, J. *et al.* (2003). EMSY links the BRCA2 pathway to sporadic breast and ovarian cancer. *Cell* **115:**523-535.

Isabel Rodriguez, M., Peralta-Leal, A., O'Valle, F., Manuel Rodriguez-Vargas, J., Gonzalez-Flores, A., Majuelos-Melguizo, J., Lopez, L. *et al.* (2013). PARP-1 Regulates Metastatic Melanoma through Modulation of Vimentin-induced Malignant Transformation. *Plos Genetics* **9**.

Jaspers, J. E., Kersbergen, A., Boon, U., Sol, W., van Deemter, L., Zander, S. A., Drost, R. *et al.* (2013). Loss of 53BP1 Causes PARP Inhibitor Resistance in Brca1-Mutated Mouse Mammary Tumors. *Cancer Discovery* **3:**68-81.

Jonkers, J., Meuwissen, R., van der Gulden, H., Peterse, H., van der Valk, M. and Berns, A. (2001). Synergistic tumor suppressor activity of BRCA2 and p53 in a conditional mouse model for breast cancer. *Nature Genetics* **29:**418-425.

Kedrin, D., Gligorijevic, B., Wyckoff, J., Verkhusha, V. V., Condeelis, J., Segall, J. E. and van Rheenen, J. (2008). Intravital imaging of metastatic behavior through a mammary imaging window. *Nature Methods* **5:**1019-1021.

Kim, K. K., Kugler, M. C., Wolters, P. J., Robillard, L., Galvez, M. G., Brumwell, A. N., Sheppard, D. *et al.* (2006). Alveolar epithelial cell mesenchymal transition develops in vivo during pulmonary fibrosis and is regulated by the extracellular matrix. *Proceedings of the National Academy of Sciences of the United States of America* **103:**13180-13185.

Kleine, H., Poreba, E., Lesniewicz, K., Hassa, P. O., Hottiger, M. O., Litchfield, D. W., Shilton, B. H. *et al.* (2008). Substrate-Assisted Catalysis by PARP10 Limits Its Activity to Mono-ADP-Ribosylation. *Molecular Cell* **32:**57-69.

Krishnakumar, R., Gamble, M. J., Frizzell, K. M., Berrocal, J. G., Kininis, M. and Kraus, W. L. (2008). Reciprocal binding of PARP-1 and histone H1 at promoters specifies transcriptional outcomes. *Science* **319:**819-821.

Laakso, M., Loman, N., Borg, A. and Isola, J. (2005). Cytokeratin 5/14-positive breast cancer: true basal phenotype confined to BRCA1 tumors. *Modern Pathology* **18:**1321-1328.

Lakhani, S. R., Ellis, I. O., Schnitt, S. J., Tan, P. H. and van de Vijver, M. J. (2012). WHO Classification of Tumours of the Breast. 4th ed. International Agency for Research on Cancer.

Langelier, M.-F. and Pascal, J. M. (2013). PARP-1 mechanism for coupling DNA damage detection to poly(ADP-ribose) synthesis. *Current Opinion in Structural Biology* **23:**134-143.

Larsen, M. J., Kruse, T. A., Tan, Q., Laenkholm, A.-V., Bak, M., Lykkesfeldt, A. E., Sorensen, K. P. *et al.* (2013). Classifications within Molecular Subtypes Enables Identification of BRCA1/BRCA2 Mutation Carriers by RNA Tumor Profiling. *Plos One* **8**.

Latifi, A., Abubaker, K., Castrechini, N., Ward, A. C., Liongue, C., Dobill, F., Kumar, J. *et al.* (2011). Cisplatin Treatment of Primary and Metastatic Epithelial Ovarian Carcinomas Generates Residual Cells With Mesenchymal Stem Cell-Like Profile. *Journal of Cellular Biochemistry* **112:**2850-2864.

Li, Q.-Q., Xu, J.-D., Wang, W.-J., Cao, X.-X., Chen, Q., Tang, F., Chen, Z.-Q. *et al.* (2009). Twist1-Mediated Adriamycin-Induced Epithelial-Mesenchymal Transition Relates to Multidrug Resistance and Invasive Potential in Breast Cancer Cells. *Clinical Cancer Research* **15:**2657-2665.

Li, X., Lewis, M. T., Huang, J., Gutierrez, C., Osborne, C. K., Wu, M.-F., Hilsenbeck, S. G. *et al.* (2008). Intrinsic resistance of tumorigenic breast cancer cells to chemotherapy. *Journal of the National Cancer Institute* **100:**672-679.

Liao, M.-J., Zhang, C. C., Zhou, B., ZimonjiC, D. B., Mani, S. A., Kaba, M., Gifford, A. *et al.* (2007). Enrichment of a population of mammary gland cells that form mammospheres and have in vivo repopulating activity. *Cancer Research* **67:**8131-8138.

Lim, E., Vaillant, F., Wu, D., Forrest, N. C., Pal, B., Hart, A. H., Asselin-Labat, M.-L. *et al.* (2009). Aberrant luminal progenitors as the candidate target population for basal tumor development in BRCA1 mutation carriers. *Nature Medicine* **15:**907-913.

Lin, Y., Tang, X., Zhu, Y., Shu, T. and Han, X. (2011). Identification of PARP-1 as one of the transcription factors binding to the repressor element in the promoter region of COX-2. *Archives of Biochemistry and Biophysics* **505:**123-129.

Liu, S., Cong, Y., Wang, D., Sun, Y., Deng, L., Liu, Y., Martin-Trevino, R. *et al.* (2014). Breast Cancer Stem Cells Transition between Epithelial and Mesenchymal States Reflective of their Normal Counterparts. *Stem Cell Reports* **2:**78-91.

Liu, T., Zhang, X., Shang, M., Zhang, Y., Xia, B., Niu, M., Liu, Y. *et al.* (2013). Dysregulated expression of Slug, vimentin, and E-cadherin correlates with poor clinical outcome in patients with basal-like breast cancer. *Journal of Surgical Oncology* **107:**188-194.

Loeffler, P. A., Cuneo, M. J., Mueller, G. A., DeRose, E. F., Gabel, S. A. and London, R. E. (2011). Structural studies of the PARP-1 BRCT domain. *Bmc Structural Biology* **11**.

Lombaerts, M., van Wezel, T., Philippo, K., Dierssen, J. W. F., Zimmerman, R. M. E., Oosting, J., van Eijk, R. *et al.* (2006). E-cadherin transcriptional downregulation by promoter methylation but not mutation is related to epithelial-to-mesenchymal transition in breast cancer cell lines. *British Journal of Cancer* **94:**661-671.

Lonn, P., van der Heide, L. P., Dahl, M., Hellman, U., Heldin, C.-H. and Moustakas, A. (2010). PARP-1 Attenuates Smad-Mediated Transcription. *Molecular Cell* **40:**521-532.

Loseva, O., Jemth, A.-S., Bryant, H. E., Schuler, H., Lehtio, L., Karlberg, T. and Helleday, T. (2010). PARP-3 Is a Mono-ADP-ribosylase That Activates PARP-1 in the Absence of DNA. *Journal of Biological Chemistry* **285:**8054-8060.

Maeda, M., Johnson, K. R. and Wheelock, M. J. (2005). Cadherin switching: essential for behavioral but not morphological changes during an epithelium-to-mesenchyme transition. *Journal of Cell Science* **118:**873-887.

Mahler-Araujo, B., Savage, K., Parry, S. and Reis-Filho, J. S. (2008). Reduction of E-cadherin expression is associated with non-lobular breast carcinomas of basal-like and triple negative phenotype. *Journal of Clinical Pathology* **61:**615-620.

Mallon, E., Osin, P., Nasiri, N., Blain, I., Howard, B. and Gusterson, B. (2000). The basic pathology of human breast cancer. *Journal of Mammary Gland Biology and Neoplasia* **5:**139-163.

Mani, S. A., Guo, W., Liao, M.-J., Eaton, E. N., Ayyanan, A., Zhou, A. Y., Brooks, M. *et al.* (2008). The epithelial-mesenchymal transition generates cells with properties of stem cells. *Cell* **133:**704-715.

Marchini, S., Fruscio, R., Clivio, L., Beltrame, L., Porcu, L., Nerini, I. F., Cavalieri, D. *et al.* (2013). Resistance to platinum-based chemotherapy is associated with epithelial to mesenchymal transition in epithelial ovarian cancer. *European Journal of Cancer* **49:**520-530.

Masutani, M., Nozaki, T., Nishiyama, E., Shimokawa, T., Tachi, Y., Suzuki, H., Nakagama, H. *et al.* (1999). Function of poly(ADP-ribose)polymerase in response to DNA damage: Gene-disruption study in mice. *Molecular and Cellular Biochemistry* **193:**149-152.

McCabe, N., Turner, N. C., Lord, C. J., Kluzek, K., Bialkowska, A., Swift, S., Giavara, S. *et al.* (2006). Deficiency in the repair of DNA damage by homologous recombination and sensitivity to poly(ADP-ribose) polymerase inhibition. *Cancer Research* **66:**8109-8115.

McMorrow, T., Gaffney, M. M., Slattery, C., Campbell, E. and Ryan, M. P. (2005). Cyclosporine A induced epithelial-mesenchymal transition in human renal proximal tubular epithelial cells. *Nephrology Dialysis Transplantation* **20:**2215-2225.

McPhee, T. R., McDonald, P. C., Oloumi, A. and Dedhar, S. (2008). Integrin-Linked Kinase Regulates E-Cadherin Expression Through PARP-1. *Developmental Dynamics* **237:**2737-2747.

Melchor, L. and Benitez, J. (2013). The complex genetic landscape of familial breast cancer. *Human Genetics* **132:**845-863.

Melchor, L., Molyneux, G., Mackay, A., Magnay, F.-A., Atienza, M., Kendrick, H., Nava-Rodrigues, D. *et al.* (2014). Identification of cellular and genetic drivers of breast cancer heterogeneity in genetically engineered mouse tumour models. *Journal of Pathology* **233:**124-137.

Mendes-Pereira, A. M., Martin, S. A., Brough, R., McCarthy, A., Taylor, J. R., Kim, J.-S., Waldman, T. *et al.* (2009). Synthetic lethal targeting of PTEN mutant cells with PARP inhibitors. *Embo Molecular Medicine* **1:**315-322.

Menear, K. A., Adcock, C., Boulter, R., Cockcroft, X.-l., Copsey, L., Cranston, A., Dillon, K. J. *et al.* (2008). 4- 3-(4-Cyclopropanecarbonylpiperazine-1-carbonyl)-4-fluorobenzyl -2H-ph thalazin-1-one: A Novel Bioavailable Inhibitor of Poly(ADP-ribose) Polymerase-1. *Journal of Medicinal Chemistry* **51:**6581-6591.

Mimeault, M., Hauke, R. and Batra, S. K. (2008). Recent advances on the molecular mechanisms involved in the drug resistance of cancer cells and novel targeting therapies. *Clinical Pharmacology & Therapeutics* **83:**673-691.

Mistry, P., Stewart, A. J., Dangerfield, W., Okiji, S., Liddle, C., Bootle, D., Plumb, J. A. *et al.* (2001). In vitro and in vivo reversal of P-glycoprotein-mediated multidrug resistance by a novel potent modulator, XR9576. *Cancer Research* **61:**749-758.

Modi, S., D'Andrea, G., Norton, L., Yao, T. J., Caravelli, J., Rosen, P. P., Hudis, C. *et al.* (2006). A phase I study of cetuximab/paclitaxel in patients with advanced-stage breast cancer. *Clinical Breast Cancer* **7:**270-277.

Molyneux, G., Geyer, F. C., Magnay, F.-A., McCarthy, A., Kendrick, H., Natrajan, R., MacKay, A. *et al.* (2010). BRCA1 Basal-like Breast Cancers Originate from Luminal Epithelial Progenitors and Not from Basal Stem Cells. *Cell Stem Cell* **7:**403-417.

Murai, J., Huang, S.-y. N., Das, B. B., Renaud, A., Zhang, Y., Doroshow, J. H., Ji, J. *et al.* (2012). Trapping of PARP1 and PARP2 by Clinical PARP Inhibitors. *Cancer Research* **72:**5588-5599.

Nie, J., Sakamoto, S., Song, D. M., Qu, Z. Q., Ota, K. and Taniguchi, T. (1998). Interaction of Oct-1 and automodification domain of poly(ADP-ribose) synthetase. *Febs Letters* **424:**27-32.

Noel, G., Godon, C., Fernet, M., Giocanti, N., Megnin-Chanet, F. and Favaudon, V. (2006). Radiosensitization by the poly(ADP=ribose) polymerase inhibitor 4-amino-1,8-naphthalimide is specific of the S phase of the cell cycle and involves arrest of DNA syntheses. *Molecular Cancer Therapeutics* **5:**564-574.

Nowsheen, S., Cooper, T., Bonner, J. A., LoBuglio, A. F. and Yang, E. S. (2012). HER2 Overexpression Renders Human Breast Cancers Sensitive to PARP Inhibition Independently of Any Defect in Homologous Recombination DNA Repair. *Cancer Research* **72:**4796-4806.

O'Shaughnessy, J., Osborne, C., Pippen, J. E., Yoffe, M., Patt, D., Rocha, C., Koo, I. C. *et al.* (2011). Iniparib plus Chemotherapy in Metastatic Triple-Negative Breast Cancer. *New England Journal of Medicine* **364:**205-214.

Oei, S. L. and Ziegler, M. (2000). ATP for the DNA ligation step in base excision repair is generated from poly(ADP-ribose). *Journal of Biological Chemistry* **275:**23234-23239.

Pajic, M., Iyer, J. K., Kersbergen, A., van der Burg, E., Nygren, A. O. H., Jonkers, J., Borst, P. *et al.* (2009). Moderate Increase in Mdr1a/1b Expression Causes In vivo Resistance to Doxorubicin in a Mouse Model for Hereditary Breast Cancer. *Cancer Research* **69:**6396-6404.

Patel, A. G., De Lorenzo, S. B., Flatten, K. S., Poirier, G. G. and Kaufmann, S. H. (2012). Failure of Iniparib to Inhibit Poly(ADP-Ribose) Polymerase In Vitro. *Clinical Cancer Research* **18:**1655-1662.

Paull, T. T., Cortez, D., Bowers, B., Elledge, S. J. and Gellert, M. (2001). Direct DNA binding by Brca1. *Proceedings of the National Academy of Sciences of the United States of America* **98:**6086-6091.

Perl, A. K., Wilgenbus, P., Dahl, U., Semb, H. and Christofori, G. (1998). A causal role for E-cadherin in the transition from adenoma to carcinoma. *Nature* **392:**190-193.

Perou, C. M., Sorlie, T., Eisen, M. B., van de Rijn, M., Jeffrey, S. S., Rees, C. A., Pollack, J. R. *et al.* (2000a). Molecular portraits of human breast tumours. *Nature* **406:**747-752.

Perou, C. M., Sorlie, T., van de Rijn, M., Jeffrey, S. S., Rees, C. A., Pollack, J. R., Ross, D. T. *et al.* (2000b). Classification of human breast tumors using cDNA microarrays and gene-clustering. *Proceedings of the American Association for Cancer Research Annual Meeting* 681-681.

Pettitt, S. J., Rehman, F. L., Bajrami, I., Brough, R., Wallberg, F., Kozarewa, I., Fenwick, K. *et al.* (2013). A Genetic Screen Using the PiggyBac Transposon in Haploid Cells Identifies Parp1 as a Mediator of Olaparib Toxicity. *Plos One* **8**.

Ponti, D., Costa, A., Zaffaroni, N., Pratesi, G., Petrangolini, G., Coradini, D., Pilotti, S. *et al.* (2005). Isolation and in vitro propagation of tumorigenic breast cancer cells with stem/progenitor cell properties. *Cancer Research* **65:**5506-5511.

Powell, S. N. and Kachnic, L. A. (2003). Roles of BRCA1 and BRCA2 in homologous recombination, DNA replication fidelity and the cellular response to ionizing radiation. *Oncogene* **22:**5784-5791.

Prasad, R., Lavrik, O. I., Kim, S. J., Kedar, P., Yang, X. P., Vande Berg, B. J. and Wilson, S. H. (2001). DNA polymerase beta-mediated long patch base excision repair - Poly(ADP-ribose) polymerase-1 stimulates strand displacement DNA synthesis. *Journal of Biological Chemistry* **276:**32411-32414.

Prat, A., Parker, J. S., Karginova, O., Fan, C., Livasy, C., Herschkowitz, J. I., He, X. *et al.* (2010). Phenotypic and molecular characterization of the claudin-low intrinsic subtype of breast cancer. *Breast Cancer Research* **12**.

Prat, A. and Perou, C. M. (2011). Deconstructing the molecular portraits of breast cancer. *Molecular Oncology* **5:**5-23.

Rebbeck, T. R., Friebel, T., Lynch, H. T., Neuhausen, S. L., van't Veer, L., Garber, J. E., Evans, G. R. *et al.* (2004). Bilateral prophylactic mastectomy reduces breast cancer risk in BRCA1 and BRCA2 mutation carriers: The PROSE study group. *Journal of Clinical Oncology* **22:**1055-1062.

Reis-Filho, J. S. and Pusztai, L. (2011). Breast Cancer 2 Gene expression profiling in breast cancer: classification, prognostication, and prediction. *Lancet* **378:**1812-1823.

Richert, M. M., Schwertfeger, K. L., Ryder, J. W. and Anderson, S. M. (2000). An atlas of mouse mammary gland development. *Journal of Mammary Gland Biology and Neoplasia* **5:**227-241.

Rios, A. C., Fu, N. Y., Lindeman, G. J. and Visvader, J. E. (2014). In situ identification of bipotent stem cells in the mammary gland. *Nature* **506:**322-+.

Rodriguez, M. I., Gonzalez-Flores, A., Dantzer, F., Collard, J., de Herreros, A. G. and Oliver, F. J. (2011). Poly(ADP-ribose)-dependent regulation of Snail1 protein stability. *Oncogene* **30:**4365-4372.

Rojo, F., Garcia-Parra, J., Zazo, S., Tusquets, I., Ferrer-Lozano, J., Menendez, S., Eroles, P. *et al.* (2012). Nuclear PARP-1 protein overexpression is associated with poor overall survival in early breast cancer. *Annals of Oncology* **23:**1156-1163.

Rottenberg, S., Jaspers, J. E., Kersbergen, A., van der Burg, E., Nygren, A. O. H., Zander, S. A. L., Derksen, P. W. B. *et al.* (2008). High sensitivity of BRCA1-deficient mammary tumors to the PARP inhibitor AZD2281 alone and in combination with platinum drugs. *Proceedings of the National Academy of Sciences of the United States of America* **105:**17079-17084.

Rouleau, M., McDonald, D., Gagne, P., Ouellet, M. E., Droit, A., Hunter, J. M., Dutertre, S. *et al.* (2007). PARP-3 associates with polycomb group bodies and with components of the DNA damage repair machinery. *Journal of Cellular Biochemistry* **100:**385-401.

Sakai, W., Swisher, E. M., Karlan, B. Y., Agarwal, M. K., Higgins, J., Friedman, C., Villegas, E. *et al.* (2008). Secondary mutations as a mechanism of cisplatin resistance in BRCA2-mutated cancers. *Nature* **451:**1116-U1119.

Sarrio, D., Rodriguez-Pinilla, S. M., Hardisson, D., Cano, A., Moreno-Bueno, G. and Palacios, J. (2008). Epithelial-mesenchymal transition in breast cancer relates to the basal-like phenotype. *Cancer Research* **68:**989-997.

Sayan, A. E., Griffiths, T. R., Pal, R., Browne, G. J., Ruddick, A., Yagci, T., Edwards, R. *et al.* (2009). SIP1 protein protects cells from DNA damage-induced apoptosis and has

independent prognostic value in bladder cancer. *Proceedings of the National Academy of Sciences of the United States of America* **106:**14884-14889.

Schreiber, V., Ame, J. C., Dolle, P., Schultz, I., Rinaldi, B., Fraulob, V., Menissier-de Murcia, J. *et al.* (2002). Poly(ADP-ribose) polymerase-2 (PARP-2) is required for efficient base excision DNA repair in association with PARP-1 and XRCC1. *Journal of Biological Chemistry* **277:**23028-23036.

Schultz, N., Lopez, E., Saleh-Gohari, N. and Helleday, T. (2003). Poly(ADP-ribose) polymerase (PARP-1) has a controlling role in homologous recombination. *Nucleic Acids Research* **31:**4959-4964.

Shackleton, M., Vaillant, F., Simpson, K. J., Stingl, J., Smyth, G. K., Asselin-Labat, M. L., Wu, L. *et al.* (2006). Generation of a functional mammary gland from a single stem cell. *Nature* **439:**84-88.

Shall, S. and de Murcia, G. (2000). Poly(ADP-ribose) polymerase-1: what have we learned from the deficient mouse model? *Mutation Research-DNA Repair* **460:**1-15.

Shen, Q. and Brown, P. H. (2005). Transgenic mouse models for the prevention of breast cancer. *Mutation Research-Fundamental and Molecular Mechanisms of Mutagenesis* **576:**93-110.

Shimo, T., Kurebayashi, J., Kanomata, N., Yamashita, T., Kozuka, Y., Moriya, T. and Sonoo, H. (2014). Antitumor and anticancer stem cell activity of a poly ADP-ribose polymerase inhibitor olaparib in breast cancer cells. *Breast Cancer* **21:**75-85.

Shiobara, M., Miyazaki, M., Ito, H., Togawa, A., Nakajima, N., Nomura, F., Morinaga, N. *et al.* (2001). Enhanced polyadenosine diphosphate-ribosylation in cirrhotic liver and carcinoma tissues in patients with hepatocellular carcinoma. *Journal of Gastroenterology and Hepatology* **16:**338-344.

Smith, S. and de Lange, T. (2000). Tankyrase promotes telomere elongation in human cells. *Current Biology* **10:**1299-1302.

Sorlie, T., Perou, C. M., Tibshirani, R., Aas, T., Geisler, S., Johnsen, H., Hastie, T. *et al.* (2001). Gene expression patterns of breast carcinomas distinguish tumor subclasses with clinical implications. *Proceedings of the National Academy of Sciences of the United States of America* **98:**10869-10874.

Sorlie, T., Tibshirani, R., Parker, J., Hastie, T., Marron, J. S., Nobel, A., Deng, S. *et al.* (2003). Repeated observation of breast tumor subtypes in independent gene expression data sets. *Proceedings of the National Academy of Sciences of the United States of America* **100:**8418-8423.

Steiglitz, B. M., Keene, D. R. and Greenspan, D. S. (2002). PCOLCE2 encodes a functional procollagen C-proteinase enhancer (PCPE2) that is a collagen-binding protein differing in distribution of expression and post-translational modification from the previously described PCPE1. *Journal of Biological Chemistry* **277:**49820-49830.

Stewart, D. J. (2007). Mechanisms of resistance to cisplatin and carboplatin. *Critical Reviews in Oncology Hematology* **63:**12-31.

Stingl, J., Eirew, P., Ricketson, I., Shackleton, M., Vaillant, F., Choi, D., Li, H. Y. I. *et al.* (2006). Purification and unique properties of mammary epithelial stem cells. *Nature* **439:**993-997.

Sung, P. and Klein, H. (2006). Mechanism of homologous recombination: mediators and helicases take on regulatory functions. *Nature Reviews Molecular Cell Biology* **7:**739-750.

Taube, J. H., Herschkowitz, J. I., Komurov, K., Zhou, A. Y., Gupta, S., Yang, J., Hartwell, K. *et al.* (2010). Core epithelial-to-mesenchymal transition interactome gene-expression signature is associated with claudin-low and metaplastic breast cancer subtypes. *Proceedings of the National Academy of Sciences of the United States of America* **107:**15449-15454.

Thomas, K. R. and Capecchi, M. R. (1987). SITE-DIRECTED MUTAGENESIS BY GENE TARGETING IN MOUSE EMBRYO-DERIVED STEM-CELLS. *Cell* **51:**503-512.

Thomson, S., Buck, E., Petti, F., Griffin, G., Brown, E., Ramnarine, N., Iwata, K. K. *et al.* (2005). Epithelial to mesenchymal transition is a determinant of sensitivity of non-small-cell lung carcinoma cell lines and xenografts to epidermal growth factor receptor inhibition. *Cancer Research* **65:**9455-9462.

Thuault, S., Tan, E. J., Peinado, H., Cano, A., Heldin, C.-H. and Moustakas, A. (2008). HMGA2 and Smads Co-regulate SNAIL1 Expression during Induction of Epithelial-to-Mesenchymal Transition. *Journal of Biological Chemistry* **283:**33437-33446.

Timmerman, L. A., Grego-Bessa, J., Raya, A., Bertran, E., Perez-Pomares, J. M., Diez, J., Aranda, S. *et al.* (2004). Notch promotes epithelial-mesenchymal transition during cardiac development and oncogenic transformation. *Genes & Development* **18:**99-115.

Tomoda, T., Kurashige, T., Moriki, T., Yamamoto, H., Fujimoto, S. and Taniguchi, T. (1991). ENHANCED EXPRESSION OF POLY(ADP-RIBOSE) SYNTHETASE GENE IN MALIGNANT-LYMPHOMA. *American Journal of Hematology* **37:**223-227.

Tryndyak, V. P., Beland, F. A. and Pogribny, I. P. (2010). E-cadherin transcriptional down-regulation by epigenetic and microRNA-200 family alterations is related to mesenchymal and drug-resistant phenotypes in human breast cancer cells. *International Journal of Cancer* **126:**2575-2583.

Turner, N. C. and Reis-Filho, J. S. (2006). Basal-like breast cancer and the BRCA1 phenotype. *Oncogene* **25:**5846-5853.

Tutt, A., Robson, M., Garber, J. E., Domchek, S. M., Audeh, M. W., Weitzel, J. N., Friedlander, M. *et al.* (2010). Oral poly(ADP-ribose) polymerase inhibitor olaparib in patients with BRCA1 or BRCA2 mutations and advanced breast cancer: a proof-of-concept trial. *Lancet* **376:**235-244.

van Amerongen, R., Bowman, A. N. and Nusse, R. (2012). Developmental Stage and Time Dictate the Fate of Wnt/beta-Catenin-Responsive Stem Cells in the Mammary Gland. *Cell Stem Cell* **11:**387-400.

Van Keymeulen, A., Rocha, A. S., Ousset, M., Beck, B., Bouvencourt, G., Rock, J., Sharma, N. *et al.* (2011). Distinct stem cells contribute to mammary gland development and maintenance. *Nature* **479:**189-U158.

van Zon, A., Mossink, M. H., Schoester, M., Houtsmuller, A. B., Scheffer, G. L., Scheper, R. J., Sonneveld, P. *et al.* (2003). The formation of vault-tubes: a dynamic interaction between vaults and vault PARP. *Journal of Cell Science* **116:**4391-4400.

Watson, C. J., Gordon, K. E., Robertson, M. and Clark, A. J. (1991). INTERACTION OF DNA-BINDING PROTEINS WITH A MILK PROTEIN GENE PROMOTER INVITRO - IDENTIFICATION OF A MAMMARY GLAND-SPECIFIC FACTOR. *Nucleic Acids Research* **19:**6603-6610.

Weigelt, B., Kreike, B. and Reis-Filho, J. S. (2009). Metaplastic Breast Carcinomas Are Basal-Like Breast Cancers: A Genomic Profiling Analysis. *Laboratory Investigation* **89:**74A-74A.

Wellings, S. R., Jensen, H. M. and Marcum, R. G. (1975). ATLAS OF SUBGROSS PATHOLOGY OF HUMAN BREAST WITH SPECIAL REFERENCE TO POSSIBLE PRECANCEROUS LESIONS. *Journal of the National Cancer Institute* **55:**231-273.

Williams, J. M. and Daniel, C. W. (1983). MAMMARY DUCTAL ELONGATION - DIFFERENTIATION OF MYOEPITHELIUM AND BASAL LAMINA DURING BRANCHING MORPHOGENESIS. *Developmental Biology* **97:**274-290.

Xia, Y., Pao, G. M., Chen, H. W., Verma, I. M. and Hunter, T. (2003). Enhancement of BRCA1 E3 ubiquitin ligase activity through direct interaction with the BARD1 protein. *Journal of Biological Chemistry* **278:**5255-5263.

Xu, J., Lamouille, S. and Derynck, R. (2009). TGF-beta-induced epithelial to mesenchymal transition. *Cell Research* **19:**156-172.

Yamaguchi, N., Ito, E., Azuma, S., Honma, R., Yanagisawa, Y., Nishikawa, A., Kawamura, M. *et al.* (2008). FoxA1 as a lineage-specific oncogene in luminal type breast cancer. *Biochemical and Biophysical Research Communications* **365:**711-717.

Yamane, K., Katayama, E. and Tsuruo, T. (2000). The BRCT regions of tumor suppressor BRCA1 and of XRCC1 show DNA end binding activity with a multimerizing feature. *Biochemical and Biophysical Research Communications* **279:**678-684.

Yap, T. A., Sandhu, S. K., Carden, C. P. and de Bono, J. S. (2011). Poly(ADP-Ribose) Polymerase (PARP) Inhibitors: Exploiting a Synthetic Lethal Strategy in the Clinic. *Ca-a Cancer Journal for Clinicians* **61:**31-49.

Yook, J. I., Li, X. Y., Ota, I., Fearon, E. R. and Weiss, S. J. (2005). Wnt-dependent regulation of the E-cadherin repressor snail. *Journal of Biological Chemistry* **280:**11740-11748.

Yu, S. W., Wang, H. M., Poitras, M. F., Coombs, C., Bowers, W. J., Federoff, H. J., Poirier, G. G. *et al.* (2002). Mediation of poly(ADP-ribose) polymerase-1-dependent cell death by apoptosis-inducing factor. *Science* **297:**259-263.

Yu, X., Jacobs, S. A., West, S. C., Ogawa, T. and Egelman, E. H. (2001). Domain structure and dynamics in the helical filaments formed by RecA and Rad51 on DNA. *Proceedings of the National Academy of Sciences of the United States of America* **98:**8419-8424.

Yuan, S. S. F., Lee, S. Y., Chen, G., Song, M. H., Tomlinson, G. E. and Lee, E. (1999). BRCA2 is required for ionizing radiation-induced assembly of rad51 complex in vivo. *Cancer Research* **59:**3547-3551.

Appendix I.

Networks of genes differentially expressed in “resistant” cohort relative to “responding” cohort.

Genes in network		Functions
Genes upregulated	Genes downregulated	
-	BLK, CARD11, CD5, CD6, CD19, CD22, CD27, CD180, CD79A, CD79B, FCRLA, ICOS, IGJ, IK2F3, LAX1, MS4A1, PIGR, POU2F2, PPP2R2C, SH2D1A, SLAMF1, SP1B, TNFRSF13C, TRAT1, UBASH3A	Haematological system development and function, humoral immune response, tissue morphology
AURKA, AUKB, BUB1, CENPA, CENP1, CKAP2, DLL4,HIST1H2AB/HIST1H2AE, HIST1H2BJ/HIST1H2BK, KIF20A, KIF4A, MAD2L1, NCAPG, NDC80, NUF2, PRC1, RACGAP1, SEPT1, SHCBP1, UBE2C	AGAP2, CD226, FYB, GIMAP5	Cell cycle, cellular assembly and organisation, DNA replication, recombination andn repair
BCAT1, CCNA2, CCNB2, CDC25C, CDKN3, CEP55, CK51B, DUSP9, HIST1H1A, HIST1H1B, HMGA2, KIF22, PLK1, PTPN22, STEAP1, TTK	ANO3, CTLA4, FREM1	Cellular assembly and organisation, DNA replication, recombination and repair, cell cycle
HMGA2, POU4F2	BTLA, CD19, CEL, CLEC2D, FAM26F, GNA14, HAAO, HEPACAM2, IPCEF1, SLAMF6, STAP1	Inflammatory response, cell-to-cell signalling and interaction, haematological system development and function
LGALS1, TOP2A	CD2, CD4,CD247,CD3E, CD3G, CD8A, DPP4, DTX1, FCRL3, GRAP2, ITK, KYNU, PTPRCAP, SH2D2A, THEMIS, ZAP70	Cellular development, cellualr growth and proliferation, haematological system development and function
ASF1B, BIRC5, CCND1, DEPDC1, FAM83D, HAS2, MNS1, PHF19, STC1	GDF6, HLA-DQA1, IKZF1, IKZF4, MUC1, SOX6	Lymphoid tissue structure and development, organ morphology, cancer
POU4F2, STEAP2	AKNA, APOD, ATP8A2, BTLA, CD28, CD40LG, COL15A1, FOXP3, HMCN1, IL2RC, IL7R, LAMA2, MMP11	Cellular development, cellualr growth and proliferation, haematological system development and function
DNPH1, HIST2H2AB,	ADIG, CACNA1E, CYP2D6, CYP4B1, H2-T24,	Energy production, endocrine system disorders,

	HLA-DOA, HLA-DOB, MS4A1, PAMR1, SOX14, TOX	gastrointestinal disease
KIAA0101, TUBB6	ATP2A3, CD74, CYFIP3, FAAH, ITGA4, KLF15, PRKAA2, WIPF3	Carbohydrate metabolism, cell morphology, organ morphology
BOK	C5, CCR6, CCR8, CCR9, CXCR6, CYGB, GPR18, GSTA3, HMGCS2, PRG2	Cell signalling, molecular transport, vitamin and mineral